THE UNIVERSITY *of* EDINBURGH

Expression and Characterisation of a Novel Poly(A)-Binding Protein, PABP5

Ross C. Anderson

PhD

The University of Edinburgh

2010

Abstract

The poly(A)-binding proteins (PABPs) are a family of eukaryotic RNA-binding proteins with key roles in mRNA translation and stability. The molecular function of PABPs have been largely revealed through study of the prototypical cytoplasmic poly(A)-binding protein, PABP1. Thus, little is known regarding other PABP family members. PABP5 contains four RNA-recognition motifs characteristic of the cytoplasmic PABPs yet is structurally distinct as it lacks a portion of the C-terminus. This region contains a proline-rich section linked to a globular domain that facilitates a number of protein-protein interactions. To date, little information has been presented regarding the expression of PABP5 and there is no data pertaining to the function of this protein, despite being mapped to a region of the X-chromosome associated with human pathological conditions.

In this thesis, I present the first data documenting the expression of PABP5 within mouse tissues, and find it to be expressed at the highest levels within the brain, ovary, and testis. The limited data available suggests that gonads may be the only tissue to contain all PABPs therefore I additionally describe the expression of PABP1 and PABP4 to ascertain their cellular distribution within these tissues. This revealed that PABPs have overlapping yet distinct expression patterns in mouse gonads.

The distinct structure of PABP5 suggested that its function may vary from PABP1. Characterisation of its activities in translational regulation was therefore investigated. When tethered to a reporter mRNA PABP5 had limited translational stimulatory activity, and in addition could not be isolated via m^7G cap chromatography and failed to interact with translation initiation factors including eIF4G and PAIP-1. These factors interact with PABP1 to positively promote translation, implying that PABP5 function in translational regulation differs from other PABPs investigated.

Examining why PABP5 failed to display translational stimulatory activity also revealed an interaction with the negative regulator of translation, PAIP-2. In summary, I present the first description of PABP5 cellular localisation, and have gone some way towards elucidating the molecular function of this uncharacterised protein.

Declaration

I declare that the work presented in this PhD is my own and has not been submitted for any other degree.

Ross C. Anderson

Acknowledgements

The last 4 years have been the source of much stress, pain and anxiety, filled with many periods where I wondered if I would ever finish, and yet seeing the following 300 pages come together as a coherent thesis is incredibly satisfying. There are so many people to thank I don't know where to start – special thanks to Niki, who after 7 years of working together I would prefer to call a friend rather than a boss. I am forever indebted as I know this thesis caused you no small amount of trauma! Thank you to Matt for the lab supervision and opening my eyes to the world of curry (maybe one day I will be able to eat a chilli without fainting). Thanks to Hannah and Pedro for sharing the PhD pain, and to Barbara for keeping me in line! Richard – has been an excellent drinking buddy and a source of infinite wisdom in the lab. Finally, William (aka the Beef from Dalkeith), - it's your round mate.

Outside the lab, I wanted to say thanks to Niall and Euan for the distracting weekends of drinking which have been excellent fun. I'd like to say a huge thank you to Claire – you have been amazing and I'll never forget the support you have given me. This thesis would not have been finished and handed in without your help. Finally, I'd like to save the biggest thank you for Babs and Stu – I know I don't pick up the phone or jump in the car often enough (unless of course I need money or food!) but you have supported me through thick and thin and I wish there was some way I could repay you. I love you both very much and I want to dedicate this thesis to you both.

To my parents.

Cheers!

Abbreviations

µg..... microgram

µl..... microlitre

µM..... micromolar

µm..... ..... micrometre

3'-UTR..... ..... 3' untranslated region

4E-BP..... ..... eukaryotic initiation factor 4E binding protein

5'-UTR..... ..... 5' untranslated region

A..... adenosine

aa-tRNA..... aminoacyl-transfer ribonucleic acid

ActD..... ..... actinomycin D

AD..... ..... activation domain

Ago..... argonaute protein

ARE..... ..... adenosine/uracil-rich element

ARE-BP..... adenosine/uracil-rich element binding protein

ARS..... autoregulatory sequence

A-site..... aminoacyl site

ATP..... adenosine triphosphate

BD..... binding domain

C..... cytosine

cDNA..... complementary DNA

Co-IP..... protein complex immunoprecipitation

CPE..... cytoplasmic polyadenylation element

CPEB..... cytoplasmic polyadenylation element binding protein

CrPV..... cricket paralysis virus

CT..... threshold cycle

C-terminus..... carboxyl terminus

CTP..... cytosine triphosphate

DAB..... diaminobenzidinetrahydrochloride

DAP5..... death associated protein 5

DAPI..... 4', 6-diamidino-2-phenylindole

DCP1..... decapping protein 1

DCP2..... decapping protein 2

Dcps..... scavenger decapping protein

ddH_2O..... double distilled water

dH_2O..... distilled water

DMEM..... Dulbecco's minimal essential medium

DNA..... deoxyribonucleic acid

DNase..... deoxyribonucleic acid nuclease

dsRNA..... double stranded ribonucleic acid

E. coli..... *Escherichia coli*

EDTA..... ethylene diamine tetraacetic acid

eEF..... eukaryotic elongation factor

EGFP..... enhanced green fluorescent protein

eIF..... eukaryotic initiation factor

EJC..... exon junction complex

EMCV..... encephalomyocarditis virus

EMSA..... electrophoresis mobility shift assay

ePABP..... embryonic polyadenylate binding protein

ePABP2..... embryonic polyadenylate binding protein 2

ER..... endoplasmic reticulum

eRF..... eukaryotic release factor

E-site..... exit site

FCS..... fetal calf serum

FMDV..... foot and mouth disease virus

G..... guanosine

g..... gram

GAC..... guanosine triphosphatase associated centre

GAP..... guanosine triphosphatase activating protein

GCN4..... general control nonderepressible 4

GEF..... guanine nucleotide exchange factor

GST..... glutathione S-transferase

GTP..... guanosine triphosphate

GTPase..... guanosine triphosphatase

H_2O..... water

HCV..... hepatitis C virus

HeLa cell..... Henrietta Lacks cell

His..... histidine

hnRNP..... heterogeneous nuclear ribonucleoprotein

HRI..... heme-regulated eukaryotic initiation factor 2 alpha kinase

HRP..... horse radish peroxidase

iPABP..... inducible polyadenylate binding protein

IPTG..... isopropyl β-D-1-thiogalactopyranoside

IRE..... iron regulatory element

IRES..... internal ribosome entry site

IRP..... iron regulatory protein

ISH..... *in-situ* hybridisation

ITAF..... internal ribosome entry site trans-acting factor

ITC..... isothermal titration calorimetry

Kb..... kilobase

K_d..... dissociation constant

kDa..... kilodalton

L..... litre

LSU..... large ribosomal subunit

M..... molar

MAPK..... mitogen activated protein kinase

Met-tRNAi..... initiator transfer ribonucleic acid

mg..... milligram

miRISC..... microribonucleic acid induced silencing complex

miRNA..... microribonucleic acid

ml..... millilitre

mM..... millimolar

mm..... millimetre

mnk1..... MAP kinase interacting serine/threonine protein kinase 1

mnk2..... MAP kinase interacting serine/threonine protein kinase 2

mRNA..... messenger ribonucleic acid

mRNP..... messenger ribonucleoprotein

mTOR..... mammalian target of rapamycin

NES..... nuclear export signal

ng..... nanogram

nl..... nanolitre

NLS..... nuclear localisation signal

nM..... nanomolar

nm..... nanometre

NMD..... nonsense mediated decay

NSP3..... non-structural protein 3

nt..... nucleotide

N-terminus..... amino terminus

O.D...... optical density

ODC..... ornithine decarboxylase

Oligo..... oligonucleotide

ORF..... open reading frame

PABC..... polyadenylate binding protein carboxy terminus

PABP..... polyadenylate binding protein

PABP1..... polyadenylate binding protein 1

PABP4..... polyadenylate binding protein 4

PABP5..... polyadenylate binding protein 5

PABPN1..... nuclear polyadenylate binding protein

PAGE..... polyacrylamide gel electrophoresis

PAIP-1..... polyadenylate binding protein interacting protein 1

PAIP-2..... polyadenylate binding protein interacting protein 2

PAM..... polyadenylate binding protein interacting motif

PAN2..... polyadenylate nuclease 2

PAN3..... polyadenylate nuclease 3

PAP..... polyadenylate polymerase

PARN..... polyadenylate ribonuclease

PCR..... polymerase chain reaction

PERK..... protein kinase R-like endoplasmic reticulum-localised kinase

PFA..... paraformaldehyde

pg..... picogram

PIC..... preinitiation complex

PKR..... protein kinase R

pM..... picomolar

poly(A)..... polyadenylate

P-site..... polyadenylate

PTC..... premature termination codon

PV..... poliovirus

QPCR..... quantitative polymerase chain reaction

rcf..... relative centrifugal force

RER..... rough endoplasmic reticulum

RLU..... relative luciferase units

RNA..... ribonucleic acid

RNA-BP..... ribonucleic acid binding protein

RNAi..... ribonucleic acid interference

RNase..... ribonucleic acid nuclease

RNMT..... messenger ribonucleic acid cap guanine N7 methyltransferase

rpm..... revolutions per minute

Rps..... ribosomal proteins

RRL..... rabbit reticulocyte lysate

RRM..... ribonucleic acid recognition motifs

rRNA..... ribosomal ribonucleic acid

RT-PCR..... reverse transcription polymerase chain reaction

SAP..... shrimp alkaline phosphatase

SG..... stress granule

siRNA..... short interfering ribonucleic acid

SSU..... small ribosomal subunit

SXL..... sex lethal

T..... thymidine

TC..... ternary complex

TD-NEM..... transcription dependent nuclear export motif

TEA..... triethanolamine

TEMED..... tetramethylethylenediamine

TOP..... terminal oligopyrimidine

tPABP..... testis polyadenylate binding protein

tRNA..... transfer ribonucleic acid

TTP..... tristetraprolin

U..... uracil

uAUG..... upstream AUG

UNR..... upstream of n-ras

uORF..... upstream open reading frame

WT..... wild-type

X-Gal..... bromochloroindolylgalactopyranoside

XRN1..... exoribonuclease 1

Y2H..... yeast two-hybrid

β-Gal..... β-galactosidase

Table of Contents

List of Figures

List of Tables

Chapter 1: Introduction

1.1 Translational Regulation

1.1.1 Translational Regulation and Disease

The synthesis of a functional gene product from its corresponding gene is a highly dynamic and regulated process. The multiple steps involved are collectively referred to as 'gene expression' and comprise many complicated molecular events. For protein coding genes messenger ribonucleic acid (mRNA) molecules are transcribed from their deoxyribonucleic acid (DNA) templates via the action of RNA polymerase, and processed to add an m^7GpppN cap and polyadenylate tail, and to remove introns via splicing. Mature mRNAs are exported from the nucleus to the cytoplasm whereupon they are decoded by ribosomes to produce proteins in a process called translation (see figure 1.1).

Aberrant expression of genes can be associated with a variety of common disorders and diseases, underlying the importance of the many layers of control that ensure genes are expressed correctly, both spatially, temporally and to an accurate level. These tiers of control cover all aspects of the gene expression pathway, including epigenetic modifications, transcription, splicing, RNA transport, mRNA translation and stability and finally modification and degradation of the protein products.

1.1.2 Translational Control as a Target for Regulation

Translation of mRNA is far from a constitutive process, and is a highly coordinated event, with approximately 1 gene in every 10 known to be strongly regulated at this level (Reynolds, 2002) while some estimates place this value considerably higher. There are notable advantages to the translational control of mRNAs. Firstly, is the speed and reversibility of many translational control mechanisms (Koritzinsky *et al.*, 2006; Ling *et al.*, 2005; Teleman *et al.*, 2005). Secondly, the spatial control of mRNA translation permits concentration gradients and regionalised protein synthesis

(Huttelmaier *et al.*, 2005; Kwon *et al.*, 1999). Finally, transcriptional inactivity can necessitate translational control, such as before the onset of zygotic transcription in developing embryos (Shen-Orr *et al.*, 2010), or during erythropoiesis where the cells undergo programmed transcriptional arrest during terminal differentiation (Ostareck *et al.*, 1997). The importance of translational control is further exemplified by the growing number of cases where translational deregulation has been shown to result in serious human pathophysiological conditions including neurological, metabolic and reproductive disorders as well as various cancers (Cazzola and Skoda, 2000; De Benedetti and Graff, 2004; Leegwater *et al.*, 2001).

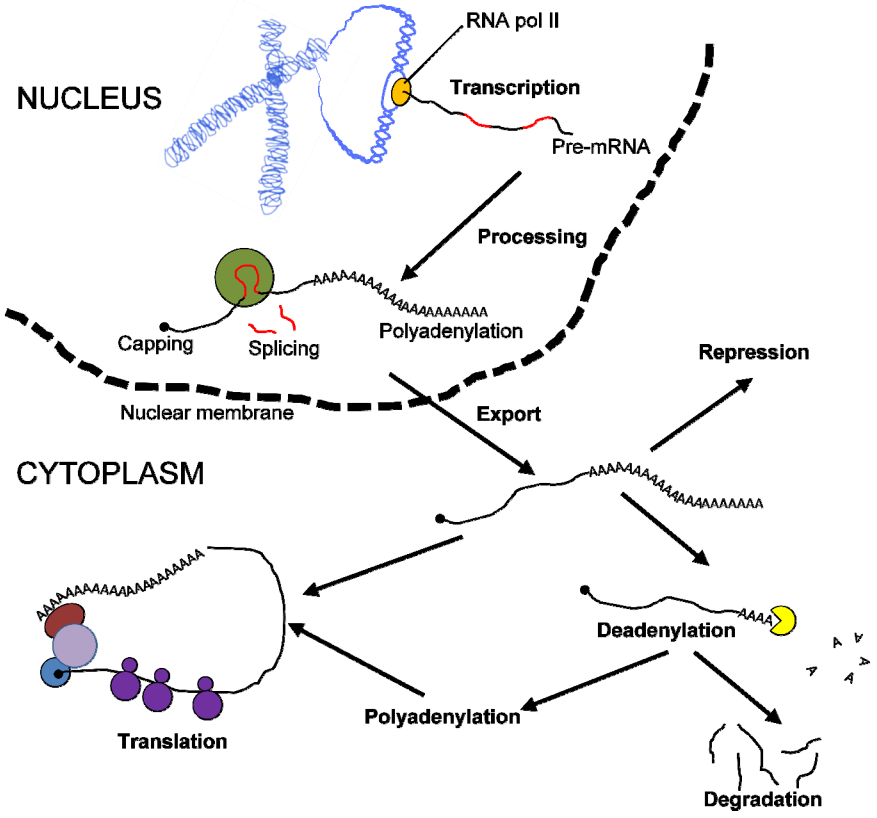

Figure 1.1 Eukaryotic gene expression. Following transcription by RNA polymerase II, pre-mRNAs are spliced to remove introns and have a polyadenylate tail added. The mRNAs are then exported through nuclear pores to the cytoplasm, where they can be translated by ribosomes to produce protein, or alternatively they can be repressed and/or degraded. Deadenylated messages can be polyadenylated in the cytoplasm to promote translation.

Many disease causing mutations affecting mRNA translation have been identified. These can take the form of mutations within mRNA *cis*-acting elements, within the *trans*-acting RNA binding proteins (RNA-BPs) that bind these elements, and within translation factors. Examples include the degenerative neurological condition termed vanishing white matter disease for which mutations in the translation factor eIF2B are known to be causative, and hereditary hyperferritinemia characterised by mutations within the mRNA of the iron storage protein ferritin that abolish binding of a translational regulatory protein. These examples serve to highlight the importance of research into the area of translational control.

1.2 Translation: Initiation, Elongation and Termination

1.2.1 Translation Overview

The process of translation can be divided into three distinct steps; termed initiation, elongation and termination. The most frequently targeted step for translational regulation is the initiation step. Multiple eukaryotic initiation factors (eIFs) are involved and these can be regulated, often to control global mRNA translation. Manipulating this step also avoids the problems associated with having to deal with partially translated protein products that may result from targeting the elongation step. Central to the translational process are the ribosomes which facilitate the production of proteins from their constituent amino acids. Ribosomes are large macromolecular structures composed of many proteins (approximately 50 proteins in humans), and also ribosomal RNAs (rRNAs). The eukaryotic ribosomal proteins are arranged into a small 40S subunit containing the 18S rRNA and a large 60S subunit containing 5S, 5.8S and 28S rRNAs. The small subunit (SSU) binds mRNA and also monitors the fidelity of codon/anticodon interactions within its rRNA composed decoding centre. The decoding centre contains three binding sites for transfer ribonucleic acids (tRNAs) – the aminoacyl site (A-site) which binds incoming aminoacylated tRNA (aa-tRNA), the peptidyl site (P-site) which binds peptidyl-tRNA and the exit site (E-site) which binds free tRNAs. The large subunit (LSU)

catalyses the formation of the peptide bond between amino acid moieties of adjacent tRNAs and also contains a guanosine-5'-triphosphatase associated centre (GAC).

1.2.2 Translation Initiation

In eukaryotes, translation initiation is defined as the events leading to the assembly of an 80S ribosome (composed of a small 40S subunit bound to a large 60S subunit), where the anticodon of the aminoacylated initiator methionyl-transfer RNA (Met-$tRNA_i$) is base-paired to the mRNA initiation codon in the ribosomal peptidyl site (P-site). The process is mediated by at least 12 eukaryotic initiation factors (eIFs) comprising >30 polypeptides (reviewed in Jackson *et al.*, 2010) as well as the hydrolysis of adenosine-5'-triphosphate (ATP) and guanosine-5'-triphosphate (GTP). In contrast, prokaryotic translation initiation requires only 3 protein factors, IF1, IF2 and IF3 which share functional and structural similarities to the eukaryotic initiation factors eIF1, eIF1A and eIF5B, known to be involved in fidelity of start codon recognition and large ribosomal subunit joining (Andreev *et al.*, 2006). While the small ribosomal subunit is recruited to the 5' terminus of eukaryotic mRNAs, in prokaryotes the ribosome appears to be directly recruited to the start codon. This is mediated via two mRNA sequence elements termed the Shine-Dalgarno sequence and an AU-rich element. These elements interact with the ribosomal 16S rRNA and ribosomal protein S1 respectively (Boni *et al.*, 1991). As a result many factors required in eukaryotes for the recruitment and scanning of the small ribosomal subunit to the start codon are dispensable in prokaryotes explaining the differing factor requirements in the 2 systems. Translation initiation in eukaryotes can be subdivided into a number of steps (see figure 1.2), discussed below.

Ternary Complex Formation

Cap-dependent translation is initiated by the formation of the ternary complex (TC) which consists of the heterotrimeric guanosine-5'-triphosphatase (GTPase) protein eIF2 bound to GTP and Met-$tRNA_i$. The TC is responsible for binding of the Met-

$tRNA_i$ to the small ribosomal subunit and possibly also commitment to the elongation phase of translation following initiation codon recognition. eIF2 consists of three subunits – α, β, and γ. eIF2β is responsible for binding to the eIF2 specific GTPase activating protein (GAP) eIF5, and also the guanine nucleotide exchange factor (GEF) eIF2B (Asano *et al.*, 1999), while eIF2γ appears to bind GTP and the Met-$tRNA_i$. GTP binding domains are present in eIF2β but these sites appear to have minimal effect on eIF2 activity (Naranda *et al.*, 1995). The Met-$tRNA_i$ binding activity of eIF2γ may be due to the structural similarity to eEF1A, the elongation factor responsible for delivering the aa-tRNAs to the ribosomal A-site (Roll-Mecak *et al.*, 2004). The availability of the ternary complex can have profound effects on global translation rates and is subject to regulation, primarily through eIF2α phosphorylation, as discussed in section 1.3.2.

Formation of 43S Pre-Initiation Complex

The ternary complex binds to the 40S ribosomal subunit along with large (~800kDa) multisubunit factor eIF3, and two small initiation factors, eIF1 and eIF1A. These three eukaryotic initiation factors are probably already associated with the 40S ribosome. Experiments *in-vitro* have identified eIF3, eIF1 and eIF1A to be required for stable quantitative binding of the TC to the 40S ribosome, with eIF3 appearing to stabilise the binding of eIF1 and eIF1A (Chaudhuri *et al.*, 1999; Majumdar *et al.*, 2003). This complex is referred to as the 43S pre-initiation complex (PIC). The GAP eIF5 may also bind to the PIC prior to mRNA recruitment as an interaction has been demonstrated between mammalian eIF5 and the p42 subunit of eIF3 (Bandyopadhyay and Maitra, 1999). This interaction has also been documented in yeast where eIF3, eIF1, eIF2 and eIF5 can associate in the absence of ribosomes in what is termed a multifactor complex (MFC), suggestive of a difference in the mechanism of PIC assembly between yeast and mammals (Valasek *et al.*, 2004).

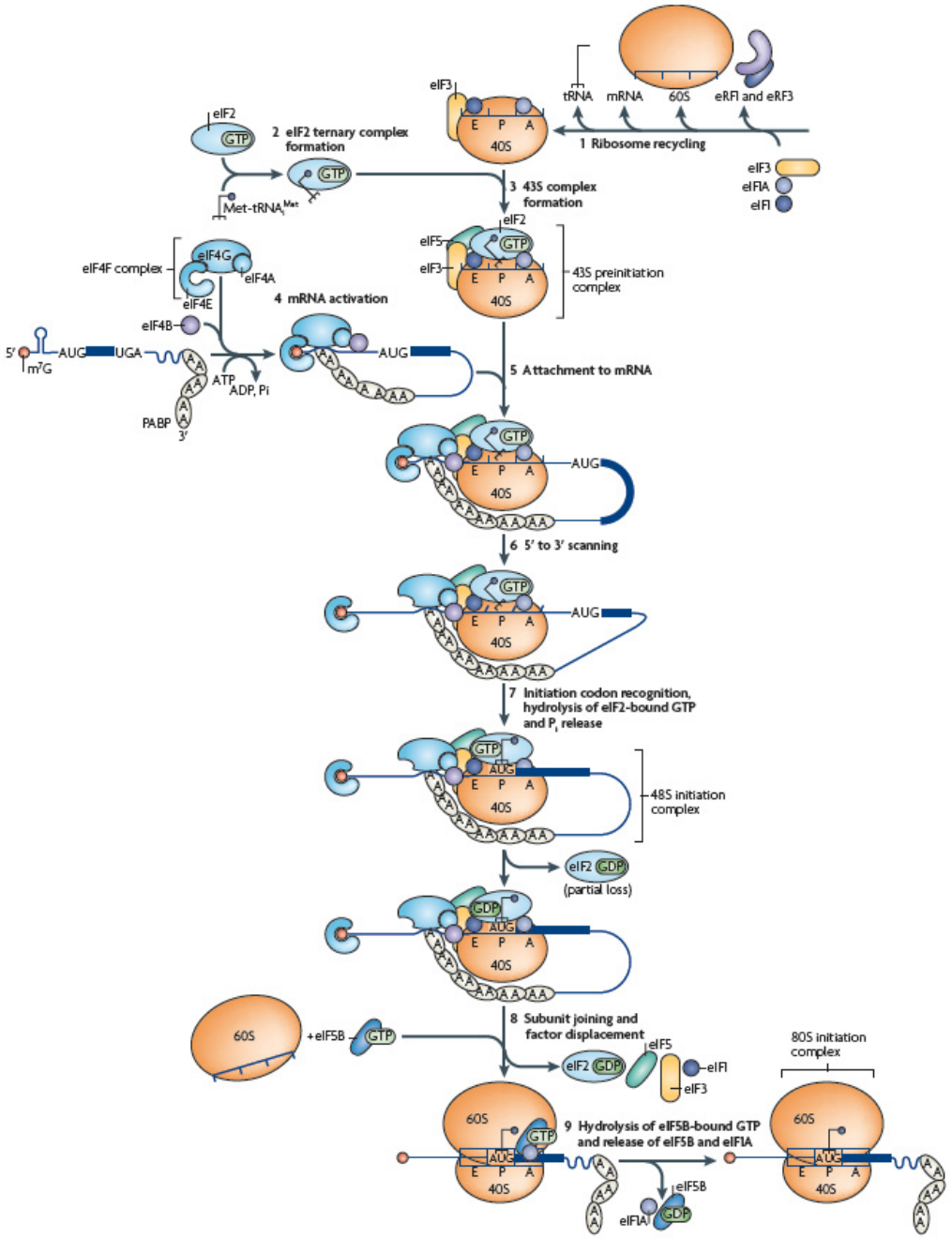

Figure 1.2 Translation initiation. The 40S subunit along with eIF1, eIF1A and eIF3 binds the ternary complex consisting of eIF2-GTP, met-tRNA$_i$ and eIF5 to form the 43S pre-initiation complex (PIC). This binds to the mRNA cap structure via an interaction between eIF3 and eIF4G which is a component of the eIF4F cap binding complex that also contains the cap-binding protein eIF4E and the helicase eIF4A. The PIC scans the 5'-UTR in a process involving eIF1, eIF1A, and eIF4A with its cofactor eIF4B until it reaches an initiation codon. The PIC then binds the mRNA to form a 48S complex, eIF2-GTP is hydrolysed by eIF5 and released, and eIF5B-GTP facilitates binding of the 60S subunit. 60S binding triggers release of initiation factors and eIF5B-GTP is hydrolysed and released from the ribosome which is now competent to begin elongation. Reproduced from Jackson *et al*. 2010.

Binding of the 43S Pre-Initiation Complex to mRNA

The PIC is recruited to the mRNA to form the 48S complex via an interaction with the heterotrimeric eIF4F complex which binds to the 7-methylguanosine cap (m^7GpppN, where N is any nucleotide) structure found at the extreme 5'-end of all nuclear transcribed eukaryotic mRNAs (Shatkin, 1985). The eIF4F complex consists of eIF4E which contains cap binding activity (Sonenberg *et al.*, 1978), eIF4G which is a large (~200kDa) scaffolding protein that mediates a number of protein-protein interactions and interacts directly with eIF4E, and the ATP-dependent DEAD-box RNA helicase eIF4A (Pestova *et al.*, 2001). One purpose of the eIF4F complex appears to be the recruitment of the PIC to the 5'-UTR of mRNA via a direct interaction between eIF4G and the eIF3 subunit eIF3e (LeFebvre *et al.*, 2006). The factors eIF1 and eIF1A also facilitate binding to the mRNA by holding the ribosomal mRNA entry channel latch in an 'open' conformation (Passmore *et al.*, 2007).

The eIF4F complex is fundamental to the initiation of cap-dependent translation (Pestova and Kolupaeva, 2002; Shatkin, 1985) and central to this is the binding of eIF4E to the m^7GpppN cap (Sonenberg *et al.*, 1980). The interaction between eIF4E/eIF4G has been demonstrated to markedly stimulate the binding of eIF4E to the cap and promote ribosome loading in eukaryotes (Friedland *et al.*, 2005; Gross *et al.*, 2003; Haghighat and Sonenberg, 1997; von Der Haar *et al.*, 2000), possibly through conformational changes that clamp eIF4E onto the cap (Volpon *et al.*, 2006). This interaction has functional consequences, with deletion or mutation of eIF4G binding residues within eIF4E resulting in reduced size of actively translating polysomes (mRNAs containing multiple ribosomes) as determined by sucrose gradient centrifugation (Gross *et al.*, 2003; Ptushkina *et al.*, 1998). In addition, an interaction between eIF4G and the polyadenylate-binding protein (PABP1) which binds the poly(A) tails of eukaryotic mRNAs has also been shown to increase the affinity of eIF4E for the cap (see figure 1.12) (Borman *et al.*, 2000; von Der Haar *et al.*, 2000). While the eIF4F complex promotes recruitment of the PIC through the eIF4G/eIF3 interaction, eIF3 may stabilise the interaction through binding to other initiation factors located at the 5'-UTR of mRNAs, including eukaryotic initiation factor 4B and PABP-interacting protein-1 (PAIP-1) (Martineau *et al.*, 2008; Methot

et al., 1996). Stable binding of the PIC is also thought to require the helicase activity of eIF4A to unwind mRNA secondary structure in cap-proximal positions, thereby preparing a 'landing platform' for the PIC (Pestova *et al.*, 2001). Thus, it appears that many interactions may contribute to the stable binding of the PIC to the mRNA cap structure.

Scanning of the 43S Complex

Once the PIC has bound to the extreme 5' end of the mRNA, the complex must move through the 5'-UTR in a poorly defined process termed scanning. The initiation factors eIF1 and eIF1A are thought to promote scanning by maintaining the 40S subunit in a scanning competent 'open' conformation (Pestova and Kolupaeva, 2002). Although PICs are capable of binding and scanning through unstructured 5'-UTRs in the absence of eIF4F (Pestova and Kolupaeva, 2002; Sonenberg *et al.*, 1982), most 5'-UTRs contain secondary structure that requires the mRNA unwinding activity of eIF4F. It is thought that eIF4A is responsible for this helicase activity, as dominant negative mutants of eIF4A confer sensitivity to mRNAs with structured 5'-UTRs (Svitkin *et al.*, 2001b). The mechanism by which eIF4A, which is an intrinsically poor helicase, promotes unwinding of mRNA secondary structure is poorly understood but is known to be stimulated by the cofactors eIF4B and eIF4H, possibly by increasing the affinity of eIF4A for RNA or ATP or by stabilising conformational changes within eIF4A during ATP hydrolysis (Marintchev *et al.*, 2009; Richter *et al.*, 1999). eIF4G also stimulates eIF4A activity through a direct interaction (Imataka and Sonenberg, 1997) although the mechanism behind this stimulatory activity is unclear and structural studies that model the interaction appear to differ in their conclusions (Oberer *et al.*, 2005; Schutz *et al.*, 2008). One model suggests a mechanism whereby components of the eIF4F complex and eIF4B/4H remain attached to the cap structure, with the 5'-UTR looping out during scanning. In this model eIF4B/4H prevent backwards movement of the ribosome during eIF4A-ADP to eIF4A-ATP recycling, and promote a 5' to 3' unidirectional translocation (Spirin, 2009). However, it is unclear how this model would allow more than one PIC to scan at a time. It has also been postulated that eIF4A may be

present on the leading edge of the PIC where its helicase activity would be utilised (Marintchev *et al.*, 2009; Spirin, 2009).

Initiation Codon Recognition

The PIC scans until it encounters an initiation codon (or start codon). Initiation codons are normally the first AUG codon the scanning ribosomal subunit encounters in a favourable context. This context is referred to as the Kozak consensus sequence and is annotated GCC(A/G)CCAUGG, with a purine at position -3 (relative to the adenine at position +1 in the initiation codon) and a guanine at position +4 (Kozak, 1987a) being the main determinants. Initiation codon recognition, GTP hydrolysis, and subsequent commitment to the elongation phase of translation requires the coordinated activities of a number of initiation factors, of which eIF1 and eIF1A appear to be the key moderators (Pestova *et al.*, 1998a). Together, these two factors appear to hold the PIC in an open scanning 'competent' form (Passmore *et al.*, 2007). During scanning, eIF1 inhibits the GAP activity of eIF5 (Unbehaun *et al.*, 2004) preventing premature hydrolysis of eIF2-GTP, and also has a role in rejecting incorrectly assembled initiation complexes at non-AUG codons (Pestova and Kolupaeva, 2002). Upon correct initiation codon/anticodon base-pairing the PIC undergoes conformational rearrangements that tighten its interaction with eIF1A (Maag *et al.*, 2006). This results in the withdrawal of an unstructured C-terminal tail of eIF1A from the ribosomal P-site, allowing the Met-tRNA$_i$ to fully enter (Saini *et al.*, 2010), and also facilitates the displacement of eIF1 (Maag *et al.*, 2005). eIF1A then contacts eIF5 (possibly linked to the movement of the C-terminal tail out of the P-site) and this interaction is thought to transform the PIC from an open form to a closed scanning 'incompetent' form that locks the PIC onto the mRNA (Maag *et al.*, 2006). The expulsion of eIF1 relieves the repression of eIF5 allowing the hydrolysis of eIF2-GTP, possibly by repositioning eIF5 relative to eIF2's GTPase active site (Nanda *et al.*, 2009), leading to the release of eIF2-GDP and inorganic phosphate (P_i), and commitment of the ribosomes to the initiation codon.

60S Ribosome Subunit Joining and Initiation Factor Release

Following initiation codon recognition, the 60S ribosomal subunit must bind to form a translationally competent 80S ribosome. This is mediated via initiation factor release facilitated by eIF1A and eIF5B-GTP. eIF5B is a ribosome dependent GTPase that promotes 60S subunit joining (Pestova *et al.*, 2000) but interestingly the GTPase activity of eIF5B is not necessary for subunit joining but rather supports its dissociation from the 60S subunit to allow the formation of a functional 80S ribosome. eIF1A interacts with eIF5B, and the hydrolytic activity of eIF5B is greatly stimulated in the presence of eIF1A (Acker *et al.*, 2006). This is thought to provide a checkpoint for correct complex assembly. A further factor, eIF6, binds the 60S subunit. eIF6 interacts with receptor for activated C kinase (RACK1) which binds the 40S subunit and interacts with protein kinase C (PKC). Phosphorylation of eIF6 via PKC results in its release from the 60S which allows joining of the two ribosomal subunits (Ceci *et al.*, 2003). The involvement of PKC potentially adds a regulatory level to subunit joining, although the recapitulation of translation initiation *in-vitro* in the absence of eIF6 (Pestova *et al.*, 1998a) suggests it may not be absolutely required. The 60S subunit joining event is thought to be responsible for the dissociation of the remaining initiation factors (Unbehaun *et al.*, 2004). The 80S ribosome is now competent to begin elongation.

1.2.3 Translation Elongation

Following the formation of a translationally competent 80S ribosome at the mRNA initiation codon, the elongation phase of translation begins and the nascent peptide chain is synthesised. This step of translation requires ancillary protein factors and these proteins are highly conserved between prokaryotes and eukaryotes (reviewed in Noble and Song, 2008). While the bacterial ribosome is much smaller than that of eukaryotes, functionally it is similar to those found in higher organisms, explaining the conservation of elongation factors (reviewed in Taylor *et al.*, 2007a). As a result, the deduction of the structure of the eukaryotic ribosome has been largely based on structural studies of its bacterial counterpart.

aa-tRNA Recruitment and Peptide Bond Formation

The eukaryotic elongation factor eEF1 is a GTPase that in metazoans consists of 4 subunits, eEF1A, eEF1Bα, eEF1Bβ, and eEF1Bγ. eEF1A binds and delivers aa-tRNA to the ribosomal A-site. Correct codon/anticodon pairing between the mRNA and the tRNA anticodon stem loop results in a tightening of domains in the ribosomal small subunit (SSU) around the tRNA (Ogle *et al.*, 2003), and leads to GTP hydrolysis of the eEF1A-GTP/aa-tRNA ternary complex. This is stimulated by the GAC of the ribosomal large subunit and promotes dissociation of eEF1A-GDP from the ribosome. Recycling of GDP for GTP is stimulated by the eEF1Bα, β, and γ subunits (Taylor *et al.*, 2007a). The LSU then rapidly catalyses the formation of a peptide bond between the amino acid moieties of the tRNAs in the A- and P-sites of the decoding centre in the SSU.

Translocation of the mRNA

To add to the growing peptide chain, the mRNA must translocate through the SSU mRNA binding channel to allow decoding of subsequent codons. This is regulated by the action of the GTPase eEF2. Upon binding to the ribosome eEF2-GTP undergoes conformational changes that result in 'ratcheting' of the SSU relative to the LSU causing partial but not complete movement of the mRNA/tRNA and decoding centre of the SSU in the direction of the translocation. A domain of eEF2-GTP then enters the A-site of the SSU, and the interactions between the mRNA/tRNA complex and the decoding centre of the SSU are severed following eEF2-GTP hydrolysis. This results in complete translocation by a movement of one codon (Taylor *et al.*, 2007b). The free tRNA in the E-site is ejected and replaced by the P-site tRNA, and the peptidyl-tRNA in the A-site moves to the P-site, leaving behind a vacant A-site, ready to accept the next aa-tRNA. The severing of the connections between the SSU and the mRNA/tRNA complex allow the SSU to back-ratchet to its original position.

1.2.4 Translation Termination and Ribosome Recycling

The elongation cycle may be repeated hundreds of times for an average protein and is terminated upon recognition of a canonical stop codon (UAA, UGA, UAG). As with the translation elongation step, termination requires few factors but is relatively poorly understood. The current model for termination involves eukaryotic release factor 1 (eRF1), which is thought to recognise all three stop codons (Konecki *et al.*, 1977) and acts as a functional mimic of a tRNA. Binding of eRF1 catalyses the hydrolysis of the ester bond linking the peptide chain to the P-site tRNA, but the mechanism behind this hydrolysis event remain obscure, although the peptidyl transferase centre of the ribosome has been hypothesised to play a role.

A second termination factor, the GTPase eRF3, is also present in eukaryotes. Interestingly, eRF3-GTP contains structural similarities to the elongation factor eEF1A, and when bound to eRF1 the complex strongly resembles that of the eEF1A-GTP/aa-tRNA complex (Cheng *et al.*, 2009). Thus, it has been proposed that eRF3 helps to deliver and correctly position eRF1 to the ribosomal A-site, much like eEF1A delivers cognate aa-tRNAs (Cheng *et al.*, 2009). Hydrolysis of eIF3-GTP to eIF3-GDP has been suggested to facilitate the correct positioning of eRF1 within the ribosome, allowing hydrolysis of peptidyl tRNA by eRF1 (Alkalaeva *et al.*, 2006). Both the GTPase activity of eRF3 and the hydrolytic activity of eRF1 are stimulated when the two factors are present in a complex that also contains the ribosome (Frolova *et al.*, 1996).

Dissociation of Ribosomes into 40S and 60S

The dissociation of post-termination ribosomes involves separation of the 40S and 60S subunits, followed by release of the deaceytlated tRNA from the P-site of the 40S and subsequent ejection of the mRNA. Although the factors eIF3, eIF1 and eIF1A have been demonstrated to be capable of promoting ribosomal dissociation, it was deemed unlikely that they were the main effectors of subunit separation as they

were effective only in a very narrow window of Mg^{2+} concentrations. Recently the involvement of ABCE1, an ATP-binding cassette protein, has been demonstrated (Pisarev *et al.*, 2010). ABCE1 only associates with post-termination ribosomes bound to eRF1, suggesting that eRF1 induces conformational rearrangements in the ribosome that facilitate ABCE1 binding (Pisarev *et al.*, 2010). ABCE1 appears to act as a molecular lever, extending from a closed to an open conformation in response to ATP hydrolysis and this extension is thought to drive the separation of the two ribosomal subunits (Pisarev *et al.*, 2010). Following subunit dissociation, P-site deaceytlated tRNA is released from the 40S by eIF1. The eIF3 subunit eIF3j which is positioned in the decoding centre, decreases the affinity of mRNA for the 40S subunit, resulting in its expulsion from the mRNA binding cleft (Fraser *et al.*, 2007). This now leaves the 40S subunit with eIF3, eIF1 and eIF1A bound, free to recruit a ternary complex and begin another round of initiation.

1.2.5 Cap-Independent Translation

It is estimated that approximately 10-15% of eukaryotic cellular mRNAs have the capability to initiate translation via cap-independent translation pathways (Spriggs *et al.*, 2008). An alternative method of initiation was first identified in the picornaviruses, where the 5'-UTRs of poliovirus (PV) and encephalomyocarditis virus (EMCV) mRNAs were demonstrated to be capable of promoting translation (Jang *et al.*, 1988; Pelletier *et al.*, 1988). These sites were predicted to recruit the ribosome directly in a cap-independent manner via mRNA structural elements which were subsequently termed internal ribosome entry sites (IRES's). While viral IRES function is independent of the cap, many utilise components of the canonical initiation factor pathway, such as foot and mouth disease virus (FMDV), while others seem to have no requirement for eIFs such as hepatitis C virus (HCV) and cricket paralysis virus (CrPV) (Pacheco *et al.*, 2008; Pestova and Hellen, 2003; Pestova *et al.*, 1998b).

In some cases viral IRES's appear to require endogenous cellular factors for their activity, termed IRES *trans*-acting factors (ITAF's). Many have been identified to date, including polypyrimidine tract binding protein (PTB), upstream of N-*ras* (UNR), La autoantigen, and a number of heterogeneous nuclear ribonucleoproteins (hnRNPs) (Costa-Mattioli *et al.*, 2004; Hunt *et al.*, 1999; Kaminski *et al.*, 1995). The mechanism by which many ITAFs infer translational activity upon viral IRES's is not known but is often linked to remodelling of secondary or tertiary structures of IRES's and/or recruitment of ribosomes (reviewed in Spriggs *et al.*, 2005). In some cases picornaviruses and retroviruses employ viral proteases to cleave initiation factors, often eIF4G and PABP (Gradi *et al.*, 1998b; Kerekatte *et al.*, 1999), which has the effect of down regulating host cell protein synthesis while promoting expression of viral IRES containing transcripts, sometimes through utilisation of the cleaved initiation factor fragments (Belsham *et al.*, 2000; Castello *et al.*, 2009; Gradi *et al.*, 1998b; Kerekatte *et al.*, 1999; Kuyumcu-Martinez *et al.*, 2004; Ventoso *et al.*, 2001).

The first human cellular IRES to be identified was that of the immunoglobulin heavy-chain binding protein (BiP) mRNA (Macejak and Sarnow, 1991), and there are now several dozen identified cellular IRES's (Elroy-Stein and Merrick, 2007). These IRES's appear to be predominantly active during periods when cap-dependent translation is severely compromised, such as apoptosis, cell stress, mitosis and viral infection (Marash and Kimchi, 2005; Qin and Sarnow, 2004; Van Eden *et al.*, 2004). Cellular IRES's also utilise ITAF's, although variation between the primary sequences and secondary structure of different IRES's make binding site predictions difficult. Polypyrimidine tracts are thought to be bound by PTB which has been demonstrated to promote translation of a number of cellular IRES's (Dhar *et al.*, 2009; Grover *et al.*, 2008).

1.3 Control of Translation

1.3.1 Global Versus Specific Control

The accurate spatial, temporal, and magnitudinal expression of proteins is of paramount importance. Control of translation can be global, affecting most cellular mRNAs, often through the modification of canonical translation factors. Global control mechanisms are often utilised during cell stress events, and the modification of translation factors during these occasions is frequently phosphorylation (Hershey, 1990). In contrast specific control only targets individual or subsets of mRNAs, through specific mRNA *cis*-acting elements frequently found in 5' and 3'-UTRs, or via modification of the *trans*-acting factors that bind these elements (reviewed in Gray and Wickens, 1998).

1.3.2 Global Control of Translation

Phosphorylation of eIF2α

The translation initiation factor eIF2 is responsible for delivering the Met-tRNA$_i$ to the 40S ribosomal subunit. Following initiation codon recognition, eIF2-GTP is hydrolysed and released from the 40S as eIF2-GDP. The GDP moiety is then exchanged for GTP by the action of the GEF eIF2B, recycling eIF2 for further rounds of translation initiation. This event appears to be regulated in part through the activity of eIF5, which stabilises the binding of GDP to eIF2, therefore acting as a GDP dissociation inhibitor (Jennings and Pavitt). Phosphorylation of serine-51 on the eIF2α subunit results in the formation of a stable complex between eIF2 and eIF2B preventing exchange of GDP for GTP (Kimball *et al.*, 1998). This stable complex depletes the available pool of eIF2B, and therefore the levels of eIF2-GTP, inhibiting translation at an early stage of initiation. eIF2B is limiting, thus phosphorylation of small amounts of eIF2 is sufficient to block protein synthesis (Dever, 2002). In eukaryotes four kinases have been identified that phosphorylate serine-51 of eIF2α in response to multiple cellular stresses. Haem-regulated inhibitor kinase (HRI)

phosphorylates eIF2α in response to oxidative stress (Lu *et al.*, 2001), protein kinase R (PKR) in response to dsRNA frequently associated with viral infection (Vattem *et al.*, 2001), PKR-like endoplasmic reticulum kinase (PERK) with ER stress, such as the unfolded protein response (UPR) (Harding *et al.*, 2000), and general control non-repressed 2 (GCN2) in reaction to amino acid starvation and the presence of uncharged tRNAs (Dever *et al.*, 1992). Paradoxically some mRNAs are upregulated in response to eIF2α phosphorylation such as the general control non-repressed 4 (GCN4) mRNA in yeast and the mammalian transcription factors ATF4 and ATF5, by a mechanism that will be discussed in section 1.3.5.

Regulation by eIF4E-Binding Proteins (4E-BPs)

Another commonly employed mechanism to regulate global cap-dependent translation is the modification of eIF4F activity. The main cellular effectors of this mechanism of translational inhibition are the 4E-binding proteins (4E-BPs). In humans, there are three 4E-binding proteins, 4E-BP1, 4E-BP2 and 4E-BP3 (Pause *et al.*, 1994; Poulin *et al.*, 1998), that associate directly with eIF4E. This association is governed by the level of phosphorylation of 4E-BP, with hyperphosphorylation causing dissociation and hypophosphorylation resulting in an interaction (Gingras *et al.*, 1998; Pause *et al.*, 1994). 4E-BPs are thought to act as molecular mimics of eIF4G, competing for binding to eIF4E (Haghighat *et al.*, 1995) as they contain the same eIF4E binding motif (Marcotrigiano *et al.*, 1999). The binding of these two proteins to eIF4E is mutually exclusive, therefore 4E-BP disrupts the formation of an active eIF4F complex. The phosphorylation status of 4E-BP is regulated by a number of cellular cues, including cell stress (Patel *et al.*, 2002), and the availability of hormones, cytokines and growth factors, such as insulin (Gingras *et al.*, 2001). The main pathway responsible for phosphorylation of 4E-BPs appears to be the murine target of rapamycin (mTOR) pathway (Burnett *et al.*, 1998; Gingras *et al.*, 1998), therefore under conditions favourable for cell growth 4E-BP is hyperphosphorylated via mTOR and does not associate with eIF4E, allowing cap-dependent translation to proceed.

Modification of eIF4E

Mammalian eIF4E is phosphorylated on serine-209 by Mnk1 and Mnk2 in response to mitogen-activated protein kinase (MAPK) signalling (Joshi *et al.*, 1995; Pyronnet *et al.*, 1999; Scheper *et al.*, 2001). The purpose of this phosphorylation is now controversial (reviewed in Scheper and Proud, 2002). eIF4E has been described as an oncogene (reviewed in Zimmer *et al.*, 2000) and phosphorylation of serine-209 is linked to its oncogenic activity and role in cellular proliferation (Wendel *et al.*, 2007). In addition, eIF4E phosphorylation is also elevated during conditions where cellular protein synthesis is stimulated (Flynn and Proud, 1996) implying that the translational activity and phosphorylation of eIF4E may be linked. Conversely, Mnk1/2 double knockout mice developed normally, in the absence of any detectable eIF4E phosphorylation (Ueda *et al.*, 2004), although phosphorylation has also been proposed to reduce eIF4E affinity for the cap by up to 2.5-fold (Scheper *et al.*, 2002).

eIF4G Decoys

The large scaffolding protein eIF4G plays a central role in translation initiation. In humans there are three family members, eIF4GI, eIF4GII, and p97/death-associated protein 5 (DAP5). eIF4GI and eIF4GII share approximately 46% identity at the protein level and appear to be functionally equivalent, as both stimulate translation and interact with eIF4E, eIF4A, and eIF3 at least *in vitro* (Gradi *et al.*, 1998a). p97/DAP5 shares homology with approximately two-thirds of the C-terminus of eIF4GI and can interact with eIF4A and eIF3, but lacks the N-terminal region containing the eIF4E and PABP binding sites (Imataka *et al.*, 1997). p97 was shown to be inhibitory to cap-dependent and cap-independent translation, possibly by forming inactive translation complexes excluding eIF4E (Imataka *et al.*, 1997) or by titrating initiation factors away from eIF4G. More recently, a caspase cleavage fragment of p97 was proposed to stimulate cap-independent translation during apoptosis, including its own translation through a 5'-UTR IRES element within its mRNA (Henis-Korenblit *et al.*, 2000), as well as cap-independent translation during

the cell-cycle (Marash *et al.*, 2008), when cap-dependent translation is downregulated.

1.3.3 Specific Control of Translation

Translational control at the level of individual mRNAs or subsets of mRNAs is usually conferred by *cis*-acting control elements within the 5' and 3'-UTRs, and the activity of *trans*-acting factors that bind these elements (reviewed in Gray and Wickens, 1998). These regulatory elements are depicted in figure 1.3. Proto-oncogenes, transcription factors and growth factors frequently have long 5'-UTRs containing multiple control elements, attesting to their requirement for stringent regulation. Control elements within 3'-UTRs often directly influence the stability, localisation and translation of mRNAs and in some cases interact with 5'-UTR bound factors to achieve this regulation (Wilkie *et al.*, 2003).

1.3.4 Primary Determinants of Translational Efficiency

m^7GpppN Cap

The 5' m^7GpppN (m^7G) cap structure is a methylated guanosine nucleotide, at the extreme 5' terminus of mRNAs with an unusual 5' to 5' triphosphate linkage. The cap must be methylated to promote translation as removal of the methyl group results in a loss of translational activity *in-vitro* (Muthukrishnan *et al.*, 1975). Cap-methylation may be subject to differential regulation as two transcription factors, c-Myc and E2F1, have been demonstrated to specifically induce the cap-methylation of their target gene transcripts (Cole and Cowling, 2009), although the mechanism by which this occurs is unknown. Moreover, differential cap-methylation appears to occur for certain transcripts such as cyclin D1 which has been found to be largely unmethylated in mammary epithelial cells (Cowling, 2010). Following overexpression of the cap-methylation effector protein RNA-guanine-7-methyltransferase (RNMT), the cyclin D1 transcript is methylated on its cap and

cyclin D1 protein expression increases (Cowling, 2010). Interestingly overexpression of RNMT can lead to cellular transformation (Cowling, 2010).

The Poly(A) Tail

The poly(A) tail is an almost universal feature of eukaryotic mRNAs located at the extreme 3' terminus of transcripts and has fundamental roles in mRNA translation and stability (Gallie, 1991; Munroe and Jacobson, 1990). The function of the poly(A) tail in translation is mediated by PABP proteins, the subject of this thesis (see section 1.4). Following transcription a 200-250 nucleotide poly(A) tail is added to pre-mRNAs within the nucleus in a process that involves a multifactorial complex of cleavage and polyadenylation factors including poly(A) polymerase (PAP) (reviewed in Millevoi and Vagner, 2010). Following nuclear export the poly(A) tail is progressively removed eventually signalling the mRNA for degradation (Sheiness *et al.*, 1975), However not all mRNAs with short poly(A) tails are degraded, and indeed *cis*-elements within the 3'-UTR of specific transcripts can direct their cytoplasmic polyadenylation (Richter, 1999). Loss of the poly(A) tail is often associated with translational silencing, while polyadenylation results in translational activation, and this has been demonstrated in a number of biological models (Gray and Wickens, 1998). For example, tissue-type plasminogen activator (tPA) mRNA is extensively deadenylated and translationally repressed upon entry into the cytoplasm in mouse primary oocytes, and during meiotic maturation is polyadenylated and translationally activated (Huarte *et al.*, 1992). Other oocyte mRNAs such as c-mos, β-actin, and cyclin B1 are also regulated in this manner (Mendez and Richter, 2001).

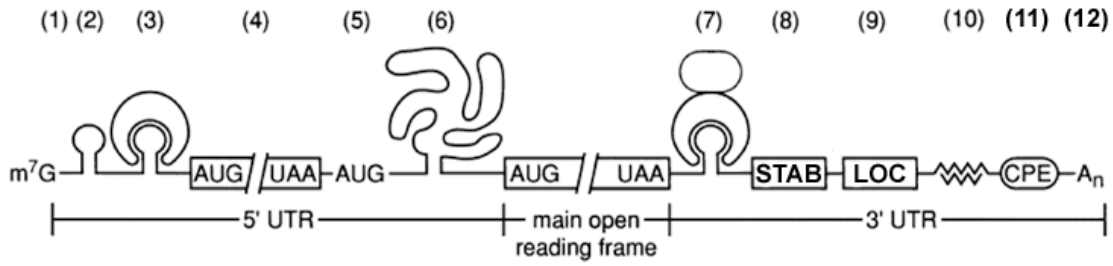

Figure 1.3 Translation control elements. mRNAs can have multiple regulatory elements. (1) m^7GpppN cap structure, (2) secondary structure, (3) 5'-UTR protein binding sites, (4) upstream ORFs, (5) upstream AUGs, (6) IRES's, (7) 3'-UTR protein binding sites, (8) stability elements, (9) localisation elements, (10) microRNA complementary sites, (11) cytoplasmic polyadenylation elements, (12) polyadenylate tail. Reproduced from Gray and Wickens, 1998.

The *cis*-elements responsible for directing the reversible mRNA polyadenylation/ deadenylation cycles have been identified in a number of higher organisms but studied most extensively in *Xenopus laevis* oocytes. Cytoplasmic polyadenylation involves two sequence elements within the 3'-UTR; the hexanucleotide AAUAAA which is bound by the cleavage and polyadenylation specificity factor (CPSF) and a second sequence element of which the best characterised example is the cytoplasmic polyadenylation element (CPE) (Mendez and Richter, 2001). CPEs are uridine-rich with a general consensus of $U_5A_{1\text{-}2}U$. The number and position of CPEs relative to the hexanucleotide can vary, and may affect the timing and/or extent of polyadenylation (Mendez and Richter, 2001). The CPE is bound by a factor called the CPE-binding protein (CPEB) (Hake and Richter, 1994; Stebbins-Boaz *et al.*, 1996).

The polyadenylation of CPE-containing mRNAs is controlled by the opposing activities of a poly(A) polymerase Gld-2 and poly(A) ribonuclease (PARN) which both reside in a CPEB containing complex that also contains the scaffolding protein symplekin (Richter, 2007). When PARN is more active than Gld-2 mRNAs are maintained with a short poly(A) tail, but following extracellular signalling cues the

kinase Aurora A is activated and phosphorylates CPEB on serine-174 (Sarkissian *et al.*, 2004) resulting in the expulsion of PARN from the complex, enabling Gld-2 to elongate the poly(A) tail (see figure 1.4) (Kim and Richter, 2006). Interestingly, this mechanism of regulation has been suggested to be important in governing synaptic plasticity, a key process underlying learning and memory. Indeed synaptic stimulation has been shown to induce the polyadenylation and subsequent translation of the α subunit of calcium-calmodulin-dependent protein kinase II (αCaMKII) mRNA in the postsynaptic compartment (Richter, 2007).

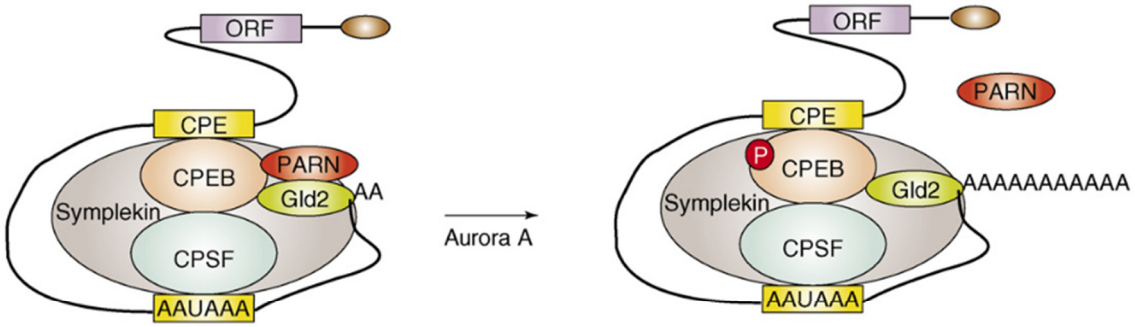

Figure 1.4 Regulation of cytoplasmic polyadenylation. PARN removes the poly(A) tail that Gld-2 is adding. PARN is more active than Gld-2 so the poly(A) tails remain short. Phosphorylation of CPEB by the kinase Aurora A results in the dissociation of PARN from the protein complex, allowing Gld-2 to default polyadenylate the mRNA. Other factors (maskin, eIF4E, eIF4G, and PABP) have been omitted for clarity. Reproduced from Richter. 2007.

1.3.5 5'-UTR Translation Control Elements

Secondary Structure

The scanning model of translation initiation posits that the 40S ribosome traverses the 5'-UTR until an initiation codon is encountered. Secondary structures can be

inhibitory to translation initiation, depending on their stability and position within the 5'-UTR. Using reporter mRNAs, it has been demonstrated that moderately stable stem loops (-30kcal/mol) located in cap-proximal regions can inhibit 43S PIC joining, but stem loops in cap-distal positions require more stable secondary structures (-61kcal/mol) to abrogate the scanning of ribosomal subunits (Kozak, 1989).

The translation of endogenous mRNAs appears to be regulated in this manner. Ornithine decarboxylase (ODC) is a rate limiting enzyme in polyamine biosynthesis. ODC mRNA contains a 160 nucleotide G/C rich region within its 5'-UTR that forms a stable stem-loop structure that inhibits translation (Manzella and Blackshear, 1990). The stem-loop retains its inhibitory function upon inversion suggesting that it is not acting as a platform for the binding of a repressor protein, but rather it is the structure itself that is inhibitory (Grens and Scheffler, 1990). It has been suggested that mRNAs containing extensive secondary structure in their 5'-UTRs are more sensitive to eIF4E activity (Koromilas *et al.*, 1992). This would appear to be true for ODC mRNA, as reporters containing the ODC 5'-UTR are more efficiently translated in a cell line overexpressing eIF4E (Shantz *et al.*, 1996).

Although secondary structure can be inhibitory, the utilisation of initiation codons in poor sequence context can be stimulated by the presence of secondary structure *in vitro*. Positioning of a stem-loop structure 14 nucleotides downstream of non-AUG initiation codons (GUG or UUG) in poor sequence context, can increase initiation at these codons 3-fold, presumably by stalling the ribosome, allowing more time for initiation codon recognition (Kozak, 1990).

RNA-Binding Proteins

Sequence elements within mRNA 5'-UTRs are often bound by regulatory protein factors that can have either a negative or positive influence on translation. The best

characterised 5'-UTR binding proteins are the iron regulatory proteins (IRPs) that modulate cellular iron homeostasis. In response to intracellular iron depletion IRP binds to a structural element termed the iron responsive element (IRE) within the 5'-UTR of mRNAs including the iron storage protein ferritin (Gray and Hentze, 1994) strongly inhibiting their translation. The IREs are positioned cap-proximally, and prevent 43S PIC recruitment to the mRNA (Gray and Hentze, 1994). This steric blocking mechanism of repression can be recapitulated with proteins that have no role in translational regulation, such as the viral coat protein MS2 and the splicing factor U1A, when binding sites for these proteins are present in cap-proximal positions within the 5'-UTRs of reporter mRNAs (Stripecke *et al.*, 1994). Positioning of the IRE in a cap-distal location in mammalian cells can also modulate translation efficiency, by sterically affecting ribosomal scanning (Paraskeva *et al.*, 1999), showing that protein-mRNA interactions within 5'-UTRs can affect both ribosome subunit binding and movement, in a position dependent manner.

Upstream Open Reading Frames and Upstream AUGs

Upstream AUGs (uAUGs) and upstream open reading frames (uORFs) are *cis*-acting elements within mRNA 5'-UTRs that generally inhibit the ribosomal selection of the primary ORF initiation codon (reviewed in Morris and Geballe, 2000). uORFs are characterised by an in-frame initiation and termination codon and generally code for very small peptides. On the contrary, uAUGs do not contain in-frame termination codons prior to the initiation codon of the primary ORF. Up to two-thirds of proto-oncogenes as well as a number of growth factors and cytokines are thought to contain uAUGs/uORFs, highlighting the importance of this mechanism of regulation (Kozak, 1991; Morris and Geballe, 2000).

In uORF and uAUG containing transcripts, translation of the main ORF has to occur by one of two mechanisms; firstly 'leaky scanning', whereupon the ribosome ignores the uAUG (a strong determinant being the strength/efficiency of the AUG context sequence), or secondly, termination of translation of the uORF and re-initiation at the

main AUG. The process of re-initiation is poorly understood but thought to involve recharging of the ribosome with initiation factors (Kozak, 1999). This is supported by evidence that increasing the intercistronic spacing between the uORF termination codon and the subsequent AUG eliminates the inhibitory effects of the uORF by allowing more time for the ribosome to reacquire necessary factors (Kozak, 1987b).

Much of our understanding of uORF function is a result of studies on the yeast GCN4 mRNA which contains four uORFs regulated in response to amino acid starvation. Phophorylation of eIF2α induced by high levels of uncharged tRNAs results in limited ternary complex availability, perturbing the re-initiation activity of the ribosomes and thus skipping of the highly inhibitory second, third and fourth uORFs and promoting initiation at the main AUG (Dever *et al.*, 1992). Other examples are BACE-1 mRNA, involved in amyloid β protein production (a hallmark of Alzheimers) which contains six inhibitory uAUGs (De Pietri Tonelli *et al.*, 2004), and the potent oncogene MDM2 which utilises alternative promoters to express an mRNA with a long 5'-UTR containing a uORF, or a short 5'-UTR that lacks the uORF and is efficiently translated (Brown *et al.*, 1999).

Increasingly, 'sequence specific' uORFs are being classified where the peptide encoded by the uORF participates directly in inhibition of a downstream ORF, such as S-adenosylmethionine decarboxylase mRNA (AdoMetDC) (Hill and Morris, 1993) and arg-2 mRNA (Wang and Sachs, 1997). AdoMetDC regulates the biosynthesis of polyamines, and contains a short uORF coding for the peptide sequence MAGDIS. Mutational analysis showed that the sequence of the uORF was important for conferring translational inhibition (Hill and Morris, 1993). Mechanisms by which these peptides interfere with translation of downstream ORFs is unclear but is thought to involve ribosomal stalling by impeding termination (Morris and Geballe, 2000). Consistent with this, in the presence of high arginine concentrations, toeprinting analysis identified stalled ribosomes within the uORF of arg-2 transcripts (Wang and Sachs, 1997).

1.3.6 3'-UTR Translational Control Elements

The 3'-UTRs of messages frequently contain *cis*-elements that are bound by multifactor protein complexes. Protein complexes associated with mRNA 3'-UTRs can affect the translation and/or stability of messages in a positive or a negative way, and in some cases these effects are linked to mRNA localization. 3'-UTR mediated regulation is important in cellular processes as diverse as embryonic patterning, differentiation, sex determination, and metabolism (Hentze *et al.*, 2007). Regulation via 3'-UTRs is often intricate and elaborate due to the spatial challenges of regulating translation initiation events at the mRNA 5' terminus (Gray and Wickens, 1998; Wilkie *et al.*, 2003). Many of the dissected mechanisms of 3'-UTR mediated regulation have been established using the genetically tractable fruit fly model *Drosophila melanogaster*, where mRNA specific translational control in oocytes and early embryos is important for axis formation and body patterning.

Regulation of Cap-Binding

In many cases, the mechanisms involved appear to be conserved in mammals such as the regulation of *Drosophila* oskar mRNA by a 4E-BP-like protein, Cup (Haghighat *et al.*, 1995; Nakamura *et al.*, 2004). CPEB is a well characterised example of a translational repressor in *Xenopus* oocytes. In translationally repressed mRNAs with short poly(A) tails CPEB binds to maskin, which in turn interacts with eIF4E. This binding precludes the interaction of eIF4G with eIF4E (Stebbins-Boaz *et al.*, 1999), therefore to promote eIF4F formation and translational activation maskin must be displaced from eIF4E. This is achieved by polyadenylation which facilitates the recruitment of PABP to the new poly(A) tail. PABP in turn binds eIF4G helping it to displace maskin from eIF4E (see figure 1.5) (Richter, 2007). Additionally, a maskin-like protein (neuroguidin) present in the brain, has been demonstrated to bind CPEB and repress translation in a CPE-dependent manner (Jung *et al.*, 2006).

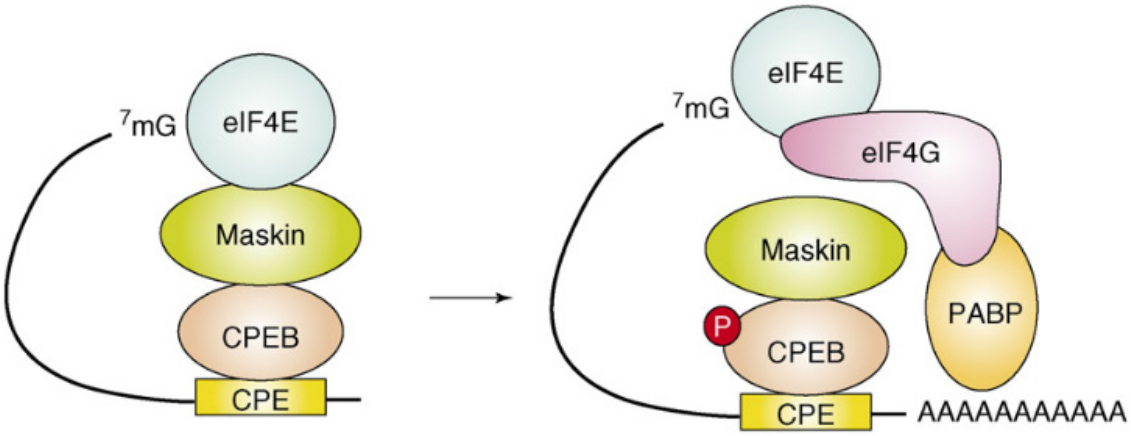

Figure 1.5 Regulation of Cytoplasmic Polyadenylation. Maskin forms a complex with eIF4E, that inhibits eIF4F formation. The newly synthesised poly(A) tail supports PABP recruitment which binds eIF4G and helps dissociate maskin, promoting translation. Other factors (CPSF, Gld-2, PARN, and symplekin) have been omitted for clarity.

Repression of 43S Recruitment

In some cases the expression of certain mRNAs has such deleterious consequences that multiple mechanisms exist to repress their translation. MSL proteins function in X-chromosome dosage compensation in males, and are responsible for recruiting factors important in chromatin remodelling and transcription. Elevated expression of the MSL complex in females is deleterious due to increased transcription from both female X-chromosomes, thus expression of the protein is tightly repressed (Kelley *et al.*, 1997).

In *Drosophila*, expression of male-specific lethal 2 (msl-2) mRNA is regulated in an unusual fashion by the female specific sex-lethal (SXL) protein which binds both the 5' and 3'-UTRs of msl-2 mRNA (Bashaw and Baker, 1997; Kelley *et al.*, 1997), with the binding sites in the 5'-UTR and 3'-UTR repressing translation via different mechanisms (see figure 1.6). Both the 5' and 3'-UTR of msl-2 are necessary for

efficient repression, with mutation of either site conferring a partial loss of inhibition (Bashaw and Baker, 1997).

The current mechanism for 3'-UTR bound SXL postulates that SXL recruits the PABP interacting protein upstream of n-ras (UNR) to the 3'-UTR (Duncan *et al.*, 2006) (Duncan *et al.*, 2009). This SXL-UNR complex inhibits 43S PIC recruitment (Gebauer *et al.*, 2003) possibly by interfering with PABP function, however the effects of SXL appear to be downstream of the eIF4G-PABP interaction and the mechanism awaits definition (Duncan *et al.*, 2009) (see section 1.4.4, The Closed Loop Model).

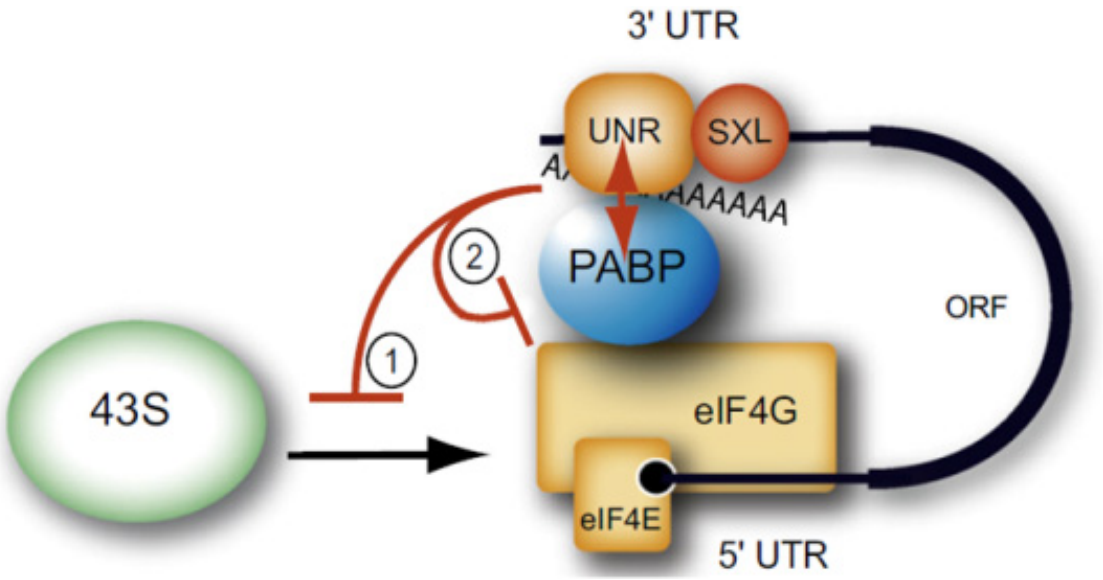

Figure 1.6 3'-UTR mediated repression of msl-2 mRNA translation. SXL recruits UNR to the 3'-UTR of msl-2 mRNA. UNR in turn interacts with PABP (red double-ended arrow) and this interaction does not preclude binding of eIF4E and eIF4G to the mRNA cap. The recruitment of the 43S PIC to the mRNA is inhibited by the repressor complex. PABP therefore acts either as a cofactor of the repressor complex enhancing its repressive function (red inhibitory bar 1), or PABP may be the effector of the repressive mechanism, with the interaction between PABP and UNR interfering with an uncharacterised function of PABP in 43S recruitment (red inhibitory bar 2). Reproduced from Duncan *et al*. 2009.

Inhibition of Scanning

SXL binding sites are found within a 5'-UTR intron of the msl-2 pre-mRNA. The binding of SXL to these intronic sites inhibits splicing by preventing recruitment of the nuclear splicing machinery (Forch *et al.*, 2001). SXL remains associated with these sites following nuclear export resulting in translational repression by a 43S PIC scanning inhibition mechanism (Forch *et al.*, 2001; Gebauer *et al.*, 1998). In males, the absence of SXL protein facilitates splicing of the 5'-UTR intron and efficient translation of msl-2 mRNA. A simple model of steric inhibition of scanning has been ruled out, as binding of a related protein to this site with a similar affinity as SXL failed to repress expression (Beckmann *et al.*, 2005). It has therefore been suggested that SXL modulates secondary structure, or facilitates the formation of a higher order repressive complex (Beckmann *et al.*, 2005). Thus, the 3' and 5'-UTR elements appear to function in a bipartite mechanism initially preventing the recruitment of 43S PIC complexes, with any ribosomal complexes escaping this block subjected to scanning inhibition.

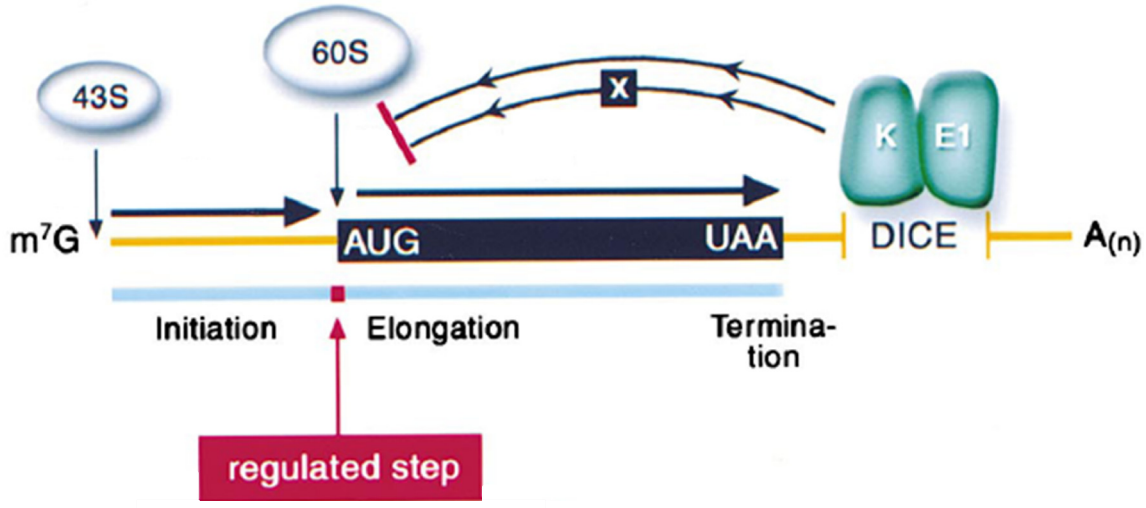

Figure 1.7 Regulation of LOX mRNA translation by DICE elements. hnRNPs K and E1 bind to the DICE element in the LOX 3'-UTR and inhibit 60S joining. Whether the inhibition is direct is unclear and may involve other factors (denoted by the white 'X' in the black box). 43S PIC binding, scanning, and 48S PIC formation all appear to proceed normally. Reproduced from Ostareck *et al*. 2001.

Repression of 60S Joining

The enzyme 15-lipoxygenase (LOX) is involved in the degradation of mitochondria during terminal erythroid differentiation. LOX mRNA is translationally repressed in erythroid precursor cells through heterogeneous nuclear ribonucleoproteins (hnRNPs) K and E1 which bind to CT rich sequence elements within the LOX 3'-UTR called differentiation control elements (DICE) (Ostareck-Lederer *et al.*, 1994; Ostareck *et al.*, 1997). 48S complex formation could be observed, but 80S formation is inhibited suggesting that 60S joining is impeded (see figure 1.7) (Ostareck *et al.*, 2001). This could be due to a direct interference with the ribosomal subunit interacting surfaces, but a DICE containing reporter mRNA was not inhibited when translation was driven by a CrPV IRES (which does not utilize eIFs) in the 5'-UTR suggesting that hnRNPs K and E1/2 are targeting an initiation factor responsible for 60S joining (Ostareck *et al.*, 2001). Interestingly, phosphorylation of a tyrosine residue in the nucleic acid binding region of hnRNPK by the tyrosine kinase c-Src prevents association with DICE, and relieves inhibition of LOX translation, suggesting that upstream signalling may play an important role in establishing repression (Messias *et al.*, 2006).

MicroRNAs

MicroRNAs (miRNAs) are nuclear transcribed short non-coding RNA molecules of approximately 22 nucleotides with a crucial role in post-transcriptional mRNA regulation. Binding of miRNAs to complementary sequences usually within the 3'-UTR of their target mRNAs induces inhibition and/or degradation of these transcripts. Computational approaches to identify miRNA binding sites within cellular mRNAs have estimated that up to 60% of all mammalian transcripts may be regulated in this manner (Friedman *et al.*, 2009). Mature miRNAs are associated with a number of protein factors including GW182 and the endonucleolytic argonaute protein Ago2, in a functional complex called the miRNA-containing RNA-induced silencing complex (miRISC). The level of complementarity between the miRNA and mRNA determines whether the target mRNA will be directed for degradation or translational inhibition with a high or perfect level of

complementarity signalling cleavage (Pillai *et al.*, 2005). The mechanism of translational inhibition remains controversial. Some reports indicate that that miRNAs target translation initiation, possibly by inhibiting eIF4E binding to the cap (Pillai *et al.*, 2005), while other reports suggest that elongation is targeted, causing ribosomal dissociation from the mRNA (Petersen *et al.*, 2006). Furthermore, a small number of miRNAs have been demonstrated to increase translation of reporter mRNAs in response to cell cycle arrest (Vasudevan *et al.*, 2007).

Stability Elements

Control of mRNA stability is an irreversible mechanism by which cells can rapidly modulate protein output. Sequence elements that regulate mRNA stability are frequently located within 3'-UTRs, and can stabilise mRNA, or prompt destabilisation and turnover, often by blocking or recruiting components of the cellular degradation machinery (Barreau *et al.*, 2005). In mammals, bulk mRNA turnover proceeds through a deadenylation-dependent pathway (see figure 1.8) (Garneau *et al.*, 2007). Poly(A) tail removal is a biphasic process requiring the actions of two deadenylases complexes, PAN2-PAN3 and CCR4-NOT (Garneau *et al.*, 2007). PAN2-PAN3 first removes the poly(A) tail to a length of approximately 110 nucleotides, which is then subsequently removed via CCR4-NOT (Yamashita *et al.*, 2005). Another deadenylase, poly(A) ribonuclease (PARN), may also be involved in poly(A) tail removal in eukaryotes, and is involved in default mRNA deadenylation during *Xenopus* oocyte meiotic maturation and early development (Korner *et al.*, 1998). Following deadenylation, the mRNA can be degraded in a 3'-5' manner by a large complex of proteins called the exosome. The decapping scavenger enzyme, DcpS, then hydrolyses the m^7GpppN cap (Liu *et al.*, 2002). Alternatively, following deadenylation the transcript can be degraded in a 5'-3' manner in a process that involves decapping by the enzymes DCP1 and DCP2, followed by degradation of the mRNA body by the exonuclease XRN1 that recognises uncapped 5'-monophosphate mRNAs (Garneau *et al.*, 2007). This process is stimulated by the Lsm1-7 complex that binds the 3' of deadenylated

messages and promotes dissociation of the cap complex (eIF4E/eIF4G) and recruitment of DCP1 and DCP2 (Tharun and Parker, 2001).

Adenosine and uridine-rich elements (AREs) are the most extensively studied 3'-UTR *cis*-acting sequences affecting mRNA stability. Approximately 5-8% of human protein coding genes are predicted to code for ARE containing transcripts, and these frequently represent mRNAs encoding oncoproteins, transcription factors and cytokines (Barreau *et al.*, 2005; Peng *et al.*, 1998). ARE sequences vary dramatically between mRNAs but appear to be based loosely on the presence of an AUUUA pentamer (Barreau *et al.*, 2005). The activity of AREs in modulating mRNA stability is driven by the binding of ARE-binding proteins (ARE-BPs) of which a multitude have been identified, including TTP, AUF1, and KSRP (Garneau *et al.*, 2007). ARE-BPs destabilise in a deadenylation-dependent manner, often by directly recruiting cellular degradation machinery, such as PARN and the exosome directly to the ARE containing mRNA (Chen *et al.*, 2001; Gherzi *et al.*, 2004; Moraes *et al.*, 2006; Tran *et al.*, 2004). It appears that ARE-BPs can also stabilise transcripts. Overexpression of HuR stabilises specific transcripts such as c-fos, p21, and cyclin D1 (Lal *et al.*, 2004; Peng *et al.*, 1998). The stabilising activity of HuR may be induced through competition for binding to AREs with destabilising factors (Lal *et al.*, 2004), and intriguingly in some cases through inhibiting the function of miRNAs (Bhattacharyya *et al.*, 2006).

As discussed above, mRNA turnover can have direct and dramatic effects on gene expression by limiting the number of transcripts available for translation. Indeed, the processes of mRNA turnover and translation are intimately linked, although the relationship appears to be complex. In yeast, degradation of cellular mRNAs has been shown to require active translation, in experiments using the elongation inhibitor cycloheximide (Herrick *et al.*, 1990) and in certain instances, such as c-fos mRNA, ribosome translocation is absolutely required for deadenylation and turnover (Chang *et al.*, 2004; Grosset *et al.*, 2000). Conversely, mutations of yeast initiation

factors that have inhibitory effects on translation still allowed efficient decapping and deadenylation of cellular mRNAs (Schwartz and Parker, 1999).

Localisation Elements

Many fundamental biological processes require the correct spatial expression of mRNAs. To this end, many mechanisms employed to accurately localise mRNAs to a particular cellular compartment frequently also result in repression of translation to prevent mis-localised proteins (Gavis *et al.*, 2007). The 3'-UTR 'zipcode' sequence element in β-actin mRNA is bound by zipcode-binding protein (ZBP1) which promotes transport to the leading edge of fibroblasts (Ross *et al.*, 1997). ZBP1 inhibits translation initiation of β-actin mRNA by preventing 60S joining (Huttelmaier *et al.*, 2005). Upon correct localisation of β-actin, ZBP1 is released through phosphorylation by the kinase c-Src relieving the repression (Huttelmaier *et al.*, 2005).

Some of the best understood mechanisms of localised mRNA translation have arisen from the model organism *Drosophila melanogaster*, where localisation is critically important during embryonic axis formation. Gurken (Grk), oskar (Osk), nanos (Nos), and bicoid (Bcd) are all proteins whose mRNAs have to be localised correctly to establish the cellular polarity necessary for anterior-posterior and dorsal-ventral body axis formation during oogenesis (Gavis *et al.*, 2007).

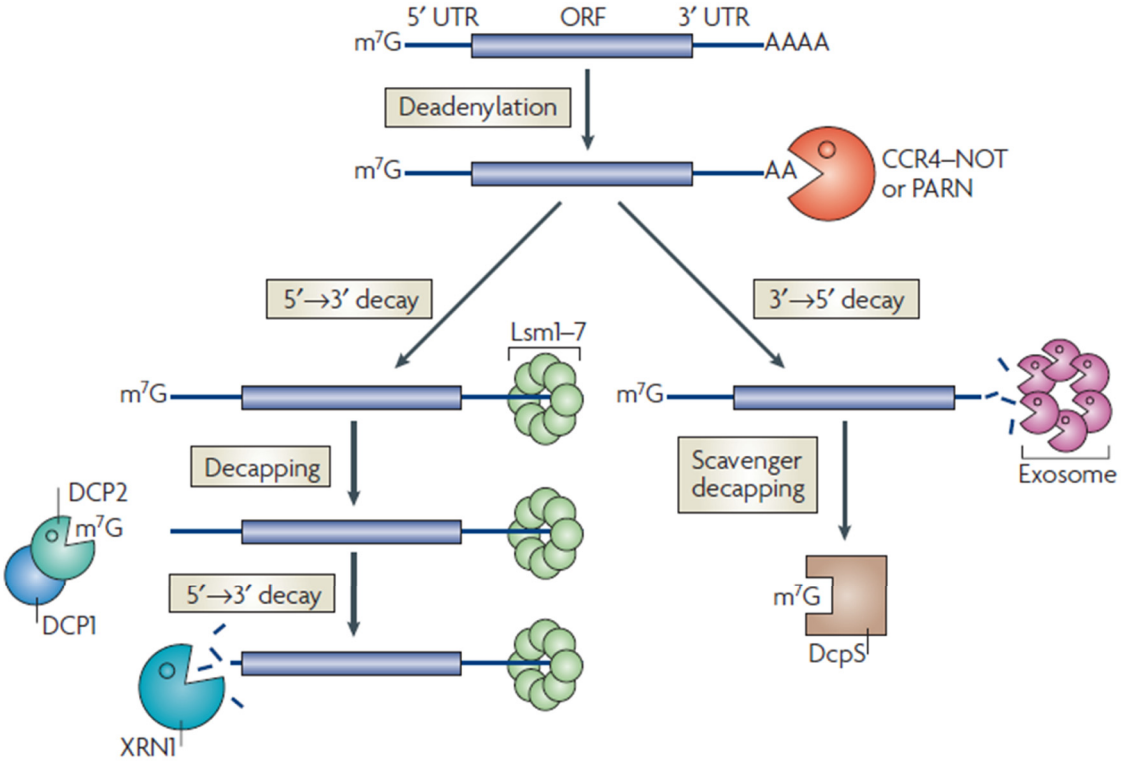

Figure 1.8 Deadenylation-dependent mRNA turnover. Following sequential deadenylation by PAN2-PAN3 then CCR4-NOT or PARN, degradation can proceed in a 3'-5' or a 5-3' direction. 5'-3' degradation requires decapping by the enzymes DCP1/DCP2, which is stimulated by the Lsm1-7 complex, followed by destruction of the mRNA body by the exonuclease XRN1. 3'-5' degradation proceeds through the activity of the exosome followed by hydrolysis of the cap structure by DcpS. Reproduced from Garneau *et al*. 2007.

During *Drosophila* oogenesis oskar (Osk) is localised to the oocyte posterior where it directs the assembly of the germ plasm, a cytoplasmic body that is required for germ cell determination and localisation of mRNAs important in posterior patterning such as nanos (Ephrussi *et al.*, 1991; Kim-Ha *et al.*, 1991). Osk is transported in a translationally repressed state that is alleviated upon correct localisation. This is achieved through the binding of a number of regulatory proteins including staufen, cup, and bruno. Staufen is required for the transport of Osk mRNA along microtubules by the motor protein kinesin 1 (Brendza *et al.*, 2000; Micklem *et al.*, 2000). The translational repression of Osk mRNA during this localisation is mediated by the 3'-UTR binding protein Bruno. Bruno interacts with a 4E-BP like

protein termed cup (Nakamura *et al.*, 2004), and prevents 43S PIC recruitment (Chekulaeva *et al.*, 2006) and additionally, promotes the oligermisation of Osk mRNAs into silenced mRNP particles, possibly facilitating bulk transport to the oocyte posterior (Chekulaeva *et al.*, 2006).

1.4 Poly(A)-Binding Proteins (PABPs)

1.4.1 The PABP Family

The cytoplasmic poly(A)-binding proteins are a family of eukaryotic multi-functional RNA binding proteins that are expressed in yeast, plants, and animals but are not conserved in prokaryotes (Gorgoni and Gray, 2004). The PABP family were first identified as proteins that bound with high affinity to the polyadenylate region of messenger RNAs in mouse L cells and rat hepatocytes (Blobel, 1973). Subsequent experimental work has shown these proteins to be involved in mRNA translation, stabilisation, and turnover (reviewed in Gorgoni and Gray, 2004; Mangus *et al.*, 2003).

Over the course of eukaryotic evolution, there appears to have been a benefit in maintaining multiple PABPs with most eukaryotic species containing a minimum of one nuclear and one cytoplasmic PABP (see table 1.10). The division of PABPs into two broad classes, nuclear and cytoplasmic, is based mainly on structural differences but also intracellular localisation, however PABP1 has been shown to shuttle to the nucleus (Afonina *et al.*, 1998). Also, *Drosophila melanogaster* nuclear PABP (PABP2) has been reported to regulate poly(A) tail length of oskar and cyclin B mRNAs in the cytoplasm (Benoit *et al.*, 2005).

The domain structure of the mammalian nuclear PABPs is strikingly different to that of the cytoplasmic PABPs (see figure 1.9 for human PABPN1 structure). Human PABPN1 contains a single RRM with a glutamate-rich N-terminus and an arginine-rich C-terminus (Kuhn and Wahle, 2004). PABPN1 is thought to play a role in pre-mRNA poly(A) tail addition in the nucleus, forming a complex with another pre-mRNA processing factor, CPSF, to stimulate the processivity of poly(A) polymerase (Bienroth *et al.*, 1993; Wahle, 1991). PABPN1 is a shuttling protein (Calado *et al.*, 2000) and there is evidence that this shuttling may facilitate the nuclear export of poly(A) mRNA (Apponi *et al.*, 2010; Chen *et al.*, 1999). Influenza A virus NS1 protein (NS1A) blocks PABPN1 shuttling as determined by heterokaryon assay, but additionally results in the retention of mRNAs within the nucleus (Chen *et al.*, 1999). In concurrence, short-interfering RNA (siRNA) knockdown of PABPN1 results in nuclear accumulation of poly(A) mRNA (Apponi *et al.*, 2010).

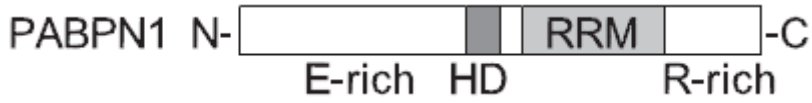

Figure 1.9 Domain structure of human PABPN1. Human PABPN1 is a small protein of 33kDa that contains a single RRM, a glutamate-rich N-terminus (E-rich) and an arginine-rich C-terminus (R-rich). A coiled α-helical domain (HD) might be involved in stimulation of poly(A) polymerase as point mutations within this region ablate this function (Kuhn and Wahle, 2004). Reproduced from Kuhn *et al*. 2004.

A protein that shares approximately 50% identity with PABPN1 was identified in *Xenopus laevis* (Cosson *et al.*, 2004). This protein specifically bound poly(A) and was called ePABP2 (Cosson *et al.*, 2004). Interestingly despite a similar domain structure and sequence homology to PABPN1 this protein is predominantly cytoplasmic (Cosson *et al.*, 2004) and appears restricted to oocytes and early

embryos (Cosson *et al.*, 2004; Good *et al.*, 2004). More recently human and mouse clones of ePABP2 have been identified (Sakugawa *et al.*, 2008).

1.4.2 PABP1

Expression of PABP1

Humans are currently known to contain five cytoplasmic PABP genes (PABP1, PABP3, PABP4, ePABP, PABP5 - see table 1.10) and a number of pseudogenes. Poly(A)-binding protein 1 (PABP1, PABPC1) is the prototypical member of the PABP family. Substantial experimental work has been directed towards understanding the molecular functions of PABP1, but surprisingly little is known regarding the physiological roles of this protein in metazoans. Whilst often regarded to be ubiquitously expressed due to the poly(A) tail being an almost universal feature of mammalian mRNAs, little is known regarding the expression of PABP1 at the tissue or cellular level. Within HeLa cells PABP1 was determined to be an abundant protein with an intracellular concentration estimated at 4μM (Gorlach *et al.*, 1994). In *Xenopus laevis* PABP1 is robustly expressed at the protein level in brain, testis, heart and muscle tissue (Cosson *et al.*, 2002b; Wilkie *et al.*, 2005), while in humans, northern blot analysis revealed a similar expression pattern with strong expression in the ovary (Yang *et al.*, 1995). Expression of PABP1 in mouse tissues has only been documented in testis (Gu *et al.*, 1995; Kleene *et al.*, 1994). It is known that PABP1 is subject to translational regulation (see section 1.4.6) emphasising the importance of analysing protein rather than mRNA levels.

Subcellular Localisation of PABP1

PABP1 is predominantly cytoplasmic (Gorlach *et al.*, 1994), but has been demonstrated to shuttle to the nucleus (Afonina *et al.*, 1998). The cellular mechanisms responsible for this relocalisation are unclear as PABP1 does not contain classic nuclear export or import signals (NES/NLS). Confusingly, inhibition of CRM1 which is responsible for the nuclear export of NES containing proteins by

treatment with leptomycin B (LMB) results in nuclear accumulation of PABP1 (Woods *et al.*, 2002), although this result has recently been challenged (Khacho *et al.*, 2008)(H. Burgess, unpublished). Interestingly the export of PABP1 from the nucleus appears to be transcription dependent. Treatment of cells with inhibitors of transcription, such as actinomycin D (ActD) and 5,6-dichlororibofuranosyl-benzimidazole (DRB) results in nuclear localisation of PABP1 (Afonina *et al.*, 1998; Khacho *et al.*, 2008) and concurrent with this a transcription-dependent nuclear export motif, $DXGX_2DX_2L$, was recently identified in PABP1 (Khacho *et al.*, 2008).

The physiological relevance of PABP1 nuclear localisation is ambiguous. PABP1 immunopurifies with PAP (Hosoda *et al.*, 2006) and accumulates in nuclear speckles containing the splicing factor SC35 (Afonina *et al.*, 1998), leading to suggestions that PABP1 may have roles in pre-mRNA processing events. Additionally, PABP1 immunoprecipitates with the adaptor protein paxillin (see figure 1.12) (Woods *et al.*, 2002). These proteins localise to the rough endoplasmic reticulum (RER) and lamellipodia, but upon LMB treatment accumulate in the nucleus, leading to the proposition that the PABP1/paxillin complex may promote mRNA nuclear export and targeting of mRNA to sites of translation (Woods *et al.*, 2005; Woods *et al.*, 2002).

Relocalisation of PABP1 to the nucleus may also represent a mechanism by which global cellular mRNA translation levels can be controlled. For instance infection with rotavirus (Harb *et al.*, 2008), gammaherpesvirus, alphaherpesvirus and bunyamwera virus all result in nuclear accumulation of PABP1, although the mechanisms by which this occurs are unclear (reviewed in Smith and Gray, 2010). Interestingly, the cytoplasmic distribution of PABP1 also changes in response to cell stress events such as heat shock and oxidative stress, localising to cytoplasmic foci termed stress granules (Kedersha *et al.*, 1999; Salaun *et al.*, 2010). Stress granules are sites of mRNA storage and contain a multitude of RNA-binding proteins and

translation initiation factors but not 60S ribosomal subunits and decapping enzymes (reviewed in Anderson and Kedersha, 2006; Anderson and Kedersha, 2009).

Organism	Poly(A)-Binding Proteins Present
Saccharomyces cerevisiae	Pab1p
Drosophila melanogaster	pAbp, [PABP2]
Caenorhabditis elegans	Pab-1, Pab-2
Xenopus laevis	PABP1, ePABP, PABP4, [ePABP2], [PABPN1/nPABP2]
Mus musculus	Pabp1, Pabp2/tPABP, ePabp, Pabp4, Pabp5, [Pabpnl1/ePABP2], [Pabpn1]
Homo sapiens	PABP1, PABP3/tPABP, ePABP/PABP1L, PABP4/iPABP, PABP5, [ePABP2], [PABPN1/ PABP2/PAB II]

Table 1.10 Poly(A)-binding proteins present in various eukaryotic species. PABP proteins are present in yeast, plants and animals but are not conserved in eukaryotes. Humans contain several cytoplasmic PABPs, nuclear PABP, and a nuclear PABP-like protein. Although *S. cerevisiae* does not appear to contain a nuclear poly(A)-binding protein, an unrelated protein, Nab2p, appears to perform similar functions to other eukaryotic nuclear PABPs. Square brackets denote nuclear PABPs.

1.4.3 PABP Protein Structure

With the exception of PABP5, all of the cytoplasmic poly(A)-binding proteins share a common protein domain structure consisting of four N-terminal RNA-recognition motifs (RRMs) which function in RNA and protein binding, followed by a relatively unstructured proline and glutamine-rich 'linker' region that is connected to a globular C-terminal module termed the PABC domain (Kuhn and Wahle, 2004). PABP5 also contains four RRMs but lacks the linker or PABC domains (see figure 1.11). The structure of RRMs 1-2 bound to RNA has been solved revealing four antiparallel β-strands backed by two α-helices. The β-strands form a trough-like orientation facilitating mRNA binding, while simultaneously leaving a face free for protein-

protein interactions (Deo *et al.*, 1999). The structure of RRMs 3-4 remains unsolved. The primary function of the PABC domain appears to be in promoting protein-protein interactions (Kozlov *et al.*, 2001) (see figure 1.12 for the binding sites of PABP1-interacting proteins). The structure of the PABC domain shows homology to other proteins, namely the E3 ubiquitin ligase hyperplastic discs (HYD) that functions in targeting ubiquitination to specific substrate proteins, consistent with PABC functioning as a platform for protein-protein interactions (Kozlov *et al.*, 2004; Lim *et al.*, 2006). Proteins that bind to PABC can do so through a conserved amino acid sequence called the PABP-interacting motif 2, (PAM2) (Kozlov *et al.*, 2001).

Bioinformatic approaches have identified a plethora of PAM2 containing proteins (Albrecht and Lengauer, 2004; Kozlov *et al.*, 2001), although only a small number have been demonstrated to bind PABC experimentally including eRF3, PAIP1, and PAIP2 (see figure 1.12) (Gray *et al.*, 2000; Kozlov *et al.*, 2004; Kozlov and Gehring, 2010).

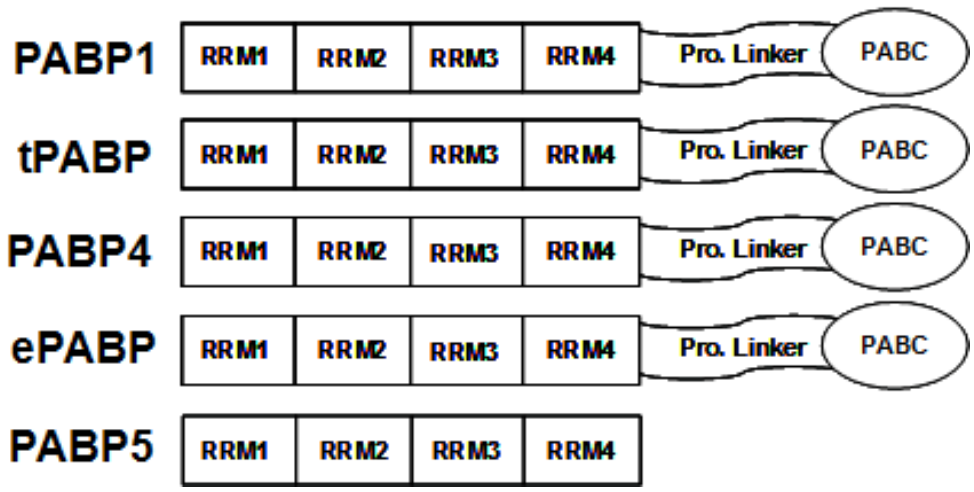

Figure 1.11 Cytoplasmic poly(A)-binding protein structure. PABP proteins share a similar protein domain structure. All human cytoplasmic PABPs contain four RNA recognition motifs (RRMs) that instigate binding to mRNA and also proteins. With the exception of PABP5, all cytoplasmic PABPs also contain a proline and glutamine-rich linker region bound to a globular C-terminal domain that facilitate protein-protein interactions and also PABP self-association. Reproduced from Gorgoni and Gray. 2004.

mRNA Binding Activity

The main mRNA substrate of PABP1 is poly(A) to which it binds with a nanomolar affinity (Gorlach *et al.*, 1994; Sladic *et al.*, 2004) although binding to poly(U) and poly(G) sequences has been shown, albeit to a lesser degree (Deardorff and Sachs, 1997; Kuhn and Pieler, 1996; Nietfeld *et al.*, 1990). No binding to poly(C) sequences has been demonstrated. When bound to mRNA, PABP1 covers approximately 25 nucleotides and requires a minimum of 12 adenosines for maximal binding (Baer and Kornberg, 1983; Sachs *et al.*, 1987). Functionally, the RRMs appear to be dissimilar in mRNA binding activity (Kuhn and Wahle, 2004). Experiments *in-vitro* have shown that the individual RRMs bind mRNA with up to 100-fold reduced affinity when compared to the wild-type protein and that typically, two RRM domains are required to impart specificity and efficient binding (Burd *et al.*, 1991; Kuhn and Pieler, 1996).

Poly(A)-binding is largely mediated by RRMs 1-2, with RRMs 3-4 displaying a reduced capacity to do so (Burd *et al.*, 1991; Deardorff and Sachs, 1997; Kuhn and Pieler, 1996) leading to the hypothesis that RRMs 3-4 may be involved in stabilising the binding to poly(A) and/or promoting binding to other mRNA sequences. Indeed, PABP1 mutations in RRMs 3 and 4 confer reduced binding affinity for poly(A) (Deardorff and Sachs, 1997), and additionally RRMs 3-4 possess an AU-rich sequence binding activity *in-vitro* and *in-vivo* that confers binding of PABP1 with only a 6-fold reduced affinity compared to poly(A) (Sladic *et al.*, 2004). In concurrence with this, PABP1 has been isolated from HeLa cell lysates by RNA affinity chromatography with the ARE of granulocyte-macrophage colony stimulating factor (GM-CSF) (Bollig *et al.*, 2003). The binding of AU-rich sequences is likely to be a conserved function of poly(A)-binding proteins as PABP4 can also bind AREs (Sladic *et al.*, 2004), and ePABP was initially identified as an ARE-binding protein by ARE-affinity selection of *Xenopus laevis* oocyte extracts (Voeltz *et al.*, 2001).

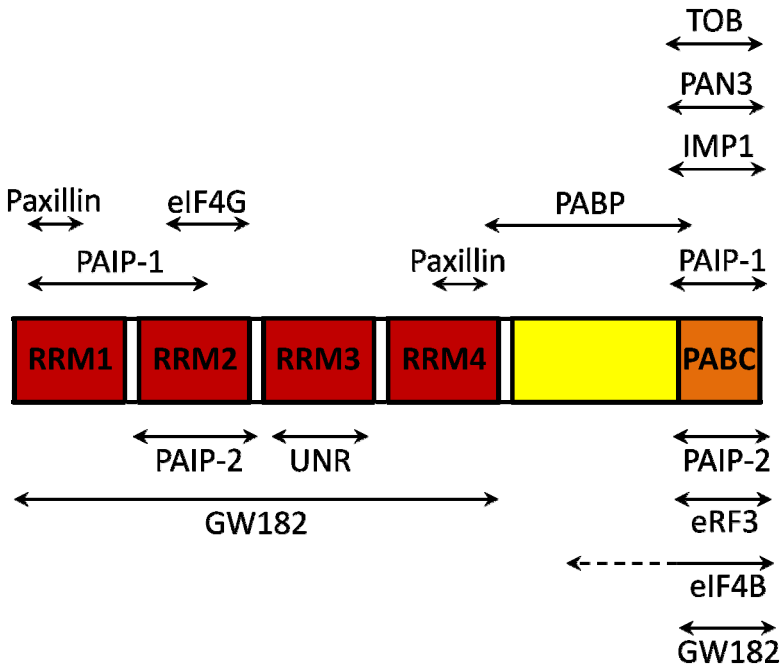

Figure 1.12 Binding sites of PABP1-interacting proteins. TOB (Ezzeddine *et al.*, 2007), PAN3 (Siddiqui *et al.*, 2007), IMP1 (Patel and Bag, 2006), PABP1 (Melo *et al.*, 2003), eIF4G (Imataka *et al.*, 1998), paxillin (Woods *et al.*, 2005), UNR (Chang *et al.*, 2004), eIF4B (Bushell *et al.*, 2001), eRF3 (Cosson *et al.*, 2002a), PAIP-1 (Roy *et al.*, 2002), PAIP-2 (Khaleghpour *et al.*, 2001a), and GW182 (Jinek *et al.*, 2010; Zekri *et al.*, 2009) have all been demonstrated to interact with PABP1. Paxillin, PAIP-1, and PAIP-2 all contain two binding sites within the PABP1 protein. The eIF4B binding site has been determined to be C-terminal but how far the region extends is not known. There are discrepancies regarding the GW182 binding site in PABP1, with data suggesting it could reside within RRMs 1-4 (Zekri *et al.*, 2009) or the C-terminus (Jinek *et al.*, 2010).

PABP1 is known to bind to poly(A) tails in an ordered repeating fashion (Baer and Kornberg, 1983; Kuhn and Pieler, 1996). Experiments *in-vitro* have shown that PABP1 can self-associate to stimulate ordered binding of multiple PABPs to mRNA and that this interaction requires the C-terminus of PABP1 containing the proline-rich linker region, but not the PABC domain (see figure 1.12) (Melo *et al.*, 2003; Wilkie *et al.*, 2005). Interestingly, the first three RRMs were suggested to be inhibitory to PABP1 dimerisation in the absence of poly(A) suggesting a mechanism whereby PABP1 cannot self-associate in the absence of a poly(A) tail (Melo *et al.*, 2003). PABP1 has also been isolated by immunoprecipitation with antibodies directed against ePABP (Wilkie *et al.*, 2005), tPABP (Kimura *et al.*, 2009) and

PABP4 (H. Burgess, unpublished) raising the possibility that different PABP proteins may bind the same transcripts.

1.4.4 PABP1 Function in Translation

The Closed Loop Model

Translation initiation at the 5' end of mRNAs is strongly enhanced in the presence of the m^7GpppG cap structure. The poly(A) tail present at the extreme 3' terminus of nearly all eukaryotic mRNAs is also a primary determinant of translational efficiency (reviewed in Jackson and Standart, 1990; Munroe and Jacobson, 1990). These two structures synergistically enhance translation (Gallie, 1991) via a mechanism termed the 'closed loop' or 'end-to-end complex' model (see figure 1.13) which postulates that the opposing termini functionally interact (Gallie, 1998; Munroe and Jacobson, 1990).

This interaction is mediated by PABP1 which binds to poly(A) (Blobel, 1973) and simultaneously interacts with factors bound to the 5' end of mRNA. PABP1 has been demonstrated to interact with eIF4G *in-vitro* (Gray *et al.*, 2000; Imataka *et al.*, 1998; Tarun and Sachs, 1996) facilitating an eIF4E-eIF4G-PABP1 chain of interactions critical to the closed loop model. The original mammalian eIF4GI (eIF4G) composite cDNA sequence was determined by screening of a human brain λ-cDNA library with labelled oligonucleotides probes that had been designed based on peptide sequences derived from a purified eIF4F preparation (Yan *et al.*, 1992). Following the subsequent publication of the eIF4GII cDNA and protein sequences it was noticed that the amino-terminus was 158 amino-acids longer than that of eIF4GI (Gradi *et al.*, 1998a). Analysis of the two cDNAs showed that sequence homology between eIF4GI and eIF4GII abruptly ends at a putative splice acceptor site and therefore it was deduced that the published eIF4GI cDNA may contain an intron at its 5' end (Gradi *et al.*, 1998a). 5'-RACE was performed using HeLa cell poly(A)+ mRNAs and an N-terminal extension of the eIF4GI mRNA was indeed discovered,

adding 156 amino-acids to the protein (Gradi *et al.*, 1998a; Imataka *et al.*, 1998). It had previously been demonstrated that yeast PABP1 could bind to the N-terminus of eIF4G (Tarun and Sachs, 1996; Tarun *et al.*, 1997) and following the discovery of the human eIF4G N-terminal extension, it too was shown to be capable of binding to PABP1 (Imataka *et al.*, 1998).

In support of this model, recombinant yeast eIF4E, eIF4G and Pab1p have been shown capable of forming ring-like structures with capped polyadenylated mRNAs by atomic force microscopy (Wells *et al.*, 1998). In addition, disruption of the PABP1-eIF4G interaction can inhibit translation of reporter mRNAs (Gray *et al.*, 2000; Imataka *et al.*, 1998; Kahvejian *et al.*, 2005; Tarun *et al.*, 1997) and in yeast translation extracts Pab1p mutants deficient in binding to eIF4G conferred a sensitivity to cap analogue and an inhibition of translation initiation as measured by toeprinting analysis of 48S complexes (Amrani *et al.*, 2008).

The closed loop model is hypothesised to promote 43S PIC recruitment to the cap (Kahvejian *et al.*, 2005; Tarun and Sachs, 1995) although how this is achieved is still unclear. In wheat germ extracts the PABP1-eIF4G interaction increases the affinity of PABP1 for the poly(A) tail (Le *et al.*, 1997) while simultaneously increasing the affinity of eIF4F for the cap structure (Wei *et al.*, 1998). It has also been suggested that the helicase activity of eIF4A doubles in the presence of PABP1 (Bi and Goss, 2000). In mammalian systems, translation of polyadenylated mRNAs was demonstrated to be more sensitive to the presence of cap analogue when the PABP1-eIF4G interaction was disrupted. This was taken to imply that the affinity of eIF4E for the cap structure was increased when PABP1 and eIF4G were complexed (Borman *et al.*, 2000) (Yanagiya *et al.*, 2009). Further interactions may also be involved in stabilising the closed loop conformation. In support of this notion, sensitivity of mRNA translation to m^7G cap analogue was only abolished when a poly(A) tail of 57 adenosines was added to the reporter, allowing binding of two

PABP1 molecules (Amrani *et al.*, 2008). This suggests that stability of the closed loop may require the activity of multiple PABPs.

PAIP-1 is a PABP1 interacting protein (Craig *et al.*, 1998) that contains two PABP-interacting motifs (PAM1 and PAM2) and binds PABP1 with a 1:1 stoichiometry through two sites in RRMs 1-2 and the C-terminus of PABP1 (Gray *et al.*, 2000; Roy *et al.*, 2002). PAIP-1 has also been shown capable of binding eIF3 through its subunit eIF3g (Martineau *et al.*, 2008), as well as interacting with eIF4A (Craig *et al.*, 1998). In addition, pulldown assays have demonstrated that PABP1 can simultaneously interact with eIF4G and PAIP-1 (Martineau *et al.*, 2008). This set of interactions is hypothesised to secure the closed loop conformation (Martineau *et al.*, 2008). Furthermore PABP1 has been shown to interact with eIF4B *in-vitro* (see figure 1.12), and in wheat germ extracts this interaction increases the affinity of PABP1 for poly(A) as well as facilitating an additional contact between the 5' and 3'-UTRs (Bushell *et al.*, 2001; Le *et al.*, 1997).

Transcripts unable to form closed loops by means of a PABP1-eIF4G interaction often utilise other methods to circularise, highlighting the importance of this configuration for stimulating translation. Histone mRNAs are capped but unadenylated, instead containing a conserved stem loop structure within their 3'-UTRs. This is bound by the stem-loop binding protein (SLBP) which stimulates histone mRNA translation (Sanchez and Marzluff, 2002). SLBP has been proposed interact with SLBP-interacting protein 1 (SLIP1) which in turn binds eIF4G (Cakmakci *et al.*, 2008). The SLBP-SLIP1-eIF4G chain of interactions is purported to circularise the transcript, driving the translation of histone mRNA. Similarly, the rotavirus family of double-stranded RNA (dsRNA) viruses produce capped but unadenylated transcripts. The transcripts are thought to circularise through a direct interaction between eIF4G and the viral non-structural protein 3 (NSP3) which binds to a conserved sequence element at the 3' end of all rotavirus mRNAs (Piron *et al.*, 1998). This interaction evicts PABP1 from the eIF4F complex and contributes to

host cell shut-off of protein synthesis probably through competition with PABP1 for eIF4F binding (Piron *et al.*, 1998).

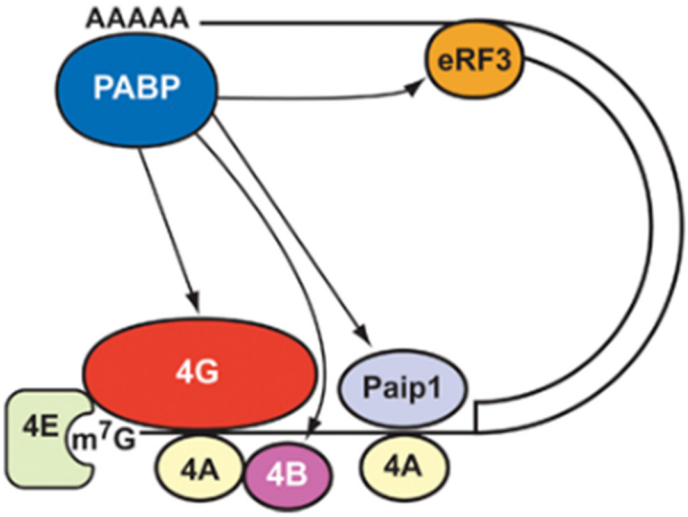

Figure 1.13 The closed loop model. PABP1 binds to the poly(A) tail and stimulates 43S PIC recruitment through an interaction with eIF4G which is part of the eIF4F cap-binding complex thus forming a 'closed loop' mRNP. The PABP-eIF4G interaction is thought to stabilise eIF4F binding to the cap and potentially stimulates the helicase activity of eIF4A. Additional interactions between PABP1 and 5'-UTR bound protein factors such as PAIP-1 and eIF4B may stabilise the closed loop. Additionally, PABP1 has been demonstrated to interact with eRF3, possibly linking translation termination and initiation thereby promoting efficient ribosome recycling. Reproduced from Smith *et al*. 2010.

Although the closed loop model is postulated to stimulate 43S PIC recruitment there is evidence that PABP1 may promote 60S ribosomal subunit joining. In yeast a temperature sensitive mutation in Pab1p that displayed a block in translation initiation could be rescued by suppressor mutations that restrict the amount of 60S subunit available (Sachs and Davis, 1989). Mutations in eIF5 and eIF5B which are involved in 60S subunit joining have also been reported to impair translation of poly(A)+ but not poly(A)- mRNAs (Searfoss *et al.*, 2001). Moreover in RRLs treated with edeine which blocks 60S joining, poly(A)+ and poly(A)- mRNAs were

equally capable of forming 48S complexes suggesting that the poly(A) tail is dispensable for 48S assembly (Munroe and Jacobson, 1990) and yet when treated with cycloheximide which inhibits peptide bond formation poly(A)+ mRNAs formed 80S complexes two and a half times more efficiently than poly(A)- mRNAs (Munroe and Jacobson, 1990). Additionally, PABP1 depleted Krebs-2 cell extracts showed a greater reduction in 80S compared to 48S ribosomal complexes implying that PABP1 could target both 43S recruitment and 60S joining (Kahvejian *et al.*, 2005)

PABP1 may also be involved in ribosome recycling through an interaction with eRF3. The interaction between the N-terminal region of eRF3 and the C-terminal domain of PABP1, has been proposed to result in eviction of PABP1 from mRNA and exposure of the poly(A) tail to deadenylases, thereby linking translation termination to mRNA turnover (Hoshino *et al.*, 1999; Hosoda *et al.*, 2003). Intriguingly, the eRF3/PABP1 interaction has also been proposed to have a stimulatory effect on translation, by physically linking the stop codon to the 5' cap complex, facilitating the efficient recycling of terminating ribosomes (Uchida *et al.*, 2002).

1.4.5 PABP1 Function in mRNA Turnover and Repression

PABP1 Role in Deadenylation

As discussed above (1.3.6 3'-UTR Translational Control Elements) deadenylation is the first step in bulk mRNA turnover (Yamashita *et al.*, 2005). PABP, as the major effector of poly(A) tail function, binds to the poly(A) tail and is proposed to stabilise the transcripts by precluding the access of deadenylases (reviewed in Mangus *et al.*, 2003). The finding that mRNA could be degraded 10-times faster in cell extracts lacking PABP1 (Bernstein *et al.*, 1989), and visualisation of deadenylation intermediates that differ in size by approximately one PABP1 binding site (approximately 30 nucleotides) suggested that this might be the case (Korner and Wahle, 1997).

This simplistic viewpoint was contested by paradoxical *in-vivo* evidence suggesting that the rate of deadenylation is slowed in Pab1p depleted yeast strains indicative of a stimulatory role for Pab1p in deadenylation (Caponigro and Parker, 1995; Sachs and Davis, 1989). The explanation for this activity could reside with the discovery that PABP1 can interact with, and stimulate the activity of the PAN2-PAN3 deadenylase complex (Funakoshi *et al.*, 2007; Siddiqui *et al.*, 2007; Uchida *et al.*, 2004) through a direct interaction with the PAN3 subunit (see figure 1.12). Interestingly the CCR4-NOT deadenylase complex also interacts with mammalian PABP1 through the anti-proliferative protein Tob (Funakoshi *et al.*, 2007). A mechanism has recently been proposed whereby PABP1 exchanges eRF3 for deadenylase complexes upon translation termination thereby linking termination to deadenylation (Funakoshi *et al.*, 2007). This is supported by evidence that the binding of eRF3, PAN2-PAN3, and CCR4-NOT to PABP1 via the PABC domain are all mutually exclusive, and that a translation-dependent exchange between eRF3 and PAN2-PAN3 occurs on PABP1 in cells (Funakoshi *et al.*, 2007).

PABP1 Requirement in miRNA Mediated Translational Repression and Turnover

PABP1 has also been implicated in miRNA directed translational repression and turnover through an interaction with GW182 (see figure 1.12), a component of the miRISC complex (Fabian *et al.*, 2009; Jinek *et al.*, 2010; Zekri *et al.*, 2009). miRNA mediated deadenylation of reporter mRNAs by the CCR4-NOT complex required the PABP1-GW182 interaction although surprisingly PABP1 recruitment of CCR4-NOT to the miRISC does not appear to be required for miRNA target deadenylation (Fabian *et al.*, 2009; Zekri *et al.*, 2009). A mechanism for deadenylase recruitment was provided upon the discovery that CAF1, a component of the CCR4-NOT complex, could be co-immunoprecipitated with the miRISC proteins Ago1 and Ago2 (Fabian *et al.*, 2009). Interestingly, *Drosophila* GW182 and eIF4G appear to compete for binding to PABP1, therefore a PABP1-GW182 interaction could possibly inhibit the formation of closed loop complexes by disrupting the PABP1-eIF4G interaction. This could result in translational repression and possibly exposure of the poly(A) tail to deadenylases (Zekri *et al.*, 2009). The PABP1-

GW182 interaction might also function in juxtaposing the poly(A) tail against the miRISC deadenylase complex (Fabian *et al.*, 2009).

PABP1 Role in Nonsense-Mediated Decay

Nonsense-mediated decay (NMD) degrades mRNAs harbouring premature termination codons (PTCs) (reviewed in Silva and Romao, 2009) that could produce deleterious truncated protein products. The NMD surveillance machinery appears to detect the exon junction complexes (EJCs) deposited at exon-exon junctions following splicing (Le Hir *et al.*, 2000). As most introns are contained within mRNA coding regions EJCs are normally displaced by translating ribosomes (Garneau *et al.*, 2007), therefore retained EJCs can indicate the presence of a PTC and signal the mRNA for decay (Nagy and Maquat, 1998; Singh *et al.*, 2007; Zhang *et al.*, 1998). The role of PABP1 in NMD appears to be antagonistic to that of EJCs and can repress NMD when tethered downstream of PTCs (Amrani *et al.*, 2004; Behm-Ansmant *et al.*, 2007; Silva *et al.*, 2008). Moreover increasing the length of the 3'-UTR is capable of triggering NMD from natural stop codons (Behm-Ansmant *et al.*, 2007). This suggests that PABP1 positioning provides information to the NMD machinery regarding natural termination events. Indeed PABP1 competes for binding to the translation termination factor eRF3 with UPF1, a core component of the NMD machinery (Ivanov *et al.*, 2008; Singh *et al.*, 2008). The ability to discriminate between normal and premature translational termination events therefore appears to be the sum of a number of antagonistic signals.

The current model speculates that at natural stop codons PABP1 interacts with eRF3 promoting normal termination, whereas at a PTC that is spatially distant to PABP1, UPF1 successfully competes for binding to eRF3 promoting NMD by a mechanism that appears to be stimulated by EJCs (Silva and Romao, 2009; Singh *et al.*, 2008). The process of NMD also appears to regulate the expression of non-PTC containing transcripts and it has recently been estimated that 5-10% of the human transcriptome is regulated in this manner. Depletion of UPF1 from mammalian cells resulted in the

upregulated expression of transposons and endogenous retroviruses. These mRNAs were found to contain introns downstream of their termination codon which would normally be sufficient to initiate NMD (Mendell *et al.*, 2004; Silva and Romao, 2009).

1.4.6 Regulation of PABP1 Expression and Activity

Terminal Oligopyrimidine Tracts

PABP1 mRNA contains a sequence element termed a terminal oligopyrimidine tract (TOP) within its 5'-UTR which is known to regulate the expression of a number of mRNAs involved in protein synthesis, including ribosomal proteins (RPs), and the translation factors eEF1A, eEF2, which are selectively repressed upon growth arrest (Hamilton *et al.*, 2006; Meyuhas, 2000). While most mRNAs have an adenosine immediately following the m^7G cap structure, TOP mRNAs contain a cytosine followed by 4-14 pyrimidine residues (Hamilton *et al.*, 2006). The mechanism of TOP mediated translational repression is controversial. Initially it was noted that the mitogen stimulated phosphorylation of RPS6 (ribosomal protein S6) by the kinase S6K correlated with the translation of TOP mRNAs in a manner that was sensitive to both mTOR and phosphatidylinositol 3-kinase (PI3K) inhibitors (Caldarola *et al.*, 2004; Dufner and Thomas, 1999; Meyuhas, 2000). Subsequent data has ruled out phosphorylation of RPS6 as a mediator of TOP regulation, although PI3K and mTOR signalling still appears to be important (Barth-Baus *et al.*, 2002; Stolovich *et al.*, 2002; Tang *et al.*, 2001). It has been hypothesised that binding of a *trans*-acting factor to TOP mRNAs may cause the translational repression. Incubation of cell free translation extracts with oligonucleotides composed of the TOP sequence from RPS16 was able to relieve the repression. This could be indicative of the presence of one or more titratable *trans*-acting factors, but while several proteins capable of binding TOP sequences have been identified, a credible candidate is yet to emerge (Biberman and Meyuhas, 1999; Intine *et al.*, 2003; Schwartz *et al.*, 2004; Zhu *et al.*, 2001).

Autoregulation of PABP1 mRNA Expression

The 5'-UTR of PABP1 mRNA contains an adenosine-rich sequence element termed the autoregulatory sequence (ARS). PABP1 has been demonstrated to bind the ARS (Patel *et al.*, 2005; Sachs *et al.*, 1986) inhibiting the translation of its own mRNA providing a feedback loop that limits the expression of PABP1 (Bag, 2001; Bag and Wu, 1996; Patel *et al.*, 2005). The ARS is proposed to inhibit 40S scanning (Bag, 2001) by acting as a binding site for the formation of a heterotrimeric complex composed of PABP1, IMP1 and UNR (Patel and Bag, 2006; Patel *et al.*, 2005). PABP1 binds to the ARS with a lower affinity than poly(A) (Patel *et al.*, 2005) and the interactions with IMP1 and UNR (see figure 1.12) are thought to be required to form a complex that is sufficient to block ribosome translocation (Patel and Bag, 2006; Patel *et al.*, 2005).

Regulation of PABP1 Activity By PAIP-2

The activity of PABP1 is also subject to regulation through an interaction with the translational inhibitory protein PABP-interacting protein 2 (PAIP-2) (reviewed in Derry *et al.*, 2006). In contrast to PAIP-1 which stimulates translation (Craig *et al.*, 1998) addition of PAIP-2 to cell-free translation extracts represses the translation of a reporter mRNA 14-fold (Khaleghpour *et al.*, 2001b). PAIP-2 binds PABP1 through two PAM domains, PAM1 and PAM2 although unlike PAIP-1, binds with a 2:1 stoichiometry (see figure 1.14A) (Albrecht and Lengauer, 2004; Khaleghpour *et al.*, 2001a; Roy *et al.*, 2002). PAIP-2 represses translation by decreasing the affinity of PABP1 for poly(A) (Khaleghpour *et al.*, 2001b) and additionally competes with eIF4G and PAIP-1 for binding to PABP1 (see figure 1.14B) (Karim *et al.*, 2006; Khaleghpour *et al.*, 2001b). A second PAIP-2 clone was identified, PAIP-2B, leading to the renaming of the original clone PAIP-2A (Berlanga *et al.*, 2006). PAIP-2B also inhibits translation *in-vitro* and *in-vivo* to the same degree as PAIP-2A (Berlanga *et al.*, 2006), although they differ in their tissue distributions with PAIP-2B being predominantly expressed in the pancreas, while PAIP-2A is expressed mainly in the testis (Berlanga *et al.*, 2006).

A.

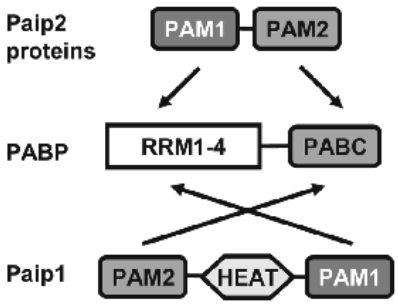

B.

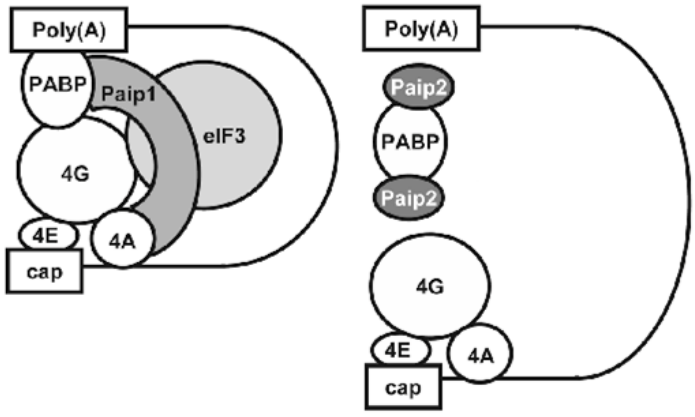

Figure 1.14 Regulation of PABP1 activity by PAIP-2. A. PAIP-1 and PAIP-2 bind PABP1 through two conserved elements called PAM1 and PAM2. PAM1 interacts with PABP1 in RRM2 while PAM2 interacts with the PABC domain. PAIP-2 binds with a 2:1 stoichiometry while PAIP-1 binds with a 1:1 stoichiometry. **B.** PAIP-2 negatively regulates PABP1 activity to repress translation. PAIP-2 competes for binding to PABP1 with eIF4G and PAIP-1, and reduces the affinity of PABP1 for poly(A). The interaction of PAIP-2 with PABP1 is therefore thought to disrupt the formation of a closed loop. Reproduced from Derry *et al*. 2006.

PABP1 and PAIP-2 cellular homeostasis is maintained through a feedback system (Yoshida *et al.*, 2006). In response to decreased PABP1 levels PAIP-2 is ubiquitinated by EDD, a member of the HECT family of E3-ubiquitin ligases (Callaghan *et al.*, 1998) and targeted for degradation by the proteasome (Yoshida *et al.*, 2006). EDD contains a PABC domain in its C-terminus (Deo *et al.*, 2001; Kozlov *et al.*, 2001). The PABC domain in EDD has a 20-fold lower affinity for PAIP-2 than the corresponding domain in PABP1, and consequently only Co-IP's with PAIP-2 in the absence of PABP1 (Yoshida *et al.*, 2006). This suggests that upon lowered PABP1 levels, PAIP-2 can interact with EDD and is ubiquitinated and degraded allowing increased PABP1 activity. PAIP-2B is also ubiquitinated implying a similar mechanism of regulation (Berlanga *et al.*, 2006). In addition to PABP1, tPABP and ePABP have also been demonstrated to bind PAIP-2 (Kim and Richter, 2007; Kimura *et al.*, 2009).

1.4.7 Other PABP Family Members

The Role of Multiple PABPs

As discussed in section 1.4.1, humans express multiple PABPs that share a similar domain structure and high level of protein sequence identity (see table 1.15). The data available on other cytoplasmic PABP family members will be discussed in the following section and indicates that they may also play roles in translational regulation. Why multiple PABPs are required in vertebrates is unclear, and to date no vertebrate PABP phenotypes have been described. In yeast deletion of the Pab1p gene is lethal (Sachs *et al.*, 1987), as is deletion of the cytoplasmic *Drosophila melanogaster* pAbp gene (Sigrist *et al.*, 2000). In an ethyl methanesulphonate (EMS) screen in *Caenorhabditis elegans*, mutation of the Pab-1 gene resulted in a fully penetrant severe germline proliferation defect resulting in sterility (Maciejowski *et al.*, 2005). RNA interference (RNAi) of the Pab-1 transcript resulted in a similar sterility phenotype with 25% of the progeny also displaying growth defects (Maciejowski *et al.*, 2005). RNAi of the Pab-2 transcript also resulted in a low

occurrence of growth defects leading to the conclusion that the Pab-1 and Pab-2 proteins act redundantly in the soma but that Pab-1 is essential in the germline (Maciejowski *et al.*, 2005). A separate RNAi knockdown of Pab-1 resulted in 50-80% embryonic lethality with the surviving progeny being sterile (Simmer *et al.*, 2003).

	htPABP	hePABP	hPABP4	hPABP5
hPABP1	92%	69%	75%	62%
htPABP		65%	70%	59%
hePABP			65%	56%
hPABP4				63%

Table 1.15 Human cytoplasmic PABP protein sequence identity. The percentage protein sequence identity between members of the human cytoplasmic PABP family was calculated. Human PABP5 lacks the proline-rich linker region and the C-terminal region conserved in other cytoplasmic PABPs, therefore the sequence identity of this protein was calculated against only RRMs 1-4 of the other family members.

ePABP

Embryonic PABP (ePABP) is probably the most extensively studied PABP apart from PABP1 and was initially described as being expressed in the oocytes and early embryos of *Xenopus laevis* where the protein could be detected up to 30 hours post-fertilisation (Voeltz *et al.*, 2001). In contrast PABP1 protein was only detectable from 1 day post-fertilisation onwards meaning that ePABP is the predominantly expressed PABP at these developmental stages when poly(A) tail length changes are important. The oocyte and early embryonic expression is borne out in mouse (Wilkie *et al.*, 2005) and human (Guzeloglu-Kayisli *et al.*, 2008) suggesting a conserved expression pattern. In adult mouse, *Xenopus* and human tissues ePABP has been detected in the ovary and testis (Guzeloglu-Kayisli *et al.*, 2008; Seli *et al.*, 2005; Wilkie *et al.*, 2005).

Initially ePABP was purified from *Xenopus laevis* oocyte extracts as an ARE-binding protein (Voeltz *et al.*, 2001). Subsequently ePABP was shown to inhibit deadenylation of ARE and non-ARE containing substrates (Kim and Richter, 2007; Voeltz *et al.*, 2001) and was implicated in regulating cytoplasmic polyadenylation possibly via a transient interaction with CPEB from where it could be transferred to the newly synthesised poly(A) tails (Kim and Richter, 2007). Given the sequence homology to PABP1 a role for ePABP in translational regulation was also examined. In *Xenopus* oocytes a reporter mRNA to which ePABP was tethered was translated 8-fold more efficiently than controls (Wilkie *et al.*, 2005), and consistent with a role in translational regulation ePABP was observed to co-sediment with polysomes from oocyte extracts (Wilkie *et al.*, 2005). Similar to PABP1, ePABP interacts with eIF4G (Kim and Richter, 2007; Wilkie *et al.*, 2005), PAIP-1 (Wilkie *et al.*, 2005), PAIP-2 (Kim and Richter, 2007) and eRF3 (Cosson *et al.*, 2002b) and accordingly can be purified by m^7G affinity chromatography from *Xenopus* oocyte extracts (Cosson *et al.*, 2002b). Interestingly, despite ePABP having the lowest protein sequence conservation across the PABP family (see table 1.15), this data is concurrent with ePABP being a genuine translation factor that appears to act in a manner similar to PABP1.

tPABP

The expression of testis PABP (tPABP) is restricted to a sub-population of germ cells within the testis of mice and humans (Feral *et al.*, 2001; Kimura *et al.*, 2009). The expression of tPABP is discussed in more detail in chapter 3. tPABP is an intronless gene and is hypothesised to have arisen through retroposition of a PABP1 transcript, explaining the high degree of sequence homology between the two PABP proteins (see table 1.15) (Kleene *et al.*, 1998). The available data suggests that tPABP may also play a role in translational regulation. It has a mainly cytoplasmic localisation and can bind poly(A) (Feral *et al.*, 2001; Kleene *et al.*, 1994), and stimulates translation to a similar degree as PABP1 in RRLs (Kimura *et al.*, 2009), although the magnitude of stimulation was only approximately 1.6-fold because the assay was undertaken in RRLs which are not cap and poly(A) sensitive. tPABP has also been

demonstrated to interact with eIF4G, PAIP-1 and PAIP-2 (Kimura *et al.*, 2009). Curiously tPABP was not observed in the polysomes of fractionated mouse testis (Kimura *et al.*, 2009), although this might reflect a detection level issue as tPABP is thought to be significantly lower in abundance than PABP1 in this tissue (Feral *et al.*, 2001).

PABP4

PABP4, also called inducible PABP (iPABP) and activated-platelet protein-1 (APP-1), was originally cloned as an inducible mRNA in activated T-cells (Yang *et al.*, 1995) and a protein that was upregulated in activated platelets (Houng *et al.*, 1997). PABP4 showed a wide expression pattern in different human tissues as determined by northern blot with particularly high mRNA levels in testis and ovary (Yang *et al.*, 1995). Moreover PABP4 was the predominant PABP mRNA species present in heart and skeletal muscle when compared to PABP1 levels (Yang *et al.*, 1995). As with other characterised PABP family members PABP4 displayed poly(A) binding affinity as determined by poly(A)-sepharose binding (Houng *et al.*, 1997; Yang *et al.*, 1995) and also by electrophoretic mobility shift assay (EMSA) (Sladic *et al.*, 2004). Quantitative EMSA experiments established that PABP4 bound poly(A) with a marginally lower affinity than PABP1 (K_d 1.1nM vs K_d 0.67nM) but bound a poly(AU) probe with higher affinity (K_d 2.4nM vs K_d 3.9nM) (Sladic *et al.*, 2004). The physiological relevance of this binding specificity has yet to be determined.

A function for PABP4 in translational regulation has yet to be firmly established although initial data appears to support a role. PABP4 was shown to modestly enhance the translation of polyadenylated interleukin-2 (IL-2) mRNA in an *in-vitro* translation system, although only in the presence of the IL-2 mRNA 3'-UTR (Okochi *et al.*, 2005). This stimulation was suppressed by the overexpression of the antiproliferative protein Tob which was shown to interact with PABP4 via the PABC domain (Okochi *et al.*, 2005).

PABP5

The least studied PABP family member is PABP5. Structurally this protein differs from the other 'classical' PABP proteins. It lacks the proline-rich linker region and the C-terminal domain, but retains four putative RRMs implying that PABP5 is capable of RNA and protein binding. PABP5 was originally identified via an exon-trapping study directed at finding expressed genes within the Xq21.3/Yp11.2 homology block of the human sex chromosomes (Blanco *et al.*, 2001). The PABP5 gene appears to be mammalian-specific and highly conserved between species (see table 1.16), coding for a protein with a predicted molecular weight of 43kDa (Blanco *et al.*, 2001). Intriguingly, like tPABP, PABP5 may have arisen by retroposition, as the gene contains a single uninterrupted ORF. The documented expression data for PABP5 is extremely preliminary, consisting of a single reverse transcriptase-polymerase chain reaction (RT-PCR) experiment on a panel of human cDNAs (Blanco *et al.*, 2001). The data shows PABP5 mRNA expression in human fetal brain, adult brain, kidney, testis, and ovary. The authors indicate that the highest expression levels are seen in the ovary, although the ovary RT-PCR is displayed on a separate figure with no other tissues for comparison. To date no functional analysis of the protein has been undertaken.

	Mus musculus	*Pan troglodytes*	*Macaca mulatta*	*Bos taurus*
Homo sapiens	94%	100%	99%	96%
Mus musculus		94%	94%	92%
Pan troglodytes			99%	96%
Macaca mulatta				96%

Table 1.16 PABP5 protein conservation across mammalian species. The putative PABP5 protein sequence identity was compared across a number of mammalian species. *Homo sapiens* = humans, *Mus musculus* = mouse, *Pan troglodytes* = chimpanzee, *Macaca mulatta* = macaque, *Bos taurus* = cow.

1.5 Thesis Aims

PABP5 is a mammalian specific protein whose physiological function is currently unknown. There is little published data available for PABP5, despite the PABP5 gene being mapped to a genetic locus associated with well-known human pathological conditions such as premature ovarian failure (see chapter 5). The expression pattern of PABP5 within mammalian tissues is poorly understood and there is currently no data pertaining to the molecular function, therefore the aim of this thesis was to examine the tissue and cellular distribution of PABP5 in mammals, and to begin to dissect the molecular role of this protein, with a longer term aim of determining its physiological importance.

Chapter 2: Materials and Methods

Note

Unless otherwise stated all tabletop centrifugation was carried out using an Eppendorf 5417R centrifuge with a fixed angle rotor (max.13,000 rpm [16,060 rcf]). All other centrifugation was carried out with a Sigma-Aldrich 6K15 centrifuge with a swing out bucket rotor (max. 4700 rpm [4495 rcf]).

2.1 General Microbiological Techniques

2.1.1 Bacterial Work

Bacterial Strains

All plasmids were prepared in the *E. coli* strain XL-1 Blue (Stratagene), genotype: *recA1 endA1 gyrA96 thi-1 hsdR17 supE44 relA1 lac* [F′ *proAB lacI*qZΔ*M15* Tn*10* (Tetr)]. All recombinant proteins were expressed and purified from the *E. coli* strain BL21(DE3) (Invitrogen), genotype: F- *ompT hsdS*B (rB-mB-) *gal dcm* (DE3).

Bacterial Growth

Bacteria were grown and maintained on Luria Bertani (LB) agar plates or in liquid LB medium containing the appropriate antibiotics (kanamycin at 40μg/ml, ampicillin at 100μg/ml, or chloramphenicol at 34μg/ml). LB agar plates and cultures were grown at 37^{o}C and stored at 4^{o}C where necessary.

Bacterial Transformations

Chemically competent XL-1 Blue *E. coli* cells were thawed on ice for 30 minutes prior to transformation. Approximately 10-100ng of plasmid DNA or 10ng of freshly ligated DNA was then added to 50μl of cells. The mixture was then incubated on ice for 30 minutes before heat shocking at 42^{o}C for 45 seconds in a

water bath. 200µl of LB medium was added and the mixture was incubated for 60 minutes at 37°C. 100µl of the mixture was then plated on LB agar containing the required antibiotic, and the plates were incubated at 37°C overnight.

2.1.2 Yeast Work

Yeast Strains

Yeast two-hybrid analysis was performed with *S. cerevisiae* strain *L40ura*$^-$ (*MATa, ura3-52, leu2-3, 112, his3, trpΔ1, ade2, Δgal4, lys::(lexAop)-HIS3, ura3::(lexAop)-LacZ*) as previously described (Zhang *et al.*, 1999).

Yeast Growth

Yeast were grown in yeast extract peptone dextrose (YPD) media (10g/l bacto-yeast extract, 20g/l bacto-peptone, 20g/l dextrose) or on YPD agar plates (10g/l bacto-yeast extract, 20g/l bacto-peptone, 20g/l dextrose, 20g/l bacto-agar) at 30°C. For yeast 2-hybrid experiments, yeast were transformed with plasmids containing selectable markers and so were grown on selective minimal media plates (6.7g/l yeast nitrogenous base, 20g/l D-glucose, 20g/l bacto-agar, 1x dropout mix [1x dropout mix = 125mg/l of each of the following: adenine, alanine, arginine, asparagine, aspartic acid, cysteine, glutamic acid, glutamine, glycine, histidine, isoleucine, lysine, methionine, phenylalanine, proline, serine, threonine, tyrosine, uracil and valine in dH_2O]).

Yeast Transformations for Yeast 2-Hybrid Assay

A single L40ura$^-$ yeast colony was used to inoculate 5ml YPD and the culture was grown overnight at 30°C. The following day, 1ml of overnight culture was used to inoculate 50ml YPD and the yeast were grown to O.D. 0.6-1.0. The culture was centrifuged at 4700 rpm for 1 minute. The supernatant was removed and the yeast

pellet was washed with 25ml dH_2O before being respun as before. The supernatant was removed and the pellet was resuspended in 25ml of buffer (100mM LiOAc, 1x TE [10mM Tris-HCl, pH7.5, 1mM EDTA]) and aliquoted into microcentrifuge tubes (500µl per reaction). The yeast were centrifuged at 7,000 rpm (5,200 rcf) for 1 minute and the supernatant was removed. The yeast were then resuspended in the transformation reaction buffer which contained 50µl 100mM LiOAc/1x TE, 6µl herring testis carrier DNA (Clontech), and 1µg of each plasmid to be transformed. 300ul of 40% PEG (M_r 3350g/mol)/100mM LiOAc/1x TE was then added to each sample, and the samples were vortexed for 10 seconds. The mixture was incubated at 30°C for 30 minutes, followed by heat shock at 42°C for 15 minutes. After centrifugation for 2 minutes at 7,000 rpm, the yeast were resuspended in 200µl of dH_2O and plated on yeast minimal media plates. The plates were incubated at 30°C for approximately 3 days to obtain colonies.

2.2 General Nucleic Acid Techniques

2.2.1 Plasmid Purification

Plasmid DNA was prepared from overnight cultures of transformed *E. coli* strain XL-1 Blue using Qiagen Mini, Midi, or Maxi-Prep kits as per the manufacturer's instructions. Plasmids were eluted and stored in Buffer EB (Qiagen) and the DNA concentration was established using a Nanodrop Spectrophotometer ND-1000 (Thermo Scientific), measuring the absorbance spectra at 260nm. DNA quality was established using agarose gel electrophoresis with the fluorescent nucleic acid dye GelRed (Biotium).

2.2.2 Phenol/Chloroform Extraction (DNA)

A 1:1 ratio of sample to phenol:chloroform:isoamyl alcohol 25:24:1 (Sigma-Aldrich) was mixed vigorously in a screw cap tube. The sample was then centrifuged at

13,000 rpm for 3 minutes. The upper (aqueous) phase was removed to a fresh tube and the extraction was repeated. The DNA was then ethanol precipitated.

2.2.3 Ethanol Precipitation of RNA/DNA

The volume of the solution containing the RNA/DNA was estimated and 0.1x volume of 3M NaOAc pH5.2 was added, followed by 2.5x volume of molecular grade ethanol (Sigma-Aldrich). The mixture was then placed at -20^{o}C for 2 hours to overnight before being spun at 13,000 rpm for 30 minutes. The RNA and DNA were then washed in large volumes of 80% and 70% molecular grade ethanol respectively, before being resuspended in dH_2O.

2.2.4 Restriction Digestion of DNA

All restriction enzymes used were supplied by New England Biolabs (NEB) or Roche. Digestions were set up as per manufacturer's instructions, using the supplied buffers. The restriction enzymes were maintained within a glycerol buffer and therefore never comprised more than 10% of the total reaction volume to avoid star activity. 1 unit of restriction enzyme was defined as the amount of enzyme required to cut 1µg of DNA in 1 hour (Roche), therefore the amount of enzyme and reaction incubation time were calculated for individual reactions. When digesting a plasmid vector for cloning, shrimp alkaline phosphatase (Roche) was added to the digestion reaction as per manufacturer's instructions and the vectors/inserts were purified using a Qiagen PCR Purification Kit as per manufacturer's instructions, prior to ligation.

2.2.5 DNA Ligations

All ligations were undertaken using T4 DNA Ligase (NEB) as per manufacturer's instructions. Ligation reactions were incubated overnight at 4^{o}C.

2.2.6 Agarose Gel Electrophoresis

Agarose gels were prepared in the range 0.8-2% (w/v) by dissolving the appropriate mass of agarose in 1x TAE buffer (40mM Tris-HCl, 20mM glacial acetic acid, 1.3mM EDTA, pH8.5) in a microwave for 1 minute. GelRed was added to the molten agarose at a 1/10,000 dilution and the solution was poured and allowed to set. 6x Gel loading buffer (0.25% bromophenol blue, 0.25% xylene cyanol FF, 30% glycerol) was added to DNA samples to a final concentration of 1x, and the samples were run at 25-100V in an EmbiTech RunOne System gel electrophoresis tank in 1x TAE buffer. The DNA was visualised under a UV light and band sizes were estimated using Promega 1kb ladder.

2.2.7 DNA Sequencing

All sequencing reactions were run on an in-house ABI 3730 DNA Analyzer machine (Applied Biosystems). The reactions were performed using a Big Dye Terminator Sequencing Kit (Applied Biosystems) as per manufacturer's instructions.

2.2.8 RNA Extraction from Tissue Samples

RNA was extracted from cells and tissue samples with Tri-Reagent (Ambion) as per manufacturer's instructions. RNA was resuspended in nuclease-free water (Ambion).

2.2.9 In-vitro Transcriptions

In-situ Hybridisation Probes

The vectors containing the template sequences for the probes were linearised by restriction enzyme digestion at a site 3' to the transcriptional end point. The construct was purified by phenol/chloroform extraction followed by ethanol

precipitation and used as a template for preparing the digoxygenin (DIG) labelled probes utilising a DIG-labelling kit (Roche) as per manufacturer's instructions.

Tethered Function Assay mRNAs

The vectors containing the template sequences for the mRNAs were linearised by restriction enzyme digestion at a site 3' to the transcriptional end point. The construct was purified by phenol/chloroform extraction followed by ethanol precipitation prior to transcription. For T7-RNA polymerase transcriptions the reactions were set up as follows: 1x transcription buffer (Stratagene), 30mM DTT, 1mM ATP, 1mM UTP, 1mM CTP, 7mM m^7G cap (New England Biolabs), 100U RNasin (Promega), 4U T7-RNA polymerase (Stratagene), 0.1µg/µl linearised DNA template. The reaction was incubated at 37^oC for 5 minutes in the absence of GTP to promote capping of the transcripts. Following the incubation 1mM GTP was added and the reaction was allowed to proceed at 37^oC for 90 minutes. The template DNA was then digested by addition of 2.5U RQ1 RNase-free DNase (Promega) followed by incubation at 37^oC for 25 minutes. The RNAs were purified by two acidic phenol/chloroform/isoamylalcohol (25:24:1) (Ambion) extractions and passed over a Chroma spin-100 DEPC-H_2O column (Clontech) to remove unincorporated m^7G cap and short partially transcribed RNA products. The RNA was then ethanol precipitated and resuspended in nuclease-free water (Ambion) and subjected to agarose gel electrophoresis to check integrity.

2.3 Polymerase Chain Reaction (PCR) Techniques

2.3.1 Polymerase Chain Reaction (PCR)

PCR reactions were set up on ice, using filter tips. The polymerase enzyme utilised for all PCR based techniques was Phusion High-Fidelity DNA polymerase

(Finnzymes) with the exception of PCR reactions to produce products for TA cloning which were undertaken with Bio-X-Act (Bioline). A typical PCR reaction contained the following components; 1x Phusion Reaction Buffer, 0.2mM dNTPs, 0.5µM sense primer, 0.5µM antisense primer, 10-50ng DNA/cDNA template, 1U Phusion DNA polymerase enzyme. The reactions were run on a Dyad DNA Engine (BioRad) with the following standard program; (1) 98^{o}C for 30 seconds, (2) 98^{o}C for 10 seconds, (3) 55-65^{o}C (dependent on the melting temperature of the oligonucleotide primers) for 30 seconds, (4) 72^{o}C for 30 seconds - 1 minute, (5) repeat steps (2) to (4) 29 - 31 times, (6) 72^{o}C for 5 minutes.

2.3.2 Reverse Trancription PCR (RT-PCR)

RT-PCR reactions were undertaken with an AMV First Strand cDNA Synthesis Kit (Roche) as per manufacturer's instructions. cDNA was then subjected to standard PCR (as above) using 1-5µl of the cDNA reaction per PCR. The mouse Pabp5 RT-PCR oligos were 5'-CGGTCATCTGGCTGTGACCAC-3' and 5'-GCGGCTGCCAGTCAGTCC-3' and the mouse aromatase RT-PCR oligos were 5'-GTTCCATGTCATGAAGCACAG-3' and 5'-TCCAGCATGATGTGTCTCATG-3'.

2.3.3 Quantitative PCR (QPCR) on Human Tissue cDNA Array

Quantitative PCR analysis was performed in a 7900HT Fast Real-Time PCR System (Applied Biosystems) using a pre-designed Taqman probe/primer set (Catalogue no. Hs01936220_s1; Applied Biosystems) with a Human QPCR Tissue Array (Origene). The reaction mix was set up on ice with the following components (per reaction); Taqman probe/primer set 2.5µl, 1x Taqman Universal PCR Master Mix (Catalogue no. 4304437; Applied Biosystems). The cycling parameters were; (1) 50^{o}C for 2 minutes, (2) 95^{o}C for 10 minutes, (3) 95^{o}C for 15 seconds, (4) 60^{o}C for 1 minute, (5) repeat steps (3) and (4) 40 times. The samples were ranked based on the $2^{(-\Delta\Delta Ct)}$ method.

2.3.4 Mutagenesis PCR

All plasmid mutagenesis reactions were carried out with the QuikChange II Site-Directed Mutagenesis Kit (Stratagene) as per manufacturer's instructions. For details of the primers and plasmids used see section 2.10.

2.4 General Protein Work

2.4.1 Bradford Assay

Sample protein concentrations were quantified by Bradford assay using Protein Assay Reagent (BioRad) as per manufacturer's instructions. A standard curve (0-20μg) was generated using bovine serum albumin (BSA) dissolved in water and the sample concentration was calculated from the values obtained from the standard curve. A Genequant Pro Spectrophotometer (GE Healthcare) was used to determine the absorbencies of the samples at 595nm.

2.4.2 Protein Extraction from Tissues and Cells

Unless stated in text, all protein preparations from tissues and cells were undertaken using phospho-RIPA buffer (50mM Tris, 150mM NaCl, 1mM EDTA, 1% NP40, 0.2% SDS, 10mM sodium pyrophosphate, 25mM β-glycerophosphate, 0.5% sodium deoxycholate, 100mM sodium orthovanadate, 5mM sodium fluoride, 2mM DTT, protease inhibitor cocktail tablets [Roche], pH7.4 with HCl). Following suspension in phospho-RIPA buffer, samples were incubated on ice for 10 minutes then passed 3-4 times through a 21-G needle. Some larger tissue samples required mechanical homogenisation with a pestle. The solution was then cleared by centrifugation at 13,000 rpm for 5 minutes at 4^{o}C.

2.4.3 Polyacrylamide Gel Electrophoresis (PAGE)

Polyacrylamide gel electrophoresis (SDS-PAGE) (Shapiro *et al.*, 1967) of protein samples was undertaken using Mighty Small II Gel Apparatus (Hoefer) with an HC PowerPac (BioRad). The gel pouring apparatus was ethanol then dH_2O cleaned and assembled, and the separating gel (0.375M Tris, 3.5mM SDS, 10-12% [v/v] acrylamide/bisacrylamide [29:1], 4.4mM APS, 6.7mM TEMED, pH8.8) was poured (0.75mm spacers). The separating gel was overlayed with dH_2O and left to set for 30 minutes. The water was then poured off and the stacking gel (0.125M Tris, 3.5mM SDS, 4% acrylamide/bisacrylamide [29:1], 4.4mM APS, 6.7mM TEMED, pH6.8) was poured and the comb inserted. Samples were heated to 99^{o}C for 5 minutes in 1x SDS-PAGE sample loading buffer (125mM Tris-HCl pH6.8, 2% SDS [w/v], 10% glycerol [v/v], 100mM DTT, 0.01% bromophenol blue [w/v]). The gels were run at 75-150V for 1-2 hours in 1x PAGE running buffer (25mM Tris, 190mM glycine, 3.5mM SDS, pH8.3). Benchmark and SeeBlue protein ladders (Invitrogen) were run as molecular weight markers. Some gels were run using the NuPAGE Bis-Tris Pre-Cast Gel System (Invitrogen) as per manufacturer's instructions. Briefly, protein samples were heated to 70^{o}C in 1x NuPAGE LDS Sample Buffer (Invitrogen) for 10 minutes. Gels were run at 100-200V (constant) for 45-90 minutes in 1x NuPAGE MOPS SDS Running Buffer (Invitrogen) with 500µl NuPAGE antioxidant (Invitrogen) added to the gel chamber. To stain the proteins, the gels were first washed 3 times in dH_2O for 10 minutes each wash. The gel was then incubated in GelCode Blue Stain Reagent (Thermo Scientific) from 1 hour to overnight before destaining in water.

2.4.4 Western Blotting

Transfer

Protein gels were incubated in 1x transfer buffer (25mM Tris, 200mM glycine, 20% methanol, pH7.4) for 5 minutes. Gels were transferred to Immobilon-P membrane (Millipore) using a V20-SBD semi-dry blotter (SCIE-PLAS) in a transfer cassette consisting of 3 pieces of blotting paper soaked in transfer buffer placed on the anode

plate, followed by the Immobilon membrane (rehydrated through methanol [1 minute] then 1x transfer buffer [3 minutes with rocking]), then the gel, and a further 3 pieces of blotting paper. Proteins were transferred at 75-100mA (constant) for 45-90 minutes. NuPAGE gels were transferred in an identical manner, except using 1x NuPAGE transfer buffer.

Blocking

Membranes were blocked in 1x Western Blocking Reagent (Roche) diluted in 1x TBS (10mM Tris, 140mM NaCl, pH7.4) or 5% non-fat dried milk powder (w/v) in TBST (0.1% Tween-20 [v/v], 1x TBS) depending on the primary antibody, for 2 hours at room temperature or overnight at 4^{o}C on a rocker. Primary antibodies were then prepared to the appropriate dilution (see table 2.1) in 0.5% Western Blocking Reagent or 5% milk TBST and applied to the membrane for 2 hours at room temperature or overnight at 4^{o}C on a rocker. Membranes were washed in TBST 3 times, for 5 minutes each wash. Secondary antibodies were applied at the appropriate dilution (see table 2.1) in 0.5% Western Blocking Reagent or 5% milk TBST and applied to the membrane for 1 hour at room temperature. Membranes were washed in TBST 3 or more times, for 15 minutes each wash and subjected to ECL (GE Healthcare) detection, as per manufacturer's instructions. The membranes were exposed to Hyperfilm ECL chemiluminescent film (GE Healthcare) unless otherwise stated and were developed through a Compact X4 Developer (XoGraph Imaging Systems).

2.4.5 TCA Precipitation of Proteins

Equal volumes of sample and 20% (v/v) trichloroacetic acid in water were mixed well and incubated on ice for 30 minutes. Samples were centrifuged at 13,000 rpm for 15 minutes then washed twice in acetone for 15 minutes each wash. Proteins were resolubilised in protein loading buffer.

2.4.6 Immunoprecipitation (IP)

1mg of protein lysate was incubated with 50µl of protein G sepharose beads (GE Healthcare) which had been washed 3 times in cold phosphor-RIPA buffer (see 2.4.2) and 1µg of the relevant antibody. The mixture was incubated for 4 hours at 4°C then the beads were washed six times in cold phosphor-RIPA buffer containing 300mM NaCl with centrifugation at 3,000 rpm (857 rcf) between washes. The beads were then were heated to 70°C in twice the bed volume of 2x NuPAGE LDS Sample Buffer (Invitrogen) for 10 minutes before being subjected to SDS-PAGE. Protein gels containing proteins labelled with ^{35}S were fixed in 3x 10 minute washes of fix solution (40% methanol, 10% acetic acid) followed by incubation in Enlightening solution (Perkin-Elmer) + 5% glycerol for 30 mins. The gels were then dried for 2 hours at 80°C in a BioRad 583 Gel Drier. The gel was then exposed to Kodak BioMax MR film overnight.

2.5 Recombinant Protein Generation

2.5.1 Recombinant Protein Inductions

BL21(DE3) *E. coli* cells were transformed with pET28c+ or pGEX6P1 vectors containing the gene of interest. Following transformation the cells were plated on LB agar plates containing an appropriate antibiotic and grown overnight at 37°C. Single colonies were picked and used to inoculate 5ml of LB media containing an appropriate antibiotic. The cultures were grown overnight at 37°C and the following day 0.5ml was used to inoculate 200ml of fresh LB media containing antibiotic and the cells grown to an optical density (O.D.) of 0.3-0.5. Isopropyl β-D-1-thiogalactopyranoside (IPTG) was then added to a final concentration of 1mM and the cells were grown for 4 hours at 22°C (pET28c+) or 3 hours at 37°C (pGEX6P1). The cells were then centrifuged at 4700 rpm for 15 minutes at 4°C and used, or frozen at -20°C. The cells were lysed as described below.

Antibody	Species Raised In	Supplier	Western Dil.
PABP1	Rabbit	N. Gray group	1/10,000
PABP4	Rabbit	N. Gray group	1/5,000
PABP5(164)	Rabbit	Atlas Antibodies	1/1,000
PABP5(165)	Rabbit	Atlas Antibodies	1/250
PABP5(Abnova)	Mouse	Abnova	1/1,000
GST	Goat	Abcam	1/5,000
Polyhistidine	Mouse	Sigma-Aldrich	1/1,000
T7	Mouse	Novagen	1/10,000
eIF4E	Rabbit	Cell Signalling Tech	1/1,000
Tubulin	Mouse	Sigma-Aldrich	1/5,000
GAPDH	Mouse	Abcam	1/1,000
LexA BD	Rabbit	Millipore	1/5,000
Gal4 AD	Mouse	BD Biosciences	1/10,000
Chicken α Goat (2^o)	Chicken	Santa Cruz	1/20,000
Goat α Mouse (2^o)	Goat	Pierce	1/20,000
Goat α Rabbit (2^o)	Goat	Sigma	1/100,000

Table 2.1 Primary and Secondary Antibodies. List of antibodies used in thesis, with dilutions used for Western blot.

2.5.2 His-PABP1 and His-PABP5 Protein Purification

Lysis buffer (20mM Tris-HCl pH8, 10mM imidazole, 150mM NaCl, 1mM DTT, 1x -EDTA protease inhibitor cocktail tablets [Roche], 1x BugBuster solution [Novagen], 25U/ml benzonase, 1KU/ml lysozyme) was added to the pelleted BL21(DE3) *E. coli* cells. The cells were then incubated on a turnwheel for 15

minutes at room temperature. The lysate was cleared by centrifugation at 4700 rpm and added to Ni-NTA agarose beads (Qiagen) which had been washed 3x in lysis buffer (centrifuging at 3,000 rpm [857 rcf] between washes). Following incubation on a coldroom turnwheel for 2 hours, the beads mixture was centrifuged at 3,000 rpm and the supernatant removed. The beads were washed 3x in wash buffer (20mM Tris-HCl pH8, 10mM imidazole, 300mM NaCl, 1mM DTT, 1x -EDTA protease inhibitor cocktail tablets [Roche]) on ice, centifuging at 3,000 rpm between washes, and the proteins were eluted in 3x 5 minute incubations in elution buffer (20mM Tris-HCl pH8, 250mM imidazole, 150mM NaCl, 1mM DTT, 1x -EDTA protease inhibitor cocktail tablets [Roche]) centifuging at 13,000 rpm between elutions. For column purifications, the same protocol was utilised except following the incubation of the Ni-NTA beads with the cell lysate, the mixture was transferred to a BioRad poly-prep chromatography column. Once the beads had settled, the column was washed 3 times with wash buffer and the proteins were eluted with elution buffer. All the washes and elutions were collected.

2.5.3 Quantification of Induced Proteins.

Serial dilutions of the recombinant proteins were prepared and subjected to SDS-PAGE alongside BSA standards (0-10µg). The protein gels were stained with SYPRO Ruby protein gel stain (Invitrogen) as per manufacturer's instructions. The gels were then scanned using a Typhoon Variable Mode Imager with a 488nm excitation laser for imaging and the proteins quantified using ImageQuant software (GE Healthcare).

2.6 Histological Analysis

2.6.1 Sectioning

Tissue samples were fixed in Bouins fluid (Clintech) overnight. Large samples such as testes were cut in half prior to immersion in Bouins. Samples were then washed in 70% ethanol followed by dehydration in increasing concentrations of alcohol, followed by xylene. The tissues were embedded in hot paraffin wax and 7µm sections were cut using a microtome and mounted on glass slides. Slides were incubated at 55°C overnight to dry.

2.6.2 Haematoxylin and Eosin Staining Tissues

The tissues were dewaxed in 3x 5 minute changes of xylene then rehydrated in 2x 5 minute washes of 100% ethanol, 1x 2 minute washes in each of 90%, 70%, 50%, 30% ethanol and finally 3x 2 minute washes in tap water. Slides containing the tissue sections were immersed in haematoxylin for 4 minutes then washed in tap water followed by acid/alcohol (1% HCl, 70% ethanol) for 5 seconds. The slides were washed again in tap water then immersed in lithium carbonate for 5 seconds followed by a 1-5 minute immersion in eosin. Following a brief immersion in water and then 3x 1 minute washes in 100% ethanol the tissue was cleared in 3x 5 minute incubations in xylene. The slides were mounted in Histomount (Invitrogen)

2.6.3 *In-situ* Hybridisation

Slides containing paraffin wax embedded tissue sections were placed in baked Coplin jars and immersed sequentially in the following: xylene (2x 5 minutes), 100% ethanol (2x 5 minutes), 90% ethanol (1x 5 minutes), 70% ethanol (1x 5 minutes), 0.2M HCl (1x 20 minutes), ddH_20 (2x 5 minutes), proteinase K solution (1x 25 minutes [2µg/ml proteinase K, 100mM Tris-HCl pH8, 50mM EDTA]), 0.2% (w/v) glycine precooled to 4^{o}C (1x 10 minutes), 0.1M triethanolamine-HCl (TEA) pH8 (1x

5 minutes), 0.1M TEA containing 0.004% (v/v) acetic anhydride (1x 10 minutes), 5x SSC (1x 15 minutes [750mM NaCl, 75mM sodium citrate, pH7]). The slides were then removed from the coplin jars and excess liquid removed. Prehybridisation buffer (50% [v/v] formamide, 3x SSC, 1x Denhardts solution) was then applied followed by coverslips and the slides were incubated for 2 hours at 50^{o}C in a humidified oven (100x Denhardts = 2% [w/v] Ficoll 400 [Pharmacia], 2% [w/v] polyvinylpyrrolidone, 2% [w/v] BSA). The hybridization mix (prehybridisation buffer containing 10% dextran sulphate, 100µg/ml yeast RNA [Ambion], 200µg/ml herring sperm DNA [Abcam]) was heated at 100^{o}C for 10 minutes to denature, then cooled on ice for 10 minutes. The digoxygenin labeled RNA probe was then added to the hybridization mix to a final concentration of 0.1-1ng/µl. The mixture was then heated to 65^{o}C and applied to the slides. Coverslips were added and the slides returned to the humidified oven overnight. The following day the slides were transferred to Coplin jars and incubated sequentially in the following: 2x SSC (1x 1 minutes), 2x SSC (1x 15 minutes), RNase A wash solution (1x 30 minutes at 37^{o}C [0.02mg/ml RNase A, 2x SSC]), 2x SSC (1x 15 minutes at 55^{o}C), 1x SSC (1x 15 minutes at 55^{o}C), 0.1x SSC (1x 15 minutes at 55^{o}C), buffer 1 (1x 5 minutes [100mM maleic acid pH7.4, 150mM NaCl]), 1x blocking solution (1x 30 minutes [buffer 1 containing 1x Roche blocking solution, 0.04% v/v fetal calf serum]). The anti-digoxygenin antibody conjugated to alkaline phosphatase (Roche) was centrifuged at 13,000 rpm for 5 minutes at 4^{o}C then 1µl was added to 200µl of 1x blocking solution and applied to the slides for 1 hour at room temperature. The slides were washed for 2x 15 minutes in buffer 1 and then equilibrated in buffer 2 (100mM Tris-HCl pH9.5, 0.1% v/v Tween-20, 0.5mg/ml levamisole) for 5 minutes. The BCIP/NBT substrate solution (Vector Laboratories) was then prepared in buffer 2 as per manufacturer's instructions and applied to the slides followed by a coverslip. Following sufficient colour development the reaction was terminated by incubating the slides in tap water. The tissues were counterstained with Nuclear FastRed Counterstain (Vector Laboratories) as per manufacturer's instructions and mounted in Histomount (Invitrogen).

2.6.4 Immunohistochemistry

The tissue sections were dewaxed and rehydrated as described in the *in-situ* hybridisation protocol. Following rehydration the slides were incubated in blocking solution (3% [v/v] hydrogen peroxide in methanol). Slides were sequentially washed in water then TBS and then incubated in blocking solution 2 (5% [v/v] goat serum, 5% [w/v] BSA in TBS) for 1 hour. After washing once in TBS the slides were treated with a Streptavidin-Biotin Blocking Kit (Vector Laboratories) as per manufacturer's instructions. The primary antibodies were diluted in blocking solution 2 (anti-PABP1: 1/10,000 and anti-PABP4: 1/500) and incubated overnight on the tissue at 4^{o}C. Slides were subsequently washed twice in TBS and incubated with biotin-conjugated secondary antibodies diluted in blocking solution 2 (anti-mouse: 1/500, anti-rabbit: 1/500). Slides were then washed twice in TBS, and incubated for 15 minutes with streptavidin conjugated to HRP (Vector Laboratories) which had been diluted 1/1000 in TBS. The slides were washed twice in TBS. The diaminobenzidinetrahydrochloride (DAB) was prepared using an ImmPACT DAB Kit (Vector Laboratories) and applied to the slides. The reaction was terminated by washing in tap water. The tissues were counterstained in haematoxylin for 1 minute followed by washing in water (1x 5 minutes), acid/alcohol (1x 5 seconds), water (1x 5 minutes), Scott's tap water (1x 30 seconds [20mM KHCO3, 81mM MgSO4.7H2O]), water (1x 5 minutes), 70% ethanol (1x 20 seconds), 95% ethanol (1x 20 seconds), 100% ethanol (2x 20 seconds), then xylene (2x 5 minutes). The slides were mounted in Pertex (Cell Path).

2.7 Cell Culture Techniques

2.7.1 Cell Culture

HeLa (human cervical carcinoma), 3T3 (mouse fibroblast), and L929 (mouse fibroblast) cells were maintained in 5% CO_2 in Dulbecco's minimal essential

medium (DMEM: Invitrogen) containing 10% fetal calf serum (FCS: Invitrogen) at 37°C. KK1 (transformed mouse granulosa) cells were grown in 5% CO_2 in DMEM-F12 media (Invitrogen) containing 10% fetal calf serum and supplemented with 4mM L-glutamine (Invitrogen) at 37°C. SK11 (transformed mouse Sertoli) cells were a kind gift from Dr Ian Adams (MRC Human Genetics Unit, Edinburgh). Cell passaging was performed by washing the cells twice in PBS that had been pre-warmed to 37°C and incubating with 10% trypsin in PBS for 2 minutes at 37°C. Cells were transferred to a 15ml centrifuge tube and pre-warmed media added. The cells were then centrifuged at 1,200 rpm (290 rcf) and the media aspirated. Following resuspension in pre-warmed media the cells were added to flasks containing pre-warmed media. To maintain stocks, cells were frozen down and stored in liquid nitrogen. To prepare the cells for freezing the cells were passaged as above, but following centrifugation were resuspended in 1ml of freeze mix (0.7ml media, 0.2ml FCS, 0.1ml DMSO) and transferred to a suitable cryovial. The cryovials were then wrapped in tissue, placed in a sealable plastic bag and moved to -80°C storage. The following day the cells were transferred to liquid nitrogen storage.

2.7.2 DNA Transfection

Cells were grown to 50-75% confluence and transfected with plasmid DNA using SuperFect transfection reagent (Qiagen) as per manufacturer's instructions. All transfections were undertaken using OPTIMEM media (Invitrogen).

2.7.3 Fixing and Imaging of Cells

For imaging cells were grown on 22mm x 22mm coverslips in 6-well plates. To fix the cells the media was aspirated and 4% paraformaldehyde in PBS was added for 15 minutes at room temperature on a rocker. The paraformaldehyde solution was aspirated and replaced with ice cold methanol for 10 minutes at room temperature, again with rocking. After a final wash in PBS the coverslips were dropped cell-side down onto droplets of Vectashield with DAPI (Vector Laboratories) on glass slides

to counterstain the cell nuclei. The coverslips were sealed onto the slides with Pang Supersolution (Pang [UK] Ltd). All fluorescent images were taken on a Coolsnap HQ CCD camera (Photometrics) on a Zeiss Axioplan II fluorescence microscope.

2.8 Pulldown Assays

2.8.1 Cap Chromatography

T75 flasks of cells were scraped in cold PBS containing 2mM benzamidine then centrifuged at 1,200 rpm for 5 minutes at 4^{o}C. The cells were resuspended in 200µl of lysis buffer (20mM MOPS.KOH pH7.2, 25mM KCl, 2mM $MgCl_2$, 2mM benzamidine, 2mM EGTA, 0.1mM GTP, 0.5mM DTT, 10% [v/v] glycerol, protease inhibitor cocktail tablets [Roche], 0.2% [v/v] IgePal [Rhodia Inc.], 0.4% [w/v] sodium deoxycholate) per T75 flask and incubated on ice for 20 minutes. The lysates were cleared by centrifugation at 13,000 rpm for 5 minutes at 4^{o}C and quantified by Bradford assay. 30µl of m^7G-sepharose (Amersham) bead slurry per point was washed twice in buffer 1 (20mM MOPS.KOH pH7.2, 20mM KCl, 2mM benzamidine, 7mM β-mercaptoethanol, 1mM magnesium acetate, 0.1mM GTP, 0.25% IgePal, protease inhibitor cocktail tablets) and 120µg of cell lysate was added. The volume was made up to approximately 250µl with buffer 1, and the beads were incubated on ice for 10 minutes with occasional gentle agitation. Following the incubation the beads were washed 2 times in buffer 1 and the factors were eluted in 25µl of protein loading buffer.

2.8.2 eIF4G-PABP Pulldowns

ANTI-FLAG M2 Affinity Resin (Sigma-Aldrich) was washed two times in binding buffer (50mM Tris-HCl pH7.5, 150mM NaCl, 1mM DTT, 0.5% [v/v] IgePal). 30µl resin slurry was used per point. The beads were incubated for 5 minutes in 1µg/µl BSA then washed a further two times in binding buffer. 200ng of the purified

recombinant FLAG-tagged eIF4G proteins were added to the resin along with 100µl of BL21 *E. coli* lysate containing the recombinant PABP proteins. The mixture was then incubated on a coldroom turnwheel for 3 hours then washed six times in binding buffer. The proteins were eluted in protein loading buffer.

2.8.3 PAIP-PABP Pulldowns

To bind GST-tagged PAIP proteins to glutathione sepharose 4B beads (GE Healthcare), 1ml of BL21 *E. coli* lysate induced to express GST, GST-PAIP-1 or GST-PAIP-2 was added to 300µl of bead slurry which had been washed two times in binding buffer (50mM Tris-HCl pH7.5, 100mM NaCl, 0.1% IgePal, protease inhibitor cocktail tablets). The mixture was incubated on a coldroom turnwheel for 3-4 hours. The beads were then washed five times in binding buffer, and could be stored at 4^{o}C in binding buffer containing 33% (v/v) glycerol. The amount of each GST protein bound per µl of beads was quantified as described in section 2.5.3. For the pulldown assay, beads containing equal quantities of the GST proteins were washed once in binding buffer, and 100µl of BL21 *E. coli* lysate induced to express PABP1 or PABP5 was added. The mixture was incubated on a coldroom turnwheel for 3 hours and then the beads were washed five times in wash buffer (50mM Tris-HCl pH7.5, 150mM NaCl, 0.1% [v/v] IgePal). The proteins were eluted in protein loading buffer.

2.9 *Xenopus laevis* Oocyte Techniques

2.9.1 Oocyte Preparation

Oocytes were collected from female Xenopus laevis frogs that were euthanised in 250ml water containing 4g 4-aminobenzoic acid for 20 minutes. The frogs were tested for their inability to 'right' themselves before delivering an intracardiac injection of 0.4ml euthatal. The neck was then dislocated and the heart removed.

The lobes containing oocytes were removed and bathed in 3 washes of 1x MMR (100mM NaCl, 2mM KCl, 5mM HEPES, 1mM $MgCl_2$, 2mM $CaCl_2$, 0.1% pen/strep). The lobes containing the oocytes were then gently torn open and incubated for 1 ½ hours in 5mg/ml collagenase B (Roche) on a turnwheel, then washed 6 times in 1x MMR.

2.9.2 Oocyte Microinjection

All microinjections were undertaken using a Harvard Apparatus (USA) Microinjector and a Narishige (Japan) Micromanipulator. Oocytes were viewed under a Leica MZ6 dissecting microscope. All microinjections were undertaken on stage VI oocytes which were sorted based on size and appearance, and 25 were injected per experimental point. The injection site was always the oocyte midline to avoid the nucleus, and each injection delivered approximately 50nl of RNA to the oocyte.

2.9.3 Tethered Function Assay

Oocytes were first injected with RNA encoding the MS2-fusion protein at a concentration of 1µg/µl. Following injection the oocytes were incubated at 18^{o}C for 6 hours before injection with reporter RNAs. Luciferase and β-galactosidase reporters were injected at 15ng/µl and 30ng/µl respectively. The oocytes were subsequently incubated overnight at 18^{o}C before assaying for luciferase and β-galactosidase. Prior to assaying any necrotic oocytes were discarded and the remaining oocytes were sorted into groups of 5. The MMR was removed and the oocytes were mechanically homogenised in 40µl lysis buffer (Tropix) per oocyte with a pestle. For the luciferase assay 5µl of oocyte extract was mixed with 100µl of Luciferase Assay Reagent (Promega) and the luciferase activity was measured using a Monolight 3010 Luminometer (Pharmingen). For the β-galactosidase assay, 2.5µl oocyte extract was added to 100µl of a 1/100 dilution of Galacton-Plus (Tropix) in Galacto Reaction Buffer Dilutent (Tropix). The samples were incubated at room

temperature in the dark for 1 hour before mixing in 100µl of Accelerator II Reaction Substrate (Tropix) and measuring β-galactosidase activity on the luminometer.

2.9.4 Radiolabelling of Oocytes

Injected oocytes were directly labelled by incubation in 1x MMR containing 5µl/ml of [^{35}S]-methionine (10µCi/ul - MP Biomedical UK) for 6 hours at 18^{o}C. Oocytes were lysed in 1x TE containing protease inhibitor cocktail tablets (Roche) with a pestle. Lysates were centrifuged at 13,000 rpm in a bench top centrifuge for 10 mins. The supernatant was removed to a fresh tube and respun for a further 10 mins. 15µl of the supernatant was mixed with 5µl 4x NuPAGE LDS sample buffer (Invitrogen) and heated at 75^{o}C for 10 mins before running on a NuPAGE Novex 4-12% Bis-Tris gel (Invitrogen). The gel was fixed in 3x 10 minute washes of fix solution (40% methanol, 10% acetic acid) followed by incubation in Enlightening solution (Perkin-Elmer) + 5% glycerol for 30 mins. The gel was then dried for 2 hours at 80^{o}C in a BioRad 583 Gel Drier. The gel was then exposed to Kodak BioMax MR film overnight.

2.9.5 Oocyte RNA Extraction

Groups of 10 oocytes were mechanically homogenised in 100µl Tri-Reagent using a pestle. Following homogenisation, the volume of the extract was increased by the addition of a further 300µl of Tri-Reagent. The lysates were centrifuged at 13,000 rpm in a bench top centrifuge for 10 mins at 4^{o}C and the supernatents were collected. 100µl of chloroform was added to each sample and vortexed for 15 seconds. The samples were then centrifuged at 13,000 rpm for 15 mins at 4^{o}C, the upper phase was collected, and the RNA precipitated by the addition of 250µl of isopropanol at room temperature followed by centrifugation at 13,000 rpm for 10 mins at 4^{o}C. The pellets were washed twice in 80% ethanol and resuspended in dH_2O.

2.9.6 QPCR RNA Stability Assay

Oocytes were injected as for the tether function assay and harvested at T=0 (immediately after injection of reporter RNAs) and T=16 (16 hours after injection of reporter RNAs). cDNA was prepared from the oocytes as above and QPCR analysis was performed using an ABI 7500 Fast Real-Time PCR System (Applied Biosystems) and measuring SYBR green incorporation with primers 5'-GGCGCGGTCGGTAAAGTT-3' and 5'-AGCGTTTTCCCGGTATCCA-3' for luciferase. The reaction mix was set up on ice with the following components; 0.5µM sense primer, 0.5µM antisense primer, 1x PowerSybr Mix (Applied Biosystems), cDNA 1µl. Data was presented as Ct scores, representing levels of luciferase RNA in the oocytes at time of harvesting.

2.10 Miscellaneous Methods

2.10.1 Cell-Free Translation Extracts

The cell-free HeLa translation extracts were a kind gift from Christian Thoma (University Hospital of Freiberg, Germany). The extracts had been prepared as previously described (Thoma *et al.*, 2004).

2.10.2 Programming the Cell-Free HeLa Extracts with mRNA

To prepare the cell-free translation extracts for programming with luciferase reporter mRNAs 4µl of extract per experimental point was initially centrifuged at 4000 rcf for 1 minute and then added to 6µl of reaction mix (0.06mM complete amino acid mix [Promega], 0.8mM ATP, 0.1mM GTP, 16mM HEPES pH7.6, 8U RNasin, 20mM creatine phosphate, 40µg/ml creatine kinase, 0.05mM spermidine, 2.5mM magnesium acetate, 40mM potassium acetate, 0-100ng reporter mRNA). The creatine kinase was reconstituted immediately prior to addition into the reaction mix. Additionally, once combined the reaction components were gently stirred rather than

vigorously pipetted to mix. The reaction was then incubated for 30 minutes at 37°C before being assayed in a luminometer using the same protocol as for oocytes in the tethered function assay (see section 2.9.3)

2.10.3 Micrococcal Nuclease Treatment of Extracts

The cell-free extracts were treated with micrococcal nuclease (0.01U per µl extract) and 1mM calcium acetate for 6 minutes at 26°C. The reaction was terminated by addition of EGTA to a final concentration of 2mM.

2.10.4 PABP Depletions from Cell-Free HeLa Extracts

GST and GST-PAIP-2 proteins were expressed in BL21 *E. coli* cells as described in section 2.5.1, and then lysed as described in section 2.5.2. 300µl of glutathione sepharose 4B bead slurry was washed three times in cold PBS and resuspended in 300µl HeLa cell extract then incubated on a coldroom turnwheel for 1 hour. The beads were then washed three times in cold PBS and resuspended in an equal volume of PBS to make a 50% slurry. Half of the slurry was added to BL21 *E. coli* lysate containing recombinant GST and half was added to lysate containing recombinant GST-PAIP-2. The mixture was incubated on a coldroom turnwheel for 3 hours before washing the beads three times in chilled buffer D (25mM HEPES.KOH pH7.3, 50mM KCl, 75mM potassium acetate, 2mM $MgCl_2$). As much buffer D was removed as possible following the final wash. Micrococcal nuclease treated extracts (see section 2.10.3) were added to the beads (approximately 3:1 ratio of extract to beads) and incubated on a coldroom turnwheel for 2 hours. The beads were then centrifuged at 6,000 rpm (3427 rcf) for 2 minutes at 4°C and the extract was removed. The whole protocol was repeated so the final extract had been subjected to two rounds of depletion. The extract was then Western blotted for the presence of PABP proteins to confirm the depletion had been successful.

2.10.5 Sucrose Gradient Fractionation

Pouring the Gradients

20-50% sucrose gradients were poured (20-50% sucrose dissolved in 15mM $MgCl_2$, 15mM Tris-HCl pH7.4, 300mM NaCl) using a dual chamber manual gradient pourer attached to a peristaltic pump. Following the pouring the gradients were balanced and left overnight at 4^{o}C to settle.

Cell Preparation

T75 flasks of cells (75-90% confluence) were treated with either 0.1mg/ml cycloheximide made up in ethanol for 7 minutes at 37^{o}C or 0.1mg/ml puromycin for 40 minutes at 37^{o}C. Following treatment the cells were removed to a coldroom and placed on a tray of ice, then washed twice in PBS containing 0.1mg/ml cycloheximide or puromycin. Cells were then lysed in 1ml lysis buffer (1% [v/v] triton-X-100 [Sigma-Aldrich], 15mM $MgCl_2$, 15mM Tris-HCl pH7.4, 300mM NaCl, 0.1mg/ml cycloheximide or puromycin, 100U RNasin) and scraped into centrifuge tubes. 200µg/ml heparin was added to the lysate followed by incubation on ice for 10 minutes. The lysates were cleared by centrifugation at 13,000 rpm for 5 minutes at 4^{o}C. The lysates were then carefully layered onto the surface of the sucrose gradients and centrifuged for 90 minutes at 39000 rpm at 4^{o}C in a Sorval TH-641 rotor.

Fraction Collection

The gradients were fractionated using a Superfrac fraction collector (Pharmacia) with the following settings: 10mV range, 0 zero suppression, 39 second fraction collect. The absorbance of RNA was measured at 254nm using an in-line UV monitor (Pharmacia) to allow identification of fractions containing mRNPs, 80S monosomes and polysomes. The proteins in each fraction were TCA precipitated and subjected to Western blotting.

2.10.6 Electrophoretic Mobility Shift Assay

The native protein gel was poured (1xTBE, 5% [v/v] acrylamide/bisacrylamide [60:1], 4.4mM APS, 6.7mM TEMED) between glass gel pouring plates (15cm by 20cm) using 1.5mm spacers) and allowed to set. The oligonucleotides AAAAAAAAAAAAAAAAAAAAAAAA and AUUUAUUUAUUUAUUUAUU UAUUUA utilised in this assay were 5'-labelled with Cy5 (Eurogentec). The reaction mixture was prepared on ice (10 or 20pmol labelled oligonucleotide, 10mM HEPES pH7.6, 5% [v/v] glycerol, 0.02% [v/v] NP40, 1mM DTT, 140mM KCl, 3mM MgCl2, 5µg/µl heparin, 40U RNasin, purified recombinant protein) and incubated on ice for 30 minutes. Protein loading buffer was then added and the mixture was electrophoresed at a constant 100V at 4^{o}C for 5-6 hours. Following electrophoresis the gel was removed from the glass plates and washed for 5 minutes in ddH_2O, then scanned using a Typhoon Variable Mode Imager.

2.11 Plasmids

All oligonucleotides (oligos) were purchased from Eurogentec unless otherwise stated.

2.11.1 IMAGE clones

IMAGE clone 6816124 (accession number: BC046233) was ordered from Geneservice and contains the full length *Mus musculus* (mouse) Pabp1 open reading frame (ORF).

IMAGE clone 40056131 (accession number: BC107362) was ordered from Geneservice and contains the full length mouse Pabp5 ORF.

IMAGE clone 6452933 (accession number: BC063113) was ordered from Geneservice and contains the full length *Homo sapiens* (human) PABP5 ORF.

2.11.2 Mutagenesis plasmids

pYXAsc-MmPab1(RRM2mut) was created by two rounds of PCR based site directed mutagenesis (see figure 4.17) of IMAGE clone 6816124 to introduce two silent restriction sites straddling RRM2. A BstB1 restriction site was introduced using oligos 5'-CGTGATCCATCACTTCGAAAAAGTGGAGTAGGCAA-3' and 5'-TTGCCTACTCCACTTTTTCGAAGTGATGGATCACG-3'. An Xma1 restriction site was then introduced using oligos 5'-CAGAGCTTGGAGCCCGGG CAAAGGAGTTC-3' and 5'-GAACTCCTTTGCCCGGGCTCCAAGCTCTG-3'. RRM2 was excised from the plasmid with BstB1 and Xma1 and replaced by the BstB1 and Xma1 cut RRM2 from pCRBluntII-MmPab5(RRM2mut).

pCRBluntII-MmPab5(RRM2mut) was created by two rounds of PCR based site directed mutagenesis (see figure 4.17) of IMAGE clone 40056131 to introduce two silent restriction sites straddling RRM2. A BstB1 restriction site was introduced using oligos 5'-TGGTCACAGCCAGATGACCGTCTTCGAAAGTCTGGAGTTG GAAATA-3' and 5'-TATTTCCAACTCCAGACTTTCGAAGACGGTCATCTG GCTGTGACCA-3'. An Xma1 restriction site was then introduced using oligos 5'-AGCAGCAGAAGTCAGAACCCGGGAAAGAGCAACATTTACCA -3' and 5'-TGGTAAATGTTGCTCTTTCCCGGGTTCTGACTTCTGCTGCT -3'. RRM2 was excised from the plasmid with BstB1 and Xma1 and replaced by the BstB1 and Xma1 cut RRM2 from pYXAsc-MmPab1(RRM2mut).

pYXAsc-MmPab1(M161V) was created by PCR based site directed mutagenesis (see figure 4.17) of IMAGE clone 6816124 to introduce a single point mutation into RRM2 of mouse Pabp1 using oligos 5'-CACTTTACGATCATTTAGAA

GCACCCCATTCATTTTTTCAATAG -3' and 5'-GAGCTATTGAAAAAATGAAT GGGGTGCTTCTAAATGATCGTAAAGTG-3'.

pCRBluntII-MmPab5(V167M) was created by PCR based site directed mutagenesis (see figure 4.17) of IMAGE clone 40056131 to introduce a single point mutation into RRM2 of mouse Pabp5 using oligos 5'-GGGCTATCTGGCACATGAAT GGAATGCGGCTCAATA-3' and 5'-TATTGAGCCGCATTCCATTCATGTGCC AGATAGCCC-3'.

2.11.3 Tethered function plasmids

pMSPN was supplied by Dr Nicola Gray (MRC Human Reproductive Sciences Unit, Edinburgh). An oligo (5'-GATCGGATCCAATTGACTAGT-3') was inserted into the BamHI site in pET-MS2 (described in Coller *et al.*, 1998).

pMSPN-U1A has been previously described (Gray *et al.*, 2000).

pMSPN-HsPab5 was created by PCR generation of a fragment containing the full length ORF of human PABP5 using oligos 5'-CAGTCAGCTAGCAT GGGGAGCGGGGAGCCTAATCCT-3' and 5'-CAGTCAACTAGTTCAGCACCT GCGCCTGGCCTG-3' using IMAGE clone 6452933 as a template. The PCR product was cut with Nhe1 and Spe1 and ligated into pMSPN which was linearised with Nhe1 and Spe1.

pMSPN-MmPab5 was created by PCR generation of a fragment containing the full length ORF of mouse Pabp5 using oligos 5'-CAGTCAGCTAGCATGAG TGGGGAGCCTAATACTGCTGGC -3' and 5'-CAGTCAACTAGTTCACCACCT GTGCCTAGCTTGCCC -3' using IMAGE clone 40056131 as a template. The PCR

product was cut with Nhe1 and Spe1 and ligated into pMSPN which was linearised with Nhe1 and Spe1.

pMSPN-hPABP1 was supplied by Dr Barbara Gorgoni (MRC Human Reproductive Sciences Unit, Edinburgh). The full length human PABP1 ORF was cloned into the Mfe1 and Spe1 sites in pMSPN.

pMSPN-xPABP has been previously described (Gray *et al.*, 2000).

pMSPN-MmPab1 was created by PCR generation of a fragment containing the full length ORF of mouse Pabp1 using oligos 5'-CAGTCAGCTAGCATGAACC CCAGCGCCCCC -3' and 5'-CAGTCAGGATCCTTAGACAGTTGGAACACC AGTGGC -3' using IMAGE clone 6816124 as a template. The PCR product was cut with Nhe1 and BamH1 and ligated into pMSPN which was linearised with Nhe1 and BamH1.

pMSPN-MmPab1(1-4) was created by PCR generation of a fragment containing RNA recognition motifs (RRMs) 1 - 4 of mouse Pabp1 using oligos 5'-CAGTC AGCTAGCATGAACCCCAGCGCCCCC -3' and 5'-CAGTCAGGATCCTCAGCG CTCTTCTTTGCGCTGAGC -3' using IMAGE clone 6816124 as a template. The PCR product was cut with Nhe1 and BamH1 and ligated into pMSPN which was linearised with Nhe1 and BamH1.

pMSPN-xPABP(1-4) has been previously described (Gray *et al.*, 2000).

pMSPN-MmPab1(RRM2mut) was created by PCR generation of a fragment containing the ORF of mouse Pabp1 with RRM2 of mouse Pabp5 using oligos 5'-CAGTCAGCTAGCATGAACCCCAGCGCCCCC -3' and 5'-CAGTCAGGATCC TTAGACAGTTGGAACACCAGTGGC -3' using pYXAsc-MmPab1(RRM2mut) as a template. The PCR product was cut with Nhe1 and BamH1 and ligated into pMSPN which was linearised with Nhe1 and BamH1.

pMSPN-MmPab5(RRM2mut) was created by PCR generation of a fragment containing the ORF of mouse Pabp5 with RRM2 of mouse Pabp1 using oligos 5'-CAGTCAGCTAGCATGAGTGGGGAGCCTAATACTGCTGGC -3' and 5'-CAGTCAACTAGTTCACCACCTGTGCCTAGCTTGCCC -3' using pCRBluntII-MmPab5(RRM2mut) as a template. The PCR product was cut with Nhe1 and BamH1 and ligated into pMSPN which was linearised with Nhe1 and BamH1.

pMSPN-MmPab1(M161V) was created by PCR generation of a fragment containing the ORF of mouse Pabp1 with a single point mutation in RRM2 using oligos 5'-CAGTCAGCTAGCATGAACCCCAGCGCCCCC -3' and 5'-CAGTCAGGATCC TTAGACAGTTGGAACACCAGTGGC -3' using pYXAsc-MmPab1(M161V) as a template. The PCR product was cut with Nhe1 and BamH1 and ligated into pMSPN which was linearised with Nhe1 and BamH1.

pMSPN-MmPab5(V167M) was created by PCR generation of a fragment containing the ORF of mouse Pabp5 with a single point mutation in RRM2 using oligos 5'-CAGTCAGCTAGCATGAGTGGGGAGCCTAATACTGCTGGC -3' and 5'-CAGTCAACTAGTTCACCACCTGTGCCTAGCTTGCCC -3' using pCRBluntII-MmPab5(V167M) as a template. The PCR product was cut with Nhe1 and BamH1 and ligated into pMSPN which was linearised with Nhe1 and BamH1.

pLG-MS2 has been previously described (Gray *et al.*, 2000).

pJK-350 has been previously described (Evans *et al.*, 1994).

2.11.4 Yeast 2-hybrid plasmids

pBTM was created by Dr David Bernstein. A kanamycin resistance cassette was inserted into the ampillicin gene of pBTM116 by transposition.

pBTM-HsPab5 was created by PCR generation of a fragment containing the ORF of human PABP5 using oligos 5'-CAGTCAGAATTCATGGGGAGCGGGGA GCCTAATCC-3' and 5'-CAGTCAGGATCCTCAGCACCTGCGCCTGGCCT GGCC-3' using pMSPN-HsPab5 as a template. The PCR product was cut with EcoR1 and BamH1 and ligated into pBTM which was linearised with EcoR1 and BamH1.

pBTM-MmPab5 was created by PCR generation of a fragment containing the ORF of mouse Pabp5 using oligos 5'-CAGTCAGAATTCATGAGTGGGGAGCCT AATACT -3' and 5'-CAGTCAGGATCCTCACCACCTGTGCCTAGC -3' using pMSPN-MmPab5 as a template. The PCR product was cut with EcoR1 and BamH1 and ligated into pBTM which was linearised with EcoR1 and BamH1.

pBTM-MmPab1(1-4) was created by PCR generation of a fragment containing RNA recognition motifs (RRMs) 1 - 4 of mouse Pabp1 using oligos 5'-CAGTCAGAATTCATGAACCCCAGCGCCCCC -3' and 5'-CAGTCAGGATCCT CAGCGCTCTTCTTTGCGCTGAGC -3' using IMAGE clone 6816124 as a template. The PCR product was cut with EcoR1 and BamH1 and ligated into pBTM which was linearised with EcoR1 and BamH1.

pBTM-xPAB1-2 has been previously described (Gray *et al.*, 2000).

pGAD-eIF1A, pGAD-eIF1, pGAD-eIF2α, pGAD-eIF2β, pGAD-eIF3S1, pGAD-eIF3S2, pGAD-eIF3S3, pGAD-eIF3S4, pGAD-eIF3S5, pGAD-eIF3S6, pGAD-eIF3S7, pGAD-eIF3S8, pGAD-eIF4AII, pGAD-eIF4H, pACTII-eIF4B, pACT-eIF4E, pGAD-eIF5, pGAD-eIF5A, and pACT-eIF5B were cloned within the laboratory of Dr Nicola K. Gray (MRC Human Reproductive Sciences Unit, Edinburgh) by Dr Barbara Gorgoni, Dr Gavin Wilkie, William Richardson and Dr Nicola K. Gray.

pACT-IRP has been previously described (SenGupta *et al.*, 1996).

pACT-hPaip1 has been previously described (Gorgoni *et al.*, 2005).

pACT2-hPaip2 was created by PCR generation of a fragment containing the ORF of human Paip2 using oligos 5'- CAGTCACCATGGCTATGAAAGATCCAAGTC GCAGC-3' and 5'- CAGTCAGGATCCTCAAATATTTCCGTACTTCACCCC-3' using pGEX6P1-HsPaip2 as a template. The PCR product was cut with Nco1 and BamH1 and ligated into pACT2 which was linearised with Nco1 and BamH1.

pACT-4GNT has been previously described (Gray *et al.*, 2000).

pBTM-MmPab1(RRM2mut) was created by PCR generation of a fragment containing the ORF of mouse Pabp1 with RRM2 of mouse Pabp5 using oligos 5'-CAGTCAGAATTCATGAACCCCAGCGCCCCC -3' and 5'-CAGTCAGGATC CTTAGACAGTTGGAACACCAGTGGC-3' using pYXAsc-MmPab1(RRM2mut) as a template. The PCR product was cut with EcoR1 and BamH1 and ligated into pBTM which was linearised with EcoR1 and BamH1.

pBTM-MmPab5(RRM2mut) was created by PCR generation of a fragment containing the ORF of mouse Pabp5 with RRM2 of mouse Pabp1 using oligos 5'-CAGTCAGAATTCATGAGTGGGGAGCCTAATACT -3' and 5'- CAGTCAGGAT CCTCACCACCTGTGCCTAGC -3' using pCRBluntII-MmPab5(RRM2mut) as a template. The PCR product was cut with EcoR1 and BamH1 and ligated into pBTM which was linearised with EcoR1 and BamH1.

pBTM-MmPab1(M161V) was created by PCR generation of a fragment containing the ORF of mouse Pabp1 with a single point mutation in RRM2 using oligos 5'-CAGTCAGAATTCATGAACCCCAGCGCCCCC -3' and 5'- CAGTCAGGAT CCTTAGACAGTTGGAACACCAGTGGC -3' using pYXAsc-MmPab1(M161V) as a template. The PCR product was cut with EcoR1 and BamH1 and ligated into pBTM which was linearised with EcoR1 and BamH1.

pBTM-MmPab5(V167M) was created by PCR generation of a fragment containing the ORF of mouse Pabp5 with a single point mutation in RRM2 using oligos 5'- CAGTCAGAATTCATGAGTGGGGAGCCTAATACT -3' and 5'- CAGTCAGGATCCTCACCACCTGTGCCTAGC -3' using pCRBluntII-MmPab5(V167M) as a template. The PCR product was cut with EcoR1 and BamH1 and ligated into pBTM which was linearised with EcoR1 and BamH1.

2.11.5 Other plasmids

pCGN has been previously described (Tanaka and Herr, 1990).

pCGN-MmPab1 was created by PCR generation of a fragment containing the full length ORF of mouse Pabp1 using oligos 5'-CAGTCATCTAGAATGAAC CCCAGCGCCCCCAGCTAC -3' and 5'-CAGTCAGGATCCTTAGACAGTTGG AACACCAGTGGCACTG -3' using pMSPN-MmPab1 as a template. The PCR

product was cut with Xba1 and BamH1 and ligated into pCGN which was linearised with Xba1 and BamH1.

pCGN-MmPab5 was created by PCR generation of a fragment containing the full length ORF of mouse Pabp5 using oligos 5'-CAGTCATCTAGAATGAGTG GGGAGCCTAATACTGCTGGC -3' and 5'-CAGTCAGGATCCTCACCACCTGT GCCTAGCTTGC -3' using pMSPN-MmPab5 as a template. The PCR product was cut with Xba1 and BamH1 and ligated into pCGN which was linearised with Xba1 and BamH1.

pCGN-SF2 was a kind gift from Dr J. Long.

pEGFP-MmPab1 was created by PCR generation of a fragment containing the full length ORF of mouse Pabp1 using oligos 5'-CAGTCAGTCGACATGAAC CCCAGCGCCCCCAGCTAC -3' and 5'-CAGTCAGGATCCTTAGACAGTTGGA ACACCAGTGGCACTG -3' using pMSPN-MmPab1 as a template. The PCR product was cut with Sal1 and BamH1 and ligated into pEGFP-C1 (Clontech) which was linearised with Sal1 and BamH1.

pEGFP-MmPab5 was created by PCR generation of a fragment containing the full length ORF of mouse Pabp5 using oligos 5'-CAGTCAGTCGACATGAGT GGGGAGCCTAATACTGCTGGC -3' and 5'- CAGTCAGGATCCTCACCACCT GTGCCTAGCTTGC -3' using pMSPN-MmPab5 as a template. The PCR product was cut with Sal1 and BamH1 and ligated into pEGFP-C1 (Clontech) which was linearised with Sal1 and BamH1.

pGEX6P1-HsPAIP-1 was a kind gift from Dr Barbara Gorgoni.

pGEX6P1-HsPAIP-2 was a kind gift from Dr Barbara Gorgoni.

pGEM-MmPab1(ISH) contained sequence derived from the 3'-UTR of mouse Pab1. The vector was linearised and used as a template for the *in-vitro* transcription of Pabp1 *in-situ* hybridisation probes. The construct was a kind gift from Dr Matthew Brook.

pGEM-MmPab5(ISH) was created by PCR generation of a fragment containing the 5'-UTR of mouse Pabp5 using oligos 5'-CGGTCATCTGGCTGTGACCAC-3' and 5'-GCGGCTGCCAGTCAGTCC-3' using mouse brain cDNA as a template. The PCR product was cloned into pGEM-T-easy (as per manufacturer's instructions) via A-overhangs incorporated by the PCR enzyme. The vector was linearised and used as a template for the *in-vitro* transcription of Pabp5 *in-situ* hybridisation probes.

2.12 Supplier List

Abcam..... Cambridge, UK

Ambion..... Austin, TX, USA

Amersham..... see GE Healthcare

Applied Biosystems..... Carlsbad, CA, USA

Bio-Rad..... Hemel Hempstead, UK

Biotium..... Hayward, CA, USA

Cell Path..... Hemel Hempstead, UK

Clintech..... Guilford, UK

Clontech..... Mountain View, CA, USA

EmbiTech..... San Diego, CA, USA

Eppendorf..... Cambridge, UK

Eurogentec..... Seraing, Belgium

Finnzymes..... Espoo, Finland

GE Healthcare..... Amersham, UK

Harvard Apparatus..... Kent, UK

Hoefer..... Holliston, MA, USA

Invitrogen..... Paisley, UK

Millipore..... Billerica, MA, USA

MP Biomedicals UK..... Cambridge, UK

Nanodrop Technologies Inc..... Wilmington, DE, USA

Narishige (Japan)..... London, UK

New England Biolabs..... Hitchin, UK

Novagen..... Nottingham, UK

Pang UK..... Suffolk, UK

Perkin-Elmer..... Beaconsfield, UK

Pharmacia..... Uppsala, Sweden

Pharmingen (BD Biosciences)..... Oxford, UK

Photometrics Ltd..... Tuscon, AZ, USA

Promega..... Southampton, UK

Qiagen..... Crawley, UK

Rhodia..... Watford, UK

Roche..... Welwyn Garden City, UK

Sigma-Aldrich..... Gillingham, UK

Stratagene..... Cedar Creek, TX, USA

Tropix..... see Applied Biosystems

Vector Laboratories..... Peterborough, UK

Chapter 3: Expression of PABP5

3.1 Introduction and Aims

Human poly(A)-binding protein 5 (PABP5) was originally identified during an exon trapping study. Subsequent RACE analysis using a fetal brain cDNA library yielded an extension product that matched a testis GenBank cDNA clone, as well as brain and fetal testis ESTs. A theoretical mRNA was compiled from available EST and RACE data that contained a polyadenylation signal in good context and a polyadenylate tail (Blanco *et al.*, 2001) implying that it is an expressed gene. Subsequent RT-PCR analysis by Blanco *et al*. using a human cDNA panel showed expression in various compartments of human brain and also within the ovary. The EST information available for human PABP5 partially overlaps with this data, with 6 out of the 16 existing ESTs being derived from human brain cDNA libraries. While this preliminary expression is available for humans, the expression of PABP5 in mouse is completely unknown and EST data is not available.

Other murine poly(A)-binding proteins display distinct yet overlapping RNA and protein tissue expression patterns. Western blotting data has shown both mouse PABP1 and PABP4 to have wide-ranging yet distinct expression patterns (Hannah Burgess, unpublished) with PABP1 expression highest in ovary and testis, and PABP4 showing robust expression within the heart. Interestingly, some tissues such as liver express both proteins, and unexpectedly tissues such as kidney appear to express neither. tPABP and ePABP have more limited expression patterns with tPABP being restricted to the pachytene spermatocytes and round spermatids of the testis (Kimura *et al.*, 2009), and ePABP, the predominant PABP protein prior to the onset of zygotic transcription during early development, is restricted to germ cells within adult ovary and testis (Seli *et al.*, 2005; Wilkie *et al.*, 2005).

In this chapter I examine the expression of PABP5, primarily in mouse tissues, and compare the cellular distribution of PABP5 with that of PABP1 and PABP4 in the mouse gonads, as these tissues express multiple PABP proteins.

3.2 *In-silico* Analysis of the PABP5 Gene

The human PABP5 gene codes for a putative 383 amino acid protein of predicted molecular weight 43.3kDa. The PABP5 gene contains only two exons with an uninterrupted ORF suggesting it arose via a retroposition event like tPABP (Kleene *et al.*, 1998). Although PABP5 is considered to be a PABP family member based on phylogeny (Gorgoni and Gray, 2004; Mangus *et al.*, 2003) the dN/dS ratio of PABP5 was calculated (see figure 3.1). dN is the non-synonymous nucleotide substitution rate and dS is the synonymous rate, therefore dN/dS is a measure of the history of selection for change in the gene, with low values indicating a selective pressure to maintain the gene sequence. The dN/dS ratio for the human PABP5 gene versus mouse PABP5 is 0.043. The 30 genes immediately adjacent to PABP5 were also analysed with the average calculated to be 0.18, which is slightly higher than the genome average (0.17). The average ratio for all genes on the X-chromosome is 0.41, implying that PABP5 has been under strong selective constraint in contrast to other genes on the X-chromosome. Upon plotting the distribution of dN/dS ratios in a histogram across the entire genome and the X-chromosome, PABP5 falls into the top 20% of genes under the strongest conservative pressure (see figure 3.1).

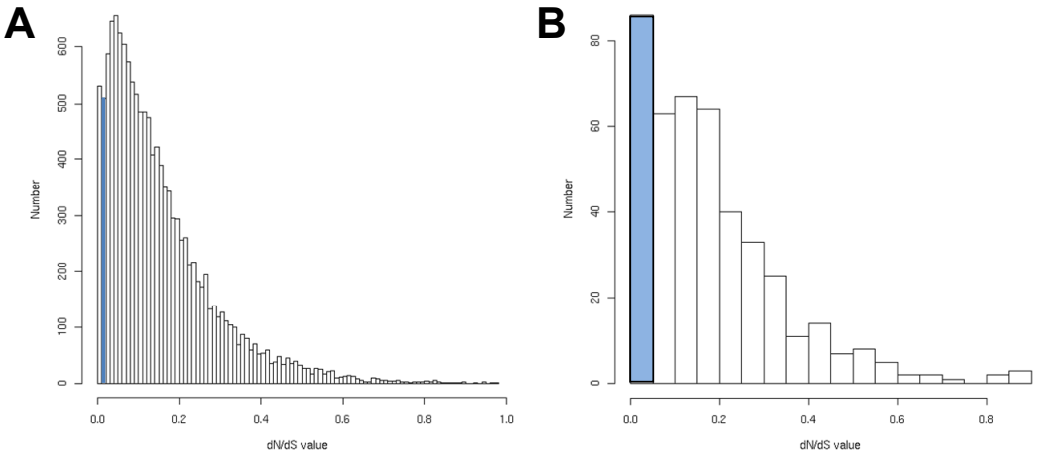

Figure 3.1 dN/dS ratios for the PABP5 gene. A. dN/dS ratio distribution - human vs. mouse genome. **B.** dN/dS ratio distribution - human vs. mouse X-chromosome genes. Blue bar represents location of PABP5 within the distribution. dN/dS ratios were calculated using MEGA2 – Molecular Evolutionary Genetic Analysis Software, Version 2 (2001) by Philippe Gautier, Bioinformatics Department, MRC Human Genetics Unit, Edinburgh.

Another useful measure of functionality is the conservation of promoter sequences. Distal enhancer, silencer and insulator sequences can be located from 10-50kb upstream or downstream of the transcription start site, but eukaryotic core promoter elements and any associated binding sites for proximal regulatory factors tend to be located within a few hundred base pairs of the transcriptional start site (Levine and Tjian, 2003). The promoter sequences for PABP5 have yet to be established, but high conservation within the region immediately upstream of the gene could suggest a conservative selective pressure. A percentage identity plot (PIP) was generated to assess whether potential upstream promoter sequences were conserved across mammalian species as an indicator of functionality (see figure 3.2). The baseline was set as human, with range of 50%-100% for the plot. The PIP shows that while the conservation is not particularly striking, the 1-2kb immediately upstream and 4-5kb downstream are relatively well conserved suggesting a selective pressure to maintain the sequence. These data support the assignment of PABP5 as a functional PABP family member.

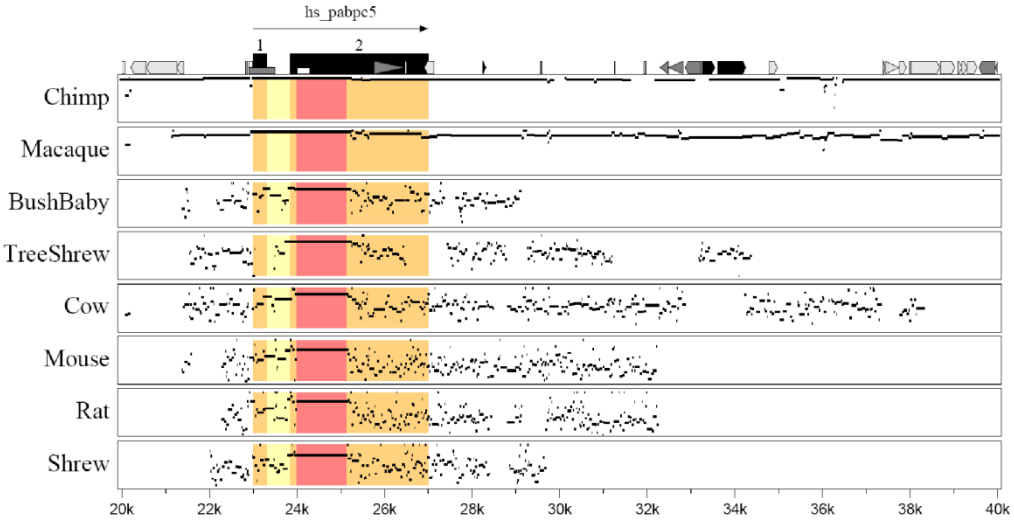

Figure 3.2 Percentage identity plot of the PABP5 gene. The human PABP5 gene was set as the baseline with a 50%-100% range. Colour code: red=coding, light orange=UTR's, light yellow=intron. Analysis was undertaken with GeneDoc version 2.0.1 (1997) by Philippe Gautier, Bioinformatics Department, MRC Human Genetics Unit, Edinburgh.

3.3 Expression Analysis of Human PABP5 mRNA

Most expression analysis of the mammalian poly(A)-binding proteins to date has been undertaken at the level of RNA, due to the high sequence homology at the protein level making it difficult to generate specific antibodies. RT-PCR analysis of PABP5 mRNA expression has only been undertaken on a limited panel of human tissues (Blanco *et al.*, 2001). To expand our knowledge of PABP5 expression in humans, quantitative PCR (qPCR) using a FAM labelled Taqman primer/probe set specific for PABP5 (Applied Biosystems) was undertaken on an Origene Human TissueScan Array (see figure 3.3), prepared from 48 human tissues. The cDNA is pre-normalised to β-actin by first northern blotting the mRNA preparations with probes specific for β-actin and adjusting the amount of mRNA added to each reverse-transcription reaction accordingly. This method of normalisation does not take into account the efficiency of individual reverse-transcriptase reactions. Following the qPCR reaction the tissues were ranked based on the $2^{(-\Delta\Delta Ct)}$ method. The brain ranked 3rd highest for PABP5 expression, correlating with previous data (Blanco *et al.*, 2001) but intriguingly the tissues ranked 1st, 2nd, and 4th for PABP5 expression were all tissues of secretory nature – the thyroid, adrenal, and pituitary glands respectively. Given the relative high level of PABP5 expression in the pituitary gland versus the whole brain, it would seem plausible that it might represent the major site of PABP5 expression within the brain. Unexpectedly, the ovary was one of the lowest ranked tissues in the panel, in disagreement with Blanco *et al*, who described the ovary as a major site of PABP5 expression in humans. Further qPCR experiments, utilising cDNA prepared from selected human tissues would need to be undertaken to determine if this discrepancy is an artefact of the TissueScan array pre-normalisation method.

3.4 Expression Analysis of Mouse PABP5 mRNA

The expression pattern of PABP5 mRNA in mouse tissues has not been addressed. The availability of tissue and the tractability of mouse as a model organism make it an ideal model in which to study the expression and function of PABP5. As an

initial approach towards determining the expression of PABP5 in mouse tissues PABP5 specific oligonucleotide primers were generated to investigate the expression of PABP5 mRNA by RT-PCR. These primers were designed to generate a 517bp amplicon and spanned the 5' intron of PABP5 to allow the identification of any contaminating genomic DNA in the RNA preparation. An additional advantage of designing primers against 5'-UTR sequence within the PABP5 transcript is that sequence homology between poly(A)-binding protein mRNAs is low within these regions. mRNA was extracted from a panel of adult mouse tissues of CD1 background and subjected to reverse-transcription followed by PCR (see figure 3.4). PABP5 was only detectable after 33 PCR cycles implying that it is a relatively low abundance transcript and appears to display a tissue specific expression pattern. The highest levels of expression was in the brain of both sexes and the ovary. Testis, heart and lung also display relatively high levels of expression. Interestingly, the relative expression levels between male and female appear to be roughly similar in these tissues, implying that PABP5 is subjected to X-inactivation in females. PABP5 was beneath detection in male but not female kidney, although this was not always observed and likely represents experimental variation due to the low levels of PABP5. Comparison with previous human RT-PCR data (Blanco *et al.*, 2001) would imply a partially conserved expression pattern between these species. Given the discrepancy between the PABP5 RT-PCR (Blanco *et al.*, 2001) and qPCR data sets (figure 3.3) regarding the expression of PABP5 in the human ovary, the mouse RT-PCR results would appear to be consistent with the analysis by Blanco *et al*., (see 3.11 for discussion).

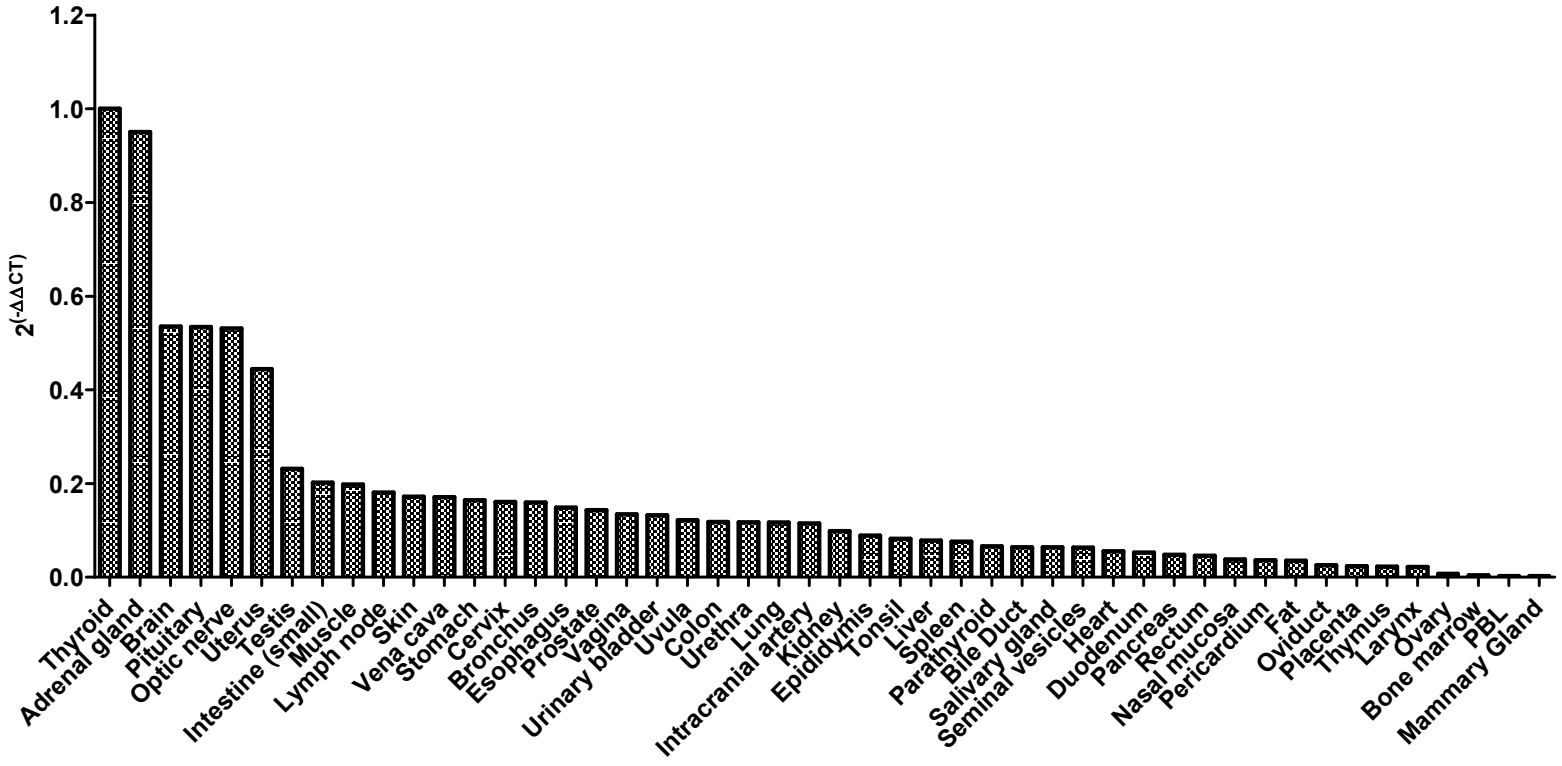

Figure 3.3 PABP5 qPCR on Origene human TissueScan array. Data is plotted as relative copy number by the $2^{(-\Delta\Delta Ct)}$ method on the Y-axis. The amount of cDNA in each reaction was pre-normalised to β-actin levels in each tissue, and $2^{(-\Delta\Delta Ct)}$ was calculated using thyroid as a reference standard. Results are the mean of two separate TissueScan arrays. With the exception of optic nerve, pituitary and skin, the $2^{(-\Delta\Delta Ct)}$ values obtained for each sample in the two arrays varied by no more than 0.2. PBL = plasma blood leucocytes.

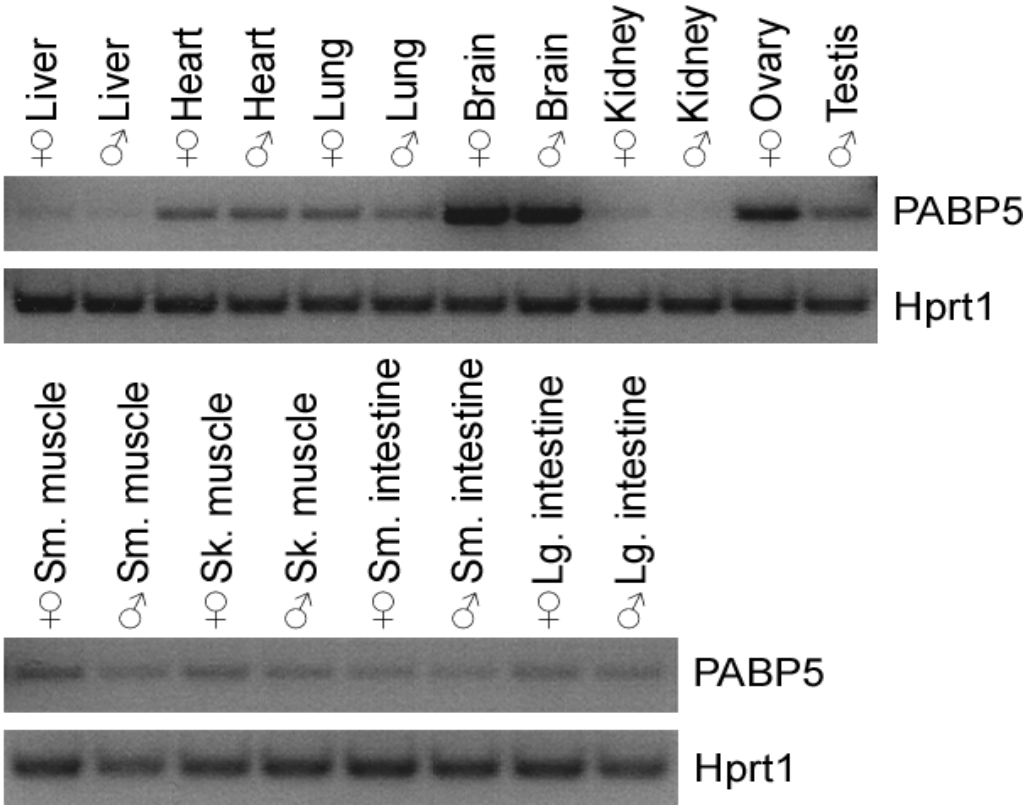

Figure 3.4 PABP5 mouse tissue RT-PCR. Mouse tissue was CD1 background and mice were approximately age matched. RT-PCR was run for 33 cycles and electrophoresed in a 1.5% TAE agarose gel. Primers were used to amplify a 350bp product from the Hprt1 transcript as a loading control. Sm. muscle = smooth muscle, Sk. muscle = skeletal muscle, Sm. intestine = small intestine, Lg. intestine = large intestine. Relative expression was highest in mouse brain and ovary. The RT-PCR reaction was performed twice with cDNA prepared from two separate mice.

3.5 Expression of PABPs in the Mammalian Gonads

Very little is known regarding the cellular distribution of the PABP family of proteins below the whole tissue level. Determining expression of PABPs at the cellular level could give insight into the physiological roles of these proteins and also raises interesting questions with respect to their relative functions. In particular, to understand PABP5 function it is important to determine whether the low levels of PABP5 represent low ubiquitous expression or high levels of expression in certain cell types and whether PABP5 is co-expressed with other PABP proteins. Gonadal tissues were chosen for analysis as they express the greatest number of PABP

proteins and represent the only tissues where any cellular expression patterns have been delineated (see below). To this end reagents specific to PABP1, PABP4 and PABP5 were generated to probe mouse histological tissue sections to determine the localisation of these PABP species.

Although limited analysis is available, the cellular distribution of poly(A)-binding proteins within mammalian gonads are still poorly understood. The histological information available pertains to the expression of ePABP, tPABP and PABP1 only. In the testis, tPABP mRNA has been shown to be present within pachytene spermatocytes and round spermatids within the seminiferous tubules by northern blot on enriched cell populations from mouse testis (Kleene *et al.*, 1994). This data overlaps with expression of human tPABP mRNA, although it appears to be absent or below the detection threshold in pachytene spermatocytes by both northern blot and *in-situ* hybridisation (Feral *et al.*, 2001). PABP1 mRNA expression in mouse testis has been documented in spermatocytes and round spermatids by northern blot (Gu *et al.*, 1995; Kleene *et al.*, 1994), and this situation is replicated in human testis (Feral *et al.*, 2001) but with the interesting observation that the protein is also present in elongating spermatids in the absence of PABP1 mRNA. In the ovary only the distribution of ePABP mRNA has been examined in mouse by *in-situ* hybridisation showing that expression is restricted to oocytes (Seli *et al.*, 2005).

3.6 Expression of PABPs in the Mouse Testes

The gonads are part of both the reproductive system and the endocrine system, being responsible for the production of gametes (via spermatogenesis and oogenesis in the testis and ovary respectively) and also sex hormones. The gonads are therefore complex organs composed of both germ cells and somatic cells.

In males, spermatogenesis is the process by which haploid gametes are generated. It occurs within the seminiferous tubules of the testis where spermatogonial stem cells

divide to produce diploid primary spermatocytes. The cellular composition of seminiferous tubules is shown in figure 3.5A and 3.5B. Two meiotic divisions results in 4 spermatids which mature through a process called spermiogenesis into round spermatids and then elongating spermatids (characterised by the presence of a tail, an acrosome and nuclear protamines). The germ cells are now referred to as spermatozoa. A process termed spermiation then results in the release of these spermatozoa into the lumen of the seminiferous tubule where further maturation results in fertilisation competent sperm. The somatic component of seminiferous tubules plays a significant role in germ cell development. In males, luteinising hormone signalling results in the production of the steroid hormone testosterone by the somatic Leydig cells of the testis. Testosterone is important in directing the process of spermatogenesis via androgen receptor signalling. Sertoli cells produce androgen binding-protein in response to follicle stimulating hormone signalling, and androgen binding-protein functions in concentrating testosterone in the luminal fluid of the seminiferous tubules.

To gain a preliminary insight into the distribution of PABP1, PABP4, tPABP and PABP5 between the somatic and germ cell components of seminiferous tubules RT-PCR was performed on cDNA prepared from the testes of wild-type or Dazl -/- mice (see figure 3.6A). Dazl is an RNA binding protein that is expressed in germ cells and is essential for gametogenesis. Dazl knockout mice display defects in spermatogenesis (see figure 3.5C), with a severe reduction of germ cells beyond the spermatogonial stage in seminiferous tubules (Ruggiu *et al.*, 1997). Thus, mRNAs expressed only in later stages of spermatogenesis will be reduced or absent in Dazl -/- mouse testes. Both tPABP and PABP1 mRNAs are essentially absent from the Dazl -/- testes cDNA preparations indicating that these mRNAs are present in post-spermatogonial germ cells, consistent with published data (Feral *et al.*, 2001; Gu *et al.*, 1995; Kleene *et al.*, 1994). Interestingly, PABP4 mRNA appears to be present in Dazl -/- testes indicating that PABP4 is partially or wholly contained within the somatic components of the testis.

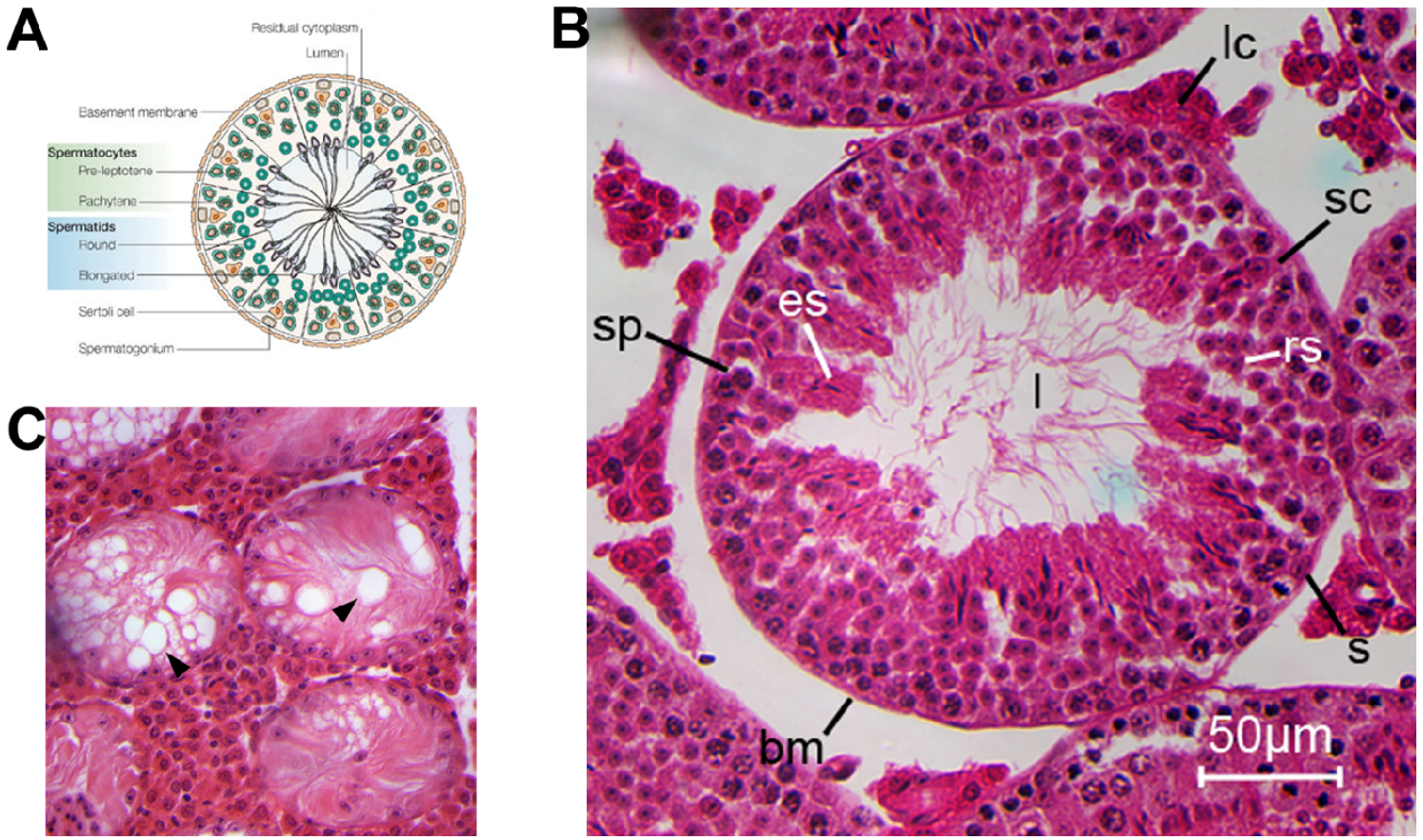

Figure 3.5 Haematoxylin and eosin staining of mouse seminiferous tubules. A. Schematic of a seminiferous tubule cross section. Adapted from Krawetz, 2005. **B.** 7µm sections were cut from wax embedded mouse testis. Seminiferous tubule cross section. BM=basal lamina, LC=leydig cell, S=spermatogonia, SP=spermatocyte, RS=round spermatid, ES=elongating spermatid, SC=sertoli cell, L=lumen. **C.** Dazl -/- testis phenotype. Loss of post-spermatogonial germ cells (indicated by black arrows). Dazl-/- tissue was a kind gift from Mary Taggart, MRC Human Genetics Unit, Edinburgh.

When an RT-PCR reaction was performed using PABP5 specific primers (see figure 3.6B) a signal was observed in the Dazl -/-testes cDNA suggesting that PABP5 is not restricted to germ cells within testes. Intriguingly there was an apparent enrichment of PABP5 within Dazl -/- testis implying that perhaps PABP5 is expressed predominantly within somatic testis cells although *in-situ* hybridisation or immunohistochemistry would be required to corroborate this statement.

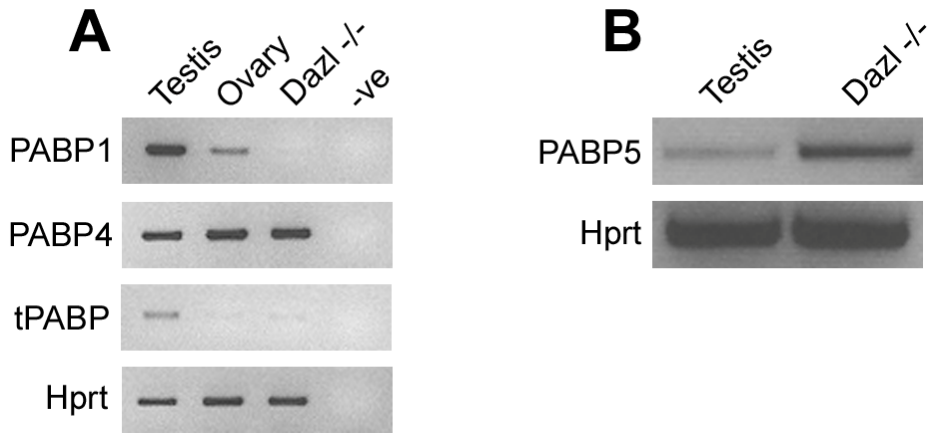

Figure 3.6 Dazl -/- RT-PCRs. cDNA was prepared from adult testes and ovaries of wild-type mice. cDNA was also prepared from the testis of Dazl -/- mice. These cDNA preparations were subjected to PCR using primers specific to (**A**) PABP1, PABP4, tPABP and Hprt or (**B**) PABP5 and Hprt. All mice were MF1 background.

3.7(A) Cellular Distribution of PABP1 and PABP4 in Mouse Testis

Immunohistochemical analysis of both PABP1 and PABP4 was performed using rabbit polyclonal antibodies generated against each protein. The peptides used to immunise the rabbits were conserved between mouse and human so that the antibodies could be used in a variety of mammalian species. In addition, they were designed against the C-terminal regions of the proteins where there is significant sequence divergence between PABP family members to minimise likelihood of cross-reactivity (see figure 3.7 for location of the peptides).

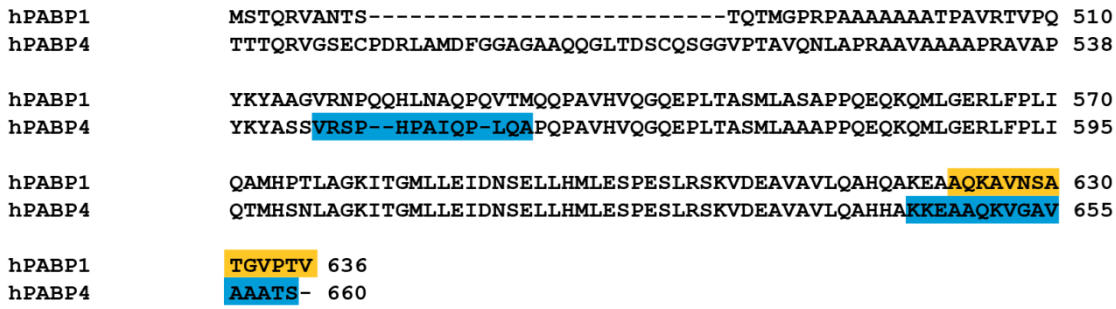

Figure 3.7 Location of peptides used to generate antibodies. Blue text denotes the peptides used to generate the PABP4 antibodies and yellow denotes the peptides used to generate the PABP1 antibodies.

The antibodies were tested by Western blotting against PABP1 and PABP4 recombinant proteins and no cross reactivity was detected (Hannah Burgess, unpublished). PABP5 does not contain the extreme C-terminal region that the peptides were generated against, and so cross-reactivity is very unlikely. Cross reactivity of the PABP1 antibody with tPABP is likely as only 1 amino acid within the peptide sequence differs between human proteins and 3 differ between the mouse proteins. This will be an issue in round spermatids, in which both proteins are expressed (Kimura *et al.*, 2009), and where determining levels of expression would be impossible to deduce as the relative contributions of each protein to the signal is unknown. PABP1 localised to the spermatocytes, round spermatids and early elongating spermatids within the seminiferous tubules with no signal detected in spermatogonial, Sertoli or Leydig cells (see figure 3.8 part 1). PABP4 displays a more wide ranging expression pattern with the protein detectable in all cell types within the tubules, including the Sertoli cells (see figure 3.8 part 2), consistent with the RT analysis (figure 3.6A). This represents the first cellular expression pattern for mouse PABP1 and PABP4 proteins and reveals that certain cells contain both PABP1 and PABP4. However, others such as spermatogonial cells which express the highest levels of PABP4 do not possess PABP1.

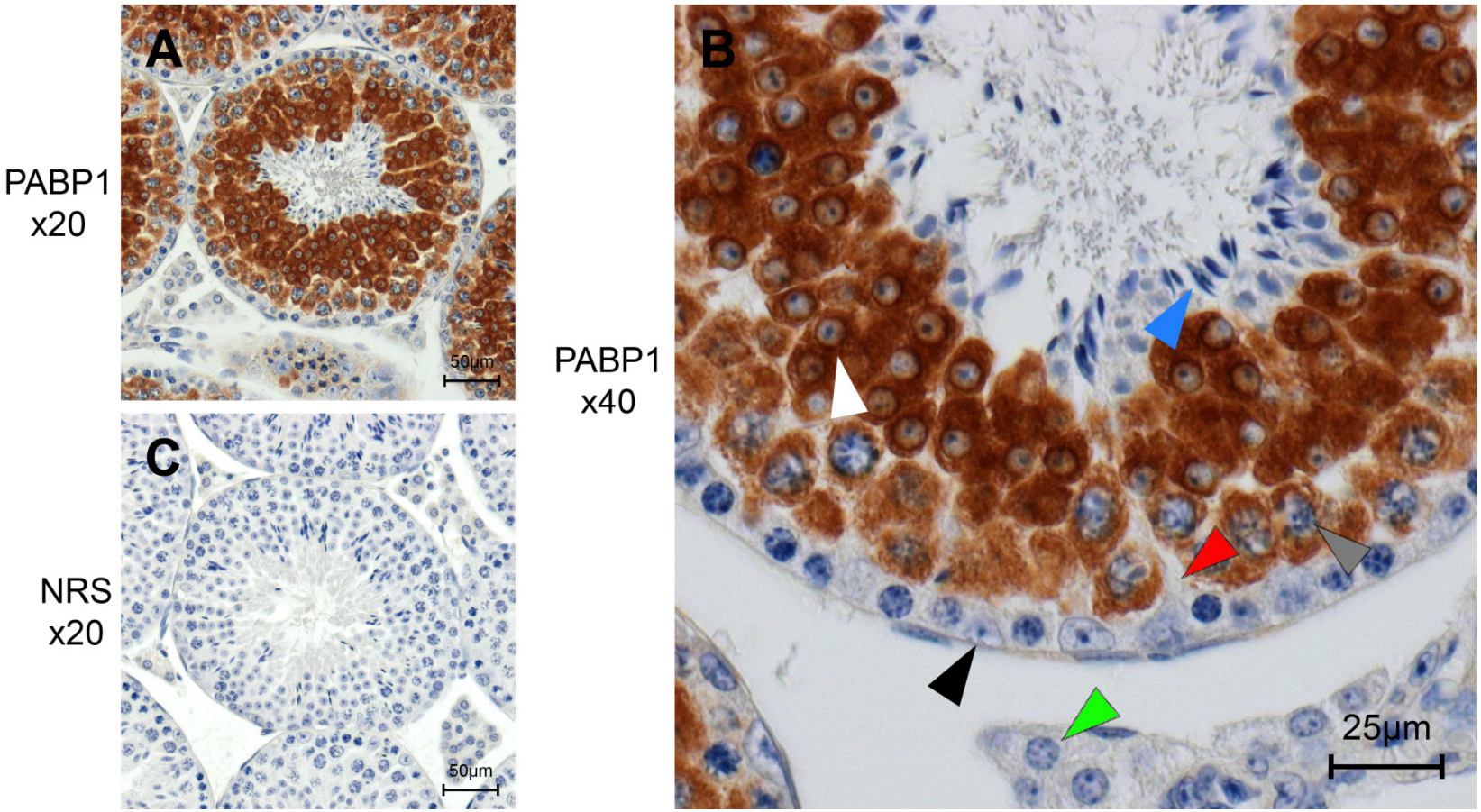

Figure 3.8 Part 1. PABP1 expression in mouse testes. Testis tissue sections were subjected to immunohistochemical analysis with α-PABP1 or α-PABP4 polyclonal antibodies at a 1/10,000 dilution or a 1/500 dilution respectively. **A.** Seminiferous tubule at 20x magnification. **B.** Seminiferous tubule at 40x magnification. Staining was seen in spermatocytes (grey arrow), and round spermatids (white arrow) but was absent in spermatogonial cells (black arrow), elongating spermatids (blue arrow), Sertoli cells (red arrow) and Leydig cells (green arrow). **C.** Control slide incubated with normal rabbit serum (NRS).

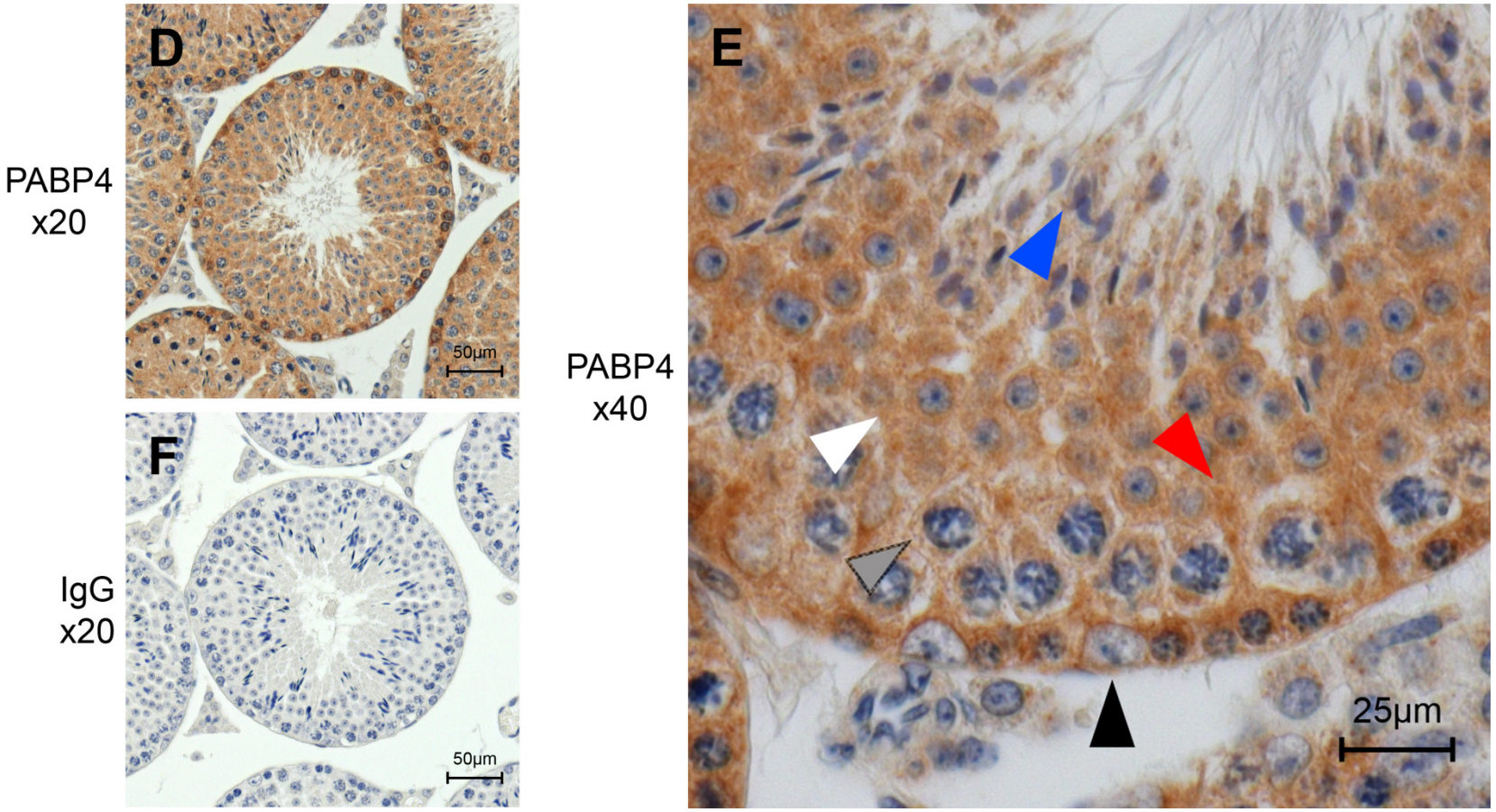

Figure 3.8 Part 2. PABP4 expression in mouse testes. **D.** Seminiferous tubule at 20x magnification. **E.** Seminiferous tubule at 40x magnification. Staining was seen in spermatocytes (grey arrow), spermatids (white arrow), and elongating spermatids (blue arrow). Stronger relative staining was observed in the sertoli cells (red arrow) and the spermatogonial cells (black arrow). **F.** Control slide incubated with rabbit IgG.

3.7(B) Cellular Distribution of PABP1 and PABP4 in Mouse Ovaries

As with the testis, the ovary is responsible for the production of hormones and female gametes (ova) and is composed of both somatic tissue as well as germ cells. Oogenesis is characterised by cyclical waves of germ cell development, maturation, and then release. Unlike males who can produce sperm for their entire adult life, the number of oocytes available for ovulation in mammals is determined during fetal development. By birth, the finite pool of immature primary oocytes are associated with granulosa cells and are referred to as primordial follicles. The oocytes within these follicles are arrested in dicytate (meiotic prophase 1) which can last up to 50 years. Primordial follicles are then selected from the pool to undergo folliculogenesis in a poorly understood process and over the course of approximately one year in humans (and approximately 20 days in mice) develop through primary, secondary, tertiary and up to pre-ovulatory follicle stages (see figure 3.9 for a schematic representation of folliculogenesis). Whilst the oocyte grows during these stages of folliculogenesis meiosis only resumes shortly before ovulation in a process termed oocyte maturation.

From the secondary follicle stage onwards this growth and development is largely directed by luteinising hormone and follicle stimulating hormone signalling through the somatic thecal cells and granulosa cells associated with the oocytes (see figure 3.9). Interestingly the granulosa and thecal cells of the ovary are often described as somatic equivalents of Sertoli and Leydig cells respectively. In females, luteinising hormone acts on the thecal cells of ovarian follicles, resulting in the production of androstenedione (a testosterone precursor). This steroid hormone is then converted into estradiol (an estrogen hormone) in granulosa cells via the action of the cytochrome P450 enzyme aromatase, which is produced in response to follicle stimulating hormone signalling to these cells. Estradiol directs folliculogenesis in the ovary via binding to its cognate receptor and initiating signalling events that result in nuclear transcription factor activity.

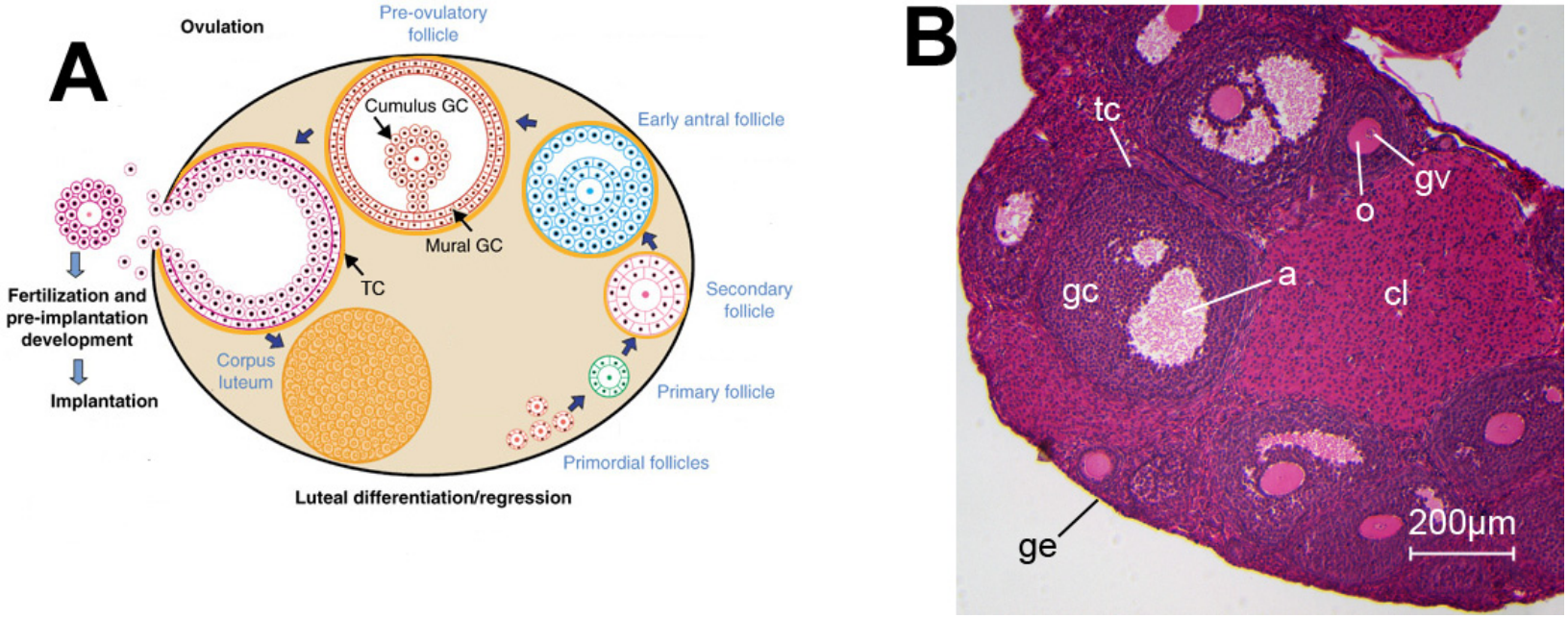

Figure 3.9 Haematoxylin and eosin staining of mouse ovarian tissue. A. Schematic of an ovary with follicles at various stages of folliculogenesis. Following selection from the primordial follicle pool the primordial follicles undergo cyclical waves of development and atresia progressing through a number of characterised stages. During this period there is a significant expansion in the granulosa and thecal cell populations, the development of an antrum and an increase in size of the oocyte arrested in dictyate. Immediately prior to ovulation the oocyte resumes meiosis. Following ovulation in response to hormonal signalling the remaining granulosa and thecal cells form an endocrine organ called the corpus luteum which releases hormones and is required to maintain the endometrium to allow implantation of the fertilised egg. Adapted from Matzuk *et al*., 2002. **B.** 7µm sections were cut from wax embedded mouse ovaries. GE=germinal epithelium, GC=granulosa cells, TC=thecal cells, A=antral cavity, O=oocyte, GV=germinal vesicle, CL=corpus luteum.

Following ovulation, the thecal and granulosa cells from the ovulated follicle that are retained within the ovary form a structure called the corpus luteum (see figure 3.9) which continues to release estrogen and progesterone which are necessary for successful implantation should the ova be fertilised.

The cellular distribution of PABPs within the mammalian ovary is poorly understood. ePABP has been shown by *in-situ* hybridisation to localise to germ cells within mammalian follicles (Seli *et al.*, 2005) consistent with the presence of ePABP in the oocytes of other vertebrate species (Voeltz *et al.*, 2001). To further investigate the distribution of PABP proteins within the mammalian ovaries immunohistochemical analysis of PABP1 and PABP4 expression was examined using the same antibodies as in figure 3.7.

In the adult mouse ovary PABP1 displays a restricted expression pattern (see figure 3.10) but unlike in the testis PABP1 is absent from the germ cells and is expressed only in somatic cells within the ovary. It appears to have the highest expression levels within the granulosa cells at multiple stages of the folliculogenesis pathway from activated primary follicles up to large antral stage follicles (figure 3.10A). The thecal cells associated with the follicles also stain weakly for PABP1 (figure 3.10C). The corpus luteum which is derived from the granulosa and thecal cells of ovulated follicles also stains for PABP1 (figure 3.10B) albeit weakly, suggesting a decline in PABP1 expression following ovulation. Thus, PABP1 is expressed in multiple cell-types within the mouse ovary. As with the testis, the expression of PABP4 in the ovary differs significantly from that of PABP1, with notable expression in the cytoplasm of developing oocytes in primordial through to antral follicles (see figure 3.11A and C). The primary oocytes within the primordial follicles stain strongly suggesting that the oocytes express PABP4 during very early stages of folliculogenesis (see figure 3.11C). The granulosa cells of activated follicles also stain for PABP4 (see figures 3.11C). Whether the squamous pregranulosa cells of primordial follicles are positive for PABP4 was undetermined due to the resolution

limit of the signal. Interestingly the corpus luteum also shows significant expression of PABP4 (see figure 3.11B) suggesting that the granulosa lutein cells continue to express PABP4 following ovulation. While the stroma appears to display low level staining it is unclear if this is background, or a result of overdevelopment of the signal. For the same reasons it is also difficult to determine if the thecal cells are positively stained (see figure 3.11C). Thus, PABP1 and PABP4 display overlapping yet distinct expression patterns within the mouse gonads.

3.8 PABP5 Antibody Generation

To investigate the localisation of PABP5 protein in mouse gonads required the generation of a PABP5 specific antibody. Two peptides were selected and each was used to immunise a pair of rabbits. One peptide was N-terminal within the mouse PABP5 protein, and the second was an internal peptide (see figure 3.12). Both were chosen to maximise the potential of cross reaction with the human protein, and to minimise the likelihood of cross reaction with other PABP proteins. Peptide A (the N-terminal peptide) failed to stimulate an immune response with the antibody titre being extremely low, as determined by an enzyme-linked immunosorbant assay (ELISA) whereby the immunogenic peptides were tested against serial dilutions of the rabbit sera. The optical density of the ELISA was measured at 450nm and the titre was calculated as the highest dilution of sera that gave an optical density reading of greater than 1. All ELISA assays were performed by Covalab.

Peptide B stimulated a moderate immune response as determined by antibody titre (rabbit 286 and rabbit 384). Rabbit 286 had an antibody titre of 16,000 compared to 4,000 for rabbit 384 and was subject to antibody purification with an immunoaffinity column containing the peptide used for immunisation.

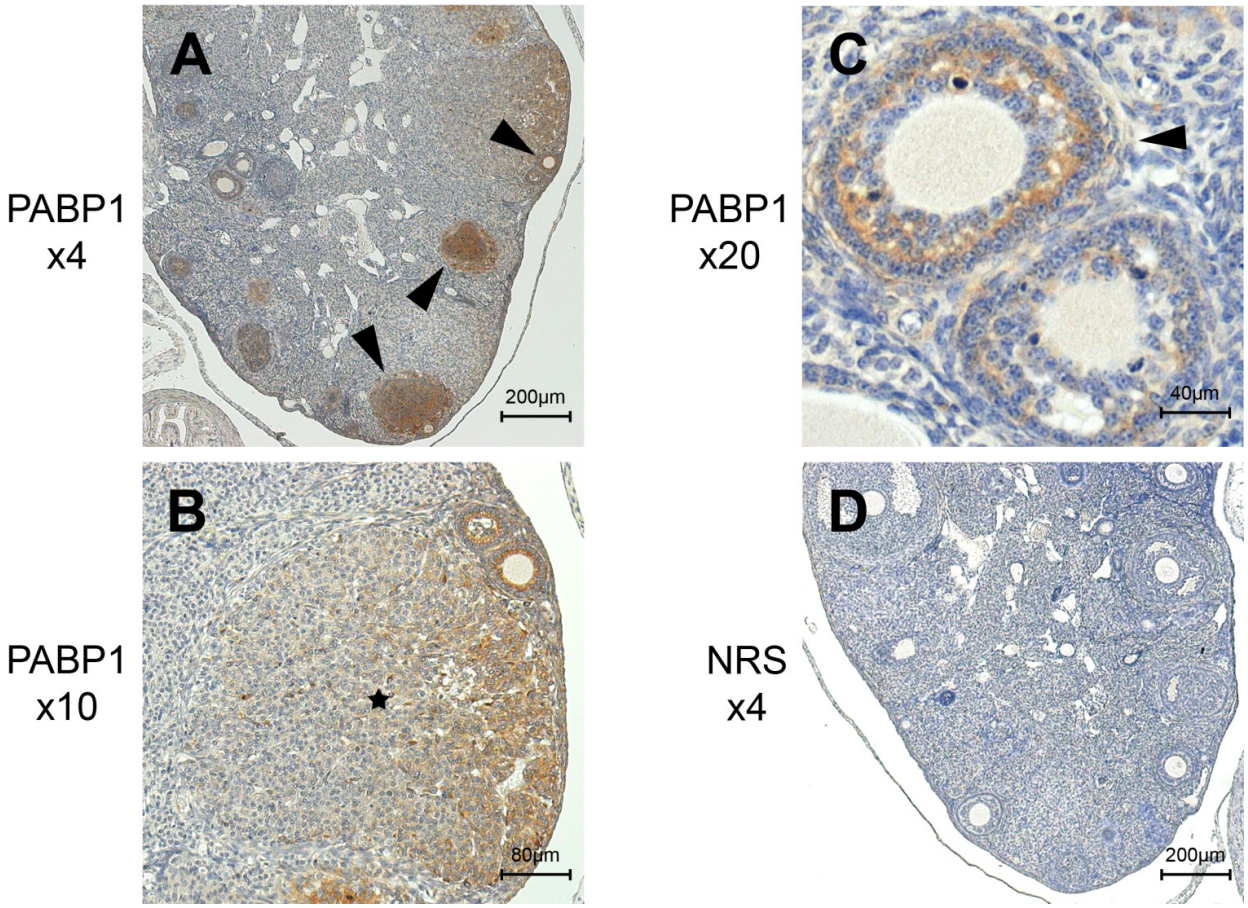

Figure 3.10 PABP1 expression in mouse ovary. Ovary tissue sections were subjected to immunohistochemical analysis with α-PABP1 polyclonal antibody at a 1/10,000 dilution. **A.** Ovary at 4x magnification. Follicles at various stages, containing PABP1 positive granulosa cells are denoted by black arrows. **B.** Ovary at 10x magnification. Corpus luteum is marked with a black star. **C.** Ovary at 20x magnification. Black arrow indicates thecal cell staining. **D.** Control slide incubated with NRS.

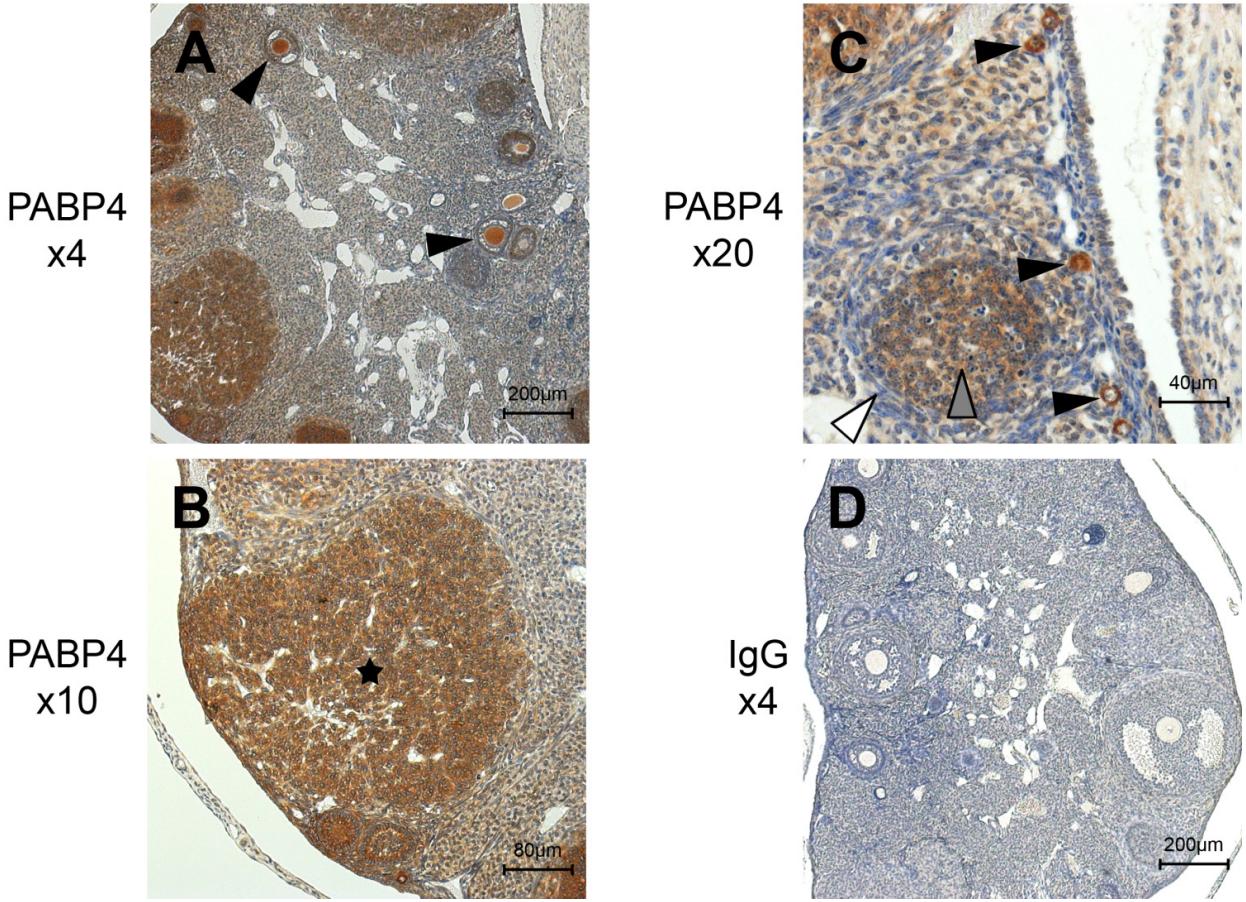

Figure 3.11 PABP4 expression in mouse ovary. Ovary tissue sections were subjected to immunohistochemical analysis with α-PABP4 polyclonal antibody at a 1/500 dilution. **A.** Ovary at 4x magnification. Antral follicles containing strongly stained oocytes are denoted by black arrows. **B.** Ovary at 10x magnification. Corpus luteum is marked with a black star. **C.** Ovary at 20x magnification. Black arrows indicate primary oocytes positive for PABP4. Grey arrow indicates granulosa cell staining, and white arrow indicates possible thecal cell staining. **D.** Control slide incubated with rabbit IgG.

When crude sera from both rabbits and the immunopurified antibody from rabbit 286 were tested against *E. coli* lysate containing recombinant polyhistidine-tagged (his-tagged) PABP5 by Western blotting (see figure 3.13A) neither generated a signal that corresponded to the predicted molecular weight for the recombinant protein despite recognising a number of *E. coli* proteins. The presence of the recombinant protein in the extracts was verified by Western blotting with an antibody raised against the his-tag. A further two peptides (peptides C and D) were then chosen for immunisation, but both failed to stimulate an immune response in the rabbits over the course of the immunisation program, as determined by ELISA. The immunisation program was extended but this failed to stimulate an immune response.

During the development of our own antibodies two commercial antibodies became available and were tested for reactivity against PABP5. The first was an affinity purified rabbit polyclonal antibody (Atlas Antibodies; cat. # HPA000164). The rabbits were immunised using a human PABP5 recombinant protein epitope signature tag (see figure 3.12). This antibody will herein be referred to as At164. The second antibody was a mouse polyclonal antibody (Abnova; cat. # H00140886-B01). The mice were immunised with full length recombinant human PABP5. This antibody will herein be referred to as Ab140886. To test the reactivity of At164 against PABP5, *E. coli* lysates containing recombinant His-tagged PABP5 were subjected to Western blotting with At164 (see figure 3.13B). Unlike the antibody generated by immunisation with peptide B, At164 recognised a band of approximately 44kDa which corresponds to the predicted molecular weight of recombinant PABP5. The specificity of the antibody for PABP5 was then tested to determine its value as an immunohistochemistry reagent. This is particularly important for antibodies raised against PABP proteins given the high level of protein sequence conservation within this family and also the common occurrence of multiple PABPs within the same tissue. The specificity was tested in two ways. Firstly, At164 was tested by Western blotting of *E. coli* lysate containing recombinant PABP1 and PABP4 (see figure 3.13C) and secondly by Western blotting of mouse tissue lysates to determine if the antibody cross-reacted with

endogenous mouse proteins (see figure 3.13D). Unfortunately At164 cross-reacts with recombinant PABP1 limiting the usefulness of the antibody for immunohistochemical analysis. Western blotting of the mouse tissue lysates revealed multiple cross reacting bands. The peptide used to immunise the rabbit covers a large proportion of the PABP5 protein and it is therefore likely that the antibody is detecting a conserved RRM motif present in other RNA-binding proteins.

```
mPABP5          -MSGEPNTAGKKKYLKAALYVGDLDPDVTEDMLYKKFRPAGPLRFTRICRDPVTRSPLG
hPABP5          MGSGEPNPAGKKKKYLKAALYVGDLDPDVTEDMLYKKFRPAGPLRFTRICRDPVTRSPLG
mPABP1          -----MNPSAP--SYPMASLYVGDLHPDVTEAMLYEKFSPAGPILSIRVCRDMITRRSLG

mPABP5          YGYVNFRFPADAEWALNTMNFDLINGKPFRLMWSQPDDRLRKSGVGNIFIKNLDKTIDNR
hPABP5          YGYVNFRFPADAEWALNTMNFDLINGKPFRLMWSQPDDRLRKSGVGNIFIKNLDKSIDNR
mPABP1          YAYVNFQQPADAERALDTMNFDVIKGKPVRIMWSQRDPSLRKSGVGNIFIKNLDKSIDNK

mPABP5          ALFYLFSAFGNILSCKVVCDDNGSKGYAYVHFDSLAAANRAIWHMNGVRLNNRQVYVGRF
hPABP5          ALFYLFSAFGNILSCKVVCDDNGSKGYAYVHFDSLAAANRAIWHMNGVRLNNRQVYVGRF
mPABP1          ALYDTFSAFGNILSCKVVCDENGSKGYGFVHFETQEAAERAIEKMNGMLLNDRKVFVGRF

mPABP5          KFPEERAAEVRTRERATFTNVFVKNFGDDIDDEKLNKLFSEYGPTESVKVIRDATGKSKG
hPABP5          KFPEERAAEVRTRDRATFTNVFVKNIGDDIDDEKLKELFCEYGPTESVKVIRDASGKSKG
mPABP1          KSRKEREAELGARAK-EFTNVYIKNFGEDMDDERLKELFGKFGPALSVKVMTDESGKSKG

mPABP5          FGFVRYETHEAAQKAVLELHGKSIDGKVLCVGRAQKKIERLAELRRRFERLKLKEKNRPS
hPABP5          FGFVRYETHEAAQKAVLDLHGKSIDGKVLYVGRAQKKIERLAELRRRFERLRLKEKSRPP
mPABP1          FGFVSFERHEDAQKAVDEMNGKELNGKQIYVGRAQKKVERQTELKRKFEQMKQDRITRYQ

mPABP5          GVPIYIKNLDETINDEKLKEEFSSFGSISRAKVMMEVGQGKGFGVVCFSSFEEACKAVDE
hPABP5          GVPIYIKNLDETINDEKLKEEFSSFGSISRAKVMMEVGQGKGFGVVCFSSFEEATKAVDE
mPABP1          GVNLYVKNLDDGIDDERLRKEFSPFGTITSAKVMMEGGRSKGFGFVCFSSPEEATKAVTE

mPABP5          MNGRIIGSKTLHVTLGQARHRW----------------------------------------
hPABP5          MNGRIVGSKPLHVTLGQARRRC----------------------------------------
mPABP1          MNGRIVATKPLYVALAQRKEERQAHLTNQYMQRMASVRAVPNPVINPYQPAPPSGYFMAA
```

Figure 3.12 Location of peptides for immunisation. Yellow represents peptide A, green represents peptide B, and blue represents the PABP5 recombinant protein epitope signature tag used to generate At164. Pink represents peptide C and grey represents peptide D used for the failed immunisation protocol. Full length recombinant PABP5 was used to generate Ab140886.

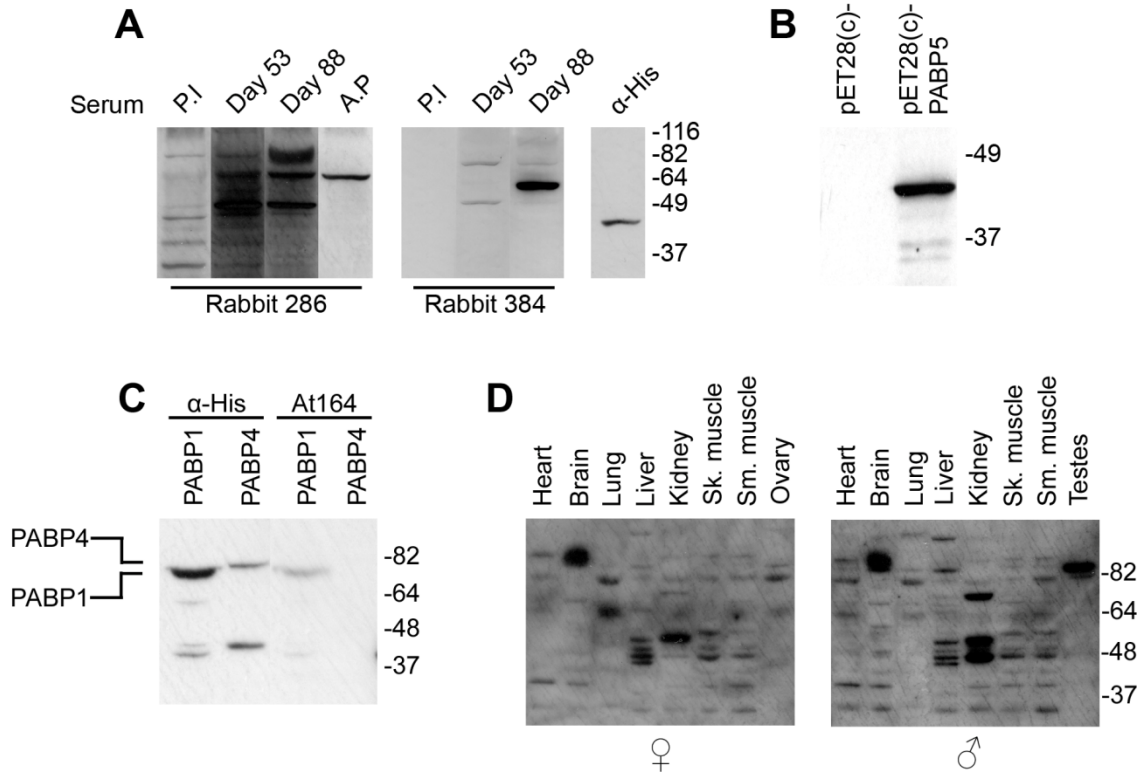

Figure 3.13 Antibody test Westerns. A. Affinity purified antibody and sera of rabbit 286 and the sera from rabbit 384 immunised with peptide B were used to Western blot *E. coli* lysates containing recombinant His-PABP5. α-histidine was used to indicate presence of recombinant protein. Both antibodies and bleeds were used at a 1/1000 dilution. **B.** At164 tested by Western blot against *E. coli* lysates containing recombinant His-PABP5. Antibody was used at a 1/250 dilution. **C.** The specificity of At164 was tested by Western blot against *E. coli* lysates containing recombinant His-PABP1 and recombinant His-PABP4. Antibody was used at a 1/250 dilution. **D.** The specificity of At164 was tested by Western blot against mouse tissue lysates containing recombinant His-PABP1 and recombinant His-PABP4. Antibody was used at a 1/250 dilution.

Of the many proteins detected by At164 in these lysates there are bands that migrate at the predicted molecular weight for both PABP1 and PABP5 (~70kDa and 43kDa respectively). Whether any of the bands represent PABP5 protein is unclear. To determine the identity of the proteins migrating at the predicted molecular weight of PABP5, immunoprecipitated (IP) protein could be analysed by mass spectroscopy. To determine the immunoprecipitating capacity of At164 an *in-vitro* coupled transcription and translation reaction was performed using a vector containing the PABP5 ORF in the presence of ^{35}S-labelled methionine to radiolabel the protein.

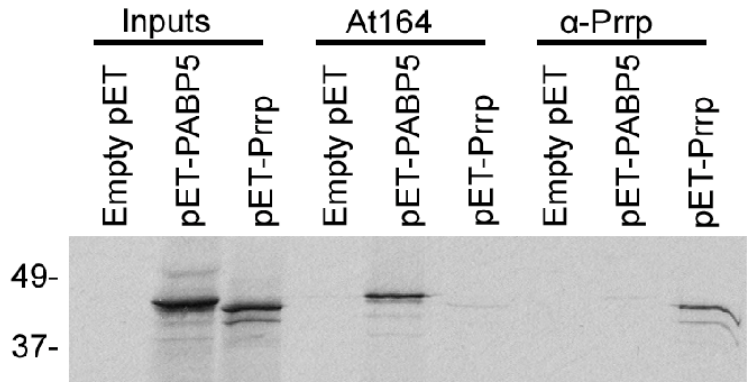

Figure 3.14 At164 can immunoprecipitate recombinant PABP5. Coupled transcription and translation reactions were carried out with empty pET vector, pET-PABP5, or pET-Prrp. At164 was then used to immunoprecipitate PABP5 but was not capable of isolating Prrp. The inputs represent 25% of the reaction used for each immunoprecipitation.

The recombinant PABP5 was then subjected to IP using At164 (see figure 3.14). This assay demonstrated the ability of At164 to recognise *in-vitro* translated recombinant PABP5. As a specificity control an antibody raised against an unrelated RRM containing protein, Prrp, was also used to IP PABP5. However the subsequent IP of mouse tissue lysates with At164 failed to isolate the 43kD protein detected in the Western blots (see figure 3.15). While there were three observable protein bands of approximately the predicted molecular weight of PABP5 they were also present in the control IgG reaction and so were deemed non-specific. It is possible that the protein bands detected by Western blot (see figure 3.13D) are at such low abundance in mouse tissues it is simply not detectable by IP. Thus the identities of the proteins detected by Western blotting with At 164 remain unknown and the antibody was deemed to have little experimental value.

The second commercially available antibody, Ab140886, was tested by Western blot against HeLa cell lysate that had been transfected with T7-tagged mouse PABP1 and PABP5 to determine if this antibody could specifically recognise mouse PABP5 (see figure 3.16).

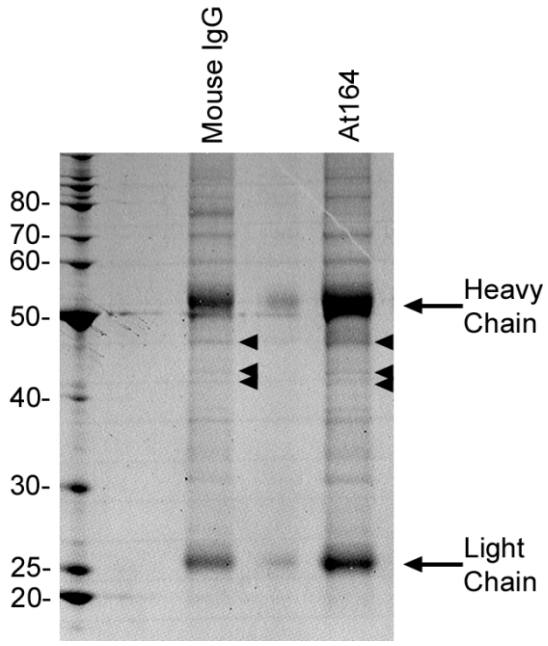

Figure 3.15 IP of mouse tissue lysate with At164. Mouse kidney tissue was lysed and subjected to immunoprecipitation with At164. A control IP reaction was set up using mouse IgG. The IP'd proteins were subjected to SDS-PAGE followed by staining with SYPRO Ruby protein stain (Invitrogen) as per manufacturer's instructions and scanned using a Typhoon Variable Mode Imager with a 488nm excitation laser. There were 3 bands of approximately the predicted molecular weight of PABP5 (44kDa) isolated by At164 but they were also isolated by the control IgG reaction and so were deemed non-specific (see small black arrows). The antibody heavy and light chains are identified.

The antibody detects a band of approximately 44kDa in the T7-PABP5 transfected lysate, and also detects a band of approximately 73kDa in the T7-PABP1 transfected lysate (PABP1 predicted mass is 71kDa) suggestive of cross reaction of the antibody with the PABP1 protein. This cross reaction appears to be limited to overexpressed protein as there is no detectable band in the untransfected and T7-SF2 transfected lysates which contain substantial amounts of endogenous PABP1. As with At164, Ab140886 demonstrated an ability to IP recombinant radiolabelled PABP5 in the same assay as undertaken in figure 3.13 (see figure 3.17A) but as before failed to specifically isolate any proteins of the predicted molecular weight of PABP5 from mouse tissue lysates (data not shown) possibly re-emphasising that PABP5 may be a low abundance protein, or alternatively is an abundant protein expressed in only a small number of cells within the tissues examined.

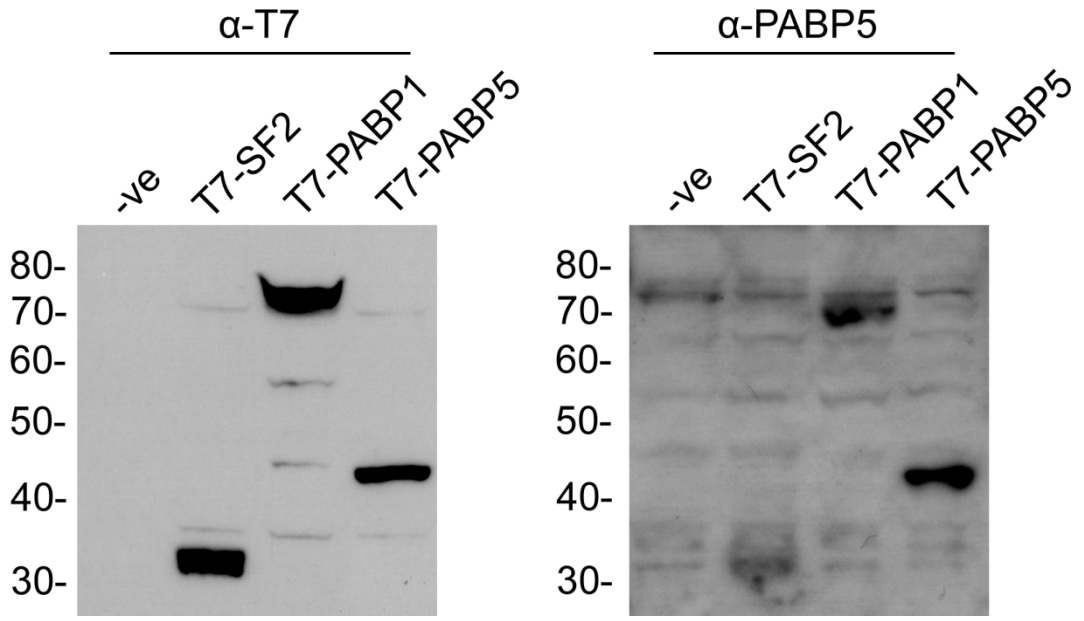

Figure 3.16 Ab140886 recognises recombinant PABP5. Ab140886 was tested against HeLa cell lysates containing mouse T7-PABP1, T7-PABP5 and T7-SF2, an RRM containing protein that is unrelated to the PABP family (right panel). The presence of the recombinant T7-tagged proteins was verified by Western blotting with an antibody raised against the T7-tag (left panel).

Ab140886 was then used to test a mouse tissue panel by Western blotting. A band was identified at 54kDa but no detectable signal at the correct mass for PABP5 was observed (data not shown) when the blot was developed using enhanced chemiluminescent (ECL) reagent (Amersham). This band could represent a post-translationally modified version of the PABP5 protein but was observable in all tissue lysates including those with negligible levels of PABP5 mRNA such as the liver. Upon development of the blot with Supersignal West Femto substrate (Thermo Scientific) which is a higher sensitivity Western blotting detection reagent a band of approximately 44kDa, the predicted mass of PABP5, was visible in both male and female brain lysates (see figure 3.17B) which have relatively high levels of PABP5 mRNA (see figures 3.3 and 3.4).

PAIP-2 is known to bind PABP1 (Khaleghpour *et al.*, 2001b) and in chapter 4 I demonstrate that recombinant PABP5 can also bind to PAIP-2 *in-vitro*. This interaction was used to test whether either the 54kDa band (upper band) and/or the 44kDa band (lower band) represent forms of PABP5. Mouse brain lysates were incubated with GST-PAIP-2 bound to glutathione sepharose beads, and the un-bound fraction was Western blotted using Ab140886. PABP1 was depleted from extracts incubated with GST-PAIP-2 but not from extracts incubated with GST alone (see figure 3.18). Neither the upper or lower putative PABP5 bands were depleted by GST-PAIP-2 incubation, suggesting that they do not represent forms of the PABP5 protein (see figure 3.18). If the upper band corresponds to a post-translationally modified version of PABP5, these modifications may preclude binding to PAIP-2.

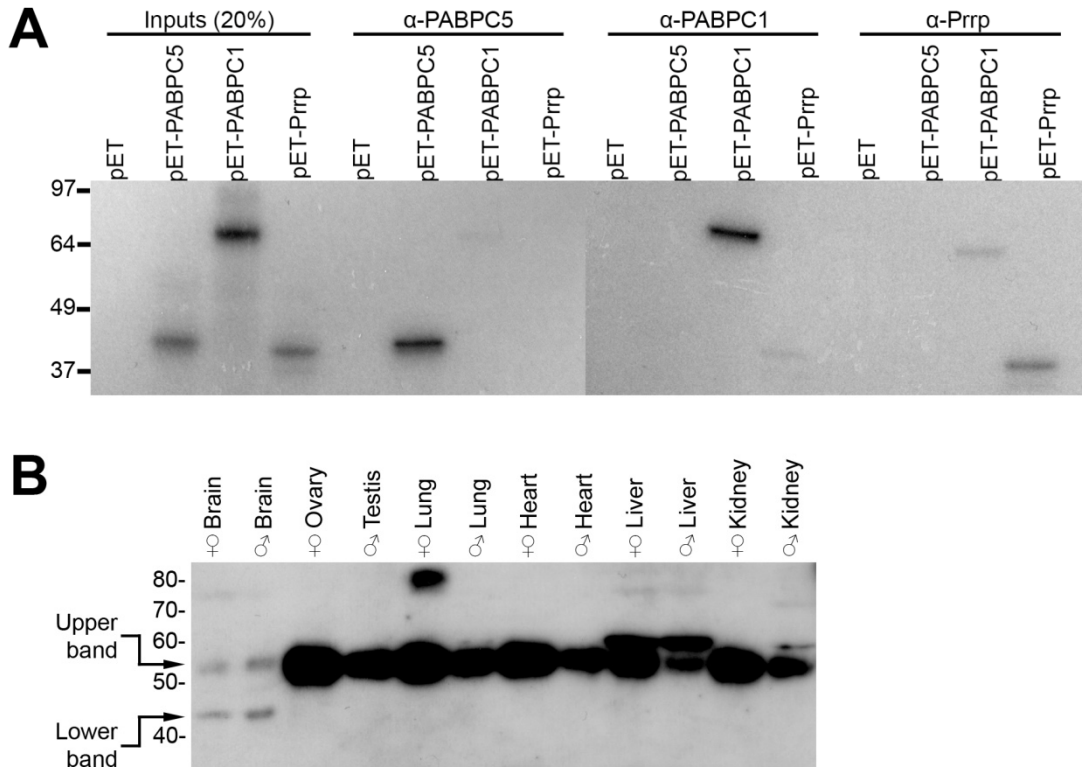

Figure 3.17 Ab140886 characterisation. A. Ab140886 can immunoprecipitate recombinant PABP5. Coupled transcription and translation reactions were carried out with empty pET vector, pET-PABP5, pET-PABP1 or pET-Prrp. Ab140886 was then used to immunoprecipitate PABP5 but was not capable of isolating PABP1 or Prrp. The inputs represent 20% of the reaction used for each immunoprecipitation. **B.** Mouse tissue lysates were subjected to Western blotting using Ab140886 at a 1/2000 dilution. Upper band at approximately 54kDa and lower band at approximately 44kDa indicated by black arrows. Supersignal West Femto Detection reagent was used to develop the blots.

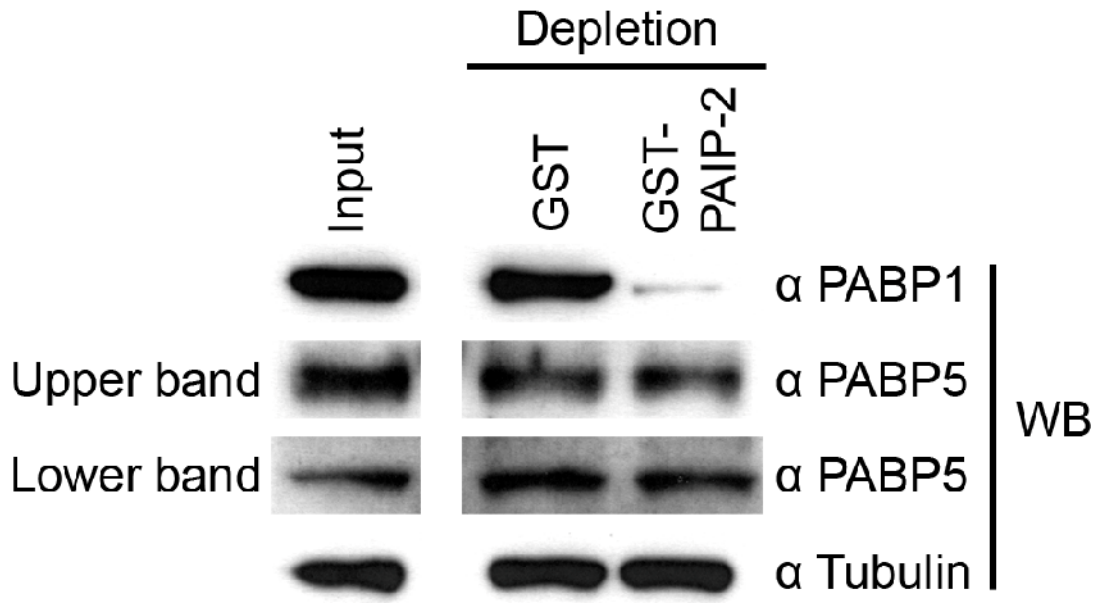

Figure 3.18 PABP depleted mouse brain lysates. Mouse brain tissue lysates were incubated with GST or GST-PAIP-2 bound to glutathione sepharose beads. The supernatant was then Western blotted with the indicated antibodies.

3.9 Localisation of PABP5 mRNA in the Mouse Gonads

Immunohistochemical analysis of PABP5 cannot be undertaken in the absence of a specific antibody. Therefore, to gain insight into likely PABP5 expressing cell populations *in-situ* hybridisation was employed. To generate a labelled PABP5 specific probe the PABP5 RT-PCR amplicon (see section 3.4) was cloned into a vector and transcribed to create digoxygenin labelled RNA probes using a DIG-labelling kit (Roche). The probe was complementary to the 5'-UTR of the PABP5 transcript, was intron spanning and was BLAST searched (NCBI) to ensure there would be minimal likelihood of cross-reactivity with transcripts containing similar sequence. The digoxygenin labelled RNA was visualised by applying an antibody raised against the digoxygenin moiety. Antibodies are coupled to alkaline phosphatase, an enzyme that catalyses the precipitation of an insoluble purple product upon addition of substrate. A corresponding sense probe was used as a control and was synthesised by transcription of the same vector but in the opposite direction to produce a non-complimentary probe of the same size as the antisense

probe. PABP1 mRNA sense and antisense digoxygenin labelled probes were also created by transcription from a vector containing the PABP1 3'-UTR. The localisation of PABP1 mRNA to a subset of male germ cells within the seminiferous tubules of mouse testis (Gu *et al.*, 1995; Kleene *et al.*, 1994) allows the PABP1 *in-situ* hybridisation to serve as a positive control for the assay and also as a measure of the integrity and condition of the tissue.

Two critical parameters that can affect the detection of an mRNA species by *in-situ* hybridisation are the temperature at which probe annealing is performed, and also the concentration at which the probe is applied to the tissues. A standard annealing temperature of 55^{o}C and probe concentration of 0.1ng/µl was initially employed. Upon performing the assay on mouse testes tissue no signal could be detected for PABP5. PABP5 mRNA remained undetectable despite increasing the probe concentration 10-fold to 1ng/µl and dropping the annealing temperature to 50^{o}C (see figures 3.19C and D). At 55^{o}C (data not shown) or 50^{o}C PABP1 localisation was observed in the spermatocytes and spermatids consistent with published data (see figures 3.19A and B) (Gu *et al.*, 1995; Kleene *et al.*, 1994). It was considered that the PABP1 probe might be binding to its mRNA with a higher affinity than the PABP5 probe, although this was deemed unlikely, as both probes were of similar length (PABP1; 439bp, PABP5; 517bp) and PABP5 had a significantly greater GC content (PABP1; 29%, PABP5; 51%). It was therefore concluded that PABP5 mRNA was below the detection threshold of this assay.

If PABP5 was below the detection limit of the assay, then employing the same assay using mouse ovarian tissue may prove to be more successful, given that higher levels of mRNA were detected in this tissue by RT-PCR (see figure 3.4). As with testes tissue there was no observable PABP5 mRNA signal using a probe annealing temperature of 55^{o}C and concentration of 0.1ng/µl, in contrast to PABP1 which showed an expression pattern reminiscent of PABP1 protein expression (see appendix figure 1).

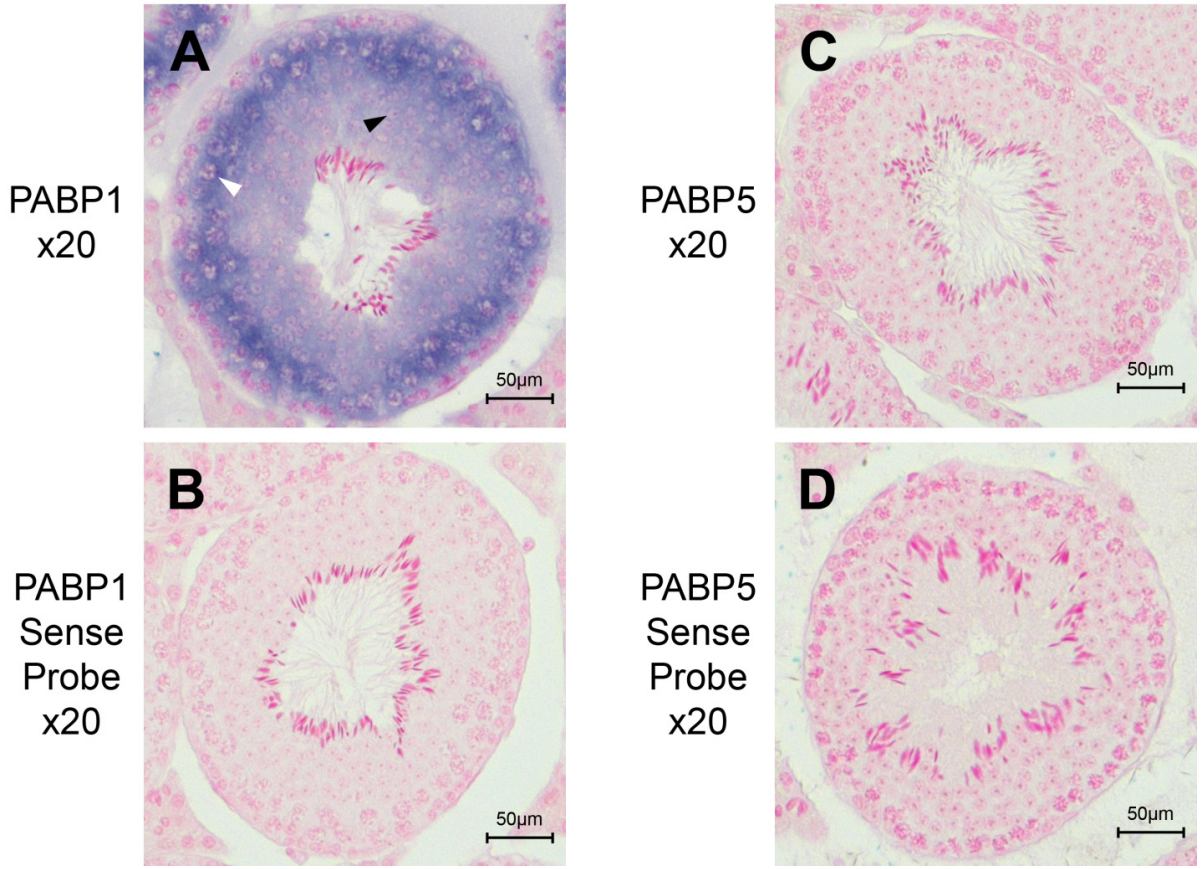

Figure 3.19 PABP5 mRNA localisation in the mouse testes. 7µm tissue sections were subjected to *in-situ* hybridisation. **A, C.** Adult mouse testes sections incubated with PABP1 and PABP5 antisense probes respectively. White arrowhead marks a spermatocyte and the black arrowhead marks a round spermatid. No signal could be seen with the PABP5 probe. PABP1 displayed strong staining in spermatocytes and round spermatids. **B, D.** Adult mouse testes sections incubated with PABP1 and PABP5 sense probes respectively. The PABP1 probes were used at a concentration of 0.1ng/µl and an annealing temperature of 50^{o}C and the PABP5 probe was used at a concentration of 1ng/µl with an annealing temperature of 50^{o}C. Nuclear counterstaining with Nuclear Fast Red Counterstain (Genetex).

However, unlike testis when the annealing temperature was dropped to 50^{o}C and the probe was applied at a concentration of 1ng/µl a PABP5 signal was observed within specific populations of cells (see figure 3.20). The signal localised to the cumulus and mural granulosa cells, and also the thecal cells, and appeared to be absent from oocytes, the stroma and ovarian surface epithelium. Thus, PABP5 would appear to be present in sub-populations of cells of somatic origin within the ovary. The resolution of the signal generated by the digoxygenin probe was not sufficient to identify the presence of PABP5 in granulosa or thecal cells in follicles below the secondary follicle stage. The corpus luteum was also positive for PABP5 but at much lower intensity than the granulosa and thecal cells, and only displayed signal with longer probe incubation times. Care must be taken in interpreting the presence of extremely low level staining in the corpus luteum given the lowered annealing temperature and higher probe concentrations used as these parameters can directly affect probe specificity.

To determine if PABP5 is present in primordial and primary follicles, tissue sections of mouse ovaries were collected at 2 days post partum (dpp) and 6 days post partum and subjected to *in-situ* hybridisation with the PABP5 probe. At 2dpp only primordial follicles inhabit the ovary, and by 6dpp there are only primary and early secondary follicles present. This facilitates the analyses of mRNAs expressed in these cell types at this developmental stage by making the precipitative staining easier to visualise as the follicles are at higher cellular densities within the ovary. At 2dpp there appears to be light staining of the squamous pregranulosa cells associated with the oocytes (see figure 3.21 part 1). This staining becomes more apparent in the granulosa cells within the primary and secondary follicles in the 6dpp ovary (see figure 3.21 part 2). Staining is also present in the thecal cells in early secondary follicles (see figure 3.21 part 2). PABP5 is therefore expressed within certain somatic cells associated with the developing follicle from very early follicular stages through to pre-ovulatory stages.

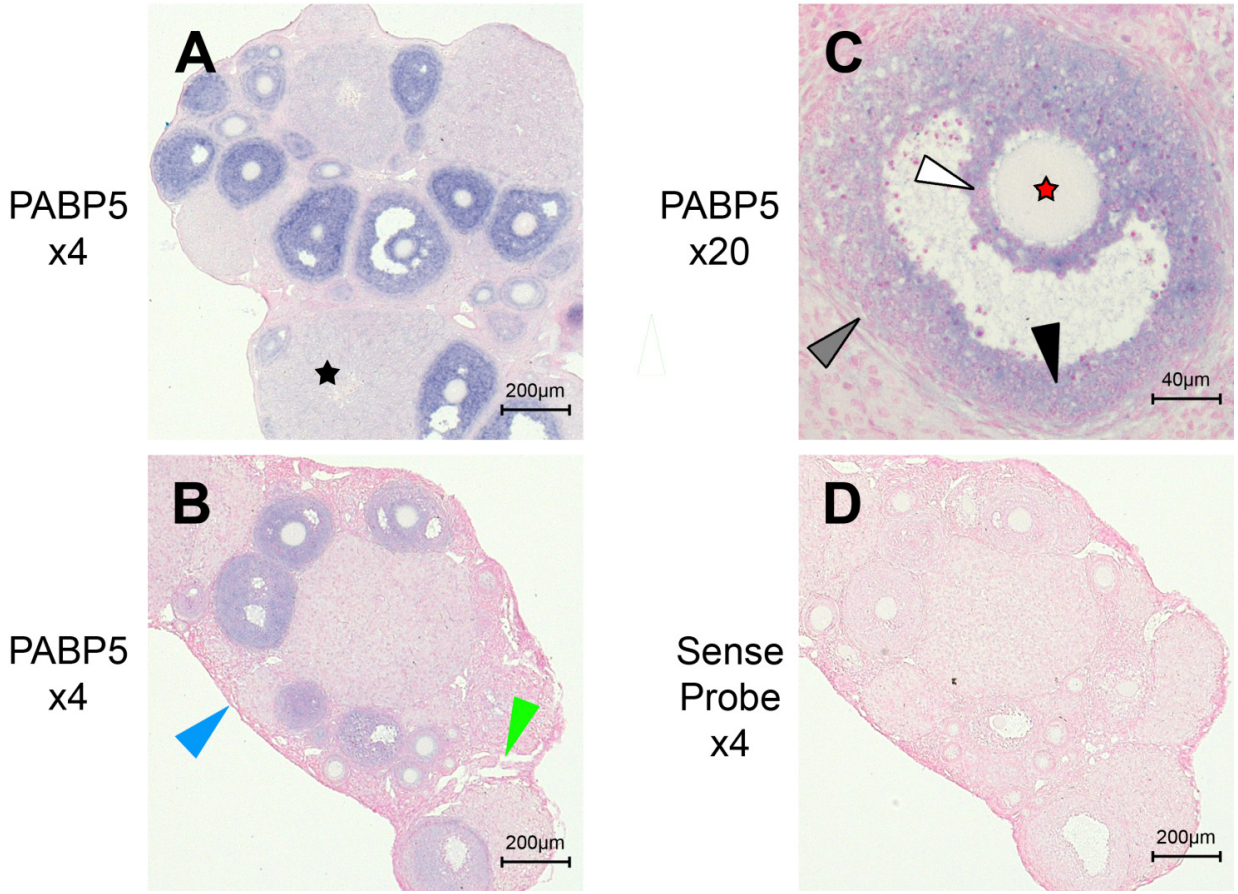

Figure 3.20 PABP5 mRNA localisation in the mouse ovary. 7µm tissue sections were subjected to *in-situ* hybridisation. **A,B,C.** Adult mouse ovary sections incubated with PABP5 antisense probe. A robust signal could be seen in mural (black arrow) and cumulus granulosa cells (white arrow), and also thecal cells (grey arrow). The corpus luteal cells also had light staining (black star). No signal could be observed in stromal tissue (green arrow) and the ovarian surface epithelium (blue arrow). The germ cells appeared negative for PABP5 staining (red star). **D.** Adult mouse ovary section incubated with PABP5 sense probe. The probes were used at a concentration of 1ng/µl and with an annealing temperature of 50^{o}C. Nuclear counterstaining with Nuclear Fast Red Counterstain.

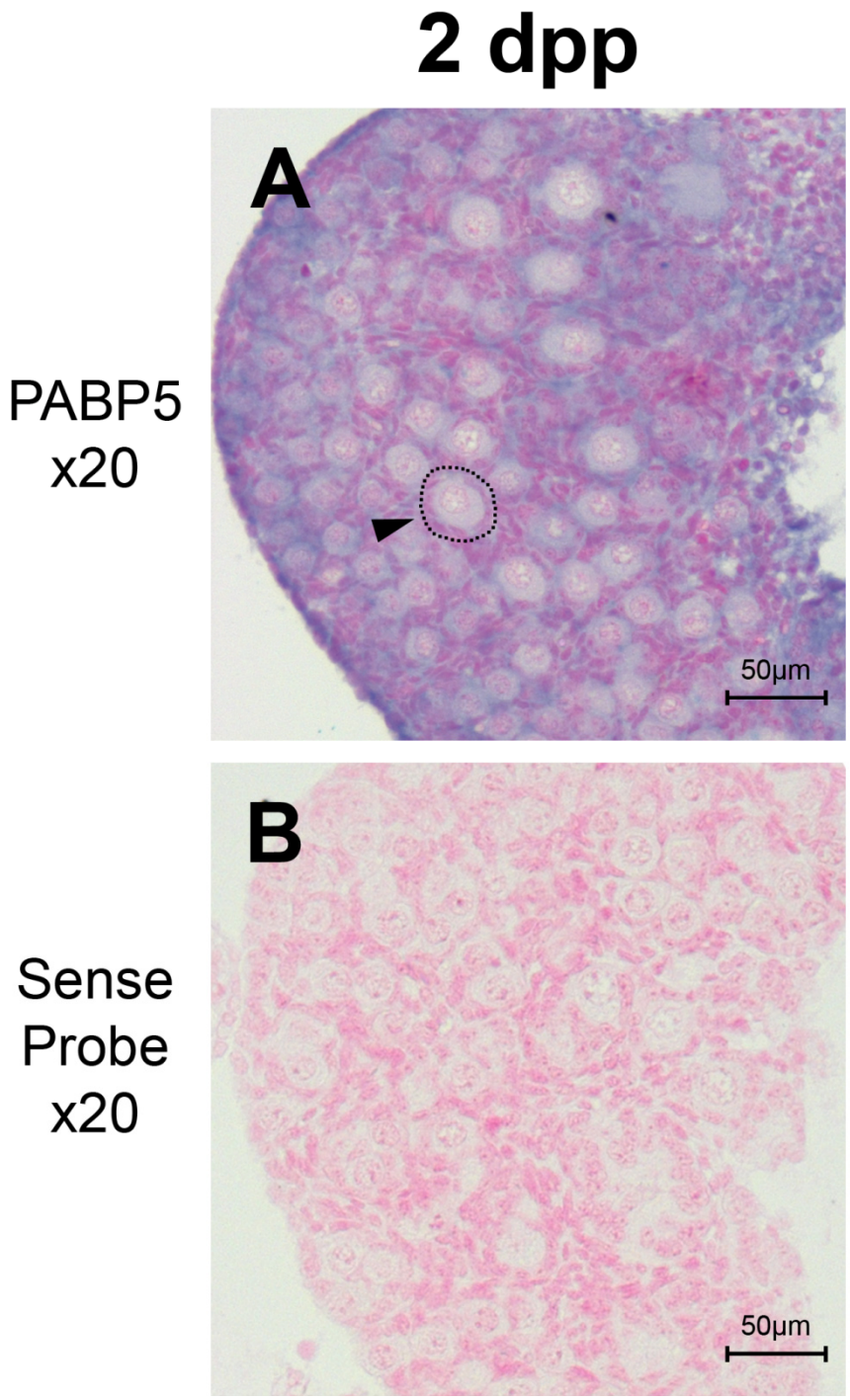

Figure 3.21 Part 1. PABP5 localisation in 2dpp mouse ovaries. 7µm tissue sections were subjected to *in-situ* hybridisation. **A.** 2dpp mouse ovary section incubated with PABP5 antisense probe. Staining was observed in the pregranulosa cells surrounding the oocyte. A primordial follicle with squamous pregranulosa cells is circled (see black arrow). **B.** 2dpp mouse ovary sections incubated with PABP5 sense probe. The probes were used at a concentration of 1ng/µl and with an annealing temperature of 50^{o}C. Nuclear counterstaining with Nuclear Fast Red Counterstain (GeneTex).

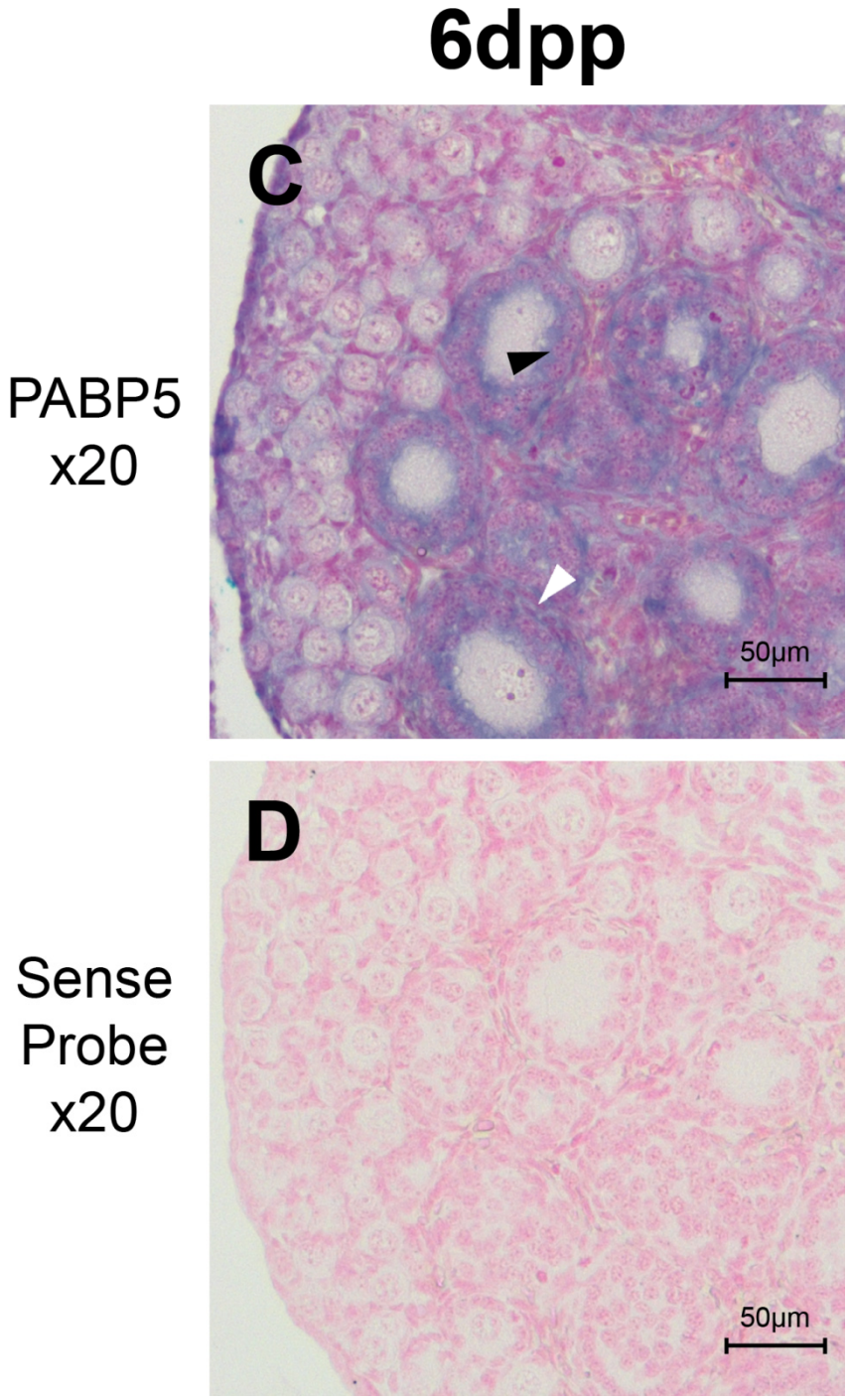

Figure 3.21 Part 2. PABP5 localisation in 6dpp mouse ovaries. 7µm tissue sections were subjected to *in-situ* hybridisation. **C.** 6dpp mouse follicle incubated with PABP5 antisense probe. The cuboidal granulosa cells of primary follicles were positively stained for PABP5 (see black arrow). In the early secondary follicles thecal cells also stained positive (see white arrow).**D.** 6dpp mouse ovary sections incubated with PABP5 sense probe. The probes were used at a concentration of 1ng/µl and with an annealing temperature of 50^{o}C. Nuclear counterstaining with Nuclear Fast Red Counterstain (GeneTex).

3.10 PABP5 Expressing Cell-Lines

That PABP5 mRNA appears to be predominantly expressed within the granulosa cells of the mouse ovary could suggest that this cell type would be a good candidate in which to study PABP5 protein. Indeed antibodies At164 and Ab140886 may be able to detect PABP5 in a pure population of granulosa cells or a granulosa cell-line compared to whole ovary extracts. However, as a preliminary line of investigation PABP5 mRNA levels were examined in a range of standard laboratory cell-lines by RT-PCR with the PABP5 specific oligonucleotide primers documented in section 3.4. As a positive control, mouse genomic DNA was also subjected to PCR with the primers. The product of this PCR reaction was expected to be 1052bp which is larger than would be generated by PCR of PABP5 cDNA (517bp) as the primers are intron spanning. Of the cell-lines tested none were positive for PABP5 mRNA (see figure 3.22A).

Expression of PABP5 mRNA in two specialised cell lines was then investigated – the immortalized murine ovarian granulosa tumour cell-line KK1, and the Sertoli cell-line SK11. The Sertoli cell-line was examined for PABP5 mRNA expression for three reasons, firstly PABP5 mRNA is known to be present within mouse testis (see figure 3.4), secondly PABP5 mRNA is still present in Dazl -/- testes suggesting that at least a proportion is expressed within somatic testes tissue (see figure 3.6), and thirdly Sertoli cells and granulosa cells are often considered functional equivalents in male and female gonads. The SK11 cell line was derived from transgenic mice expressing a temperature sensitive form of the Simian virus 40 (SV40) large T antigen. At the permissive temperature (33^{o}C) the cells are mitotically active, but when they are grown at the non-permissive temperature (39^{o}C) they stop proliferating, start expressing Sertoli cell markers and undergo cytoskeletal changes consistent with the changes seen during functional maturation of Sertoli cells during the first wave of spermatogenesis (Sneddon *et al.*, 2005). If PABP5 was expressed in these granulosa or Sertoli cell lines they could prove to be useful molecular biology tools in which to study the molecular function of PABP5.

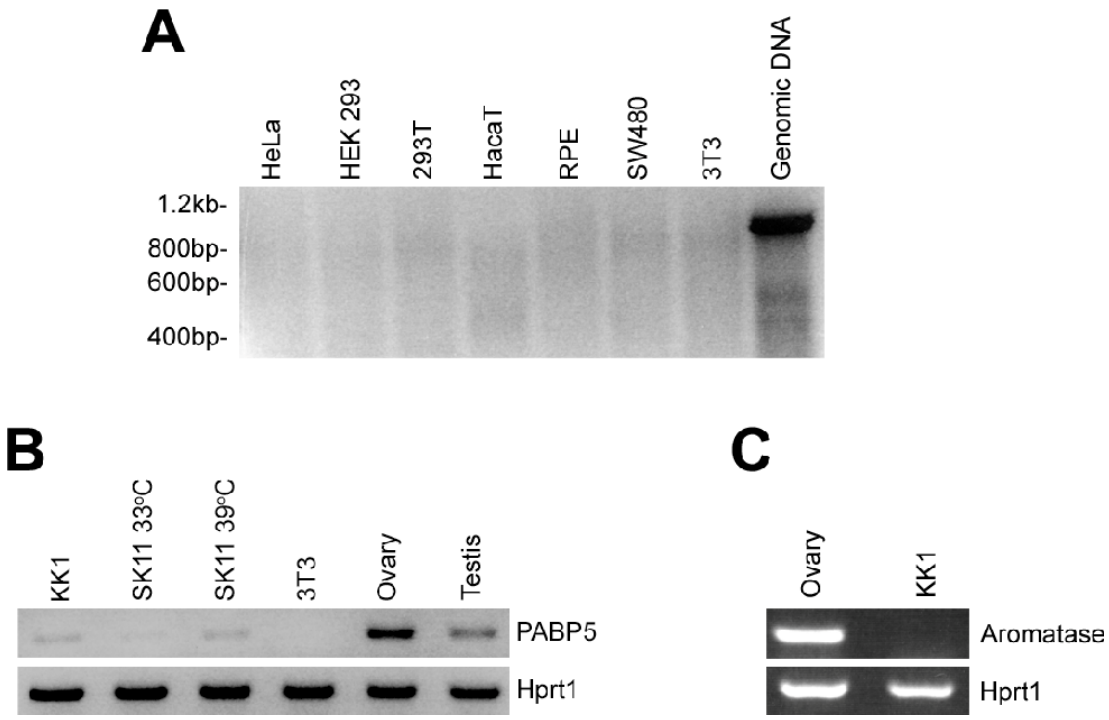

Figure 3.22 Expression of PABP5 mRNA in cell-lines. A. Various cell-lines were tested for the expression of PABP5 mRNA by RT-PCR. The expected amplicon was 517bp. Genomic mouse DNA was subjected to PCR as a control. The expected amplicon for this reaction was 1052bp as the primers are intron spanning. **B.** PABP5 RT-PCR on cDNA derived from granulosa and Sertoli cell lines. HIH/3T3 cells are a mouse fibroblast line that are negative for PABP5 expression. PABP5 expresses at low levels in SK11 cells grown at 39°C and also in KK1 cells. **C.** Aromatase RT-PCR on cDNA derived from mouse ovary or KK1 cell mRNA. PCR reactions were 32 cycles.

cDNA was prepared from these cell-lines and RT-PCR was performed. When SK11 cells were grown at the permissive and non-permissive (Sertoli cell- like) temperatures, the latter appeared to induce a slight increase in PABP5 mRNA levels but this was relatively low compared to ovary and testis cDNA expression (see figure 3.22B). PABP5 levels were also relatively low in the SK11 granulosa cell line. It is known that the KK1 cells luteinise in culture, a process in which the granulosa cells undergo radical changes in gene expression and endocrine function in preparation for implantation. This often occurs at especially high cell densities or passage numbers (Portela *et al.*, 2010). This could in part explain the low expression of PABP5 in these cells, as the *in-situ* data in mouse ovary implied that there was severely reduced expression of PABP5 in corpus luteal tissue. RT-PCR was performed on RNA extracted from KK1 cells using primers against aromatase, a granulosa expressed

gene, as a marker of how granulosa cell 'like' the cultured KK1 cells are (see figure 3.22C). The KK1 cells fail to express aromatase in culture, possibly through a lack of FSH signalling, suggesting that they are more luteal than granulosa like and indicating that they are not an ideal cellular background in which to perform PABP5 functional assays.

3.11 Discussion

The PABP5 gene contains no introns within its ORF. Thus, it is likely to have originated through a retroposition event analogous to tPABP, a mammalian testis specific poly(A)-binding protein (Feral *et al.*, 2001; Kleene *et al.*, 1998) that appears to share many of the functional characteristics of PABP1 (Kimura *et al.*, 2009). The high degree of sequence conservation of the PABP5 gene across mammals implies a degree of selective pressure acting upon this gene to maintain the sequence. While no promoter sequences have been determined for PABP5, there is conservation of the DNA sequence upstream of the gene. It would be interesting to run the upstream sequence through a transcription factor binding site predictor program such as rVista to establish if there are any conserved recognisable transcription factor binding sites within this genomic region that may account for regulation of its transcription. Alternatively, PABP5 mRNA may be expressed then rapidly turned over in cells where it appears absent, and interestingly the 3'-UTR of PABP5 contains a number of putative stability or AU-rich elements, suggestive of regulation via this mechanism although this is purely speculative.

The main sites of expression of PABP5 mRNA appeared to overlap between species. In mice a primary site of expression was the brain (see figure 3.4), correlating with qPCR analysis of human tissues (see figure 3.3) and published human data (Blanco *et al.*, 2001). Localisation and translation of mRNAs in neurons has been shown to be important for a number of processes, particularly synaptic plasticity and axon growth cone movement (reviewed in Lin and Holt, 2007; Schuman *et al.*, 2006), therefore it is interesting to find expression of poly(A)-binding proteins within the

brain. The human qPCR cDNA arrays suggest relatively high PABP5 mRNA expression within the pituitary gland suggesting it is the main site of expression. Whether expression in this gland is conserved in mouse remains to be determined. *In situ* hybridisation of mouse brains was undertaken but resulted in destruction of the tissue and further optimisation of the protocol would be required to facilitate these experiments. Expression within the pituitary is particularly intriguing given that in mouse ovarian tissue PABP5 is expressed in the granulosa cells which are a direct downstream target of follicle stimulating hormone which is produced in the anterior portion of the pituitary. The so called hypothalamic-pituitary-gonadal axis is central to gonad function.

Also of interest was the implication that PABP5 may be expressed predominantly in endocrine organs. Besides the brain, ovary and testis, other endocrine organs such as the thyroid and adrenal glands were ranked highly in the qPCR assay. Whether PABP5 has a particular subset of mRNA targets that are in some way associated with sending or receiving signals, such as cellular receptors or factors involved in the packaging of secreted signals in these cell types is unclear. Certainly investigation into PABP5 expression within these organs warrants further attention.

There remains a discrepancy between the human RT-PCR data (Blanco *et al.*, 2001) and the qPCR data presented in figure 3.3 regarding the expression of PABP5 in human ovarian tissue. Whilst the higher levels of PABP5 observed in mouse ovaries would appear consistent with the results of Blanco *et al*, it is possible that PABP5 levels may differ significantly in human and mouse ovaries. Humans are mono-ovulatory, and generally produce one ova for each menstrual cycle while mice are poly-ovulatory resulting in the production of multiple ovulatory follicles each cycle. As a result the PABP5 expressing granulosa cells may represent a higher proportion of the cellular mass of a mouse ovary.

In-situ hybridisation of the testis failed to identify the sites of PABP5 mRNA expression. Since PABP5 is expressed in the granulosa cells of the ovary, it is possible that PABP5 may be expressed within the Sertoli cells of the seminiferous tubules. Low abundance transcripts are notoriously difficult to visualise in this cell-type due to the diffuse nature of their cytoplasm. As a result, a more sensitive assay such as tyramide signal amplification (TSA) or fluorescent *in-situ* hybridisation may prove appropriate. Alternatively, RT-PCR could be undertaken on isolated primary Sertoli cells to confirm the presence of PABP5 transcript in this cell type.

As a result of the failure of the antibodies tested to detect endogenous PABP5, the localisation of PABP5 protein at both the whole tissue and cellular level remains to be characterised. Both commercial antibodies, At164 and Ab140886 detected recombinant PABP5 protein by Western blot, implying that the levels of endogenous PABP5 may be below the detection threshold of the antibodies rather than being non-immunoreactive against PABP5 antigen. This would correlate with the levels of PABP5 mRNA which appears to be a low abundance transcript.

My results extend the existing literature with regard to the expression pattern of PABPs revealing that PABP1, PABP4, ePABP, tPABP and PABP5 are all expressed in gonadal tissues, as detailed below (see table 3.23). This suggests that PABP proteins may have important roles in mammalian gametogenesis consistent with tPABP and ePABP being gonad specific.

Expression of PABPs in the Mouse Testes

Investigation into the subcellular localisation of PABP proteins is largely hampered by the high levels of sequence homology between the proteins making generation of specific reagents difficult. Available data shows that PABP proteins are present within both the somatic tissues and germ cells within the testes, although the distribution of PABP proteins varies between cell types, with some cells containing

multiple PABP proteins, yet others apparently only containing one. The non-ubiquitous nature of the PABP proteins within the cells of the seminiferous tubules might argue against functional redundancy between these proteins, perhaps implicating that within certain cell-types different physiological requirements necessitate different functional activities. It is distinctly possible that within these cell-types the PABP proteins have specific mRNA targets, thus requiring cell-type specific expression.

The Sertoli cells and Leydig cells of the testis are somatic endocrine and paracrine cells. I have shown that PABP4 is expressed in Sertoli and more weakly in Leydig cells. Kimura *et al*. document weak PABP1 expression in Leydig cells but this may represent cross-reaction with PABP4 as PABP1 mRNA is not present in these cells. Moreover, a second in-house PABP1 specific antibody also failed to detect PABP1 in Leydig cells (L. McCracken, unpublished). RT analysis would suggest that PABP5 may be expressed in at least one of these cell types, however this requires further verification. tPABP is restricted to specific germ cell stages and is not expressed in these somatic cells. Within the germ cell population, it was extremely interesting to note that the cells expressing the highest levels of PABP4 protein, the mitotically dividing spermatogonia, were completely devoid of PABP1 and tPABP. Kimura et al report weak PABP1 expression which for the reasons given above is likely to be cross-reaction. PABP4 levels are reduced in later germ cell stages concomitant with the initial expression of PABP1 and tPABP in spermatocytes. tPABP and PABP1 expression peaks in round spermatids (Gu *et al.*, 1995; Kimura *et al.*, 2009; Kleene *et al.*, 1994), however only PABP1 expression persists into early elongating spermatids.

The loss of PABP proteins during elongation correlates with an important deadenylation event within elongating spermatids, where the mRNAs coding for protamines and transition proteins involved in chromatin remodelling and packaging within the spermatozoa undergo a loss of their poly(A) tails (Kleene, 1989; Kleene,

1993; Kleene *et al.*, 1984). Counter-intuitively, inhibition of PABP protein activity appears to be required to facilitate the translational activation of these mRNAs (Yanagiya *et al.*, In press). ePABP mRNA is weakly expressed in testis and this may represent its presence in specific germ cell stages as it is restricted to oocytes within the ovary in several species (Seli *et al.*, 2005; Wilkie *et al.*, 2005). No evidence supporting PABP5 expression in germ cells is available.

Expression of PABPs in the Mouse Ovaries

As with the testes, mouse ovaries display a distinct yet overlapping expression pattern of PABPs. Only tPABP is not expressed within this tissue, underlining the importance of the PABP proteins and translational regulation in oogenesis. While PABP5 was hypothesised to be expressed predominantly within the Sertoli and Leydig cells of the testes, the functional equivalents within the ovary, the granulosa and thecal cells, were positively identified as sites of expression of PABP5 mRNA. PABP1 and PABP4 were also documented in these cell-types. The granulosa and thecal cells have both endocrine and paracrine functions in follicular development, and additionally undergo an enormous expansion in cell number during folliculogenesis, therefore it could be argued that there is a requirement for high levels of active translation within these cells.

The oocytes within the follicles also appear to express more than one PABP with ePABP mRNA (Seli *et al.*, 2005) and PABP4 protein both expressed within these germ cells. While ePABP expression is independent of the follicular stage PABP4 appears to be less abundant in late ovulatory follicles (L. McCracken, unpublished). The necessity for translational regulation in oocytes is well established, because the transcriptionally quiescent oocytes rely on proteins produced from maternally derived mRNAs. In particular, changes in poly(A) tail length are important for progression through pachytene, dictyate and oocyte maturation in mouse (Gebauer *et al.*, 1994; Racki and Richter, 2006; Tay and Richter, 2001).

	PABP1		ePABP		PABP4		PABP5		tPABP	
	RNA	Protein	RNA	Protein	RNA	Protein	RNA	Protein	RNA	Protein
Spermatogonia	x	x				✓✓✓				
		Kimura								
Spermatocytes	✓✓✓	✓				✓				
	Gu	Gu Kimura							Kleene	Kimura
Round spermatids	✓✓	✓✓				✓				
	Gu	Gu Kimura							Kleene	Kimura
Elongating spermatids	✓	✓				✓				
		Gu Kimura								
Sertoli cells	x	x				✓				
Leydig cells	x	x				✓				
		Kimura								
Primary oocyte	x	x				✓✓✓	x			
			Seli							
Granulosa cell	✓✓	✓✓				✓✓	✓✓✓			
Thecal cell	✓	✓				✓/x	✓✓			
Stroma	x	x				✓/x	x			
OSE	x	x					x			
Corpus luteum	✓	✓				✓✓	✓			

Table 3.23 PABP distributions within mouse gonads. Ticks and crosses represent expression levels documented within thesis. ✓✓✓ = strong expression observed, ✓✓ = moderate expression observed, ✓ = weak expression observed, X = no expression observed. Blank boxes represent cell types in which expression levels remain to be determined. Gu = expression in this cell type reported by Gu *et al*. 1995, Kimura = expression in this cell type reported by Kimura *et al*. 2009, Seli = expression in this cell type reported by Seli *et al*. 2005, Kleene = expression in this cell type reported by Kleene *et al*. 1994.

Following ovulation the remaining granulosa and thecal cells of the follicle form an endocrine structure called the corpus luteum. PABP1 and PABP4 protein, as well as PABP5 mRNA was documented in this tissue with PABP1 and PABP5 being at lower levels than other positively staining cell types. Whether this is residual expression from follicles that have recently undergone ovulation or is physiologically important is unclear.

PABP Gametogenesis Phenotypes

Unfortunately, there are no published mouse models for any of the PABP proteins, and therefore no attributable mammalian phenotypes. In the available invertebrate models, roles in gametogenesis have been suggested based on the phenotypes. In *Caenorhabditis elegans* for example ethyl methanesulphonate (EMS) screens and RNAi knock-downs of the Pab-1 and Pab-2 genes suggest that the proteins may have a redundant function within the soma but that Pab-1 is essential in the germline (Maciejowski *et al.*, 2005). P-element insertions that disrupt pAbp function in *Drosophila* can also lead to meiotic defects during spermatogenesis (Fasulo *et al.*, 1999). The data described here suggest that loss of PABP function in mammals is also likely to result in gametogenesis defects. In support of this loss of function of the PABP regulatory protein PAIP2 disrupts spermatogenesis in mouse (Yanagiya *et al.*, In press).

In this chapter I have described the expression of a novel mammalian poly(A)-binding protein, PABP5, and characterised its mRNA distribution within mouse ovarian tissue. I have shown that the mRNA localises to somatic cells within the ovary that also contains the PABP proteins PABP1 and PABP4. The requirement for multiple PABP proteins in single cells is unclear, although interestingly, recently submitted data from within our laboratory (B. Gorgoni, submitted) suggests that despite a high degree of protein sequence conservation PABP1, PABP4 and ePABP only have partially redundant roles. The difference in domain structure between PABP5 and the other PABP proteins raises interesting questions pertaining to its molecular function, which is addressed in chapter 4.

Chapter 4: Functional Analysis of PABP5

4.1 Introduction and Aims

Most functional data pertaining to the poly(A)-binding proteins is derived from studies of the prototypical family member, PABP1. While little is known regarding the functions of the other PABP proteins, a conserved role in the regulation of mRNA translation and stability appears likely from the limited experimental evidence available. There is currently no data pertaining to the physiological or molecular functions of PABP5.

PABP5 is frequently referred to as a cytoplasmic PABP (Gorgoni and Gray, 2004; Mangus *et al.*, 2003), although there is no published evidence of its subcellular distribution. The classification of PABP5 as a cytoplasmic protein is based on phylogeny, as PABP5 shares a common RRM domain structure with other cytoplasmic PABPs, and bears little structural homology to the nuclear PABPs (see figure 1.9 and figure 1.11). PABP5 lacks both the proline-rich linker region and the C-terminal domain present within other cytoplasmic poly(A)-binding proteins, and the functional implications of this are unknown. Given that these domains facilitate a number of interactions with protein factors promoting PABP1 activity (Mangus *et al.*, 2003) PABP5 could be envisaged to have a function that differs from that of PABP1. In opposition to this, there is data suggesting that PABP5 might share a degree of functional similarity to PABP1 even in the absence of a C-terminal domain. Firstly, yeast growth was completely unaffected by the removal of the entire yeast Pab-1 C-terminus (Sachs *et al.*, 1987) and secondly, a truncation mutant of *Xenopus* PABP1 that contains only RRMs 1-4 was capable of stimulating translation *in-vivo* when tethered to a reporter mRNA (Gray *et al.*, 2000). Indeed the closed loop model facilitated by the PABP1-eIF4G interaction occurs within PABP1 RRM2 (Imataka *et al.*, 1998; Kessler and Sachs, 1998) which could feasibly still occur within PABP5, although this remains to be determined.

Within this chapter I begin to dissect the molecular functions and interactions of PABP5 with regards to a potential role in translational regulation by direct comparison with PABP1.

4.2 EGFP-tagged PABP5 is Localised to the Cytoplasm

While PABP1 is localised predominantly to the cytoplasm the subcellular localisation of PABP5 is unknown. A predominantly cytoplasmic localisation would be consistent with a role in translational regulation or mRNA stability. Since lack of a functional antibody prohibits the determination of the subcellular localisation by immunofluoresence it was decided to clone mouse PABP5 into a mammalian expression vector. HeLa cells were transiently transfected with the resulting vector which expressed PABP5 as an N-terminally tagged fusion with enhanced green fluorescent protein (EGFP). A vector expressing only EGFP was also transfected. GFP is known to localise to both the nucleus and cytoplasm in transfected vertebrate cells (Ogawa *et al.*, 1995). Mouse PABP1 was also cloned into the same vector to establish any effects of overexpression on subcellular localisation. It has previously been reported that overexpressing GFP-PABP1 in a HeLa cell-line can result in a homogeneous cellular distribution of the protein (Afonina *et al.*, 1998), but that cells expressing low levels of GFP-PABP1 display a predominantly cytoplasmic localisation, mirroring the endogenous protein (Afonina *et al.*, 1998). It was therefore decided to transfect 100ng of the EGFP-PABP constructs rather than 3µg which was sufficient to drive nuclear accumulation of the GFP-PABP1 protein (Afonina *et al.*, 1998). Upon transfection EGFP-PABP5 predominantly localised to the cytoplasm, as did EGFP-PABP1 (see figure 4.1). EGFP had a homogeneous cellular distribution as was expected. A number of cells (approximately 10%) contained nuclear localised EGFP-PABP1 and EGFP-PABP5. Whether this is physiologically relevant is unclear. These cells could simply represent cells with higher levels of expression, but quantification of the signal intensity to score cells would be required to validate this.

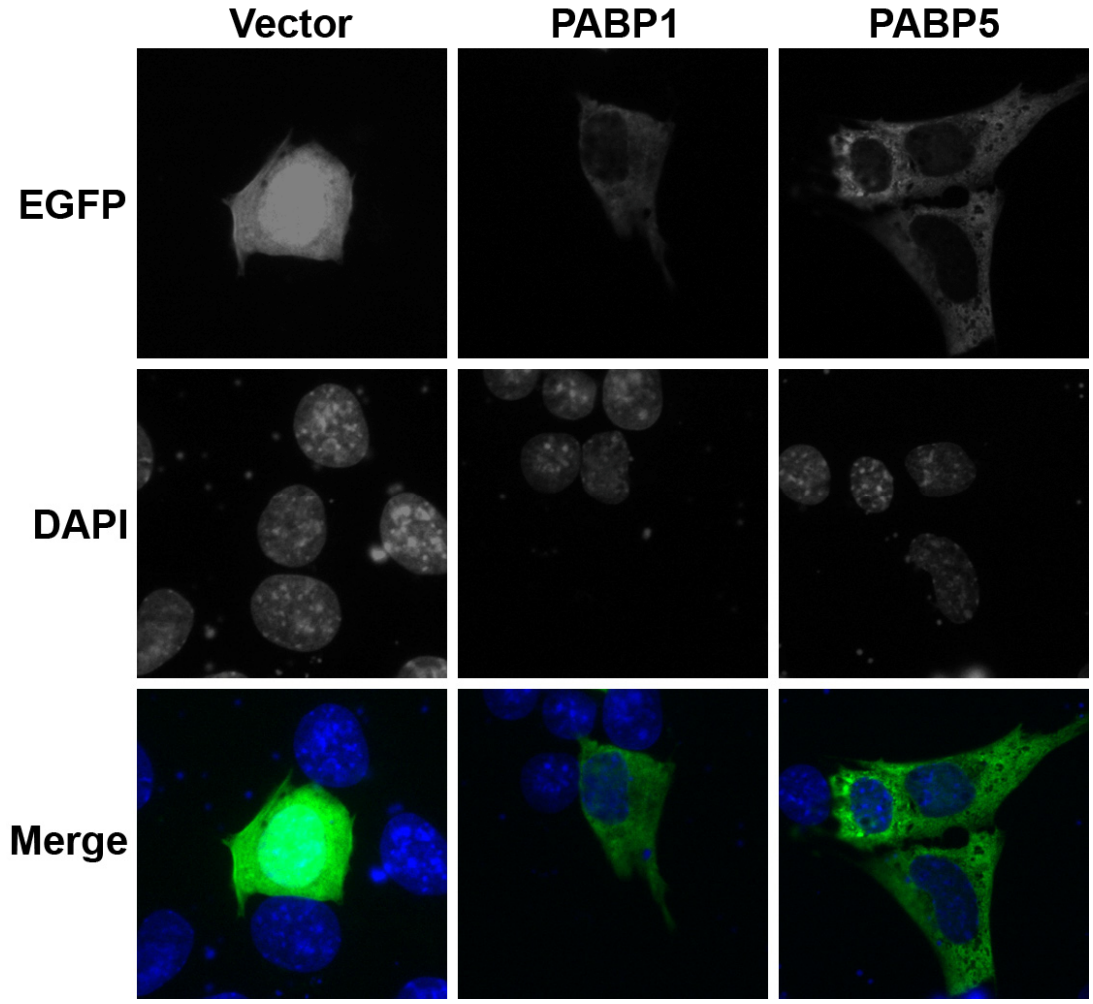

Figure 4.1 Localisation of EGFP-PABP proteins. HeLa cells were transiently transfected with 100ng of EGFP, EGFP-mouse PABP1, or EGFP-mouse PABP5 mixed with 1.9µg of carrier DNA. Cells were counterstained with DAPI (blue) to mark the nucleus. Single channel images in grayscale are shown.

The cytoplasmic distribution of EGFP-PABP5 was then determined in two further cell lines – the mouse fibroblast cell-lines 3T3 and L929. As with HeLa cells, PABP5 localised predominantly to the cytoplasm suggesting that the localisation is likely conserved between mammalian species (see figure 4.2).

4.3 Overexpressed PABP5 Co-Localises with Polysomes

Cellular translation occurs within the cytoplasm, therefore the localisation of PABP5 to the cytoplasm is in agreement with a potential role in translational regulation. If PABP5 is a stimulator of translation it could be expected to associate with polysomes. Sucrose gradient fractionation of cell and tissue lysates is a widely utilised tool, used to establish if proteins co-sediment with polysomes, and indeed PABP1, PABP4 and ePABP are present in the polysomal fractions (Gu *et al.*, 1995; Proweller and Butler, 1996; Wilkie *et al.*, 2005) (H.Burgess, unpublished). HeLa cells transfected with T7-tagged PABP1 and PABP5 were treated with cycloheximide prior to extracts being resolved on 20-50% sucrose gradients.

Cycloheximide affects the translocation step during translation elongation to 'freeze' translating ribosomes on the mRNAs. As a control untransfected HeLa cells were also subjected to fractionation. As expected a proportion of PABP1 (both endogenous and overexpressed) localised to the polysomal regions of the sucrose gradient as determined by Western blotting (see figure 4.3). Interestingly a similar proportion of PABP5 also co-sedimented with the polysomal fractions.

To determine if this co-sedimentation was likely to represent bona fide polysomal association a puromycin 'release' experiment was performed in tandem. Puromycin is an aminonucleoside antibiotic that causes premature chain termination during translation by entering the ribosomal A-site and joining the growing peptide causing premature release and dissociation of the ribosome. Thus, factors associated with polysomes will shift towards free messenger ribonucleoprotein (mRNP) fractions. Investigators frequently utilise ethylenediamine-tetraacetic acid (EDTA) as a similar control, but this treatment is not specific to ribosomes and can lead to erroneous conclusions regarding whether factors are truly polysome associated. While all the PABP proteins appeared to release with puromycin treatment, and this corresponded to a resulting increase in 'free' 80S monoribosomes, the release was far from satisfactory. This could reflect only some of the PABP proteins in these fractions

associating with polysomes, as previous puromycin release experiments have demonstrated that some PABP1 remains in polysomal fractions (Kozak *et al.*, 2006). Alternatively, this may reflect the effectiveness of puromycin which functions best in salt concentrations greater than 300mM, higher than in our assays (Blobel and Sabatini, 1971).

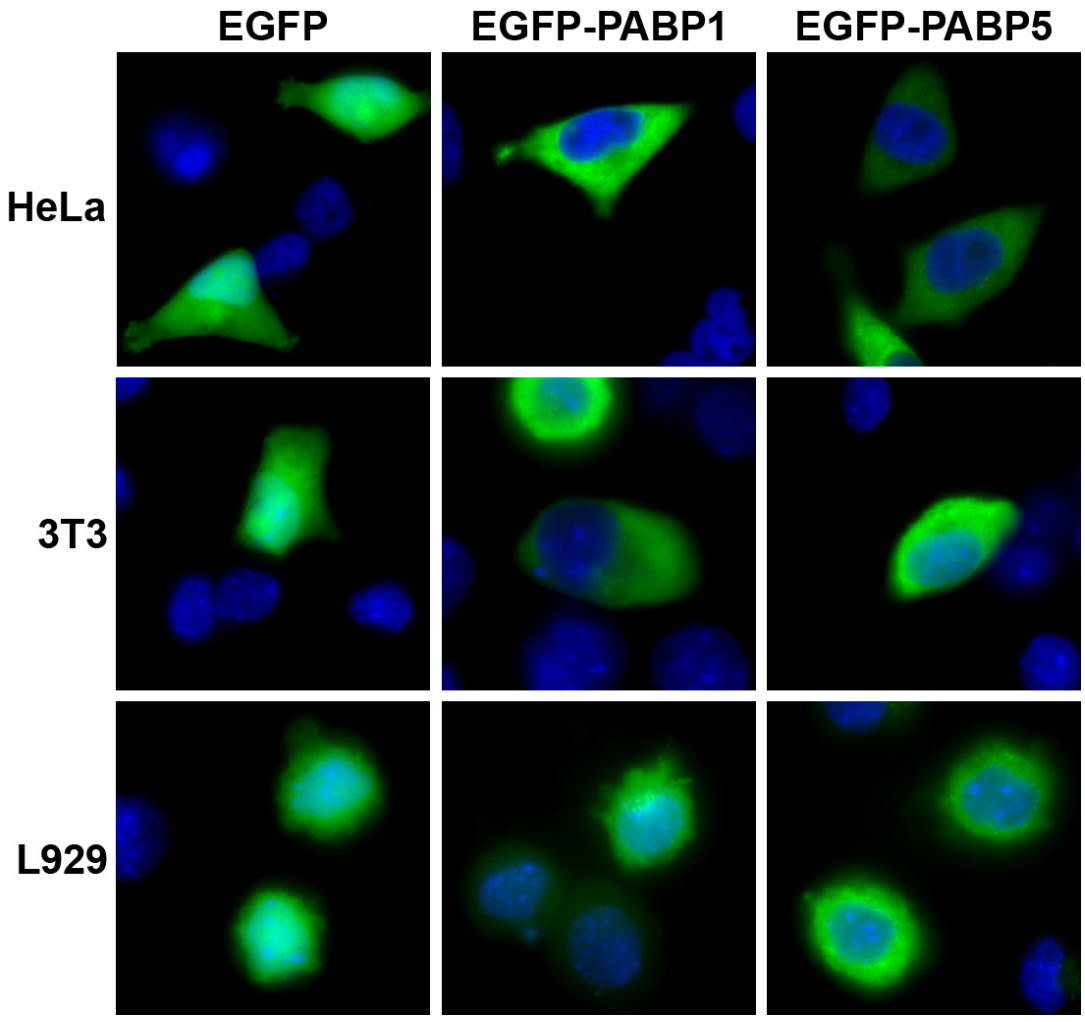

Figure 4.2 Localisation of EGFP-PABP proteins in different cell types. HeLa, 3T3, or L929 cells were transiently transfected with 100ng of EGFP, EGFP-PABP1, or EGFP-PABP5 mixed with 1.9µg of carrier DNA. Cells were counterstained with DAPI (blue) to mark the nucleus. See appendix 5 for single channel images.

Of interest was the observation that ectopically expressed PABP5 appeared to have little effect on the polysome profile when compared to the untransfected cells (see figure 4.3). If PABP5 was a potent general translational repressor or stimulator overexpression might be expected to promote or inhibit the formation of polysomes. Overexpression of PABP1 also appeared to have little effect on mRNA distribution perhaps suggesting that the HeLa cells are unresponsive to overexpression of PABP1. Perhaps a more likely explanation is that overexpression of PABP1 results in downregulation of endogenous PABP1 via the ARS in the 5'-UTR of PABP1 mRNA, thus maintaining similar levels of the protein.

It was concluded from the polysome analysis that at least a proportion of the overexpressed PABP5 protein was possibly associated with polysomes, although care must be taken when interpreting these experiments as a polysomal association does not imply a direct role in translation and it is possible that PABP5 could be performing a function that requires association with mRNA in a non-translational capacity, such as that of a stability factor. Thus, the translational stimulatory activity of PABP5 requires testing.

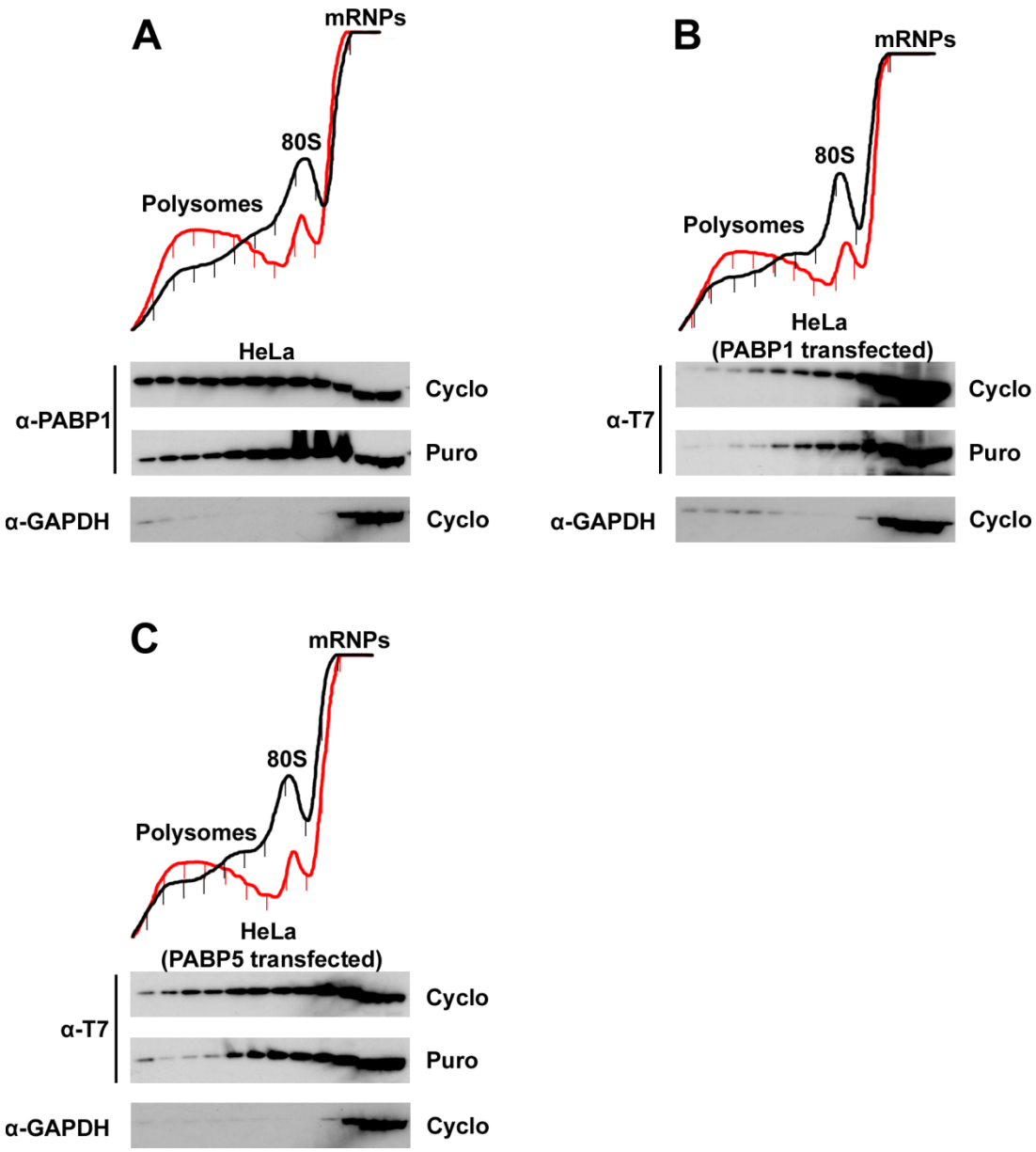

Figure 4.3 Polysome association of PABP proteins. **(A)** Untransfected **(B)**, T7-PABP1 transfected or **(C)** T7-PABP5 transfected HeLa cells were lysed in buffer containing cycloheximide or puromycin and subjected to sucrose gradient fractionation. Absorbance of the collected fractions was measured at 254nm and plotted. Red line = cycloheximide treatment, black line = puromycin treatment. The protein was extracted from the fractions by trichloroacetic acid precipitation and was subjected to Western blotting with relevant antibodies. GAPDH was included as a non-polysomal associated protein control.

4.4 PABP5 Has Little Activity in The Tether Function Assay

The Tethered Function Assay

The finding that PABP5 was possibly polysomal fitted with the hypothesis that PABP5 may indeed be a translational regulatory protein. To investigate the translational stimulatory activity of PABP5 directly the tethered function assay was utilised (depicted in figure 4.4). The tethered function assay has the advantage of being able to test the function of a protein without needing to know the endogenous target binding sequence as the ability of PABP5 to bind poly(A) has not been determined. Additionally, tethering avoids the complications of other endogenous PABP proteins which would otherwise need to be depleted (Kahvejian *et al.*, 2005). A number of tethering approaches have been described, each of which revolves around the generation of a fusion protein containing the protein of interest fused to a second peptide or protein that binds with high affinity to a known sequence element inserted into a reporter mRNA. The most common tethered function assays utilise the RNA-binding domain of the λ phage antiterminator protein N with its specific λ-N binding site (called a boxB site) (Baron-Benhamou *et al.*, 2004; De Gregorio *et al.*, 2001) or conversely the bacteriophage coat protein, MS2, which recognises a structural stem loop termed an MS2-binding site. This assay has been utilised to investigate the translational activity of other PABPs (Gray *et al.*, 2000; Wilkie *et al.*, 2005).

All tethered function assays performed within this thesis were undertaken in microinjected stage VI oocytes derived from *Xenopus laevis* frogs. While translation assays could be performed in cultured cell-lines, reporter mRNAs with no poly(A) tail would not be efficiently exported from the nucleus and so RNA transfections would be required. Additionally, the lack of a poly(A) tail would render the reporter mRNAs vulnerable to degradation. In contrast mRNAs can be injected directly into the cytoplasm of *Xenopus* oocytes, and have been demonstrated to be highly stable within these cells (see figure 1D in Gray *et al.*, 2000).

Oocytes were injected with *in-vitro* transcribed mRNAs coding for the test and control proteins fused to an N-terminal MS2 tag. MS2-U1A mRNA serves as a negative control (Gray *et al.*, 2000). U1A is an RRM containing protein that forms part of the U1 small nuclear ribonucleoprotein (snRNP) complex that is essential in pre-mRNA splicing, but does not regulate translation (Jovine *et al.*, 1996).

Following a six hour incubation to allow expression of the fusion protein two mRNA reporters were simultaneously co-injected, a m^7G capped unadenylated luciferase reporter mRNA and an internal control β-galactosidase (β-gal) mRNA (see figure 4.4). The luciferase reporter contains three MS2-binding sites within its 3'-UTR that serve as tethering sites for the fusion protein. The translational effects of tethering the fusion protein to the reporter mRNA can then be directly measured by luciferase protein production. The β-gal reporter is incapable of binding the fusion protein as it contains no MS2 sites within its 3'-UTR. Therefore, variability in injection volumes and also the translational capacities of different oocytes can be corrected for by normalising the luciferase units to the β-gal light units. The β-gal reporter mRNA was unadenylated and contained an artificial ApppG (ApG) cap and a CSFV IRES within the 5'-UTR rather than a physiological m^7G cap. The utilisation of a β-gal reporter that lacks a functional cap and a poly(A) tail decouples translation of this reporter from the effects of overexpressing PABP proteins. After reporter mRNA injections the oocytes were incubated overnight before assaying.

Oocytes were assayed in batches of five, with a minimum of twenty oocytes per experimental point. The value obtained from the MS2-U1A fusion protein was always set to one. All other values were then corrected relative to MS2-U1A. Multiple experiments were undertaken to generate a data set, using oocytes collected from different female *Xenopus* frogs. The stimulation values were averaged to give a final value and the standard error was calculated.

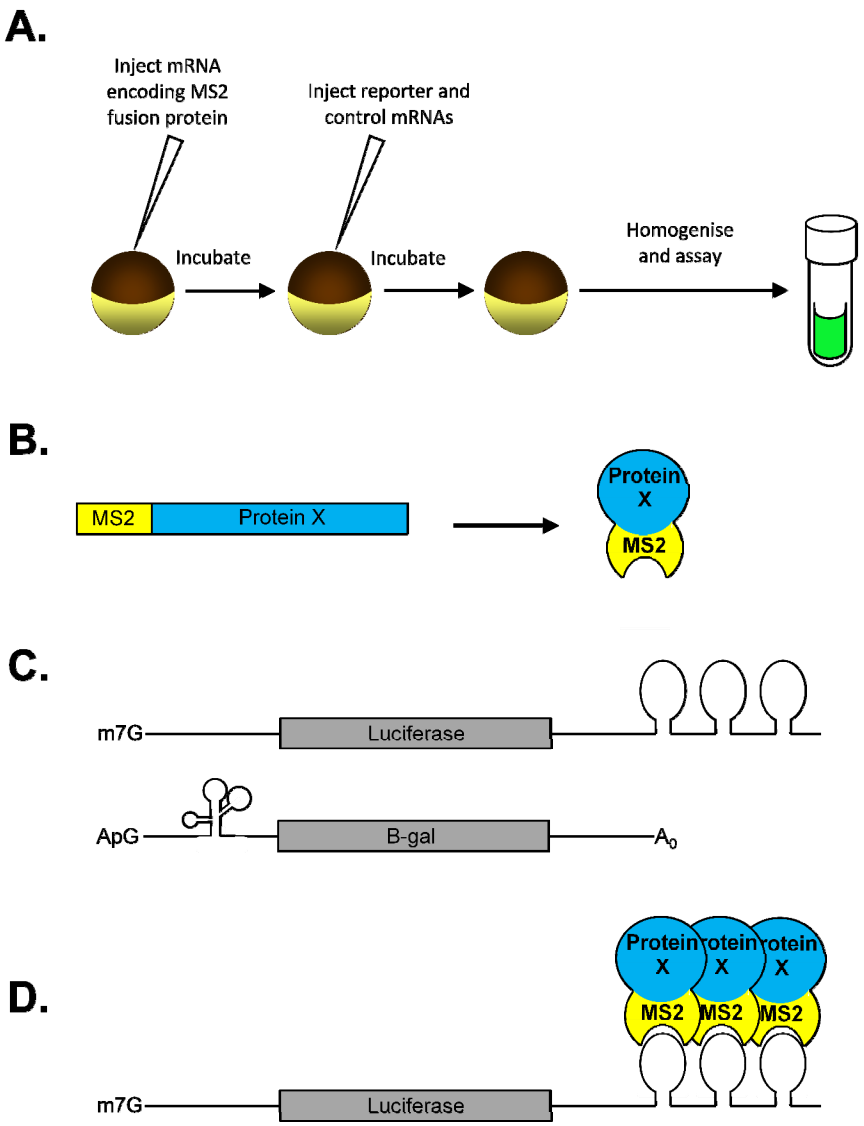

Figure 4.4 The tethered function assay. A. Oocytes collected from *Xenopus laevis* are injected with mRNA encoding a fusion protein (depicted in B) consisting of the protein to be tested fused to bacteriophage MS2 coat protein. Following incubation the oocytes are simultaneously injected with a luciferase reporter containing MS2-binding sites within its 3'-UTR, and a control β-galactosidase mRNA (depicted in C). The fusion protein MS2-proteinX then binds the MS2-binding sites within the luciferase reporter mRNA 3'-UTR (depicted in D). Following a further incubation, the effect of tethering protein X on the translation of the reporter can be assessed by directly measuring luciferase protein production. Luciferase units are normalised to β-galactosidase units to correct for small variations in the amount of reporter mRNA injected and the differing translational capacities of individual oocytes.

Human PABP5 Activity in the Tethered Function Assay

To investigate the ability of human PABP1 and PABP5 to stimulate translation tethered function assays were performed as described above, with mRNAs coding for MS2-PABP5, MS2-U1A and MS2-PABP1 (see figure 4.5A). MS2-PABP1 stimulated translation approximately 6-fold over MS2-U1A. In contrast, MS2-PABP5 only stimulated translation approximately 2-fold (see figure 4.5A), with a lowest stimulation value of 0.66-fold over MS2-U1A and a highest of 3.1-fold. The average stimulation value for PABP5 represents the lowest value reported for a PABP protein using this assay, as various *Xenopus* PABP proteins have been demonstrated to stimulate translation up to 7-fold over the control injected protein (Gray *et al.*, 2000; Wilkie *et al.*, 2005). To demonstrate the specificity of the fusion protein activity on the reporter mRNAs the raw luciferase and β-gal values from five different experiments were plotted (see figure 4.5B). The β-gal values appeared to be largely consistent between different experiments, suggesting that the β-gal reporter values were unaffected by the overexpressed fusion protein, and that the translational stimulation was through stimulatory effects on the luciferase reporter.

Mouse PABP5 Activity in the Tethered Function Assay

Previously published data has shown that PABP1 proteins from different species have differing capacities to stimulate translation in the tethered function assay. For example *Saccharomyces cerevisiae* Pab-1 stimulates translation 35-fold over a control protein, compared to 7-fold for *Xenopus laevis* PABP1 (Gray *et al.*, 2000). To determine if the reduced translational activity observed by human PABP5 is a species specific effect, mouse PABP5 and mouse PABP1 were also tested by tethered function assay (see figure 4.6A). As with the human protein, mouse PABP5 had a reduced capacity to stimulate translation compared to mouse PABP1, with an average stimulation value of approximately 1.5-fold over MS2-U1A. Thus, in a tethered function assay mammalian PABP5 appears to have limited translational stimulatory activity.

A.

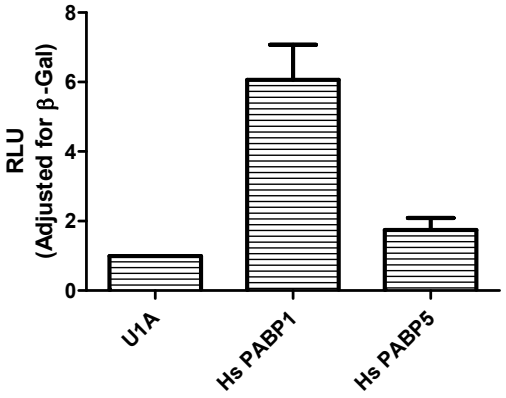

B.

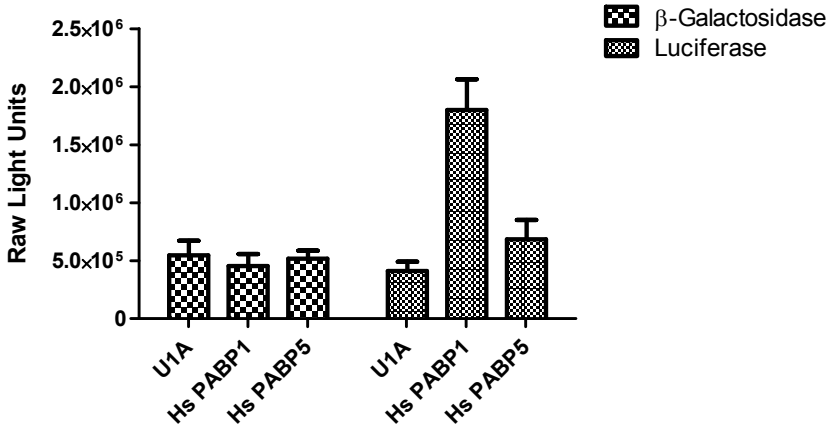

Figure 4.5 Human PABP5 has a reduced capacity to stimulate translation compared to human PABP1. A. The translational stimulatory activity of human PABP1 (Hs PABP1) and human PABP5 (Hs PABP5) on a luciferase reporter mRNA was tested by tethered function assay in *Xenopus* oocytes. Relative luciferase units (RLU) were calculated by normalising luciferase reporter units to the β-galactosidase internal control units. The stimulation values for five separate experiments were averaged and the standard error calculated. MS2-U1A was set to one and all other values were corrected to MS2-U1A. While PABP1 stimulated translation approximately 6-fold over U1A, PABP5 only stimulated approximately 2-fold. **B.** The raw luciferase and β-galactosidase values generated by the tether function assay.

To determine the extent to which this result reflects a translational effect, effects on luciferase reporter mRNA stability must be formally ruled out. Indeed, the levels of luciferase protein may be the net effect of a large increase in reporter translation combined with a simultaneous increase in mRNA degradation. Conversely, the stimulatory activity seen by PABP1 could be a result of the tethered PABP1 protein stabilising the reporter mRNAs. As mentioned previously, exogenously introduced mRNAs are remarkably stable within *Xenopus* oocytes and therefore stabilisation is unlikely to result in the 5- to 6-fold stimulation visualised by tethering PABP1 to the reporter. Previously, *Xenopus laevis* PABP1 and ePABP and *Saccharomyces cerevisiae* Pab-1 have been demonstrated to have minimal effects on reporter mRNA stability in a tethered function assay (Collier *et al.*, 2005; Gray *et al.*, 2000; Wilkie *et al.*, 2005).

Effects on stability were determined by harvesting oocytes immediately (t=0) or 16 hours (t=16) following the luciferase reporter injection. Total mRNA from the oocytes was extracted and cDNA was prepared. The cDNA was then subjected to quantitative real-time PCR (QPCR) using primers specific for the luciferase reporter. This assay was chosen to circumvent the need to use radioactive material, and also due to the high sensitivity offered by using a PCR based assay. SYBR green QPCR assays have been used previously in the laboratory to determine mRNA stability (Wilkie *et al.*, 2005). SYBR green fluorescence increases dramatically upon binding the minor-groove of DNA and can therefore be used as a direct readout of the level of PCR product present within a reaction.

Oocytes were injected with MS2-U1A, MS2-PABP1 (mouse), MS2-PABP5 (mouse) and MS2-PABP5 (human) and harvested as described above. The mRNA was harvested from batches of five oocytes and 1µg of total mRNA was added to each reverse-transcriptase reaction to produce cDNA. Following cDNA production, the equivalent of 0.1µl from each reverse-transcriptase reaction was added to each QPCR reaction. The data was subsequently plotted as a measure of cycle threshold

(C_T) number, that is the number of PCR cycles required for the fluorescent signal to cross a defined threshold value (i.e. exceeds the background level). The results of two separate experiments were averaged and standard error calculated. The data is plotted in figure 4.6B. There appeared to be little difference between the luciferase reporter CT scores at t=0 and t=16 for all the fusion proteins injected. Two-tailed Student's *t*-tests were performed and differences between the paired time-points were deemed not statistically significant for all samples ($p>0.05$). This shows that the differences in expression levels of luciferase protein are true translational effects and are not a function of altered luciferase reporter mRNA stability within oocytes as a result of tethering the MS2-fusion proteins.

PABP1 Truncation Mutant Activity in the Tethered Function Assay

Why PABP5 has a markedly reduced translational stimulatory activity is unclear. PABP5 lacks the proline-rich linker region and PABC domain important for facilitating a number of protein-protein interactions. It was therefore hypothesised that these missing regions may be partially or wholly responsible for the lack of translational activity. To test this hypothesis, full-length and truncation mutants of *Xenopus laevis* and mouse PABP1 were cloned and transcribed as MS2-fusion mRNAs for tethered function assay (see figure 4.7A). Interestingly, mouse PABP1 RRMs 1-4 was capable of stimulating translation of the luciferase reporter 4-fold over MS2-U1A which is similar to the full-length fusion protein (5-fold).

A.

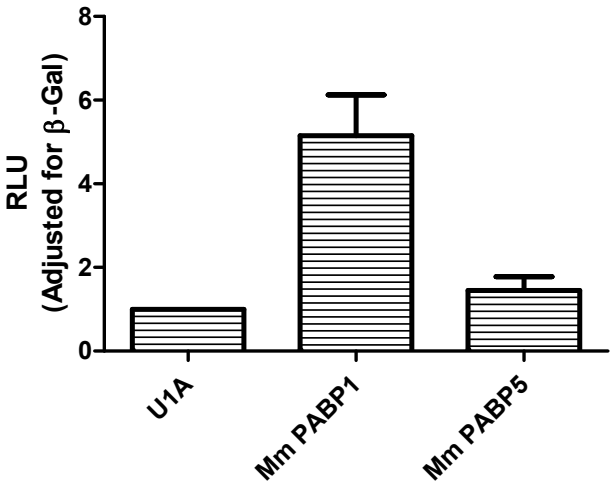

B.

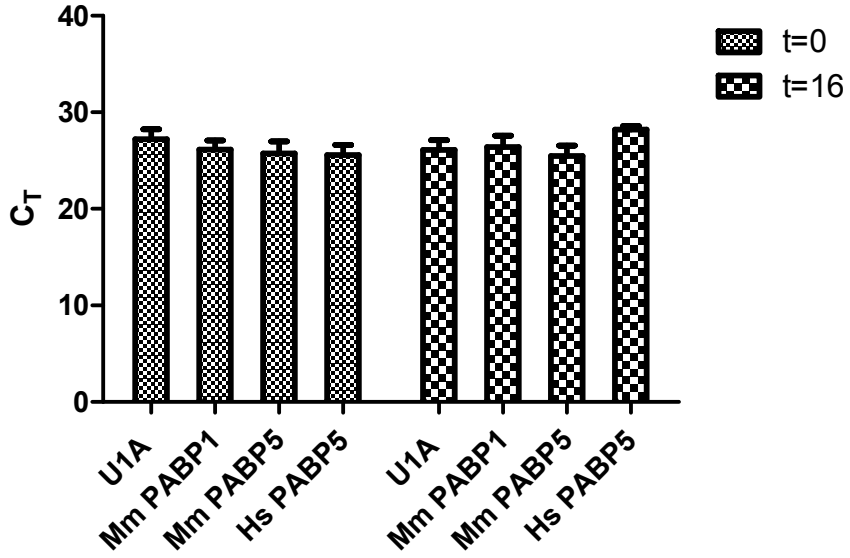

Figure 4.6 The low translational stimulatory activity of PABP5 is conserved between species. A. The translational activities of mouse PABP1 (Mm PABP1) and mouse PABP5 (Mm PABP5) were tested by tethered function assay. The stimulation values for four separate experiments were averaged and the standard error calculated. RLU = relative luciferase units. **B.** Oocytes expressing MS2-U1A, MS2-PABP1 (mouse), MS2-PABP5 (mouse) and MS2-PABP5 (human) were injected with luciferase reporter mRNA. Total mRNA was extracted from the oocytes immediately following reporter injection (t=0) or following a 16 hour incubation (t=16). cDNA was prepared from the mRNA and used for SYBR green QPCR. The variability between time points for each MS2-fusion protein injection was calculated as not significant by two-tailed Student's *t*-test ($p>0.05$).

This result mirrored that of *Xenopus* PABP1 RRMs 1-4 against the full-length protein (5-fold and 7-fold respectively). Of all the full-length PABP1 proteins tested, *Xenopus laevis* PABP1 stimulated translation of the luciferase reporter to the highest degree. This could be a result of the tethered function assays being performed in a *Xenopus* oocyte background, with endogenous factors perhaps having a lower functional affinity for the mammalian fusion proteins. These data imply that lacking the C-terminus is not the sole reason for a lack of translational activity, although both the *Xenopus* and mouse PABP1 RRM 1-4 truncation mutants stimulate translation to a lesser degree than the full-length wild-type protein suggesting that the C-terminus of PABP1 does contribute to the translational activity. Indeed the previously published data showed that both the ePABP and PABP1 C-termini could stimulate translation 2-fold over MS2-U1A in a tethered function assay, although the mechanism of this stimulation was unclear and the authors warn that it may be a result of endogenous PABP recruitment to the luciferase reporter mRNA (Gray *et al.*, 2000).

Lack of translational activity shown by PABP5 in this assay might be the poor expression of the MS2-PABP5 fusion protein. To determine that the fusion proteins were being efficiently expressed, oocytes were injected with mRNAs coding for the fusion proteins and were metabolically labelled by incubation in a buffer containing ^{35}S-methionine for six hours. Following the incubation the oocytes were collected, lysed and subjected to SDS-PAGE, then the labelled proteins were visualised by autoradiography. All newly synthesised proteins were visible including the fusion proteins (see figure 4.7B). The signals for the mouse and human PABP5 fusion proteins were visibly weaker than their corresponding PABP1 counterparts. However, this is largely a reflection of the number of methionines within the proteins as mouse and human PABP5 only contain 8 methionines whereas mouse PABP1 RRMs 1-4 contains 15 methionines. These data suggest that the lack of translational activity is not as a result of the MS2-PABP5 mRNA failing to express the MS2-PABP5 fusion protein.

A.

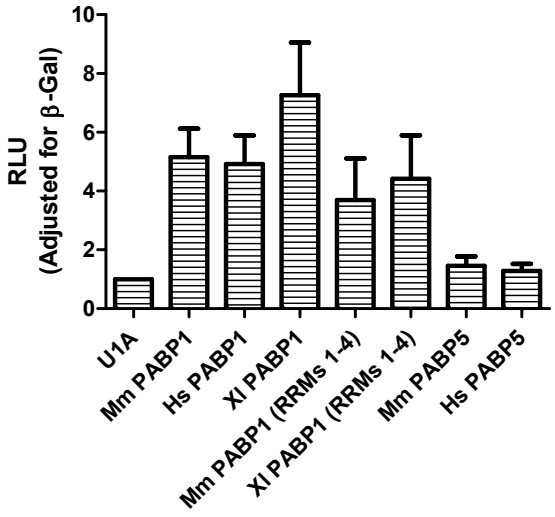

B.

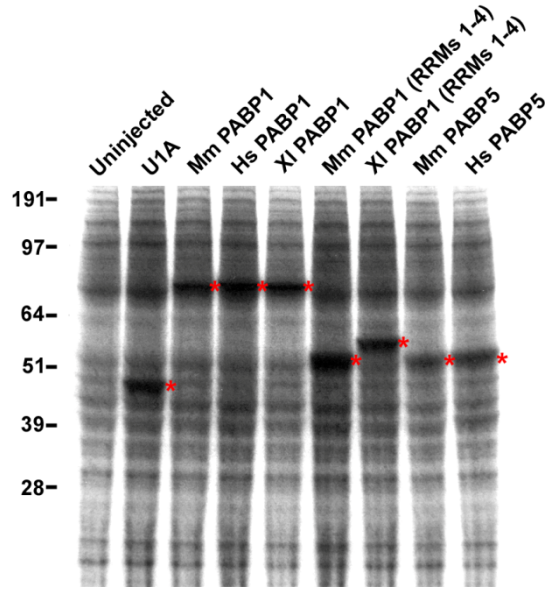

Figure 4.7 PABP1 C-terminal truncation mutants have translational stimulatory activity. A. The translational activities of U1A, PABP1, PABP5 and PABP1 truncation mutants were tested by tethered function assay as described above. The stimulation values for four separate experiments were averaged and the standard error calculated. RLU = relative luciferase units. Mm = mouse, Hs = human, Xl = *Xenopus laevis*. **B.** The fusion proteins are expressed. Oocytes were injected with mRNA coding for the fusion proteins then incubated in buffer containing ^{35}S methioine to label new proteins. After incubating for 6 hours oocyte lysates were prepared and run on an SDS-PAGE gel before being subjected to autoradiography. Fusion proteins are indicated by red stars.

4.5 PABP5 Fails to Interact with Translation Initiation Factors

Data in the previous section suggest that PABP5 has a severely reduced capacity to stimulate translation of a reporter mRNA compared to PABP1. The reasons behind the lack of translational activity are unclear. A number of PABP1 protein interactions are thought to promote mRNA circularisation in the closed loop model of translational stimulation, including eIF4G (Gray *et al.*, 2000; Imataka *et al.*, 1998; Kessler and Sachs, 1998), PAIP-1 (Craig *et al.*, 1998; Roy *et al.*, 2002) and eIF4B (Bushell *et al.*, 2001; Cheng and Gallie, 2007). These interactions have been demonstrated to be important for stimulating translation (Bushell *et al.*, 2001; Craig *et al.*, 1998; Imataka *et al.*, 1998; Kahvejian *et al.*, 2005). In addition, other PABP1 interacting proteins such as PAIP-2, can directly affect PABP1 activity (reviewed in Derry *et al.*, 2006). Thus, interacting proteins play a key role in moderating PABP1 translational activity. In the following section I address the possibility that the lack of PABP5 activity in the translational assay may be in part due to failure of PABP5 to bind proteins central to the closed loop mechanism of translational stimulation.

4.6 The Yeast 2-Hybrid Assay

The yeast 2-hybrid (Y2H) assay is a yeast-based genetic assay utilised to identify protein-protein interactions, by taking advantage of the modular nature of transcription factors (Fields and Song, 1989). The reconstitution of a functional transcription factor through interacting proteins is exploited in the Y2H assay to drive transcription of a reporter gene, often LacZ, allowing quick identification of positive yeast colonies by treatment with the β-galactosidase substrate X-gal (see figure 4.8 for a schematic of the Y2H assay).

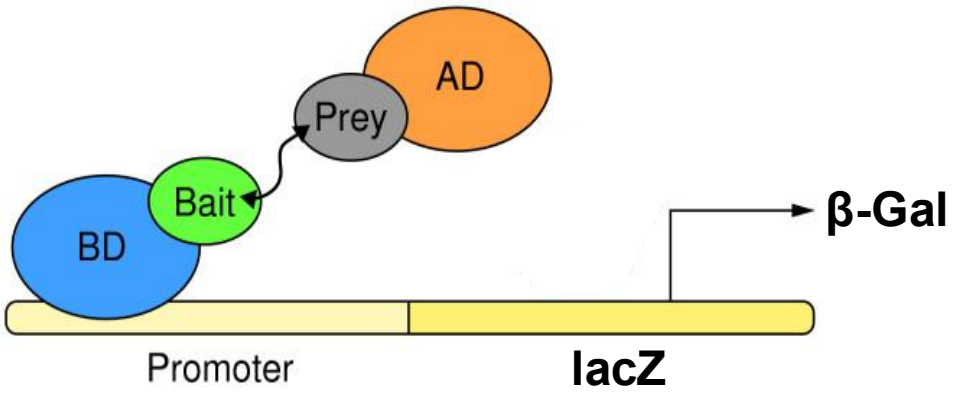

Figure 4.8 The yeast 2-hybrid assay. Fusions consisting of 'bait' and 'prey' proteins fused to the DNA-binding domain (BD) or activating domain (AD) of a transcription factor are expressed in yeast. Upon interaction between bait and prey the transcription factor is reconstituted, resulting in the transcription of a reporter gene, LacZ.

4.7 PABP5 Fails to Interact with Translation Factors by Y2H Assay

The Y2H assay was chosen to identify any potential interactions between PABP5 and known translation factors. An in-house library of translation factors cloned into suitable Y2H GAL4-AD vectors was utilised. This library has been pre-validated for yeast expression within the laboratory (B. Richardson and B. Gorgoni, unpublished). Mouse and human PABP5 were therefore cloned into a corresponding Y2H BD vector. The controls used in this assay were *Xenopus laevis* PABP1 RRMs 1-2 tested against IRP (negative control) and the N-terminus of human eIF4G (positive control). Both these interactions have been tested by Y2H previously, in the yeast strain used here (Gray *et al.*, 2000).

Mouse PABP5 failed to interact with any of the human translation factors tested by Y2H (see figure 4.9A). In particular, the lack of an interaction with eIF4G could be considered unusual as this interaction has been demonstrated for *Xenopus* ePABP (Wilkie *et al.*, 2005) and mouse tPABP (Kimura *et al.*, 2009) in addition to PABP1 from a variety of species (Imataka *et al.*, 1998; Kimura *et al.*, 2009; Tarun and Sachs,

1996), suggesting that it may be a conserved interaction of all the other cytoplasmic PABPs. However, the lack of interaction could be due to PABP5-BD not being expressed correctly. Also, the lexA-BD is approximately 24 kDa therefore represents a large peptide which could affect the folding or protein interacting capacity of a relatively small protein such as PABP5. The lack of a positive control for PABP5 also makes validation of the expression of PABP5-BD in yeast a necessity. To this end yeast were transformed with mouse PABP5-BD and following growth were lysed and subjected to SDS-PAGE followed by Western blotting with a primary antibody directed against the LexA-BD. The PABP5 fusion protein was present in all the yeast transformations and was also expressed to a similar degree (see figure 4.9B). In addition, the PABP1 RRMs 1-2 also showed robust expression.

The absence of interaction with eIF4G would reconcile with a lack of translational activity in the tethered function assay. Human PABP5 also failed to interact with eIF4G (see figure 4.9C) suggesting that this may be a conserved property of PABP5 proteins. Confirmation of this lack of interaction in a second assay is required such as a pulldown assay utilising recombinant proteins, or an immunoprecipitation (IP) from cells or tissues (see section 4.10).

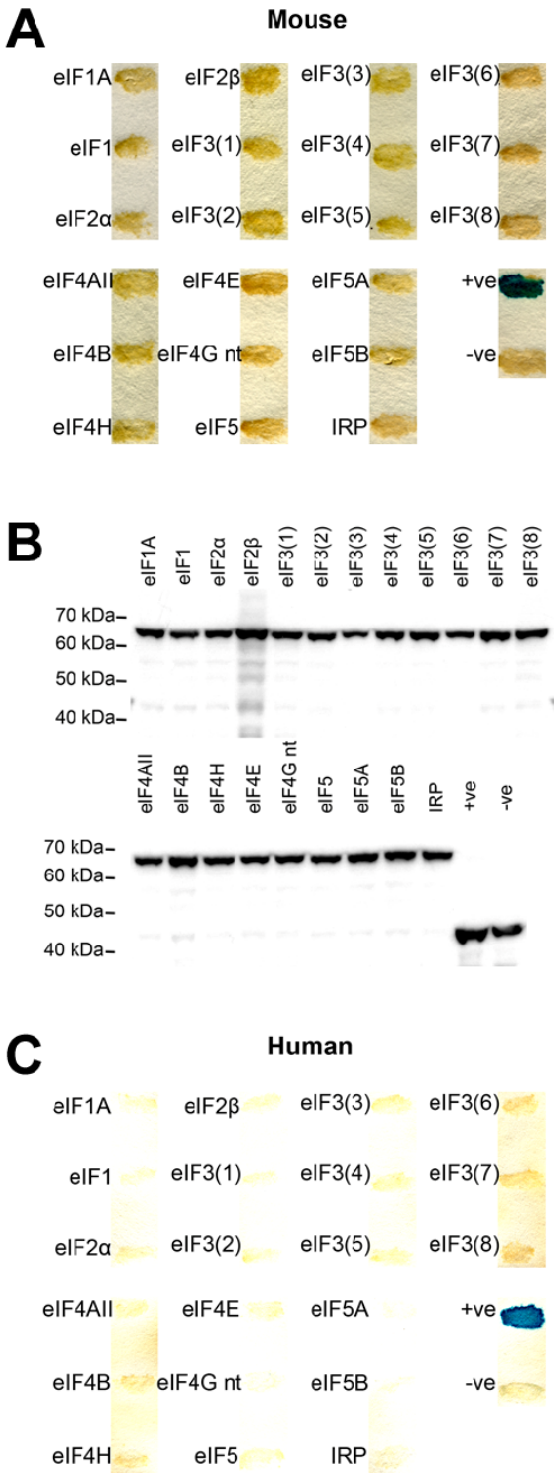

Figure 4.9 Yeast 2-hybrid PABP5 versus translation initiation factors. A,C. Mouse and human PABP5 respectively were expressed in yeast as fusion proteins with the LexA-BD. The translation initiation factors were expressed in the same yeast as fusion proteins with the GAL4-AD. Positive colonies were identified by incubation with X-gal resulting in a blue colouration. Positive control (+ve) = *Xenopus laevis* PABP1 RRMs 1-2 versus N-terminus of human eIF4G, negative control (-ve) = *Xenopus laevis* PABP1 RRMs 1-2 versus IRP. **B.** Expression of mouse PABP5-BD fusion protein in yeast. Antibody was directed against the LexA-BD. PABP5 fusion protein = 67 kDa, PABP1 RRMs 1-2 fusion protein = 43 kDa.

4.8 The eIF4G Residue Responsible for PABP1 Binding is Not Conserved in PABP5

It is known that disruption of the mammalian PABP1-eIF4G interaction is sufficient to inhibit translation of reporter mRNAs *in-vitro* and *in-vivo* (see chapter 1, section 1.4.4) (Imataka *et al.*, 1998; Kahvejian *et al.*, 2005), therefore failure of PABP5 and eIF4G to interact by Y2H could explain the low levels of translational stimulation observed with PABP5 in the tethered function assay.

The eIF4G binding site in PABP1 has been previously mapped to RRM2 (Gray *et al.*, 2000; Imataka *et al.*, 1998; Kessler and Sachs, 1998; Otero *et al.*, 1999). Further investigations using isothermal titration calorimetry (ITC) narrowed the binding site to a handful of conserved residues (Groft and Burley, 2002). ITC is a technique that is used to determine the thermodynamic parameters of chemical reactions and directly measures the heat taken up or evolved upon addition of a ligand to its binding molecule. Thus, binding curves can be determined by plotting heat changes in response to increasing amounts of ligand. Two residues within PABP1 RRM2 were described as critical for eIF4G binding, methionine 161 (M161) and leucine 162 (L162). Mutation of these residues to alanine resulted in complete abolition of the interaction (Groft and Burley, 2002). An additional residue, lysine 157 (K157), resulted in significantly decreased eIF4G binding affinity (K_d of 170μM compared to the 27μM calculated for wild-type PABP1 RRMs 1-2) (Groft and Burley, 2002).

The M161 to alanine (M161A) PABP1 mutant has been demonstrated to be functionally compromised. In Krebs-2 cell extracts depleted of PABP1, translation of a reporter was inhibited 7-fold. Addition of recombinant wild-type PABP1 but not the M161A PABP1 mutant restored translation to levels comparable to undepleted extracts (Kahvejian *et al.*, 2005). Crucially it was demonstrated that the M161A mutation does not affect poly(A)-binding activity of PABP1, therefore a deficit in translational activity was likely due to inhibition of the PABP1-eIF4G interaction (Groft and Burley, 2002).

The critical residues M161 and L162 have been described as being conserved between PABP1 species from yeast to man (Groft and Burley, 2002). Upon sequence alignment of RRM2 across all the cytoplasmic PABPs in mouse and human (see figure 4.10) it was apparent that PABP5 was the only cytoplasmic PABP species in which these residues were not conserved, with a valine residue replacing M161 and an arginine residue replacing L162. In addition K157 which was described as being important for eIF4G binding was substituted with a histidine residue. Interestingly K157 is replaced with a threonine in ePABP although this appears to be insufficient to prevent binding of *Xenopus laevis* ePABP to eIF4G (Wilkie *et al.*, 2005). In addition to these substitutions in PABP5 which may have functional implications, the region around M161 and L162 is not particularly well conserved as highlighted by the sequence alignment (see figure 4.10). This observation could therefore represent an explanation as to why PABP5 might not interact with eIF4G.

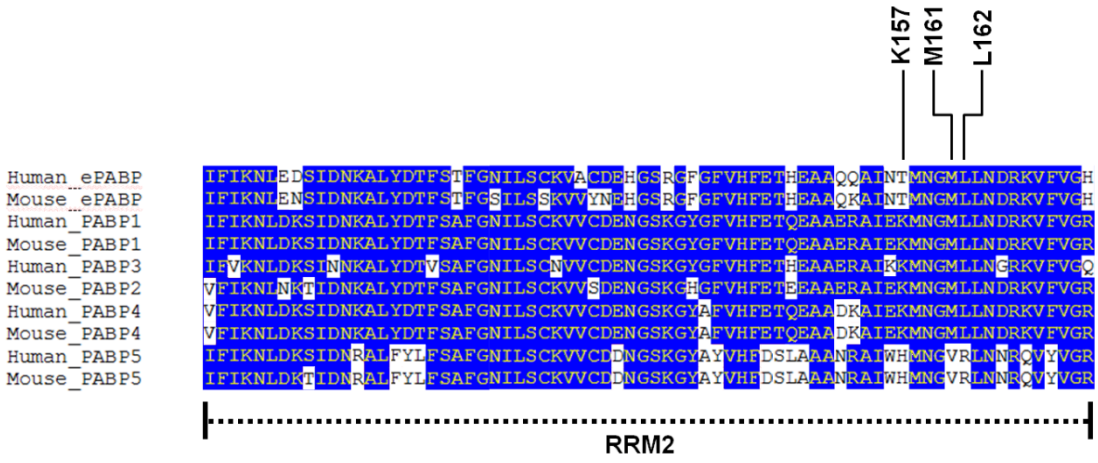

Figure 4.10 PABP RRM2 sequence homology. Mouse and human cytoplasmic PABP RRM2 sequence conservation. Blue shading represents conserved sequence. The position of three amino acids, K157, M161, and L162, are indicated. These amino acids have been identified as important for eIF4G binding and are not conserved in PABP5.

4.9 Recombinant Protein Generation

The sequence alignment mapping the critical eIF4G binding residues would appear to correlate with the Y2H data. Therefore, to confirm that PABP5 and eIF4G fail to interact a pulldown assay was performed. This required generation of recombinant proteins. Both human PABP1 and PABP5 were cloned into the pET28(c)+ bacterial expression vector which is based on a T7 promoter driven system. These clones were used to transform *E. coli* cells expressing the bacteriophage T7-RNA polymerase under the control of the lac promoter. Thus, supplementing the growth media with the allolactose analogue isopropyl β-D-1-thiogalactopyranoside (IPTG) results in inhibition of the lac repressor and strong expression of T7-RNA polymerase. This in turn induces the rapid expression of the target gene within the vector. The vector contains sequence coding for six consecutive histidine (his) residues immediately upstream of the cloning site that forms a tag incorporated into the extreme N-terminus of the recombinant protein. This allows identification of the recombinant proteins by Western blotting with a primary antibody raised against the his-tag, and additionally can be used to purify the proteins by affinity chromatography using a nickel column.

Protocols for T7-promoter driven expression of recombinant PABP5 in *E. coli* cells have previously never been detailed but have been described for the generation of recombinant PABP1. These protocols suggest growth of the transformed *E. coli* to an optical density (O.D.) of 0.3 at 37^{o}C then induction with 0.5mM IPTG at 22^{o}C (Woods *et al.*, 2002). These conditions were used to set up the initial inductions, and subsequent optimisation was based around these parameters. See table 4.11 for all induction conditions used. It was determined that the optimal induction conditions differed for the two recombinant proteins with optimal PABP1 induction occurring at 22^{o}C with 0.5mM IPTG as previously described (Woods *et al.*, 2002). PABP5 inductions were more robust at higher temperature and IPTG concentrations (22-30^{o}C, with 1mM IPTG). All subsequent inductions post-optimisation were undertaken at 22^{o}C with 1mM IPTG. The recombinant proteins were clearly visible after IPTG induction followed by lysis and analysis by SDS-PAGE (see figure

4.12A). The his-tag and the associated vector polylinker region were estimated to add approximately 3kDa to the mass of the protein, giving his-PABP1 an estimated mass of 75kDa (72kDa + 3kDa) and his-PABP5 a mass of 47kDa (44kDa + 3kDa). The induced proteins appeared to migrate in a manner consistent with these predictions suggesting that the majority of the recombinant protein produced was full-length.

Induction Temperature	Induction Time (hours)	IPTG Concentration	PABP1 Expression	PABP5 Expression
16°C	4	0.5	✓	-
22 °C	4	0.5	✓✓✓	✓
22 °C	4	1	✓✓	✓✓
22 °C	4	1.5	✓✓	✓
6 °C	Overnight	1	ND	-
30 °C	4	1	ND	✓✓

Table 4.11 E. coli induction conditions. *E. coli* cells were transformed with pET28-PABP1 or pET28-PABP5 and grown to an optical density of 0.3-0.5 before being induced using one of the above induction protocols. ND = not determined. A hyphen (-) indicates that no expression was detectable. The ticks represent the level of induction as determined by SDS-PAGE analysis with one tick indicating a poor induction, two ticks indicating moderate induction, and three ticks indicating robust induction. All inductions post-optimisation were undertaken at the highlighted parameters.

To confirm that the induced proteins were indeed his-tagged, lysates were subjected to SDS-PAGE followed by Western blotting with a primary antibody directed against the his-tag (see figure 4.12B). The majority of the detectable signal for each of the proteins corresponded to molecular masses consistent with full-length PABP1 and PABP5 proteins. However, in the PABP1 lysate there was an additional signal running at approximately 47kDa.

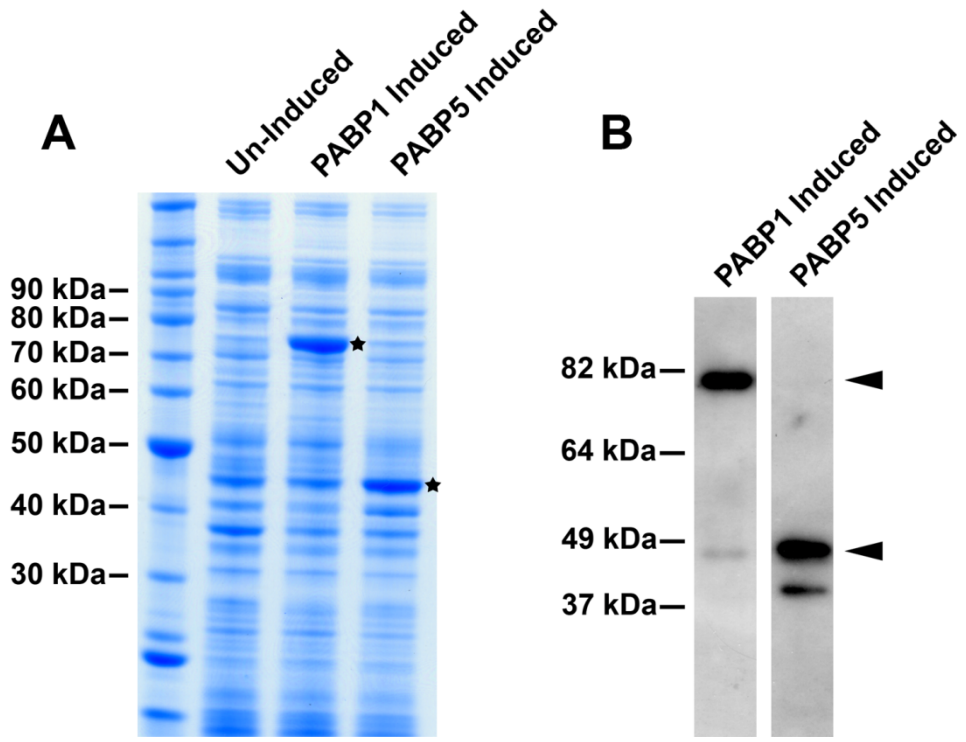

Figure 4.12 Recombinant protein inductions. A. *E. coli* cells were transformed with pET28-PABP1 or pET28-PABP5 and induced to express the recombinant proteins. The cells were then lysed and 10µg of the lysate was subjected to SDS-PAGE. The gel was then stained with GelCode Blue (Thermo Scientific). The PABP1 and PABP5 histidine-tagged proteins had predicted molecular masses of 75kDa and 47kDa respectively. The black stars indicate the induced proteins. **B.** Lysate containing recombinant Histidine-tagged PABP1 or PABP5 was subjected to SDS-PAGE followed by Western blotting with an anti-polyhistidine antibody. The his-PABP1 and his-PABP5 signals are indicated by black arrows.

The fact that it is detectable implies that it contains a his-tag, therefore this was considered a breakdown product of the full-length protein. Given that the his-tag is N-terminal and that the signal is of very similar mass to PABP5, it is possible that this signal represents RRMs 1-4 of PABP1. The flexible proline-rich linker region is known to be vulnerable to protease attack (Joachims *et al.*, 1999; Kuyumcu-Martinez *et al.*, 2002; Kuyumcu-Martinez *et al.*, 2004). The PABP5 Western also picks up an additional signal running immediately underneath the full-length protein at approximately 43kDa. Again this protein must represent a C-terminal truncation as the his-tag is still present.

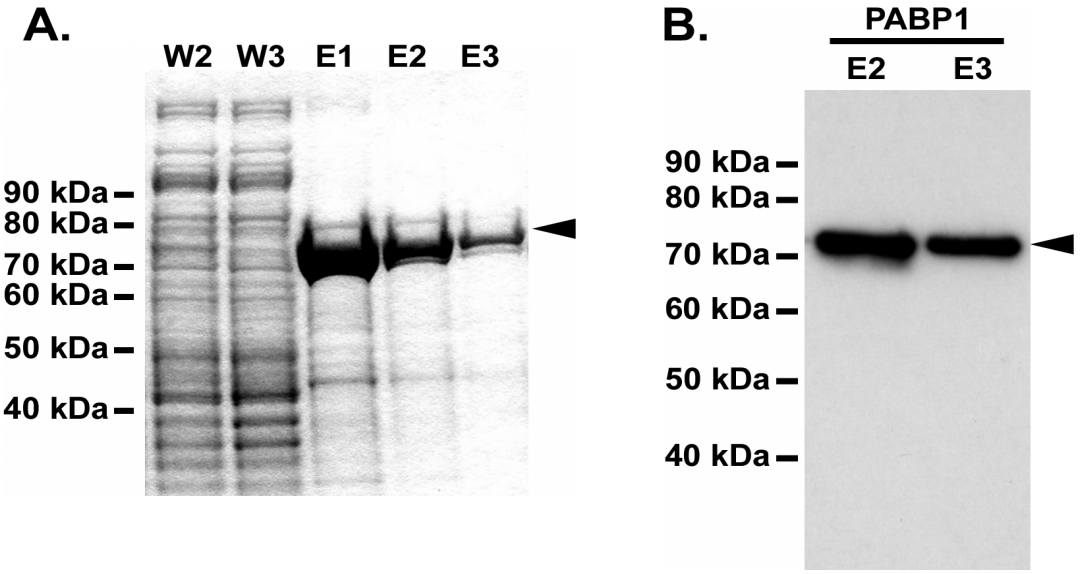

Figure 4.13 Recombinant PABP1 purification. A. His-PABP1 was purified from *E. coli* lysate by affinity chromatography using nickel agarose. 15µl of the two final bead washes (W2 and W3) and the elutions from the beads (E1, E2, and E3) were subjected to SDS-PAGE followed by staining with GelCode Blue (Thermo Scientific). The arrow indicates full-length PABP1 protein. In lane E1 the possible his-tagged RRM 1-4 breakdown product is visible. **B.** 0.1µl of purified recombinant PABP1 from E2 and E3 was subjected to Western blotting with an anti-PABP1 antibody raised against a peptide derived from the extreme C-terminus of the human PABP1 protein. The arrow indicates the presence of the full-length protein.

E. coli cell lysates containing recombinant PABP1 and PABP5 were subsequently subjected to affinity chromatography with a nickel column to purify the his-tagged proteins. While PABP1 purified in significant quantity and to relative homogeneity (see figure 4.13A) PABP5 could not be purified in quantity under the conditions used (figure 4.14A). The presence of recombinant PABP5 within the unbound fraction (flow-through) of the purification procedure implied that the protein was not binding the nickel-agarose beads with high affinity (see figure 4.14A). A possible explanation could be that the his-tag was partially buried within the protein so as not to be accessible to the nickel-agarose.

Following purification both PABP1 and PABP5 were subjected to Western blotting (figures 4.13B and 4.14B respectively). To test for the presence of PABP1 N-terminal truncations which would not be detectable by Western blot against the N-terminal his-tag, Western blotting was performed with an antibody raised against an

extreme C-terminal peptide of the PABP1 protein (see figure 3.7; Chapter 3). The resulting signal corresponded only to the full length protein (see figure 4.13B) therefore it was concluded there were no N-terminal truncations suggesting that PABP1 was not subject to breakdown following purification. The only available antibodies for PABP5 were raised against full-length PABP5 protein, therefore the epitopes are unknown and the same conclusions could not be drawn regarding PABP5 N-terminal truncations.

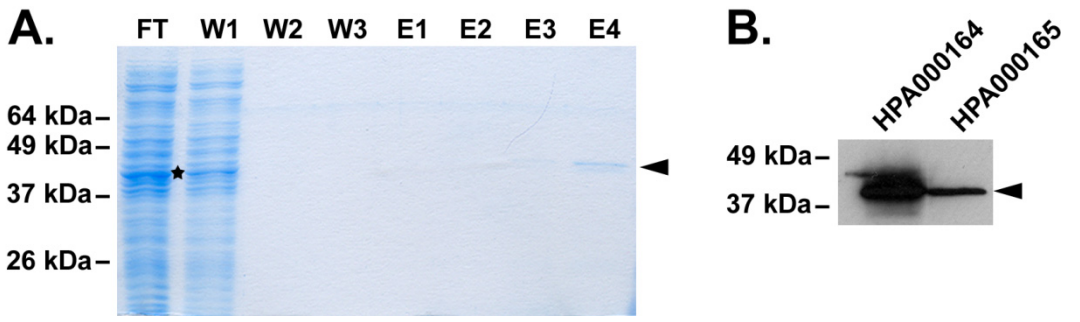

Figure 4.14 Recombinant PABP5 purification. A. his-PABP5 was purified from *E. coli* lysate by affinity chromatography using nickel agarose. 10µl of the flow-through (FT) bead washes (W1, W2, and W3) and elutions from the beads (E1, E2, E3, and E4) were subjected to SDS-PAGE followed by staining with Coomassie protein stain. The arrow indicates full-length PABP5 protein. The star indicates the recombinant PABP5 protein in the flow-through. **B.** 1µl of purified recombinant PABP5 from E4 was subjected to Western blotting with two antibodies raised against PABP5 (HPA000164 and HPA000165). The arrow indicates the presence of the full-length protein.

The quantities of PABP5 recombinant protein retrieved by affinity chromatography were below the detection threshold for quantification by Bradford assay, therefore it was decided to quantify the proteins using SYPRO Ruby protein stain (Invitrogen). SYPRO Ruby is a sensitive luminescent stain that is not amino acid biased therefore is suitable for quantitation of proteins. The proteins were subjected to SDS-PAGE along with BSA standards. The gel was then stained with SYPRO Ruby protein stain as per manufacturer's instructions and scanned using a Typhoon Variable Mode

Imager with a 488nm excitation laser. The PABP5 protein was calculated to be at a concentration of 15.44ng/µl (0.357µM) while PABP1 was calculated to be at a concentration of 1342ng/µl (18.99µM).

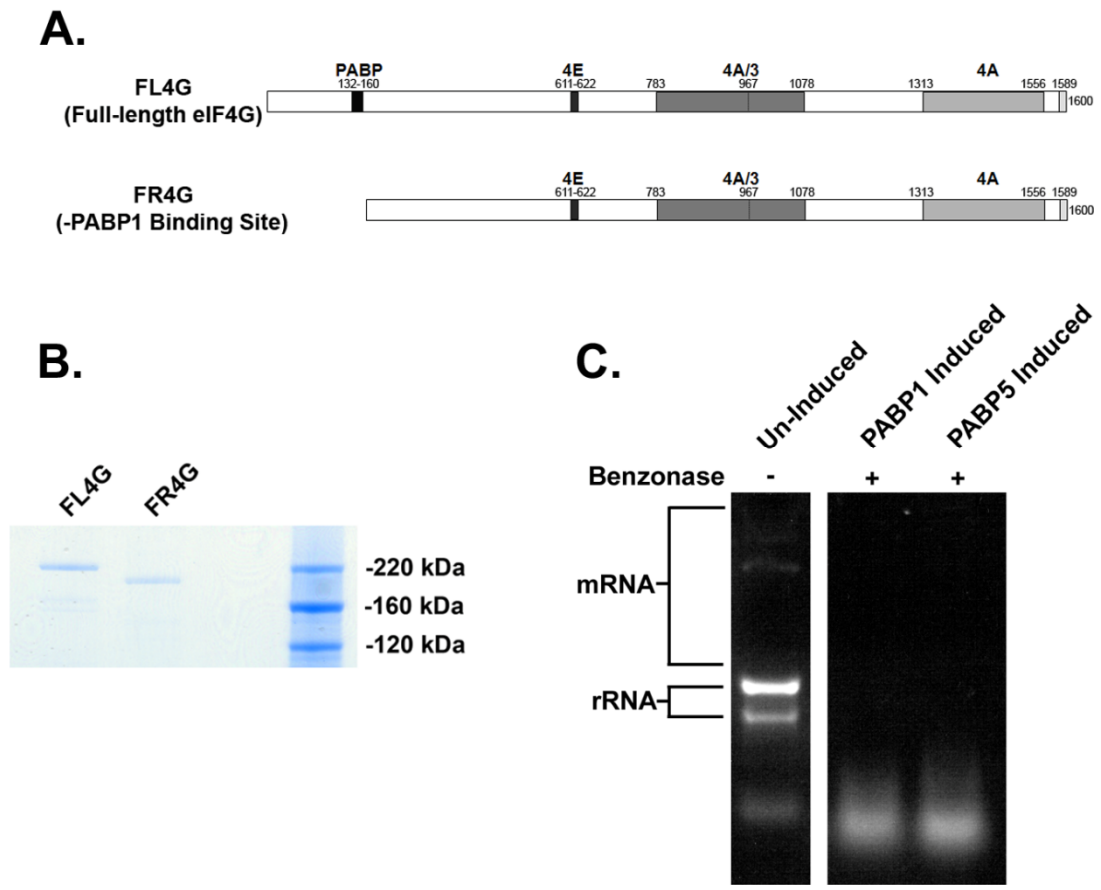

Figure 4.15 Recombinant eIF4G proteins. A. Schematic representation of the eIF4G recombinant proteins. Both proteins are C-terminally FLAG-tagged. FR4G lacks the N-terminal PABP1 binding site that is retained in the full-length protein (FL4G). The binding sites of other eukaryotic initiation factors are depicted (eIF4E, eIF4A, and eIF3). **B.** 200ng of each recombinant eIF4G protein was subjected to SDS-PAGE and the gel was stained with GelCode Blue. **C.** *E. coli* cells containing recombinant PABP1 or recombinant PABP5 were lysed in a buffer containing 25 units of benzonase per ml of buffer. As a control un-induced *E. coli* lysate was lysed in the same buffer but lacking benzonase. The RNA was extracted from the samples using Tri-Reagent (Ambion) and was subjected to agarose gel electrophoresis. The rRNA and mRNA are degraded in the presence of benzonase.

4.10 PABP5 Does Not Interact With eIF4G By Pulldown Assay

The importance of the PABP1-eIF4G interaction in facilitating closed loop or end-to-end complex formation is documented in chapter 1, section 1.4.4. A schematic of the full-length eIF4G protein with key binding sites is depicted in figure 4.15A. To further substantiate the finding that PABP5 and eIF4G do not interact in a Y2H assay pulldown experiments using recombinant proteins were performed. Two recombinant human FLAG-tagged-eIF4G proteins were utilised for this experiment, one containing the N-terminal PABP1 binding site (FL4G) and one lacking this site (FR4G). The FL4G and FR4G samples were estimated to be ≥95% pure and ≥75% pure respectively. These proteins were a kind gift from Dr Simon Morley (University of Sussex) and are schematically depicted in figure 4.15A and visualised on a protein gel in figure 4.15B. These proteins could be bound to anti-FLAG antibodies conjugated to an agarose affinity resin (Sigma-Aldrich) and tested for binding to recombinant PABP5. Given the problems in purifying significant quantities of PABP5 protein, it was decided to undertake the assay using *E. coli* lysate containing either recombinant PABP1 or recombinant PABP5, as the proteins could both be expressed to a significant and similar degree within these cells (see figure 4.12B). The *E. coli* lysates were prepared with a lysis solution containing benzonase which has both RNA and DNA endonuclease activity to avoid indirect interactions mediated by mRNA-binding. The activity of the benzonase in the lysis solution was sufficient to promote degradation of the bacterial RNAs to small oligonucleotide fragments which can be visualised in 4.15C.

FLAG-tagged eIF4G was bound to the anti-FLAG antibody agarose affinity resin and was subsequently incubated with *E. coli* lysate containing either recombinant PABP1 or recombinant PABP5. Following the incubation the beads were washed and the proteins eluted into protein loading buffer for analysis by SDS-PAGE followed by Western blotting with an anti-his antibody. PABP1 could be pulled down using full-length eIF4G, and as expected could not be isolated using the eIF4G truncated protein lacking the PABP1 binding site (see figure 4.16A). Interestingly in the same pulldown assay recombinant PABP5 could not be pulled down with the

full-length or truncated eIF4G proteins. This is in agreement with the Y2H assay and the PABP5 protein sequence data.

It is known that PABP1 can also interact with eIF4GII *in-vivo* (Imataka *et al.*, 1998). The binding site for PABP1 within eIF4GI was determined and found to be remarkably well conserved in eIF4GII (see figure 4.16B) (Imataka *et al.*, 1998), thus while any interaction between PABP5 and eIF4GII has yet to be investigated, it is predicted that PABP5 will not interact with eIF4GII.

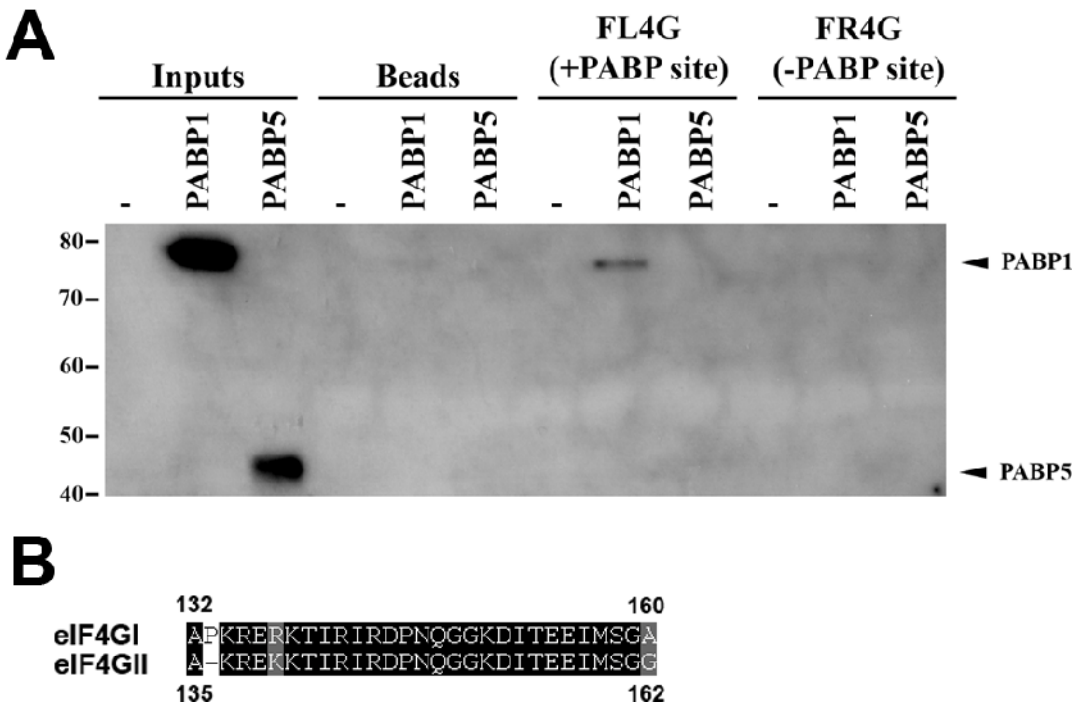

Figure 4.16 Pulldown of PABP proteins with eIF4G. A. FLAG-tagged full-length eIF4G (FL4G) or truncated eIF4G lacking the PABP1 binding site (FR4G) were bound to anti-FLAG affinity resin and incubated with *E. coli* lysate containing his- tagged PABP1 or PABP5. Resin containing no bound eIF4G protein was included as a control pulldown. The inputs represent 3% of the lysate added to the eIF4G resin. Proteins were eluted and subjected to SDS-PAGE followed by Western blotting with an anti-polyhistidine antibody. **B.** Sequence conservation of the PABP1 binding site in human eIF4GI and eIF4GII.

4.11 PABP5 is Poorly Isolated by m^7G-cap Chromatography

The binding of PABP1 and eIF4G is one of the core interactions responsible for the formation of the closed loop conformation of mRNAs that promotes their translation. PABP1 has also been demonstrated to interact with other proteins associated with the cap-binding complex to stabilise the closed loop conformation, such as eIF4B and PAIP-1. As a result of these interactions PABP1 can be isolated as part of the eIF4F complex by m^7G-cap affinity chromatography (Bradrick and Gromeier, 2009; Gallie *et al.*, 2000; Willett *et al.*, 2006). Whether the lack of an observable interaction between PABP5 and eIF4G would preclude an association of PABP5 with the cap complex is unknown.

To investigate whether PABP5 can associate with the cap-binding complex m^7G-cap affinity chromatography was performed using lysate derived from HeLa cells that had been transiently transfected with T7-tagged PABP5. As a positive control untransfected HeLa cell lysate was also assayed for the association of endogenous PABP1 with the cap-complex, as well as lysate derived from HeLa cells transiently transfected with T7-tagged PABP1. Western blotting with an antibody directed against the T7-tag allows for the levels of T7-PABP1 and T7-PABP5 isolated in this assay to be determined, and assuming equal expression levels allows their relative affinities for the cap-complex to be directly compared. Western blotting with antibodies against eIF4E and tubulin was also undertaken to determine the specificity of the assay as tubulin is not predicted to bind cap complexes, while it could be predicted that eIF4E would be enriched. The results of the m^7G-cap chromatography assay are depicted in figure 4.17.

The inputs represent 7.5% of the amount of lysate subjected to cap-chromatography. Interestingly, eIF4E was undetectable in the input lysate lanes. This was attributed to two factors. Firstly was the detection level of the antibody, as the signal for eIF4E was only observable upon extended film development times compared to the other blots which were developed simultaneously and with shorter development times, and

secondly was the level of eIF4E which is frequently described as being a limiting initiation factor and rate limiting in eIF4F complex formation (Duncan *et al.*, 1987; Goss *et al.*, 1990; Hiremath *et al.*, 1985).

In the untransfected cell lysates a small amount of PABP1 can be isolated by cap-chromatography. In the T7-PABP1 overexpressed lysates PABP1 is expressed to a markedly higher degree than the endogenous protein and this is reflected in the greater amount of PABP1 in the pulldowns. Thus, the more PABP1 present, the more can be isolated by cap-chromatography. This suggests that not all cap complexes associated with the m^7G-sepharose in the untransfected lysates are bound by PABP1, although whether this is physiologically relevant or simply represents the transient nature of the interaction between PABP1 and the cap complex in this assay is unclear.

Importantly PABP1 and PABP5 appear to be overexpressed to the same degree in the HeLa cells (see input lanes) allowing a more direct comparison of the amount of each that is isolated by cap-chromatography. Interestingly, there is a significant difference between PABP1 and PABP5 pulldowns with less PABP5 appearing to associate with the cap-complex. This suggests that PABP5 has reduced affinity for the cap-complex, consistent with an unobservable interaction with eIF4G. There is a small amount of PABP5 present in the pulldown lane and this may represent an association with the cap-complex via a protein other than eIF4G, or residual eIF4G binding activity. Alternatively this signal could represent background contamination as there is a faint tubulin signal detectable in the pulldown lanes suggesting that there is a small level of non-specific binding occurring.

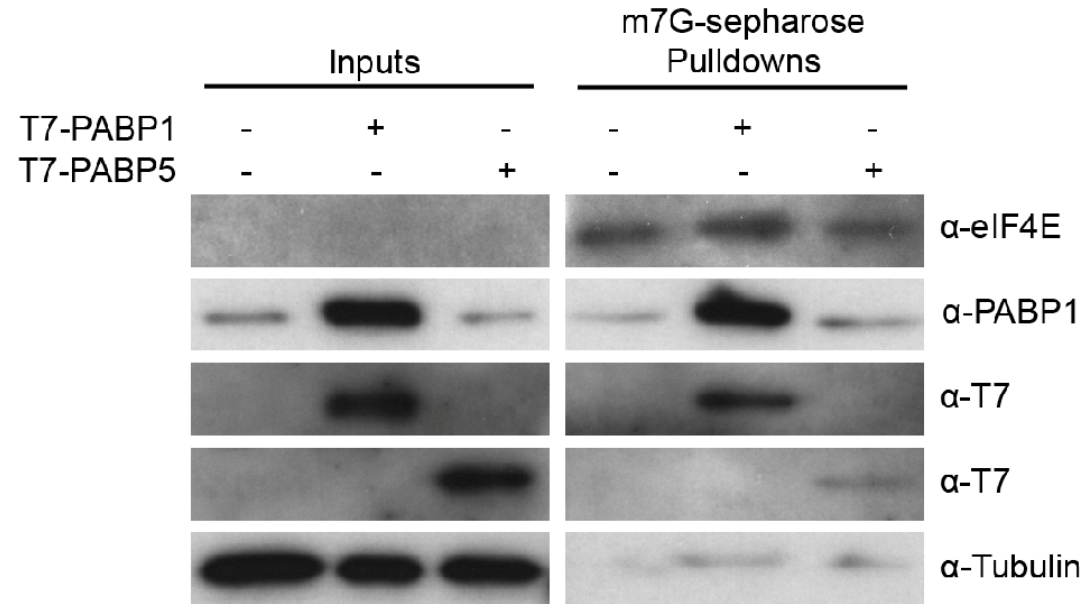

Figure 4.17 m7G-cap affinity chromatography. Untransfected, T7-PABP1 or T7-PABP5 transfected HeLa cell lysates were subjected to m^7G-cap affinity chromatography by incubating the lysates in the presence of m^7G-sepharose resin, followed by washing and elution of bound proteins into SDS-PAGE loading buffer. Western blotting was performed using the antibodies indicated on the right. The inputs represent 7.5% of the lysates used for the cap-chromatography.

Taken together the results thus far provide a speculative model whereby PABP5 failing to interact with eIF4G precludes its association with the cap-binding complex and as a result has little translational activity. In keeping with this model it is interesting to note that the presence of overexpressed T7-PABP5 protein does not appear to affect the level of endogenous PABP1 protein associating with the cap-binding complex. Assuming PABP5 did interact with eIF4G it could be expected that overexpression of PABP5 might result in a competition with PABP1 for binding to eIF4G.

4.12 Mutagenesis of PABP5

The suggested model would imply that 'rescuing' the ability of PABP5 to interact with eIF4G may promote PABP5 translational activity. To test this hypothesis a

mutagenesis approach was undertaken. In section 4.8 amino-acids in PABP1 critical for the eIF4G interaction were discussed. These amino-acids are not conserved in the PABP5 protein. In the mouse PABPs these residues are methionine-161 (M161) and leucine-162 (L162) which are substituted for valine (V167) and arginine (R168) respectively in PABP5. Since M161 ablates the activity of PABP1 (Kahvejian *et al.*, 2005; Karim *et al.*, 2006) a PABP5 point mutant, in which V167 of the MS2-PABP5 construct was mutated to a methionine (V167M) to resemble M161 in PABP1, was created. In contrast, M161 in PABP1 was mutated to a valine (M161V) to determine whether this would inhibit the translational activity of PABP1 in a tethered function assay.

The mutagenesis strategy was based upon the Stratagene QuikChange XL site directed mutagenesis kit in which the mutations are incorporated in a PCR based approach (see figure 4.18 for a schematic of the mutagenesis protocol). In abridged form the strategy involves designing two oligonucleotide primers containing the desired mutation that are complementary to opposite strands of the DNA. The primers are then extended by PCR. The PCR reaction is then treated with the Dpn1 endonuclease which is specific for hemimethylated and methylated DNA. As most DNA isolated from *E. coli* is methylated Dpn1 treatment results in removal of the parental vector. The PCR product is then transformed into *E. coli* where the staggered nicked ends generated by the PCR reaction are repaired and the vector is replicated.

4.13 PABP Point Mutants Have Little Translational Activity

Following cloning of the mouse PABP1 and PABP5 point mutants (M161V and V167M respectively), *in-vitro* transcribed mRNA was prepared and injected into stage VI *Xenopus laevis* oocytes.

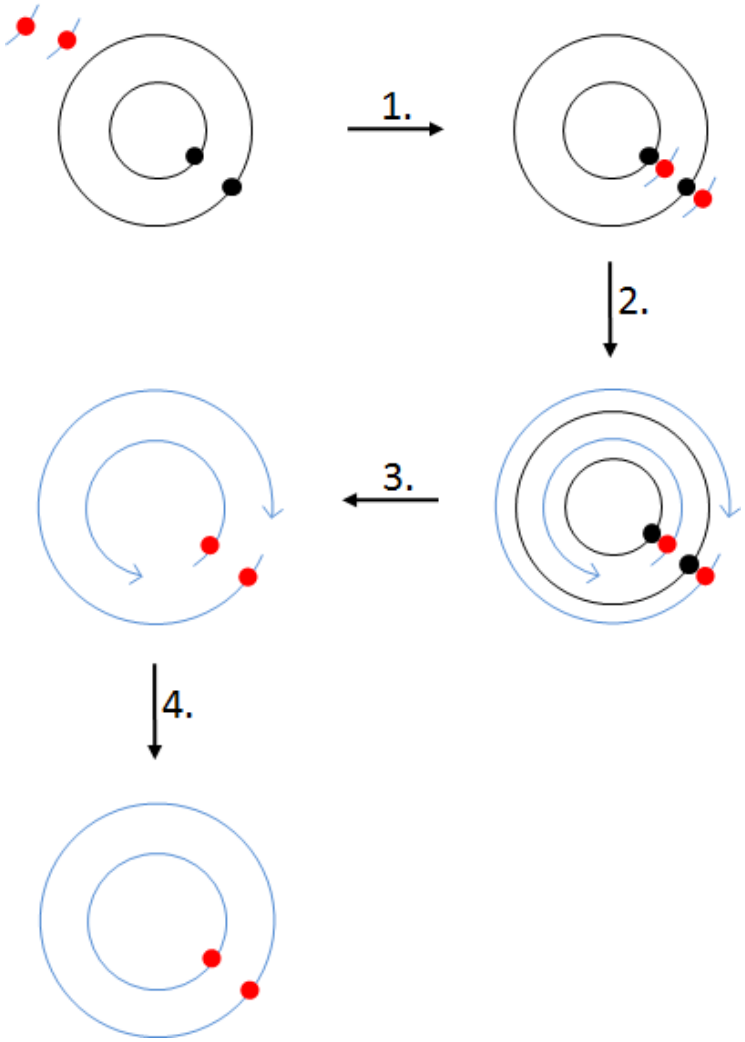

Figure 4.18 Mutagenesis strategy. Oligonucleotide primers are designed that contain the desired mutation (represented by a red dot). The vector contains the insert with the target site for mutation (represented by a black dot). **(1)** The primers are annealed to the vector and **(2)** are extended by PCR. **(3)** The methylated parental vector is digested by Dpn1 endonuclease treatment and **(4)** the remaining PCR product is transformed into *E. coli* where the nicked ends are repaired and the vector is replicated.

The M161V mutation was sufficient to reduce the translational activity of PABP1 from approximately 8-fold to approximately 4-fold over MS2-U1A (see figure 4.19). While this represents a significant loss in activity of PABP1 it is clearly not translationally inactive. In contrast, previous data has indicated that mutation of PABP1 M161 to alanine is sufficient to abolish binding of eIF4G (Groft and Burley, 2002) resulting in an almost complete loss of translational activity (Kahvejian *et al.*, 2005). The reason for the discrepancy is unclear, but raises the possibility that the mutation also affects RNA-binding, although this possibility was addressed in the original study.

Alternatively, the M161V mutation may not be adequate to completely abolish eIF4G binding but instead results in a reduced affinity, or conversely other factors that still interact with PABP1 may be sufficient to promote PABP1 activity. It should be noted that the original binding assay that determined a PABP1 M161 to alanine mutation was sufficient to eliminate a PABP1-eIF4G interaction was undertaken using only RRMs 1-2 of PABP1 rather than full-length protein (Groft and Burley, 2002). As a result issues regarding whether the protein folds correctly and supports binding of eIF4G in a manner consistent with full-length protein must be considered.

Importantly, the corresponding V167M PABP5 mutation failed to stimulate the translational activity of PABP5, with both the wild-type and mutant proteins stimulating translation about 3-fold over MS2-U1A (see figure 4.19). This could imply that either the V167M PABP5 mutant still does not interact with eIF4G, or conversely V167M PABP5 interacts with eIF4G but that this interaction is insufficient to stimulate translation. As discussed with the M161V PABP1 point mutant, it is possible that a single residue swap is not adequate to alter the activity of these proteins and that efficient binding of eIF4G is an additive effect of multiple interaction sites.

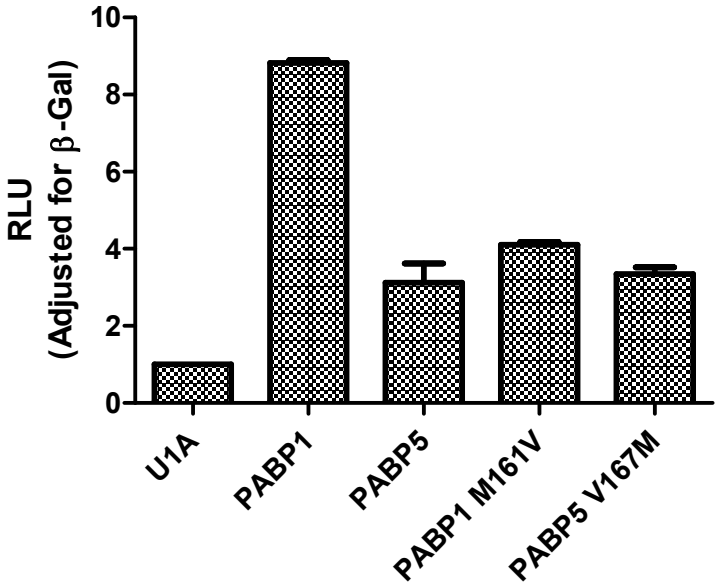

Figure 4.19 Translational activity of mouse PABP point mutants. The translational activities of U1A, PABP1, PABP5, PABP1 M161V and PABP5 V167M were tested by tethered function assay. The stimulation values of two separate experiments were averaged and the standard error calculated. RLU = relative luciferase units.

4.14 PABP RRM2 Domain Swap Mutants Have Little Translational Activity

As the V167M PABP5 mutation appears to be inadequate in promoting eIF4G binding, a PABP5 mutant in which RRM2 is substituted for the RRM2 of PABP1 was produced. This approach allows relocation of the mapped eIF4G binding region of PABP1 into the corresponding region of PABP5. As with the point mutations, the reciprocal domain swap was undertaken in PABP1 with RRM2 being replaced by the corresponding domain in PABP5.

As there were no appropriate endogenous restriction sites in the wild-type sequences to facilitate the domain swap a mutagenesis approach was undertaken. Two rounds of mutagenesis were performed on each clone to create novel BstB1 and Xma1

restriction sites at opposite ends of the RRM2 regions. These sites were incorporated into both the PABP1 and PABP5 sequences allowing a direct transfer of the regions between the two clones. Importantly these mutations were silent, not altering the amino-acids incorporated at these sites in the translated proteins.

The RRM2 domain swap mutant constructs were subjected to tethered function assay (see figure 4.20A). In a result consistent with abolishment of eIF4G binding, the PABP1 RRM2 mutant only stimulates translation 2-fold over MS2-U1A compared to the wild-type protein (approximately 7-fold). Comparison of the results from the point mutant and RRM2 mutant injections it would appear that the RRM2 mutant has less activity in the tethered function assay (4-fold versus 2-fold respectively) although the wild-type PABP1 protein also stimulates to a lesser degree in the RRM2 domain swap experiment. A tethered function assay in which all the mutants were injected simultaneously revealed a slight difference between the PABP1 point and RRM2 domain swap mutants (4-fold stimulation versus 3-fold stimulation). This analysis was only undertaken once. Therefore, to determine if this difference is statistically significant, more repeats would be required (see figure 4.20B).

The PABP5 domain swap mutant containing the RRM2 of PABP1 also failed to stimulate translation (see figure 4.20A). As with the PABP5 point mutant, this could be due to a failure of PABP5 and eIF4G to interact or alternatively might represent an interaction between the two proteins that is not stimulatory to translation. In the case of both RRM2 mutants it is possible that the swapping of the large RRM2 domains impacts upon the folding of the proteins which could directly affect activity.

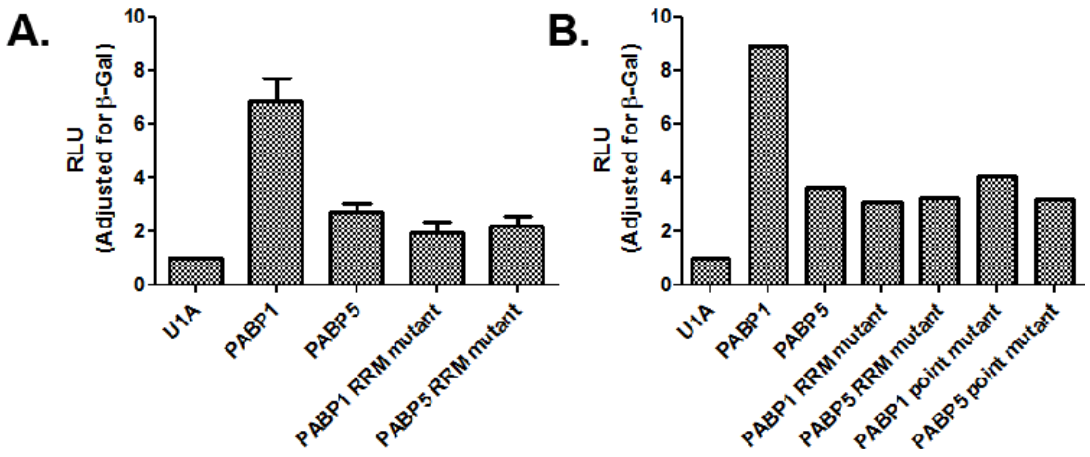

Figure 4.20 Translational activity of mouse PABP RRM2 domain swap mutants. A. The translational activities of U1A, PABP1, PABP5, PABP1 RRM2 mutant and PABP5 RRM2 mutant were tested by tethered function assay. The stimulation values of four separate experiments were averaged and the standard error calculated. RLU = relative luciferase units. **B.** The translational activities of all the mutant PABPs were tested in parallel by tethered function assay. The results are representative of one experiment.

4.15 PABP Mutants Fail To Interact With eIF4G

The ability of the mutant PABP proteins to interact with eIF4G was investigated by Y2H. This would identify whether the PABP5 mutants fail to support eIF4G binding or simply that an interaction between PABP5 and eIF4G is insufficient to promote translation. To this end the V167M and RRM2 domain swap mutants were subcloned into Y2H bait vectors to be tested against the N-terminus of eIF4G (eIF4GNT). As a positive control PABP1 RRMs 1-4 was tested against eIF4GNT, and all the clones were tested against IRP as a negative control. None of the PABP mutant proteins interacted with eIF4G by Y2H (see figure 4.21A). This is consistent with a loss of translational activity in the PABP1 mutant proteins and offers a possible explanation as to the lack of increased activity of the PABP5 mutants. Expression of the mutant constructs in yeast was confirmed by Western blotting with an antibody raised against the LexA-BD region of the fusion proteins (see figure 4.21B). Since the PABP5 RRM2 domain swap mutant failed to interact with eIF4G despite containing PABP1 RRM2 which is capable of binding eIF4G (Groft and Burley, 2002; Imataka *et al.*, 1998) this raised the possibility that interchanging such large regions of the PABP proteins could disrupt the folding of the proteins.

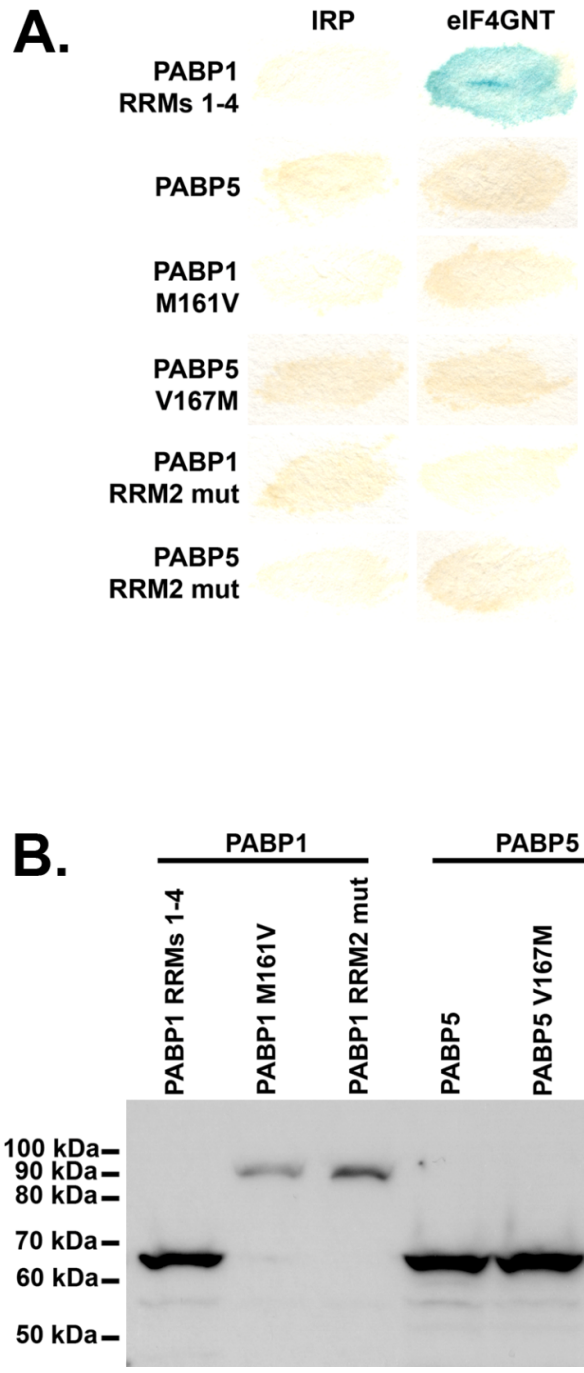

Figure 4.21 The PABP mutants fail to interact with eIF4G by Y2H. A. The PABP mutants were expressed in yeast as fusion proteins with the LexA-BD. eIF4G and IRP were expressed as fusion proteins with the GAL4-AD. Positive colonies were identified by incubation with X-gal resulting in a blue colouration. The positive control is mouse PABP1 RRMs 1-4 tested against the N-terminus of human eIF4G, and the negative control is mouse PABP1 RRMs 1-4 tested against IRP. **B.** Yeast expressing the mutant-LexA fusion proteins were lysed and subjected to SDS-PAGE followed by Western blotting with an antibody raised against the LexA-BD. LexA-BD is approximately 24 kDa therefore PABP1 RRMs 1-4 and the PABP5 proteins were predicted to run at approximately 67 kDa (24 kDa LexA-BD + 43kDa) and the full-length PABP1 proteins were predicted to run at approximately 94 kDa (24 kDa + 70 kDa).

The X-ray crystal structure of human PABP1 RRMs 1-2 complexed with poly(A) is available at a 2.6 Angstrom resolution (Deo *et al.*, 1999). To assess whether the PABP5 RRM2 mutant fails to interact with eIF4G because the chimeric protein is significantly unstructured across RRMs 1-2 it was decided to use this PABP1 model as a template to predict the structure of PABP5 RRMs 1-2, and the subsequent effect of introducing PABP1 RRM2. Given the high level of sequence identity between PABP1 and PABP5 RRMs 1-2 (69%) the prediction was likely to be accurate. Also, given the high level of sequence homology between mouse and human PABP5 proteins (95%) the results were deemed applicable to both species. An algorithm designed to find the most probable structure for a given amino-acid sequence based on alignments with related structures was utilised (Sali and Blundell, 1993). The analysis was undertaken by Dr Jonathan Manning (Bioinformatics, Queens Medical Research Institute, University of Edinburgh).

Within the PABP1 RRMs 1-2 model structure 8 amino-acid residues serve to mediate inter-domain contacts between RRM1 and RRM2 and were predicted to be important for maintenance of the RRM 1-2 structure (Deo *et al.*, 1999). Two of these residues are not conserved in RRMs 1-2 of PABP5, an aspartate at position 70 (Asp-70) is substituted with an asparagine (Asn-77), and a tyrosine at position 116 (Tyr-116) is substituted with a phenylalanine (Phe-123). Interestingly these substitutions can be considered conservative as tyrosine and phenylalanine are of similar size and contain aromatic side-chain moieties, whereas aspartate and asparagine both represent polar hydrophilic amino-acids of similar size.

The Tyr-116 and Asp-70 residues do not interact within PABP1 RRMs 1-2 (Deo *et al.*, 1999) presumably due to the spatial distance between them (5.4 Angstroms) as was similarly predicted for their conservative substitutions Phe-123 and Asn-77 within PABP5 RRMs 1-2. As these substituted residues do not interact but mediate contacts between the two RRMs via conserved residues it was predicted that loss of structure within RRMs 1-2 of the domain swap proteins was unlikely.

4.16 PABP5 Interaction with the PAIP Proteins

Within the closed loop model of translational stimulation the PABP1-eIF4G interaction is implied to be the key contact that facilitates 5'- and 3'-UTR communication, however several other factors may also be important for PABP1 mediated translational stimulation.

The translational enhancer PAIP-1 interacts with PABP1 both *in-vitro* and *in-vivo* via two binding motifs termed PAM-1 and PAM-2 which interact with RRMs 1-2 and the C-terminus of PABP1 respectively (Craig *et al.*, 1998; Roy *et al.*, 2002)(see figure 1.14A). PAIP-1 contains homology to the central domain of eIF4G and can also interact with eIF3 and eIF4A in addition to PABP1 (Craig *et al.*, 1998; Martineau *et al.*, 2008). This is suggested to offer an alternative mechanism for the circularisation and translational activation of mRNAs (Derry *et al.*, 2006). Given that the PAM-1 domains bind to the RRMs region of PABP1 it is feasible that these interactions may be conserved within PABP5 contributing to its residual ability to stimulate translation. Indeed, although PAIP-1 binds PABP1 RRMs 2-3 and C-terminus with a 1:1 stoichiometry it would appear that the PAM-1 and PAM-2 motifs can interact with PABP1 independently as truncation mutants of *Xenopus laevis* PABP1 consisting of either RRMs 1-2 or the C-terminus alone can support binding of PAIP-1 (Gray *et al.*, 2000). Similarly, the negative regulator of PABP1 activity, PAIP-2, also contains a PAM-1 and PAM-2 motif which bind a region within RRMs 2-3 and also the C-terminus of PABP1 respectively. In distinction to PAIP-1, PAIP-2 binds PABP1 with a 2:1 stoichiometry (Khaleghpour *et al.*, 2001a).

To investigate the ability of PABP5 to interact with PAIP-1 and PAIP-2 a Y2H approach was taken. The mouse and human PABP5 Y2H LexA-BD constructs utilised in figure 4.9, and mouse PABP1 RRMs 1-4 cloned into the same vector (as a positive control) were tested against human PAIP-1 and PAIP-2.

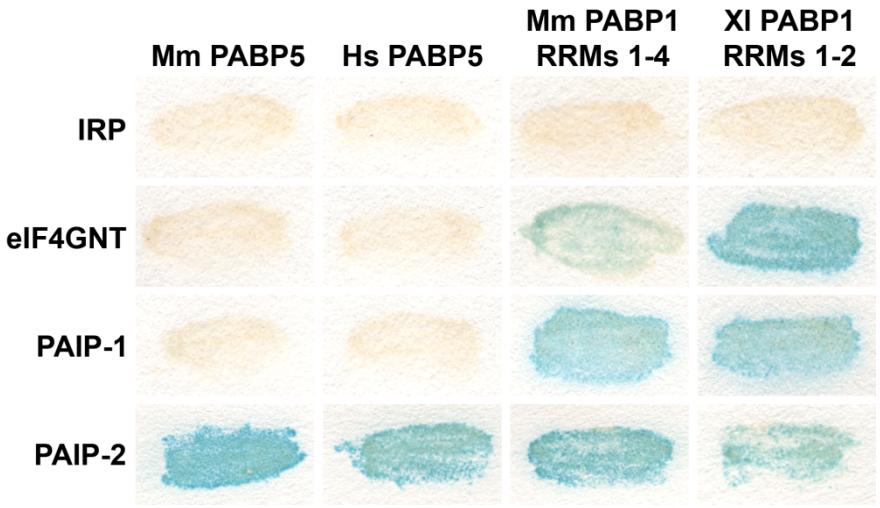

Figure 4.22 PABP5 interacts with PAIP-2. The PABP proteins were expressed in yeast as fusion proteins with the LexA-BD. eIF4GNT, IRP, PAIP1 and PAIP-2 were expressed as fusion proteins with the GAL4-AD. Positive colonies were identified by incubation with X-gal resulting in a blue colouration. The controls are Mm PABP1 RRMs 1-4 and Xl PABP1 RRMs 1-2 tested against eIF4G and PAIP-1 (+ve), and IRP (-ve). Mm = *Mus musculus*, Hs = *Homo sapiens*, Xl = *Xenopus laevis*.

The results of the Y2H are presented in figure 4.22. As was anticipated, the reactions containing the *Xenopus* and mouse PABP1 proteins were positive for an eIF4GNT interaction and negative for an interaction with IRP. Additionally these proteins also interacted with PAIP-1 as has been previously shown (Gray *et al.*, 2000; Kimura *et al.*, 2009). Interestingly, both PABP1 proteins interacted with PAIP-2. While this has been documented for the mouse protein (Kimura *et al.*, 2009) *Xenopus laevis* PABP1 has never been previously been demonstrated to interact with PAIP-2 and therefore represents a conserved interaction.

Remarkably the mouse and human PABP5 proteins interacted with PAIP-2 yet failed to bind PAIP-1. The inability of PABP5 to bind the translational enhancer protein PAIP-1 is consistent with its relative inability to stimulate translation. The interaction of PABP5 with PAIP-2 is interesting. Available evidence demonstrates that the association of PAIP-2 is sufficient to down-regulate the activity of PABP1 via multiple mechanisms (reviewed in Derry *et al.*, 2006), including competition for

eIF4G binding. Therefore, the interaction between PABP5 and PAIP-2 could be construed as further evidence supporting the lack of translational activity of PABP5.

4.17 PABP5 Interacts with PAIP-2

To verify the Y2H results and confirm an interaction of PABP5 with PAIP-2 a pulldown experiment using recombinant proteins was performed. To this end human PABP1 and PABP5 were expressed as described in section 4.9 and cell lysates were prepared. Human PAIP-1 and PAIP-2 were cloned into the pGEX-6P-1 bacterial expression vector which produces recombinant proteins N-terminally tagged with glutathione S-transferase (GST). The GST-PAIP proteins were produced in *E. coli* cells, using 1mM IPTG and inducing for 3 hours at 37^{o}C. Lysates were passed over glutathione sepharose beads which bind the GST proteins. The beads were washed and the presence of the GST-PAIP proteins was verified by incubating the beads in protein loading buffer and subjecting the eluted proteins to SDS-PAGE followed by staining of the gel with GelCode Blue. Three distinct proteins were observed that corresponded to the predicted masses for GST, GST-PAIP-1, and GST-PAIP-2 (see figure 4.23A). To verify that these protein bands represented the induced GST proteins the samples were subjected to Western blotting with an antibody raised against GST. Again three distinct signals were observed that corresponded to the predicted masses of the recombinant proteins (see figure 4.23B).

As with the PABP1 and PABP5 inductions in figure 4.12B, some lower molecular weight proteins co-purified with GST-PAIP-1 and GST-PAIP-2. Western blotting revealed that the majority of these were breakdown products of the recombinant proteins that still retained the GST-tag.

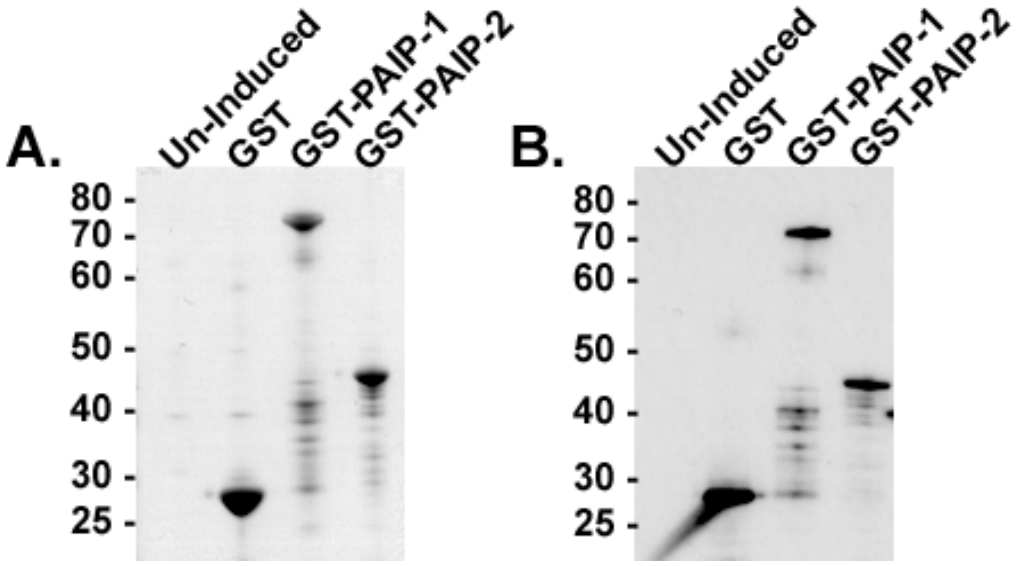

Figure 4.23 GST proteins induction. A. *E. coli* cells were transformed with the pGEX-6P-1 constructs and induced to express recombinant proteins. The cells were lysed and the lysate added to glutathione sepharose. Following washing the bound proteins were eluted in protein loading buffer and subjected to SDS-PAGE. The gel was then stained with GelCode Blue (Thermo Scientific). GST = 26kDa, GST-PAIP-1 = 79kDa, GST-PAIP-2 = 41kDa. **B.** The same protein samples were subjected to Western blotting using an anti-GST antibody.

For the purposes of the pulldown assay, GST proteins (GST, GST-PAIP-1, and GST-PAIP-2) were induced in *E. coli* cells, bound to glutathione sepharose and washed as before. Prior to undertaking the assay the amount of each protein bound per µl of beads was quantified to ensure similar levels of the proteins were utilised in each pulldown experiment. To this end the proteins were eluted from various quantities of the beads and subjected to SDS-PAGE alongside BSA standards. The protein gel was then stained with SYPRO Ruby (Invitrogen) and the proteins imaged and quantified as described in section 4.9. The results of this quantification are shown in appendix 2.

Three different quantities of glutathione-sepharose beads corresponding to 5µg, 2.5µg, and 0.5µg of each GST-protein were added to *E. coli* lysates containing

PABP1 or PABP5. Following incubation the beads were washed and the bound proteins were eluted in protein loading buffer. The proteins were subjected to SDS-PAGE followed by Western blotting with an anti-his antibody directed against the N-terminal his-tag present on the PABP proteins (see figure 4.24). The pulldowns indicate that PABP1 can interact with both GST-PAIP-1 and GST-PAIP-2 but does not cross-react with GST alone. That the PABP1 signal decreases in response to decreasing amounts of the GST-PAIP proteins could suggest that the GST proteins are limiting. Interestingly, the amount of PABP1 isolated with GST-PAIP-1 and GST-PAIP-2 is comparable. PABP5 on the other hand appears to bind PAIP-2 with a significantly higher affinity than PAIP-1 based on the amount of PABP5 pulled down with each of the proteins (see figure 4.24). Thus, the pulldown corroborates with the Y2H data indicating that in these assay systems PABP5 interacts with PAIP-2 but fails to show significant binding to PAIP-1. Whether the inability to interact with PAIP-1 is because PABP5 lacks the C-terminal binding site present in the PABP1 protein, or rather the RRM 1-2 binding site is not conserved within PABP5 is not known. In support of the latter PABP1 RRMs 1-2 can sustain binding of PAIP-1 in the absence of the C-terminus (Gray *et al.*, 2000).

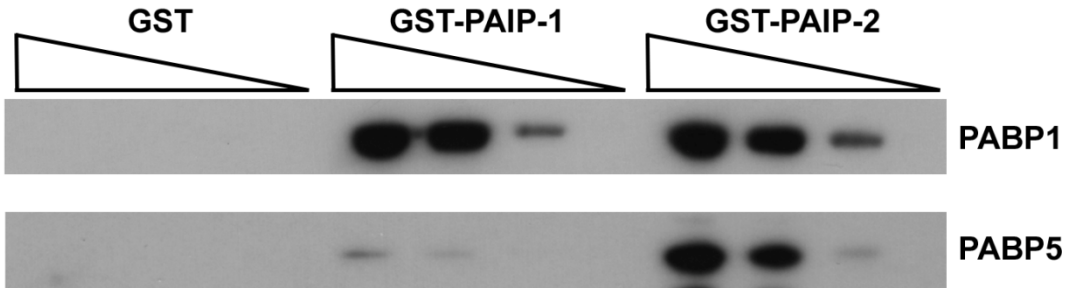

Figure 4.24 PABP5 interacts with PAIP-2 by pulldown assay. GST, GST-PAIP-1, and GST-PAIP-2 were bound to glutathione-sepharose beads. A volume of beads corresponding to 5µg, 2.5µg, 0.5µg, and 0µg of the bound GST-proteins was incubated with *E. coli* lysate containing either his-tagged PABP1 or PABP5. Following the incubation the beads were washed and the bound proteins were eluted in protein loading buffer. The proteins were subjected to SDS-PAGE followed by Western blotting with an anti-polyhistidine antibody.

4.18 Discussion

Within this chapter I have examined the molecular function of a novel uncharacterised poly(A)-binding protein, PABP5. Ectopically expressed PABP5 protein appears to be predominantly cytoplasmic in accord with other PABP family members. Interestingly *in-vitro* and *in-vivo* analysis suggests that PABP5 may have a molecular role that is distinct from the other characterised PABP family members.

PABP5 Localisation

The cytoplasmic localisation of GFP-PABP5 is consistent with a role in the regulation of mRNA translation or stability as this cellular compartment contains the protein synthesis machinery. However it remains to be determined whether endogenous PABP5 exhibits a similar predominantly cytoplasmic distribution. In the absence of an antibody that can detect endogenous PABP5 protein, construction of a stably expressing PABP5 granulosa cell-line would permit PABP5 subcellular localisation to be examined in a cell-type in which it is endogenously expressed. This would also allow other *in-vivo* assays to be performed in an appropriate cellular background, although the ability to maintain a 'granulosa like' pattern of gene expression could be problematic given their propensity to luteinise in culture.

The presence of PABP5 within the nucleus of some of the transfected cells is interesting. Whether this is linked to PABP5 function, or is simply an artefact of overexpressing PABP5 is unclear, as overexpressing PABP1 can result in nuclear accumulation (Afonina *et al.*, 1998). However, nuclear import of PABP1 is an energy dependent process requiring ATP (Afonina *et al.*, 1998) and endogenous PABP1 can also localise to the nucleus (Afonina *et al.*, 1998; Woods *et al.*, 2002). Thus PABP5 may also be a true shuttling protein. The TD-NEM motif recently implied to be responsible for nuclear export of PABP1 (Khacho *et al.*, 2008) does not appear to be conserved in PABP5 suggesting an alternative mechanism for nuclear export of PABP5. Interestingly, a PABP1-paxillin interaction has also been

suggested to facilitate PABP1 nuclear export (Woods *et al.*, 2005), and the two characterised paxillin binding sites in PABP1 appear to be highly conserved in PABP5. Demonstration of a PABP5-paxillin interaction could imply a conserved mechanism of nuclear-cytoplasmic transport.

PABP5 Translational Activity

Based on the function of other PABP proteins PABP5 was hypothesised to have a role in translational activation. The association of ectopically expressed PABP5 with actively translating mRNAs would seemingly corroborate this. While the co-sedimentation of factors with polysomes can be indicative of an association with actively translating mRNAs great care must be taken in interpreting the results of these experiments, as other large molecular weight complexes also sediment within these gradient fractions. Moreover mRNA binding factors with no intrinsic translational stimulatory activity have been isolated from the polysomal fractions of sucrose gradients, such as the decapping enzyme Dcp2 (Wang *et al.*, 2002).

A tethered function assay was employed to determine whether PABP5 had translational stimulatory activity. Surprisingly, mouse and human PABP5 were found to have only limited translational stimulatory activity relative to PABP1 which has been described as a canonical translation factor (Kahvejian *et al.*, 2005). The activity of mouse and human PABP1 proteins in this assay indicate that the result is unlikely to be an artefact of assaying mammalian proteins in *Xenopus* cells.

While the translational activity of many of the mammalian PABP proteins has not been established, other vertebrate PABPs such as *Xenopus* ePABP (Wilkie *et al.*, 2005), *Xenopus* PABP4 (B. Gorgoni, submitted) and mouse tPABP (Kimura *et al.*, 2009), all stimulated translation to a similar degree as PABP1 in translation assays. Thus the lack of translational activity appears unique to PABP5. Nonetheless, PABP5 consistently stimulated translation of the reporter approximately 2-fold over

the U1A control protein. The physiological relevance of this residual stimulatory activity remains unclear, although it could be an artefact of the high affinity MS2/MS2-binding site interaction given that the mRNA binding activity of PABP5 has never been experimentally determined. Two important questions therefore require addressing. Firstly, is the relative inactivity of PABP5 reproducible in translational assays utilising reporters containing endogenous PABP5 binding sites, and secondly, what is the mRNA substrate preference of PABP5.

PABP5 mRNA Binding

The mRNA-binding activity of characterised PABP proteins is critical to their function. The binding affinity of PABP1, tPABP, PABP4 and ePABP for poly(A) mRNAs has been established using electrophoretic mobility shift assay (EMSA) (Kim and Richter, 2007; Sladic *et al.*, 2004) or via poly(A)-sepharose columns (Houng *et al.*, 1997; Kimura *et al.*, 2009). In contrast the mRNA-binding activity of PABP5 remains to be addressed and if determined would allow formulation of a more informed hypotheses regarding PABP5 molecular function. In yeast, and human PABP1 proteins poly(A) recognition activity was determined to be largely mediated by RRMs 1-2 (Burd *et al.*, 1991; Deardorff and Sachs, 1997; Sladic *et al.*, 2004).

In the molecular modelling study described in chapter 4 (section 4.15), the poly(A)-binding potential of PABP5 RRMs 1-2 was investigated in relation to the structure of PABP1 RRMs 1-2 bound to poly(A). Some 22 amino-acid residues in PABP1 RRMs 1-2 are involved in mediating contacts with poly(A) RNA (Deo *et al.*, 1999). Of these residues, there are 4 substitutions in the PABP5 protein: S12A, M46P, R89P and F142Y (PABP1 numbering) of which the first 3 are non-conservative. Of these 3 non-conservative substitutions, residues S12 and M46 have been suggested to be important in adenine recognition (Deo *et al.*, 1999) leading to speculation that base preference of PABP5 may be more flexible or that poly(A)-binding affinity may be reduced. Highlighting the importance of the substitutions, in yeast Pab1p a single

mutation in RRM2, F170V, was capable of almost completely ablating binding to poly(A) (Deardorff and Sachs, 1997). Furthermore, PABP5 also lacks the proline-rich C-terminal domain that functions in PABP1 oligomerisation to mediate ordered binding to poly(A) (Melo *et al.*, 2003). Several PABP proteins have been demonstrated to have an affinity for AU-rich sequences (Sladic *et al.*, 2004; Voeltz *et al.*, 2001), with PABP4 having only a two-fold lower affinity for poly(AU) than for poly(A) (Sladic *et al.*, 2004), suggesting that PABP5 may also bind AU sequences.

To directly test the affinity of PABP5 for poly(A) RNA binding assays must be utilised. To this end I have undertaken preliminary EMSA experiments using poly(A) and poly(AU) fluorescently labelled RNA probes. These experiments are detailed in appendix 3. Intriguingly, whilst highly preliminary, these assays suggest that PABP5 displays a strong preference for poly(AU) compared to poly(A). This finding warrants further investigation as, if verified, it would describe the first PABP protein with an affinity for an mRNA substrate higher than poly(A) and would have interesting implications for the function of PABP5. Indeed, if PABP5 proves to have a negligible affinity for poly(A) and instead binds specific target mRNAs through AU-rich sequences or other motifs, it may be possible to perform meaningful RNA-IP experiments without isolating unmanageable numbers of polyadenylated mRNAs.

Translation Assays

One approach to validating the results of the tethered function assay is the utilisation of *in vitro* cell-free translation extracts. Recently, cell-free translation extracts have been described that display cap-poly(A) synergy (Michel *et al.*, 2000; Thoma *et al.*, 2004), overcoming the problem with many of the previous *in-vitro* translation systems with respect to assaying for PABP activity. To this end active HeLa cell-free translation extracts were prepared and demonstrated to display cap-poly(A) synergy (see appendix 4). These extracts could be programmed with reporter mRNAs, and identification of the mRNA substrates of PABP5 would facilitate the use of reporter mRNAs containing endogenous PABP5 binding sites.

To investigate the function of PABP5 these assays would ideally be performed in both the presence and absence of competing PABP proteins (see chapter 5 for discussion of models). Cell-free translation extracts depleted of PABP proteins have been described (Thoma *et al.*, 2004). Active cell-free HeLa extracts depleted of PABP1 were prepared (see appendix 4). HeLa cells are also known to contain PABP4 (H. Burgess, unpublished) which would also require depletion. Interestingly depletion of PABP1 by passing the extracts over PAIP-2 columns similarly depleted PABP4 (see appendix 4), suggesting that PAIP-1 and PABP4 may also interact. Thus these extracts would be suitable for undertaking experiments in the absence of other cytoplasmic PABPs. As HeLa cells do not express PABP5 mRNA, purified recombinant PABP5 protein would have to be added to these extracts. While purified PABP1 was generated in significant quantities, PABP5 was not.

PABP5 Protein Interactions

A molecular explanation for the relative inactivity of PABP5 in the tethered function assay could be its reduced affinity for the factors that are known to promote PABP1 mediated translational stimulation. The Y2H and *in vitro* binding assays undertaken with PABP5 and the initiation factors eIF4G and PAIP-1 show clearly reduced affinity. However, if the interactions are particularly RNase sensitive or reliant on post-translational modifications they may not be detectable in the assays undertaken. It is known that the phosphorylation status of wheat germ PABP1 affects its ability to interact with both eIF4B and eIF4G for example (Le *et al.*, 2000). Therefore, the inability to interact with PABP5 must be confirmed by Co-IP of endogenous proteins.

Furthermore the absence of the C-terminus which interacts with eIF4B and eRF3 precludes a role for these proteins (Bushell *et al.*, 2001; Cosson *et al.*, 2002a), and indeed an interaction between PABP5 and eIF4B was not observed by Y2H. It is therefore tempting to speculate that the functional differences between PABP1 and PABP5 may be linked to its inability to circularise and therefore promote the

translation of mRNAs. In support of this hypothesis PABP5 could not be isolated by m^7G-cap chromatography indicating that PABP5 does not interact with the cap complex.

The closed loop model of translational stimulation is suggested to be mediated primarily through an interaction between eIF4G and PABP1. To determine whether the low translational stimulatory activity of PABP5 was indeed through a reduced affinity for eIF4G, attempts were made to create a mutant PABP5 protein that bound eIF4G but were unsuccessful. Molecular modelling suggested the failure of the PABP5 RRM2 mutant to interact with eIF4G may not have had a structural basis but rather reflected additionally required eIF4G contact sites that are present within full-length wild-type PABP1 protein. Although mammalian PABP1 RRM2 contains residues deemed critical for eIF4G interaction (Groft and Burley, 2002), and this region is solely responsible for the yeast PABP1-eIF4G interaction (Kessler and Sachs, 1998; Otero *et al.*, 1999) it is possible that RRM1 may also influence binding. In support of this the ability of RRM2 to interact with eIF4G was significantly enhanced by the presence of RRM1 *in-vitro* despite RRM1 containing no intrinsic eIF4G binding activity (Imataka *et al.*, 1998). Similarly the ITC binding assay that determined the critical eIF4G binding residues in RRM2 was performed using a PABP1 RRMs 1-2 fragment (Groft and Burley, 2002). Hence, the RRM2 domain alone may not be sufficient to promote robust binding of eIF4G. The results of the Y2H assay utilising the mutant proteins would appear to be supportive of a larger eIF4G binding site.

Intriguingly, despite stimulating translation to a lesser degree than PABP1, PABP5 clearly has some low level stimulatory activity in the tethered function assay. This activity of PABP5 may be the result of a residual affinity for these factors, or reflect a high affinity interaction with a yet to be described factor that contributes to PABP1 activity. Indeed, RRMs 3-4 of PABP1 and ePABP have been demonstrated to stimulate translation of a reporter mRNA (Gray *et al.*, 2000; Wilkie *et al.*, 2005),

implying that factors other than eIF4G and PAIP-1 can contribute to PABP1 mediated translational activation.

Interestingly PABP5 failed to interact with PAIP-1 but was positive for an interaction with PAIP-2 by Y2H thus representing the first example of a PABP protein differentially interacting with the PAIP proteins. The interaction of PABP5 with PAIP-2 was verified by pulldown assay but requires confirmation with endogenous proteins, possibly through Co-IP. This interaction could be taken as further evidence that PABP5 has no role in translational stimulation given that it fails to interact with PAIP-1 yet binds PAIP-2 which is a characterised negative regulator of translation. Conversely, it could be argued that if PABP5 had no intrinsic translational stimulatory activity it would not need repressed in a PAIP-2 mediated mechanism. To this end it would be interesting to test PABP5 in a translational assay in which the PAIP-2 binding was ablated by mutation or depleted by siRNA.

In conclusion, within this chapter I have demonstrated that PABP5 does not appear to act as a translation factor, at least not in a manner analogous to the prototypical PABP1. PABP5 has limited ability to stimulate translation in a well characterised translational assay, and has not maintained protein interactions conserved by other PABPs, integral to their function. Indeed the only interaction preserved would appear to be with the negative regulator of translation, PAIP-2. Further experimental work will be required to elucidate the significance of this interaction and models for the function of PABP5 are discussed in chapter 5.

Chapter 5: General Discussion

5.1 Summary of Findings

The role of mammalian PABP1 as a translation factor is well established. While the mechanism of PABP1 mediated translational stimulation is still a subject of investigation it is apparent that several other mammalian cytoplasmic PABP proteins may also share a similar role in translational regulation through conserved protein-protein interactions (Cosson *et al.*, 2002a; Kimura *et al.*, 2009; Okochi *et al.*, 2005) and the ability to bind poly(A) (Sladic *et al.*, 2004). PABP5 represents a largely uncharacterised member of the PABP family. Within this thesis I have examined the expression pattern of PABP5 mRNA showing that PABP5 has both a tissue and cell-type restricted expression pattern within mice. In particular PABP5 was found to be co-expressed with PABP1 and PABP4 in granulosa cells. Furthermore I have demonstrated that PABP5 represents the first PABP protein to display an inability to bind the translation factors eIF4G and PAIP-1 and that PABP5 has little translational stimulatory activity. These data strongly suggest that the function of PABP5 is distinct from that of other PABP proteins, performing a different molecular role within granulosa and other cell types. Possible models for the function are presented below.

5.2 PABP5 as a Translational Activator

Although PABP5 has little translational stimulatory activity relative to PABP1 in the tethered function assay it clearly has a weak but positive stimulatory effect on luciferase reporter expression and may function as a weak translational activator. Consistent with this PABP5 co-sediments with the polysomes in HeLa cell lysates and was partially released upon treatment with puromycin. While the latter does not identify a direct role in translational stimulation, it is potentially indicative of an association with actively translating mRNAs.

If PABP5 is a potent translational stimulatory protein, it is unclear why such a low level of activity in the tethered function assay was observed. One drawback of the

tethered function assay is that PABP5 is interacting with the mRNA via the MS2/MS2-binding site interaction. PABP5 may undergo conformational rearrangements in response to mRNA binding that would not occur upon tethering. It could be speculated that this may affect PABP5-protein interactions and subsequent translational activity. Indeed the interaction of yeast Pab-1 with eIF4G is RNA-dependent, requiring Pab-1 to be complexed with poly(A) (Tarun and Sachs, 1996). As PABP5 is mammalian specific it is also possible that PABP5 cap-dependent translation requires an unidentified mammalian specific bridging protein to contact the cap-complex (see figure 5.1). Undertaking translational assays in mammalian cell free extracts (described in chapter 4, section 4.18), could validate this theory. The development of a functional antibody to PABP5 could allow IP of endogenous PABP5 interacting proteins. A more comprehensive understanding of the PABP5 interactome would be highly informative with respect to the putative translational activity of PABP5.

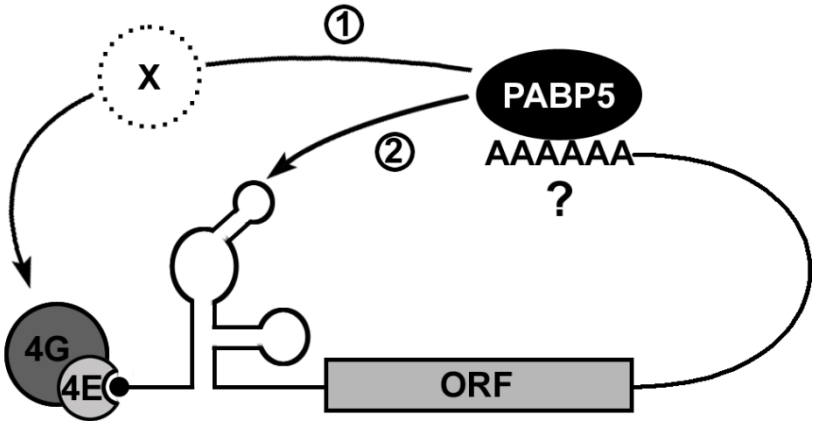

Figure 5.1 PABP5 may be a translational stimulatory protein. Possible mechanisms of PABP5 mediated translational stimulation include the formation of alternative closed-loop conformations. The mRNA binding activity and mRNA substrate of PABP5 remain to be experimentally determined and PABP5 may bind poly(A) or other elements such as AU-rich sequences within the 3'-UTR. Arrow number 1 depicts a cap-dependent mechanism of translational stimulation whereby PABP5 interacts with the cap-complex via an unknown interacting protein thus forming the closed-loop. Arrow number 2 depicts a cap-independent mechanism of translational stimulation whereby PABP5 interacts with mRNA sequences in the 3'-UTR of target mRNAs and simultaneously binds an element within the 5'-UTR thereby forming an alternative closed-loop. The 5' element may be an IRES. It is possible that the interaction is not direct and may be facilitated by an unknown bridging protein.

It remains to be determined whether any ability of PABP5 to stimulate translation is specific to IRES dependent translation. PABP1 has been shown to directly interact with the IRES of platelet-derived growth factor-2 (PDGF2) to stimulate the translation of this mRNA (Koloteva-Levine *et al.*, 2004) suggesting that this alternative mechanism of closed-loop formation can be used to regulate the translation of cellular mRNAs. PABP1 has also been shown to stimulate viral IRESs via interaction with other initiation factors such as eIF4G (Burgui *et al.*, 2003; Svitkin *et al.*, 2001a). Thus, mechanisms exist for the direct and indirect associations of PABP proteins with IRES elements facilitating translational stimulation (see figure 5.1). Fascinatingly the viral HIV-1 and HIV-2 proteases are known to cleave PABP1 liberating the C-terminus from the RRM domains producing a truncated PABP protein with resemblance to PABP5 (Alvarez *et al.*, 2006). It has been postulated that the viral mRNAs may recruit the PABP1 cleavage product to promote translation of the viral transcripts in a cap-independent mechanism (Collier and Gray, 2006).

5.3 PABP5 as an Indirect Translational Activator

PAIP-2 regulates the activity of PABP1 by reducing the affinity of PABP1 for poly(A) (Khaleghpour *et al.*, 2001b) and competing with eIF4G and PAIP-1 for binding to PABP1 (Karim *et al.*, 2006). The functional consequences of the interaction between PAIP-2 and PABP5 remain to be examined. It could be envisaged to function in a manner analogous to its regulation of PABP1 activity, promoting a reduction in PABP5 mRNA binding affinity although testing this requires knowledge of the mRNA substrate preference of PABP5.

Alternatively the interaction between PAIP-2 and PABP5 may affect the availability of PAIP-2 for other PABP proteins. PABP1 is a known target of PAIP-2 and my data suggests that PABP4 could also be a PAIP-2 interacting protein (appendix figure 4). Mouse tPABP and *Xenopus laevis* ePABP similarly interact with PAIP-2 suggesting that this interaction is highly conserved within the PABP family. Thus

the interaction between PABP5 and PAIP-2 could represent a plausible mechanism by which PAIP-2 is sequestered promoting the translational activity of other PABP proteins (see figure 5.2A) such as PABP1 and PABP4 which are expressed within granulosa cells alongside PABP5. Certainly the predicted low affinity for poly(A) and an inability to bind eIF4G and PAIP-1 would support a model of this nature. The ability to isolate PABP1 and PAIP-2 by Co-IP in the presence versus absence of PABP5 would inform whether the PABP proteins are directly competing for PAIP-2 binding. An assumption of the sequestration model would be that the presence of PABP5 should result in a relative increase in PABP1/PABP4 activity. Again this could be directly tested within the cell-free translation extracts subject to the production of recombinant PABP5 protein. This model is an example of PABP5 acting as an indirect activator of translation and therefore the cell-free translation assay would have to be performed in the presence of PABP1, as a polyadenylated reporter mRNA would not be stimulated in the presence of PABP5 alone.

While this mechanism seems plausible there are certain pieces of evidence that would appear contradictory. Firstly, overexpression of PABP5 fails to result in a simultaneous increase in the amount of PABP1 isolated with the cap complex. Secondly, PAIP-2 levels are already known to be regulated in response to PABP1 levels by ubiquitination and proteasomal degradation therefore why a further mechanism of regulation would be required is unclear. It is also feasible that the PABP5 interaction with PAIP-2 could act as a form of 'failsafe'. Finally, the cell-type specific expression of PABP5 would imply that this is not a general mechanism of regulation, and it is unclear why this additional tier of regulation is only required in these restricted cell populations.

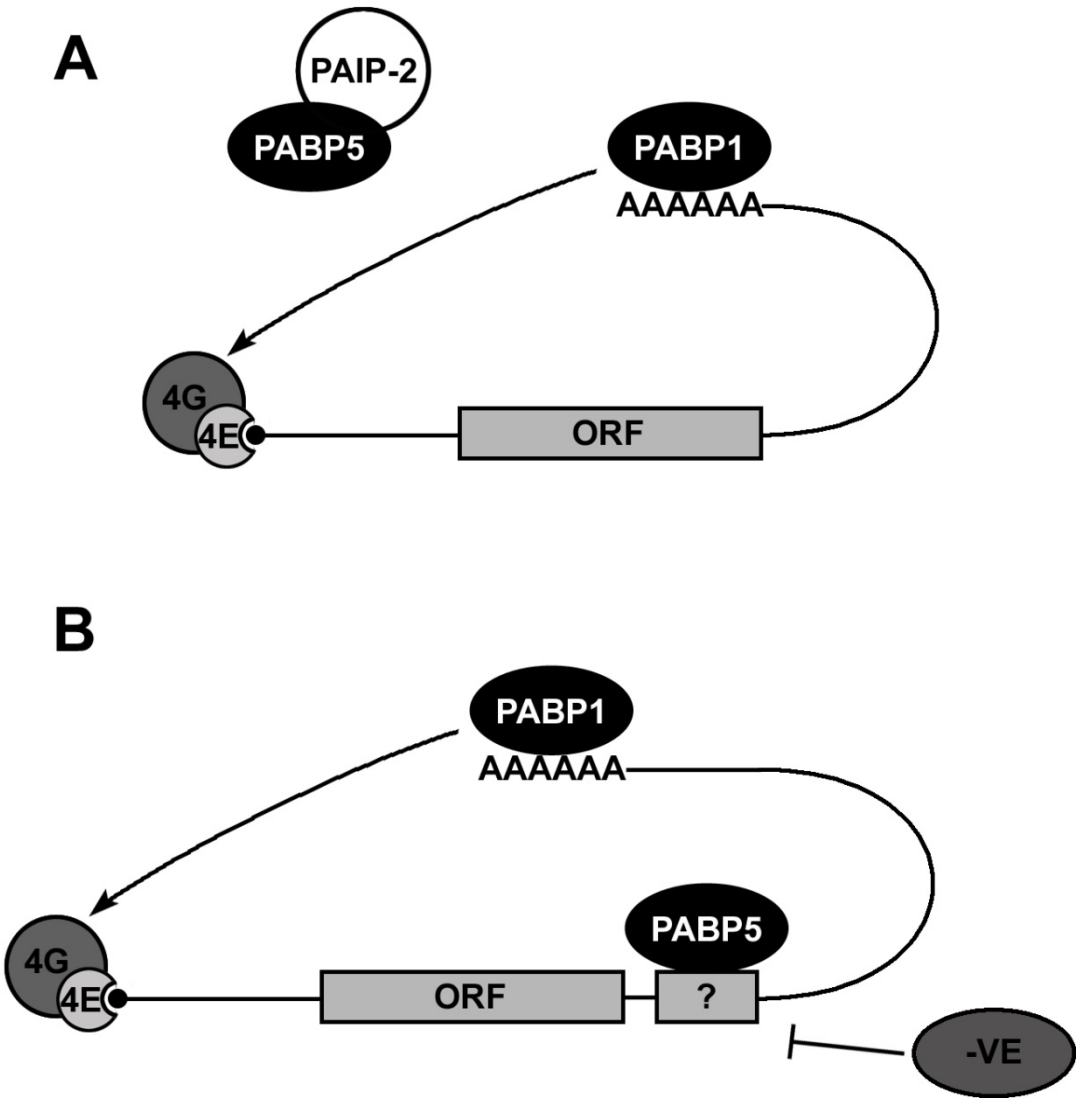

Figure 5.2 PABP5 may stimulate translation via an indirect mechanism. A. PABP5 binding to PAIP-2 could indirectly stimulate the translation of mRNAs by sequestering PAIP-2, allowing PABP1 to bind poly(A) and interact with the translation initiation factors eIF4G and PAIP-1 supporting closed loop formation. **B.** PABP5 binds to an unidentified sequence element and inhibits the binding of a negative regulator of translation supporting PABP1 mediated translational activation.

There are also examples of PABP proteins having positive roles in translation independent of their interactions with poly(A). Y-box binding protein-1 (YB-1) autoregulates the translation of its own mRNA through binding an A-rich element within the 3'-UTR and inhibiting translation initiation. PABP1 relieves this repression by competing with YB-1 for binding to this element (Skabkina *et al.*,

2005; Skabkina *et al.*, 2003). The possibility that PABP5 could bind 3'-UTR elements and promote translation by preventing the association of negative regulatory factors is intriguing (see figure 5.2B). For this postulated mechanism poly(A) binding could potentially be redundant, as would an interaction with eIF4G. It would also explain the presence of PABP5 only polysomes despite having little intrinsic translational activity, and reconciles with a lack of interaction with the cap complex. Furthermore, regulation of transcripts via binding to 3'-UTR elements could explain the restricted expression pattern of PABP5 if the target mRNAs are cell specific.

5.4 PABP5 as a Stability Factor

It is possible that the primary role of PABP5 is not in mRNA translation but in mRNA stability. Consistent with this hypothesis PABP5 has little translational stimulatory activity but is found in the polysomal fractions of a sucrose gradient. Given the results of the bioinformatic modelling and the very preliminary EMSA binding experiments it would be tempting to speculate that PABP5 could potentially bind ARE sequences and affect mRNA stability in a manner independent of poly(A) binding (see figure 5.3). In support ARE-BPs are known to associate with polysomes (Nguyen Chi *et al.*, 2009). The ARE-BP HuR has been demonstrated to co-localise with polysomes and competes for binding to the AREs of cyclin D1 and p21 with the destabilising ARE-BP AUF1 (Lal *et al.*, 2004). Thus a similar model to that of figure 5.2B could be conceived. In this model, PABP5 might bind mRNA ARE sequences precluding the binding of destabilising factors, therefore allowing stabilisation of these transcripts (see figure 5.3). The purpose of its interaction with PAIP-2 in the models 5.2B and 5.3 are unclear but may regulate PABP5 mRNA substrate binding or interactions with additional protein partners.

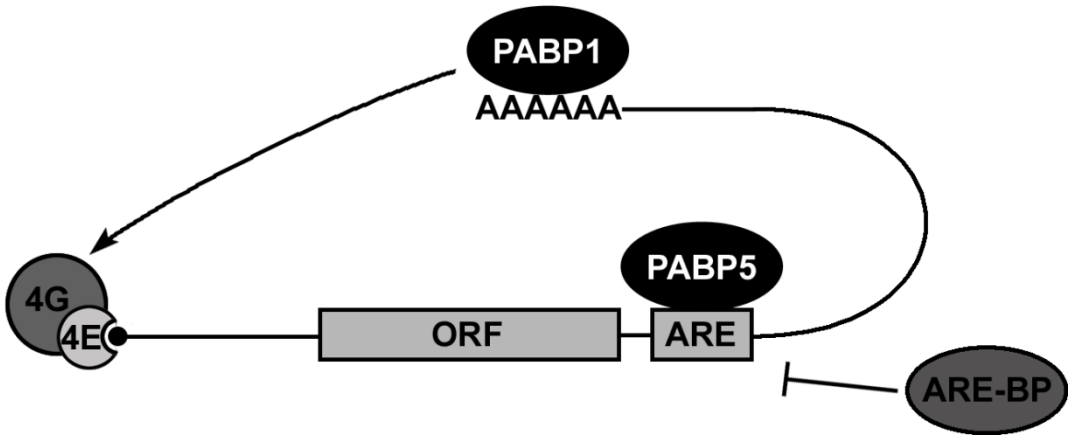

Figure 5.3 PABP5 may be an mRNA stabilising factor. PABP5 may bind to mRNA stability elements, possibly AREs, and prevent association of destabilising factors such as ARE-BPs to these elements. The stabilised messages can then be translated via PABP1.

Determination of the mRNA targets of PABP5 would allow investigation into the ability of PABP5 to promote translation/stabilisation of a specific reporter mRNA in a mammalian cell background in addition to validating the very preliminary data documenting the AU-rich sequence binding ability of PABP5 noted in appendix 3.

5.5 PABP Family Functional Redundancy

While there are a number of putative models for PABP5 function the physiological purpose of expressing multiple PABPs in the same cell types remains enigmatic. I have established that both PABP1 and PABP4 proteins are expressed within granulosa cells alongside PABP5. From the data presented in this thesis it would appear unlikely that PABP5 is capable of promoting translation activity of mRNAs in a manner similar to that of PABP1 and PABP4. Indeed PABP5 is the first example of a PABP protein that displays differential binding to certain translation factors. PABP1 has a large interactome and in a number of cases these interacting proteins have been tested for binding against other PABPs. Of the tested proteins none appear to be PABP1 specific. This is clearly not the case for PABP5 which lacks the PABP C-terminus, the major platform for the binding of a number of

PABP1 proteins including eRF3 (Cosson *et al.*, 2002a) and eIF4B (Bushell *et al.*, 2001). If PABP5 truly has an altered mRNA substrate affinity as postulated by the bioinformatic modelling and preliminary EMSA experiments, it is conceivable that PABP5 not only has an alternative function from that of other PABPs but might additionally be specific to a particular subset or group of mRNA targets expressed within the granulosa cells. Limited mRNA-specific roles for PABP1 have been described (reviewed H. Burgess and N. Gray, In press).

Mammalian PABP phenotypes have not yet been described. Understanding of the physiological role of PABP5 would benefit from the product of a knockout mouse model, allowing the characterisation of phenotypes. Generation of a PABP5 knockout mouse is complicated by its location in an X-specific subinterval of the Xq21.3/Yp11.2 homology block (Blanco *et al.*, 2001), therefore lethality or sterility in males would prevent the generation of homozygous mice. Given the expression pattern of PABP5 within the ovary, pituitary, and testis, the risk of sterility is relatively high. Therefore a more prudent approach might be the generation of conditional knockout mice to allow the knockout of PABP5 in a temporal and spatial specific manner. As a further tool for analysing the physiological role of PABP5 in granulosa cells mouse oocyte-granulosa complexes can be cultured *in-vitro*, from primary through to pre-ovulatory stages of follicle development (Qvist *et al.*, 1990). Viral transduction can be utilised to deliver small hairpin mRNAs to knockdown the expression of PABP5 in these cells (P. Brown, personal communication) to establish effects on folliculogenesis.

It is interesting to note that while PABP5 is found within a subinterval of the X-chromosome that is known to be gene poor, this subinterval is found within a larger X-Y homology block that has been linked to normal ovarian function and to premature ovarian failure by mapping translocations (Sala *et al.*, 1997). Premature ovarian failure is the cessation of ovulation in women below the average menopausal age. Symptoms vary but can include amenorrhea, hypoestrogenism and elevated

gonadotrophin levels (Shelling, 2010). In most cases the loss of fertility directly correlates with a severe reduction or loss of the follicles available for recruitment into folliculogenesis therefore factors regulating follicular recruitment and development have been investigated (Shelling, 2010). Establishing the causes of premature ovarian failure are difficult due to the heterogeneity of the condition and as a result it is usually idiopathic, but has been suggested in certain cases to be genetic in origin (Shelling, 2010). Intriguingly, several candidate genes regulate folliculogenesis through directly targeting the granulosa and thecal cell function (reviewed in Goswami and Conway, 2005). Thus although the link to PABP5 expression is tenuous it warrants further investigation, utilising the mouse model and oocyte-granulosa complexes mentioned above.

5.6 Final Summary

In conclusion, while much is known regarding the function of PABP1 in eukaryotes there are clearly large gaps in our knowledge regarding the additional PABP family members. Functional redundancy between PABP proteins and the necessity of expressing multiple PABPs within a single cell is a largely unanswered question. Recently submitted work from within my laboratory implies that PABP1 and PABP4 have overlapping but also distinct functions within *Xenopus laevis*, as determined by morpholino knockdown and cross-rescue experiments within embryos, possibly explaining the requirement for multiple PABPs of similar domain organisation within a single cell. In contrast, the work outlined in this thesis suggests that the function of PABP5 is highly distinct from the other PABP proteins. It appears unique with regard to both its roles as a basal translation factor and in its molecular interactions. These results highlight the importance of future work aimed at a more complete understanding of the molecular and physiological roles of PABP5 in human health and disease.

Appendices

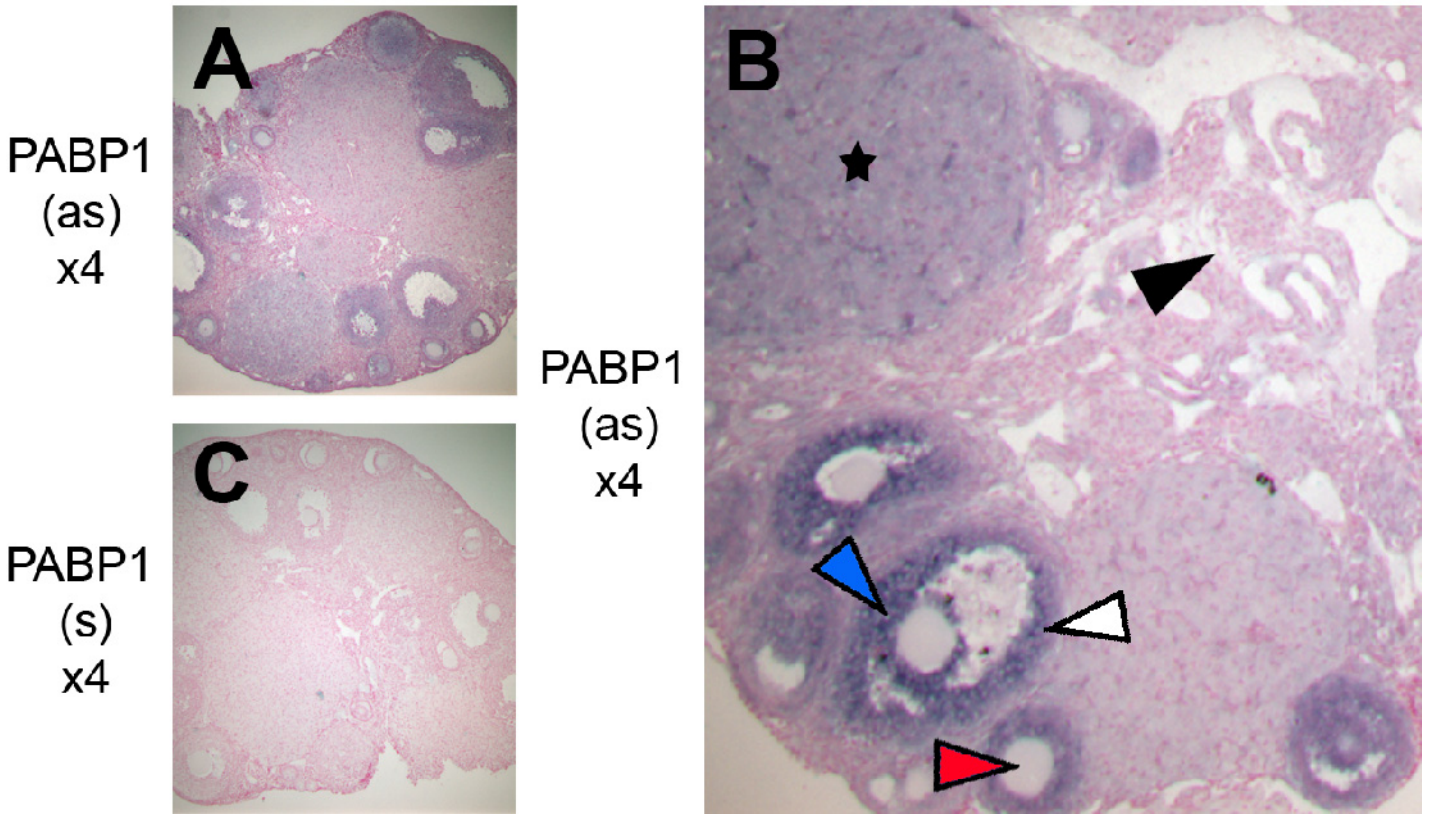

Appendix 1. PABP1 mRNA localisation in the mouse ovary. 7µm tissue sections were subjected to *in-situ* hybridisation. **A,B.** Adult mouse ovary sections incubated with PABP1 antisense probe. A robust signal could be seen in mural granulosa cells (white arrow), and cumulus granulosa cells (blue arrow). The corpus luteal cells also had staining (black star). No signal could be observed in stromal tissue (black arrow). The germ cells appeared negative for PABP5 staining (red arrow). **C.** Adult mouse ovary section incubated with PABP1 sense probe. The probes were used at a concentration of 0.1ng/µl and with an annealing temperature of 50°C. Nuclear counterstaining with Nuclear Fast Red Counterstain.

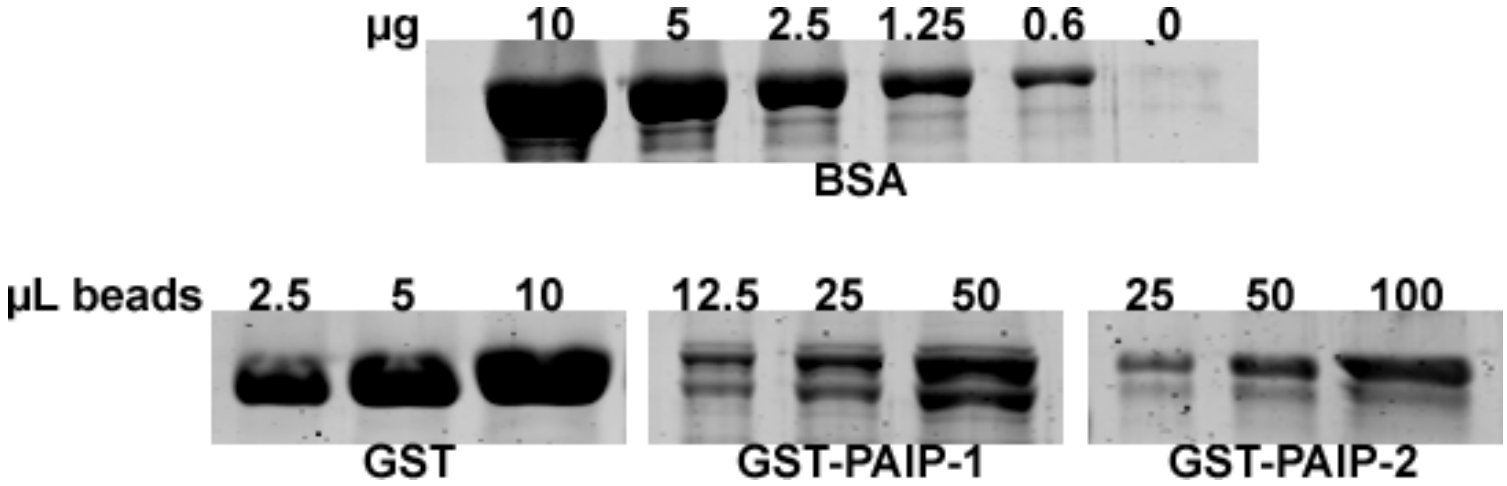

Appendix 2. Quantification of GST proteins. GST-proteins were eluted from various volumes of the beads and subjected to SDS-PAGE alongside BSA standards. The protein gel was then stained with SYPRO Ruby (Invitrogen) and the proteins imaged and quantified using a Typhoon Variable Mode Imager with a 488nm excitation laser. GST protein = 1.1µg/µl beads, GST-PAIP-1 = 0.0365µg/µl beads, and GST-PAIP-2 = 0.0173µg/µl beads.

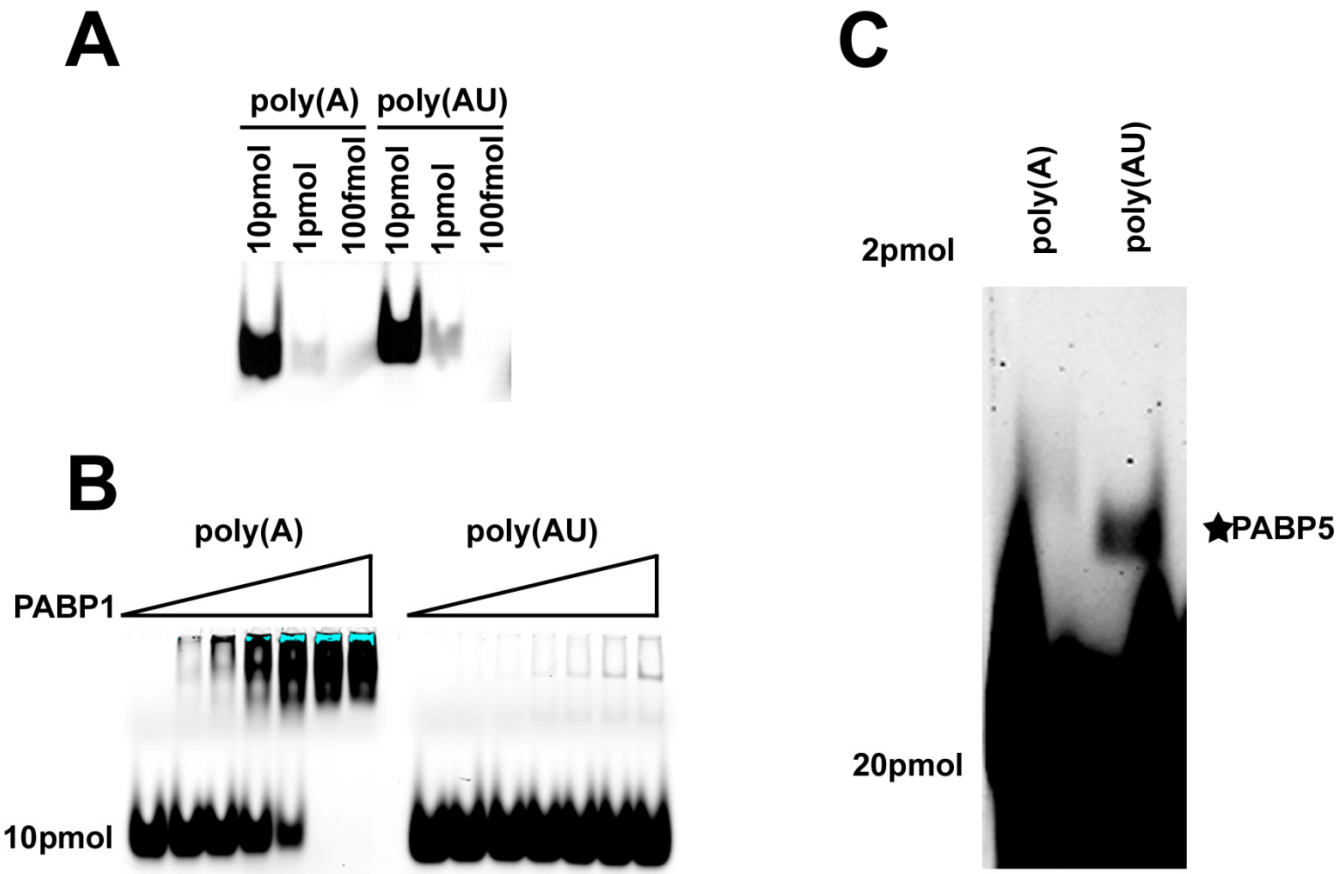

Appendix 3. Electrophoretic mobility shift assays. A. Oligonucleotide RNA probes (A_{25} and $AUUU_6$) were 5'-labelled with Cy5 (Eurogentec) and subjected to PAGE with a non-denaturing gel. **B.** Increasing concentrations of purified recombinant PABP1 (0-20pmol) were incubated with 10pmol poly(A) or poly(AU) RNA probes and subjected to PAGE with a non-denaturing gel. **C.** 2pmol of recombinant PABP5 protein was incubated with either 20pmol poly(A) or poly(AU) RNA probes and subjected to PAGE with a non-denaturing gel. Images were scanned with a Typhoon Variable Mode Imager.

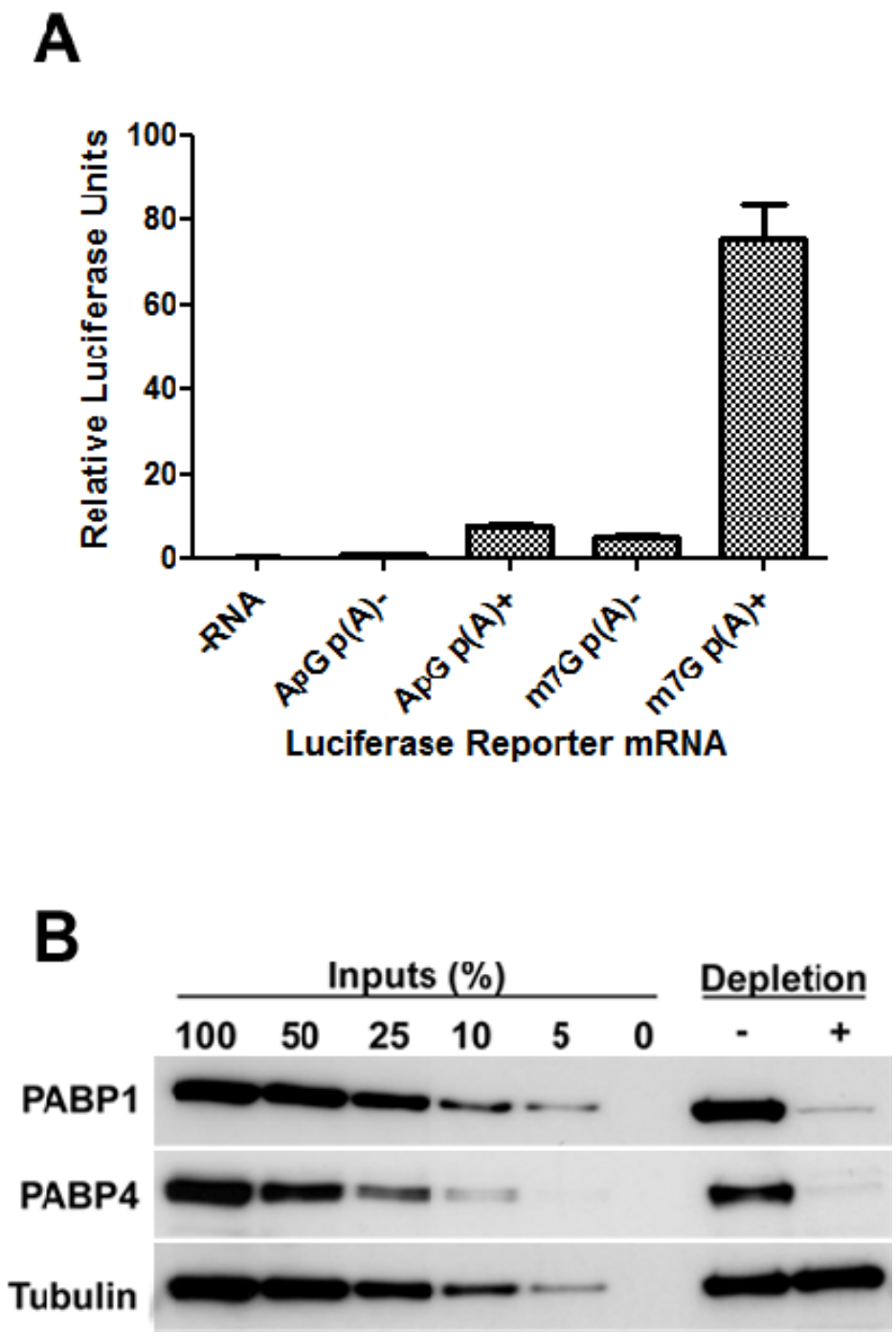

Appendix 4. Cell-free translation extracts. A. HeLa cell-free translation extracts were programmed with luciferase reporter mRNAs containing an ApG or m^7G cap and/or poly(A) tail. Luciferase units were normalised to the ApG capped poly(A) – mRNA which was set to 1. **B.** HeLa cell-free translation extracts could be successfully depleted of PABP1 and PABP4 by incubation with GST-PAIP-2.

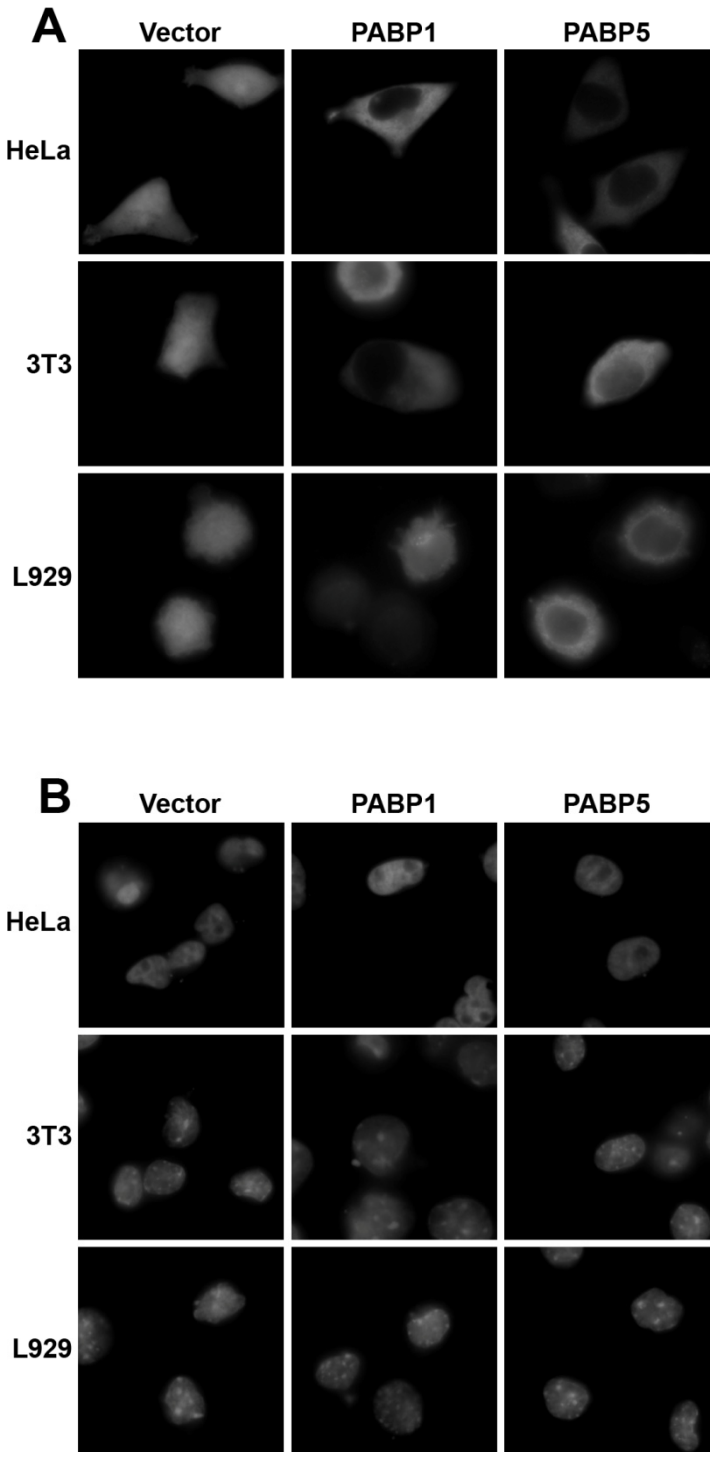

Appendix 5. Single channel images for figure 4.2. A. EGFP channel. **B.** DAPI channel.

References

Acker, M.G., B.S. Shin, T.E. Dever, and J.R. Lorsch. 2006. Interaction between eukaryotic initiation factors 1A and 5B is required for efficient ribosomal subunit joining. *J Biol Chem*. 281:8469-75.

Afonina, E., R. Stauber, and G.N. Pavlakis. 1998. The human poly(A)-binding protein 1 shuttles between the nucleus and the cytoplasm. *J Biol Chem*. 273:13015-21.

Albrecht, M., and T. Lengauer. 2004. Survey on the PABC recognition motif PAM2. *Biochem Biophys Res Commun*. 316:129-38.

Alkalaeva, E.Z., A.V. Pisarev, L.Y. Frolova, L.L. Kisselev, and T.V. Pestova. 2006. In vitro reconstitution of eukaryotic translation reveals cooperativity between release factors eRF1 and eRF3. *Cell*. 125:1125-36.

Alvarez, E., A. Castello, L. Menendez-Arias, and L. Carrasco. 2006. HIV protease cleaves poly(A)-binding protein. *Biochem J*. 396:219-26.

Amrani, N., R. Ganesan, S. Kervestin, D.A. Mangus, S. Ghosh, and A. Jacobson. 2004. A faux 3'-UTR promotes aberrant termination and triggers nonsense-mediated mRNA decay. *Nature*. 432:112-8.

Amrani, N., S. Ghosh, D.A. Mangus, and A. Jacobson. 2008. Translation factors promote the formation of two states of the closed-loop mRNP. *Nature*. 453:1276-80.

Anderson, P., and N. Kedersha. 2006. RNA granules. *J Cell Biol*. 172:803-8.

Anderson, P., and N. Kedersha. 2009. RNA granules: post-transcriptional and epigenetic modulators of gene expression. *Nat Rev Mol Cell Biol*. 10:430-6.

Andreev, D.E., I.M. Terenin, S.E. Dmitriev, and I.N. Shatskii. 2006. [Similar features in mechanisms of translation initiation of mRNAs in eukaryotic and prokaryotic systems]. *Mol Biol (Mosk)*. 40:694-702.

Apponi, L.H., S.W. Leung, K.R. Williams, S.R. Valentini, A.H. Corbett, and G.K. Pavlath. 2010. Loss of nuclear poly(A)-binding protein 1 causes defects in myogenesis and mRNA biogenesis. *Hum Mol Genet*. 19:1058-65.

Asano, K., T. Krishnamoorthy, L. Phan, G.D. Pavitt, and A.G. Hinnebusch. 1999. Conserved bipartite motifs in yeast eIF5 and eIF2Bepsilon, GTPase-activating and GDP-GTP exchange factors in translation initiation, mediate binding to their common substrate eIF2. *EMBO J*. 18:1673-88.

Baer, B.W., and R.D. Kornberg. 1983. The protein responsible for the repeating structure of cytoplasmic poly(A)-ribonucleoprotein. *J Cell Biol*. 96:717-21.

Bag, J. 2001. Feedback inhibition of poly(A)-binding protein mRNA translation. A possible mechanism of translation arrest by stalled 40 S ribosomal subunits. *J Biol Chem*. 276:47352-60.

Bag, J., and J. Wu. 1996. Translational control of poly(A)-binding protein expression. *Eur J Biochem*. 237:143-52.

Bandyopadhyay, A., and U. Maitra. 1999. Cloning and characterization of the p42 subunit of mammalian translation initiation factor 3 (eIF3): demonstration that eIF3 interacts with eIF5 in mammalian cells. *Nucleic Acids Res*. 27:1331-7.

Baron-Benhamou, J., N.H. Gehring, A.E. Kulozik, and M.W. Hentze. 2004. Using the λN Peptide to Tether Proteins to RNAs *In* mRNA Processing and Metabolism. Vol. 257. D.R. Schoenberg, editor. Humana Press. 135-153.

Barreau, C., L. Paillard, and H.B. Osborne. 2005. AU-rich elements and associated factors: are there unifying principles? *Nucleic Acids Res*. 33:7138-50.

Barth-Baus, D., C.A. Stratton, L. Parrott, H. Myerson, O. Meyuhas, D.J. Templeton, G.E. Landreth, and J.O. Hensold. 2002. S6 phosphorylation-independent pathways regulate translation of 5'-terminal oligopyrimidine tract-containing mRNAs in differentiating hematopoietic cells. *Nucleic Acids Res*. 30:1919-28.

Bashaw, G.J., and B.S. Baker. 1997. The regulation of the Drosophila msl-2 gene reveals a function for Sex-lethal in translational control. *Cell*. 89:789-98.

Beckmann, K., M. Grskovic, F. Gebauer, and M.W. Hentze. 2005. A dual inhibitory mechanism restricts msl-2 mRNA translation for dosage compensation in Drosophila. *Cell*. 122:529-40.

Behm-Ansmant, I., D. Gatfield, J. Rehwinkel, V. Hilgers, and E. Izaurralde. 2007. A conserved role for cytoplasmic poly(A)-binding protein 1 (PABPC1) in nonsense-mediated mRNA decay. *Embo J*. 26:1591-601.

Belsham, G.J., G.M. McInerney, and N. Ross-Smith. 2000. Foot-and-mouth disease virus 3C protease induces cleavage of translation initiation factors eIF4A and eIF4G within infected cells. *J Virol*. 74:272-80.

Benoit, B., G. Mitou, A. Chartier, C. Temme, S. Zaessinger, E. Wahle, I. Busseau, and M. Simonelig. 2005. An essential cytoplasmic function for the nuclear poly(A) binding protein, PABP2, in poly(A) tail length control and early development in Drosophila. *Dev Cell*. 9:511-22.

Berlanga, J.J., A. Baass, and N. Sonenberg. 2006. Regulation of poly(A) binding protein function in translation: Characterization of the Paip2 homolog, Paip2B. *RNA*. 12:1556-68.

Bernstein, P., S.W. Peltz, and J. Ross. 1989. The poly(A)-poly(A)-binding protein complex is a major determinant of mRNA stability in vitro. *Mol Cell Biol*. 9:659-70.

Bhattacharyya, S.N., R. Habermacher, U. Martine, E.I. Closs, and W. Filipowicz. 2006. Relief of microRNA-mediated translational repression in human cells subjected to stress. *Cell*. 125:1111-24.

Bi, X., and D.J. Goss. 2000. Wheat germ poly(A)-binding protein increases the ATPase and the RNA helicase activity of translation initiation factors eIF4A, eIF4B, and eIF-iso4F. *J Biol Chem*. 275:17740-6.

Biberman, Y., and O. Meyuhas. 1999. TOP mRNAs are translationally inhibited by a titratable repressor in both wheat germ extract and reticulocyte lysate. *FEBS Lett*. 456:357-60.

Bienroth, S., W. Keller, and E. Wahle. 1993. Assembly of a processive messenger RNA polyadenylation complex. *EMBO J*. 12:585-94.

Blanco, P., C.A. Sargent, C.A. Boucher, G. Howell, M. Ross, and N.A. Affara. 2001. A novel poly(A)-binding protein gene (PABPC5) maps to an X-specific subinterval in the Xq21.3/Yp11.2 homology block of the human sex chromosomes. *Genomics*. 74:1-11.

Blobel, G. 1973. A protein of molecular weight 78,000 bound to the polyadenylate region of eukaryotic messenger RNAs. *Proc Natl Acad Sci U S A*. 70:924-8.

Blobel, G., and D. Sabatini. 1971. Dissociation of mammalian polyribosomes into subunits by puromycin. *Proc Natl Acad Sci U S A*. 68:390-4.

Bollig, F., R. Winzen, M. Gaestel, S. Kostka, K. Resch, and H. Holtmann. 2003. Affinity purification of ARE-binding proteins identifies polyA-binding protein 1 as a potential substrate in MK2-induced mRNA stabilization. *Biochem Biophys Res Commun*. 301:665-70.

Boni, I.V., D.M. Isaeva, M.L. Musychenko, and N.V. Tzareva. 1991. Ribosome-messenger recognition: mRNA target sites for ribosomal protein S1. *Nucleic Acids Res*. 19:155-62.

Borman, A.M., Y.M. Michel, and K.M. Kean. 2000. Biochemical characterisation of cap-poly(A) synergy in rabbit reticulocyte lysates: the eIF4G-PABP interaction increases the functional affinity of eIF4E for the capped mRNA 5'-end. *Nucleic Acids Res*. 28:4068-75.

Bradrick, S.S., and M. Gromeier. 2009. Identification of gemin5 as a novel 7-methylguanosine cap-binding protein. *PLoS One*. 4:e7030.

Brendza, R.P., L.R. Serbus, J.B. Duffy, and W.M. Saxton. 2000. A function for kinesin I in the posterior transport of oskar mRNA and Staufen protein. *Science*. 289:2120-2.

Brown, C.Y., G.J. Mize, M. Pineda, D.L. George, and D.R. Morris. 1999. Role of two upstream open reading frames in the translational control of oncogene mdm2. *Oncogene*. 18:5631-7.

Burd, C.G., E.L. Matunis, and G. Dreyfuss. 1991. The multiple RNA-binding domains of the mRNA poly(A)-binding protein have different RNA-binding activities. *Mol Cell Biol*. 11:3419-24.

Burgui, I., T. Aragon, J. Ortin, and A. Nieto. 2003. PABP1 and eIF4GI associate with influenza virus NS1 protein in viral mRNA translation initiation complexes. *J Gen Virol*. 84:3263-74.

Burnett, P.E., R.K. Barrow, N.A. Cohen, S.H. Snyder, and D.M. Sabatini. 1998. RAFT1 phosphorylation of the translational regulators p70 S6 kinase and 4E-BP1. *Proc Natl Acad Sci U S A*. 95:1432-7.

Bushell, M., W. Wood, G. Carpenter, V.M. Pain, S.J. Morley, and M.J. Clemens. 2001. Disruption of the interaction of mammalian protein synthesis eukaryotic initiation factor 4B with the poly(A)-binding protein by caspase- and viral protease-mediated cleavages. *J Biol Chem*. 276:23922-8.

Cakmakci, N.G., R.S. Lerner, E.J. Wagner, L. Zheng, and W.F. Marzluff. 2008. SLIP1, a factor required for activation of histone mRNA translation by the stem-loop binding protein. *Mol Cell Biol*. 28:1182-94.

Calado, A., U. Kutay, U. Kuhn, E. Wahle, and M. Carmo-Fonseca. 2000. Deciphering the cellular pathway for transport of poly(A)-binding protein II. *RNA*. 6:245-56.

Caldarola, S., F. Amaldi, C.G. Proud, and F. Loreni. 2004. Translational regulation of terminal oligopyrimidine mRNAs induced by serum and amino acids involves distinct signaling events. *J Biol Chem*. 279:13522-31.

Callaghan, M.J., A.J. Russell, E. Woollatt, G.R. Sutherland, R.L. Sutherland, and C.K. Watts. 1998. Identification of a human HECT family protein with homology to the Drosophila tumor suppressor gene hyperplastic discs. *Oncogene*. 17:3479-91.

Caponigro, G., and R. Parker. 1995. Multiple functions for the poly(A)-binding protein in mRNA decapping and deadenylation in yeast. *Genes Dev*. 9:2421-32.

Castello, A., D. Franco, P. Moral-Lopez, J.J. Berlanga, E. Alvarez, E. Wimmer, and L. Carrasco. 2009. HIV- 1 protease inhibits Cap- and poly(A)-dependent translation upon eIF4GI and PABP cleavage. *PLoS One*. 4:e7997.

Cazzola, M., and R.C. Skoda. 2000. Translational pathophysiology: a novel molecular mechanism of human disease. *Blood*. 95:3280-8.

Ceci, M., C. Gaviraghi, C. Gorrini, L.A. Sala, N. Offenhauser, P.C. Marchisio, and S. Biffo. 2003. Release of eIF6 (p27BBP) from the 60S subunit allows 80S ribosome assembly. *Nature*. 426:579-84.

Chang, T.C., A. Yamashita, C.Y. Chen, Y. Yamashita, W. Zhu, S. Durdan, A. Kahvejian, N. Sonenberg, and A.B. Shyu. 2004. UNR, a new partner of poly(A)-binding protein, plays a key role in translationally coupled mRNA turnover mediated by the c-fos major coding-region determinant. *In* Genes Dev. Vol. 18. 2010-23.

Chaudhuri, J., D. Chowdhury, and U. Maitra. 1999. Distinct functions of eukaryotic translation initiation factors eIF1A and eIF3 in the formation of the 40 S ribosomal preinitiation complex. *J Biol Chem*. 274:17975-80.

Chekulaeva, M., M.W. Hentze, and A. Ephrussi. 2006. Bruno acts as a dual repressor of oskar translation, promoting mRNA oligomerization and formation of silencing particles. *Cell*. 124:521-33.

Chen, C.Y., R. Gherzi, S.E. Ong, E.L. Chan, R. Raijmakers, G.J. Pruijn, G. Stoecklin, C. Moroni, M. Mann, and M. Karin. 2001. AU binding proteins recruit the exosome to degrade ARE-containing mRNAs. *Cell*. 107:451-64.

Chen, Z., Y. Li, and R.M. Krug. 1999. Influenza A virus NS1 protein targets poly(A)-binding protein II of the cellular 3'-end processing machinery. *EMBO J*. 18:2273-83.

Cheng, S., and D.R. Gallie. 2007. eIF4G, eIFiso4G, and eIF4B bind the poly(A)-binding protein through overlapping sites within the RNA recognition motif domains. *J Biol Chem*.

Cheng, Z., K. Saito, A.V. Pisarev, M. Wada, V.P. Pisareva, T.V. Pestova, M. Gajda, A. Round, C. Kong, M. Lim, Y. Nakamura, D.I. Svergun, K. Ito, and H. Song. 2009. Structural insights into eRF3 and stop codon recognition by eRF1. *Genes Dev*. 23:1106-18.

Cole, M.D., and V.H. Cowling. 2009. Specific regulation of mRNA cap methylation by the c-Myc and E2F1 transcription factors. *Oncogene*. 28:1169-75.

Coller, J.M., N.K. Gray, and M.P. Wickens. 1998. mRNA stabilization by poly(A) binding protein is independent of poly(A) and requires translation. *Genes Dev*. 12:3226-35.

Collier, B., B. Gorgoni, C. Loveridge, H.J. Cooke, and N.K. Gray. 2005. The DAZL family proteins are PABP-binding proteins that regulate translation in germ cells. *Embo J*. 24:2656-66.

Collier, B., and N.K. Gray. 2006. Cleavage, a real turn-off? HIV-mediated proteolysis of PABP1. *Biochem J*. 396:e9-11.

Cosson, B., N. Berkova, A. Couturier, S. Chabelskaya, M. Philippe, and G. Zhouravleva. 2002a. Poly(A)-binding protein and eRF3 are associated in vivo in human and Xenopus cells. *Biol Cell*. 94:205-16.

Cosson, B., F. Braun, L. Paillard, P. Blackshear, and H. Beverley Osborne. 2004. Identification of a novel Xenopus laevis poly (A) binding protein. *Biol Cell*. 96:519-27.

Cosson, B., A. Couturier, R. Le Guellec, J. Moreau, S. Chabelskaya, G. Zhouravleva, and M. Philippe. 2002b. Characterization of the poly(A) binding proteins expressed during oogenesis and early development of Xenopus laevis. *Biol Cell*. 94:217-31.

Costa-Mattioli, M., Y. Svitkin, and N. Sonenberg. 2004. La autoantigen is necessary for optimal function of the poliovirus and hepatitis C virus internal ribosome entry site in vivo and in vitro. *Mol Cell Biol*. 24:6861-70.

Cowling, V.H. 2010. Enhanced mRNA cap methylation increases cyclin D1 expression and promotes cell transformation. *Oncogene*. 29:930-6.

Craig, A.W., A. Haghighat, A.T. Yu, and N. Sonenberg. 1998. Interaction of polyadenylate-binding protein with the eIF4G homologue PAIP enhances translation. *Nature*. 392:520-3.

De Benedetti, A., and J.R. Graff. 2004. eIF-4E expression and its role in malignancies and metastases. *Oncogene*. 23:3189-99.

De Gregorio, E., J. Baron, T. Preiss, and M.W. Hentze. 2001. Tethered-function analysis reveals that elF4E can recruit ribosomes independent of its binding to the cap structure. *RNA*. 7:106-13.

De Pietri Tonelli, D., M. Mihailovich, A. Di Cesare, F. Codazzi, F. Grohovaz, and D. Zacchetti. 2004. Translational regulation of BACE-1 expression in neuronal and non-neuronal cells. *Nucleic Acids Res*. 32:1808-17.

Deardorff, J.A., and A.B. Sachs. 1997. Differential effects of aromatic and charged residue substitutions in the RNA binding domains of the yeast poly(A)-binding protein. *J Mol Biol*. 269:67-81.

Deo, R.C., J.B. Bonanno, N. Sonenberg, and S.K. Burley. 1999. Recognition of polyadenylate RNA by the poly(A)-binding protein. *Cell*. 98:835-45.

Deo, R.C., N. Sonenberg, and S.K. Burley. 2001. X-ray structure of the human hyperplastic discs protein: an ortholog of the C-terminal domain of poly(A)-binding protein. *Proc Natl Acad Sci U S A*. 98:4414-9.

Derry, M.C., A. Yanagiya, Y. Martineau, and N. Sonenberg. 2006. Regulation of poly(A)-binding protein through PABP-interacting proteins. *Cold Spring Harb Symp Quant Biol*. 71:537-43.

Dever, T.E. 2002. Gene-specific regulation by general translation factors. *Cell*. 108:545-56.

Dever, T.E., L. Feng, R.C. Wek, A.M. Cigan, T.F. Donahue, and A.G. Hinnebusch. 1992. Phosphorylation of initiation factor 2 alpha by protein kinase GCN2 mediates gene-specific translational control of GCN4 in yeast. *Cell*. 68:585-96.

Dhar, D., M. Venkataramana, A. Ponnuswamy, and S. Das. 2009. Role of polypyrimidine tract binding protein in mediating internal initiation of translation of interferon regulatory factor 2 RNA. *PLoS One*. 4:e7049.

Dufner, A., and G. Thomas. 1999. Ribosomal S6 kinase signaling and the control of translation. *Exp Cell Res*. 253:100-9.

Duncan, K., M. Grskovic, C. Strein, K. Beckmann, R. Niggeweg, I. Abaza, F. Gebauer, M. Wilm, and M.W. Hentze. 2006. Sex-lethal imparts a sex-specific function to UNR by recruiting it to the msl-2 mRNA 3' UTR: translational repression for dosage compensation. *Genes Dev*. 20:368-79.

Duncan, K.E., C. Strein, and M.W. Hentze. 2009. The SXL-UNR corepressor complex uses a PABP-mediated mechanism to inhibit ribosome recruitment to msl-2 mRNA. *Mol Cell*. 36:571-82.

Duncan, R., S.C. Milburn, and J.W. Hershey. 1987. Regulated phosphorylation and low abundance of HeLa cell initiation factor eIF-4F suggest a role in translational control. Heat shock effects on eIF-4F. *J Biol Chem*. 262:380-8.

Elroy-Stein, O., and W.C. Merrick. 2007. Translation Initiation Via Cellular Internal Ribosome Entry Sites. *In* Translational Control in Biology and Medicine. M.B. Mathews, N. Sonenberg, and J.W. Hershey, editors. Cold Spring Harbor Laboratory Press, New York. 155-172.

Ephrussi, A., L.K. Dickinson, and R. Lehmann. 1991. Oskar organizes the germ plasm and directs localization of the posterior determinant nanos. *Cell*. 66:37-50.

Evans, T.C., S.L. Crittenden, V. Kodoyianni, and J. Kimble. 1994. Translational control of maternal glp-1 mRNA establishes an asymmetry in the C. elegans embryo. *Cell*. 77:183-94.

Ezzeddine, N., T.C. Chang, W. Zhu, A. Yamashita, C.Y. Chen, Z. Zhong, Y. Yamashita, D. Zheng, and A.B. Shyu. 2007. Human TOB, an antiproliferative transcription factor, is a poly(A)-binding protein-dependent positive regulator of cytoplasmic mRNA deadenylation. *Mol Cell Biol*. 27:7791-801.

Fabian, M.R., G. Mathonnet, T. Sundermeier, H. Mathys, J.T. Zipprich, Y.V. Svitkin, F. Rivas, M. Jinek, J. Wohlschlegel, J.A. Doudna, C.Y. Chen, A.B. Shyu, J.R. Yates, 3rd, G.J. Hannon, W. Filipowicz, T.F. Duchaine, and N. Sonenberg. 2009. Mammalian miRNA RISC recruits CAF1 and PABP to affect PABP-dependent deadenylation. *Mol Cell*. 35:868-80.

Fasulo, B., R. Becattini, G. Cenci, M.G. Giansanti, M.P. Somma, and M. Gatti. 1999. Doppio fuso (Duo), a gene required for spindle pole assembly during Drosophila male meiosis.

Feral, C., G. Guellaen, and A. Pawlak. 2001. Human testis expresses a specific poly(A)-binding protein. *Nucleic Acids Res*. 29:1872-83.

Fields, S., and O. Song. 1989. A novel genetic system to detect protein-protein interactions. *Nature*. 340:245-6.

Flynn, A., and C.G. Proud. 1996. Insulin and phorbol ester stimulate initiation factor eIF-4E phosphorylation by distinct pathways in Chinese hamster ovary cells overexpressing the insulin receptor. *Eur J Biochem*. 236:40-7.

Forch, P., L. Merendino, C. Martinez, and J. Valcarcel. 2001. Modulation of msl-2 5' splice site recognition by Sex-lethal. *RNA*. 7:1185-91.

Fraser, C.S., K.E. Berry, J.W. Hershey, and J.A. Doudna. 2007. eIF3j is located in the decoding center of the human 40S ribosomal subunit. *Mol Cell*. 26:811-9.

Friedland, D.E., W.N. Wooten, J.E. LaVoy, C.H. Hagedorn, and D.J. Goss. 2005. A mutant of eukaryotic protein synthesis initiation factor eIF4E(K119A) has an increased binding affinity for both m7G cap analogues and eIF4G peptides. *Biochemistry*. 44:4546-50.

Friedman, R.C., K.K. Farh, C.B. Burge, and D.P. Bartel. 2009. Most mammalian mRNAs are conserved targets of microRNAs. *Genome Res*. 19:92-105.

Frolova, L., X. Le Goff, G. Zhouravleva, E. Davydova, M. Philippe, and L. Kisselev. 1996. Eukaryotic polypeptide chain release factor eRF3 is an eRF1- and ribosome-dependent guanosine triphosphatase. *RNA*. 2:334-41.

Funakoshi, Y., Y. Doi, N. Hosoda, N. Uchida, M. Osawa, I. Shimada, M. Tsujimoto, T. Suzuki, T. Katada, and S. Hoshino. 2007. Mechanism of mRNA deadenylation: evidence for a molecular interplay between translation termination factor eRF3 and mRNA deadenylases. *Genes Dev*. 21:3135-48.

Gallie, D.R. 1991. The cap and poly(A) tail function synergistically to regulate mRNA translational efficiency. *Genes Dev*. 5:2108-16.

Gallie, D.R. 1998. A tale of two termini: a functional interaction between the termini of an mRNA is a prerequisite for efficient translation initiation. *Gene*. 216:1-11.

Gallie, D.R., J. Ling, M. Niepel, S.J. Morley, and V.M. Pain. 2000. The role of 5'-leader length, secondary structure and PABP concentration on cap and poly(A) tail function during translation in Xenopus oocytes. *Nucleic Acids Res*. 28:2943-53.

Garneau, N.L., J. Wilusz, and C.J. Wilusz. 2007. The highways and byways of mRNA decay. *Nat Rev Mol Cell Biol*. 8:113-26.

Gavis, E.R., R.H. Singer, and S. Huttelmaier. 2007. Localized Translation through Messenger RNA Localisation. *In* Translational Control in Biology and Medicine. M.B. Mathews, N. Sonenberg, and J.W. Hershey, editors. Cold Spring Harbor Laboratory Press.

Gebauer, F., M. Grskovic, and M.W. Hentze. 2003. Drosophila sex-lethal inhibits the stable association of the 40S ribosomal subunit with msl-2 mRNA. *Mol Cell*. 11:1397-404.

Gebauer, F., L. Merendino, M.W. Hentze, and J. Valcarcel. 1998. The Drosophila splicing regulator sex-lethal directly inhibits translation of male-specific-lethal 2 mRNA. *RNA*. 4:142-50.

Gebauer, F., W. Xu, G.M. Cooper, and J.D. Richter. 1994. Translational control by cytoplasmic polyadenylation of c-mos mRNA is necessary for oocyte maturation in the mouse. *EMBO J*. 13:5712-20.

Gherzi, R., K.Y. Lee, P. Briata, D. Wegmuller, C. Moroni, M. Karin, and C.Y. Chen. 2004. A KH domain RNA binding protein, KSRP, promotes ARE-directed mRNA turnover by recruiting the degradation machinery. *Mol Cell*. 14:571-83.

Gingras, A.C., S.G. Kennedy, M.A. O'Leary, N. Sonenberg, and N. Hay. 1998. 4E-BP1, a repressor of mRNA translation, is phosphorylated and inactivated by the Akt(PKB) signaling pathway. *Genes Dev*. 12:502-13.

Gingras, A.C., B. Raught, S.P. Gygi, A. Niedzwiecka, M. Miron, S.K. Burley, R.D. Polakiewicz, A. Wyslouch-Cieszynska, R. Aebersold, and N. Sonenberg.

2001. Hierarchical phosphorylation of the translation inhibitor 4E-BP1. *Genes Dev*. 15:2852-64.

Good, P.J., L. Abler, D. Herring, and M.D. Sheets. 2004. Xenopus embryonic poly(A) binding protein 2 (ePABP2) defines a new family of cytoplasmic poly(A) binding proteins expressed during the early stages of vertebrate development. *Genesis*. 38:166-75.

Gorgoni, B., S. Andrews, A. Schaller, D. Schumperli, N.K. Gray, and B. Muller. 2005. The stem-loop binding protein stimulates histone translation at an early step in the initiation pathway. *Rna*. 11:1030-42.

Gorgoni, B., and N.K. Gray. 2004. The roles of cytoplasmic poly(A)-binding proteins in regulating gene expression: a developmental perspective. *Brief Funct Genomic Proteomic*. 3:125-41.

Gorlach, M., C.G. Burd, and G. Dreyfuss. 1994. The mRNA poly(A)-binding protein: localization, abundance, and RNA-binding specificity. *Exp Cell Res*. 211:400-7.

Goss, D.J., S.E. Carberry, T.E. Dever, W.C. Merrick, and R.E. Rhoads. 1990. Fluorescence study of the binding of m7GpppG and rabbit globin mRNA to protein synthesis initiation factors 4A, 4E, and 4F. *Biochemistry*. 29:5008-12.

Goswami, D., and G.S. Conway. 2005. Premature ovarian failure. *Hum Reprod Update*. 11:391-410.

Gradi, A., H. Imataka, Y.V. Svitkin, E. Rom, B. Raught, S. Morino, and N. Sonenberg. 1998a. A novel functional human eukaryotic translation initiation factor 4G. *Mol Cell Biol*. 18:334-42.

Gradi, A., Y.V. Svitkin, H. Imataka, and N. Sonenberg. 1998b. Proteolysis of human eukaryotic translation initiation factor eIF4GII, but not eIF4GI, coincides with the shutoff of host protein synthesis after poliovirus infection. *Proc Natl Acad Sci U S A*. 95:11089-94.

Gray, N.K., J.M. Coller, K.S. Dickson, and M. Wickens. 2000. Multiple portions of poly(A)-binding protein stimulate translation in vivo. *Embo J*. 19:4723-33.

Gray, N.K., and M.W. Hentze. 1994. Iron regulatory protein prevents binding of the 43S translation pre-initiation complex to ferritin and eALAS mRNAs. *EMBO J*. 13:3882-91.

Gray, N.K., and M. Wickens. 1998. Control of translation initiation in animals. *Annu Rev Cell Dev Biol*. 14:399-458.

Grens, A., and I.E. Scheffler. 1990. The 5'- and 3'-untranslated regions of ornithine decarboxylase mRNA affect the translational efficiency. *J Biol Chem*. 265:11810-6.

Groft, C.M., and S.K. Burley. 2002. Recognition of eIF4G by rotavirus NSP3 reveals a basis for mRNA circularization. *Mol Cell*. 9:1273-83.

Gross, J.D., N.J. Moerke, T. von der Haar, A.A. Lugovskoy, A.B. Sachs, J.E. McCarthy, and G. Wagner. 2003. Ribosome loading onto the mRNA cap is driven by conformational coupling between eIF4G and eIF4E. *Cell*. 115:739-50.

Grosset, C., C.Y. Chen, N. Xu, N. Sonenberg, H. Jacquemin-Sablon, and A.B. Shyu. 2000. A mechanism for translationally coupled mRNA turnover: interaction between the poly(A) tail and a c-fos RNA coding determinant via a protein complex. *Cell*. 103:29-40.

Grover, R., P.S. Ray, and S. Das. 2008. Polypyrimidine tract binding protein regulates IRES-mediated translation of p53 isoforms. *Cell Cycle*. 7:2189-98.

Gu, W., Y. Kwon, R. Oko, L. Hermo, and N.B. Hecht. 1995. Poly (A) binding protein is bound to both stored and polysomal mRNAs in the mammalian testis. *Mol Reprod Dev*. 40:273-85.

Guzeloglu-Kayisli, O., S. Pauli, H. Demir, M.D. Lalioti, D. Sakkas, and E. Seli. 2008. Identification and characterization of human embryonic poly(A) binding protein (EPAB). *Mol Hum Reprod*. 14:581-8.

Haghighat, A., S. Mader, A. Pause, and N. Sonenberg. 1995. Repression of cap-dependent translation by 4E-binding protein 1: competition with p220 for binding to eukaryotic initiation factor-4E. *EMBO J*. 14:5701-9.

Haghighat, A., and N. Sonenberg. 1997. eIF4G dramatically enhances the binding of eIF4E to the mRNA 5'-cap structure. *J Biol Chem*. 272:21677-80.

Hake, L.E., and J.D. Richter. 1994. CPEB is a specificity factor that mediates cytoplasmic polyadenylation during Xenopus oocyte maturation. *Cell*. 79:617-27.

Hamilton, T.L., M. Stoneley, K.A. Spriggs, and M. Bushell. 2006. TOPs and their regulation. *Biochem Soc Trans*. 34:12-6.

Harb, M., M.M. Becker, D. Vitour, C.H. Baron, P. Vende, S.C. Brown, S. Bolte, S.T. Arold, and D. Poncet. 2008. Nuclear localization of cytoplasmic poly(A)-binding protein upon rotavirus infection involves the interaction of NSP3 with eIF4G and RoXaN. *J Virol*. 82:11283-93.

Harding, H.P., Y. Zhang, A. Bertolotti, H. Zeng, and D. Ron. 2000. Perk is essential for translational regulation and cell survival during the unfolded protein response. *Mol Cell*. 5:897-904.

Henis-Korenblit, S., N.L. Strumpf, D. Goldstaub, and A. Kimchi. 2000. A novel form of DAP5 protein accumulates in apoptotic cells as a result of caspase cleavage and internal ribosome entry site-mediated translation. *Mol Cell Biol*. 20:496-506.

Hentze, M.W., F. Gebauer, and T. Preiss. 2007. cis-Regulatory Sequences and trans-Acting Factors in Translational Control. *In* Translational Control in Biology and Medicine. M.B. Mathews, N. Sonenberg, and J.W. Hershey, editors. Cold Spring Harbor Laboratory Press, New York. 269-295.

Herrick, D., R. Parker, and A. Jacobson. 1990. Identification and comparison of stable and unstable mRNAs in Saccharomyces cerevisiae. *Mol Cell Biol*. 10:2269-84.

Hershey, J.W. 1990. Overview: phosphorylation and translation control. *Enzyme*. 44:17-27.

Hill, J.R., and D.R. Morris. 1993. Cell-specific translational regulation of S-adenosylmethionine decarboxylase mRNA. Dependence on translation and coding capacity of the cis-acting upstream open reading frame. *J Biol Chem*. 268:726-31.

Hiremath, L.S., N.R. Webb, and R.E. Rhoads. 1985. Immunological detection of the messenger RNA cap-binding protein. *J Biol Chem*. 260:7843-9.

Hoshino, S., M. Imai, T. Kobayashi, N. Uchida, and T. Katada. 1999. The eukaryotic polypeptide chain releasing factor (eRF3/GSPT) carrying the translation termination signal to the 3'-Poly(A) tail of mRNA. Direct association of erf3/GSPT with polyadenylate-binding protein. *J Biol Chem*. 274:16677-80.

Hosoda, N., T. Kobayashi, N. Uchida, Y. Funakoshi, Y. Kikuchi, S. Hoshino, and T. Katada. 2003. Translation termination factor eRF3 mediates mRNA decay through the regulation of deadenylation. *J Biol Chem*. 278:38287-91.

Hosoda, N., F. Lejeune, and L.E. Maquat. 2006. Evidence that poly(A) binding protein C1 binds nuclear pre-mRNA poly(A) tails. *Mol Cell Biol*. 26:3085-97.

Houng, A.K., L. Maggini, C.Y. Clement, and G.L. Reed. 1997. Identification and structure of activated-platelet protein-1, a protein with RNA-binding domain motifs that is expressed by activated platelets. *Eur J Biochem*. 243:209-18.

Huarte, J., A. Stutz, M.L. O'Connell, P. Gubler, D. Belin, A.L. Darrow, S. Strickland, and J.D. Vassalli. 1992. Transient translational silencing by reversible mRNA deadenylation. *Cell*. 69:1021-30.

Hunt, S.L., J.J. Hsuan, N. Totty, and R.J. Jackson. 1999. unr, a cellular cytoplasmic RNA-binding protein with five cold-shock domains, is required for internal initiation of translation of human rhinovirus RNA. *Genes Dev*. 13:437-48.

Huttelmaier, S., D. Zenklusen, M. Lederer, J. Dictenberg, M. Lorenz, X. Meng, G.J. Bassell, J. Condeelis, and R.H. Singer. 2005. Spatial regulation of beta-actin translation by Src-dependent phosphorylation of ZBP1. *Nature*. 438:512-5.

Imataka, H., A. Gradi, and N. Sonenberg. 1998. A newly identified N-terminal amino acid sequence of human eIF4G binds poly(A)-binding protein and functions in poly(A)-dependent translation. *EMBO J*. 17:7480-9.

Imataka, H., H.S. Olsen, and N. Sonenberg. 1997. A new translational regulator with homology to eukaryotic translation initiation factor 4G. *EMBO J*. 16:817-25.

Imataka, H., and N. Sonenberg. 1997. Human eukaryotic translation initiation factor 4G (eIF4G) possesses two separate and independent binding sites for eIF4A. *Mol Cell Biol*. 17:6940-7.

Intine, R.V., S.A. Tenenbaum, A.L. Sakulich, J.D. Keene, and R.J. Maraia. 2003. Differential phosphorylation and subcellular localization of La RNPs associated with precursor tRNAs and translation-related mRNAs. *Mol Cell*. 12:1301-7.

Ivanov, P.V., N.H. Gehring, J.B. Kunz, M.W. Hentze, and A.E. Kulozik. 2008. Interactions between UPF1, eRFs, PABP and the exon junction complex suggest an integrated model for mammalian NMD pathways. *EMBO J*. 27:736-47.

Jackson, R.J., C.U. Hellen, and T.V. Pestova. 2010. The mechanism of eukaryotic translation initiation and principles of its regulation. *Nat Rev Mol Cell Biol*. 11:113-27.

Jackson, R.J., and N. Standart. 1990. Do the poly(A) tail and 3' untranslated region control mRNA translation? *Cell*. 62:15-24.

Jang, S.K., H.G. Krausslich, M.J. Nicklin, G.M. Duke, A.C. Palmenberg, and E. Wimmer. 1988. A segment of the 5' nontranslated region of encephalomyocarditis virus RNA directs internal entry of ribosomes during in vitro translation. *J Virol*. 62:2636-43.

Jennings, M.D., and G.D. Pavitt. eIF5 has GDI activity necessary for translational control by eIF2 phosphorylation. *Nature*. 465:378-81.

Jinek, M., M.R. Fabian, S.M. Coyle, N. Sonenberg, and J.A. Doudna. 2010. Structural insights into the human GW182-PABC interaction in microRNA-mediated deadenylation. *Nat Struct Mol Biol*. 17:238-40.

Joachims, M., P.C. Van Breugel, and R.E. Lloyd. 1999. Cleavage of poly(A)-binding protein by enterovirus proteases concurrent with inhibition of translation in vitro. *J Virol*. 73:718-27.

Joshi, B., A.L. Cai, B.D. Keiper, W.B. Minich, R. Mendez, C.M. Beach, J. Stepinski, R. Stolarski, E. Darzynkiewicz, and R.E. Rhoads. 1995. Phosphorylation of eukaryotic protein synthesis initiation factor 4E at Ser-209. *J Biol Chem*. 270:14597-603.

Jovine, L., C. Oubridge, J.M. Avis, and K. Nagai. 1996. Two structurally different RNA molecules are bound by the spliceosomal protein U1A using the same recognition strategy. *Structure*. 4:621-31.

Jung, M.Y., L. Lorenz, and J.D. Richter. 2006. Translational control by neuroguidin, a eukaryotic initiation factor 4E and CPEB binding protein. *Mol Cell Biol*. 26:4277-87.

Kahvejian, A., Y.V. Svitkin, R. Sukarieh, M.N. M'Boutchou, and N. Sonenberg. 2005. Mammalian poly(A)-binding protein is a eukaryotic translation initiation factor, which acts via multiple mechanisms. *Genes Dev*. 19:104-13.

Kaminski, A., S.L. Hunt, J.G. Patton, and R.J. Jackson. 1995. Direct evidence that polypyrimidine tract binding protein (PTB) is essential for internal initiation of translation of encephalomyocarditis virus RNA. *RNA*. 1:924-38.

Karim, M.M., Y.V. Svitkin, A. Kahvejian, G. De Crescenzo, M. Costa-Mattioli, and N. Sonenberg. 2006. A mechanism of translational repression by competition of Paip2 with eIF4G for poly(A) binding protein (PABP) binding. *Proc Natl Acad Sci U S A*. 103:9494-9.

Kedersha, N.L., M. Gupta, W. Li, I. Miller, and P. Anderson. 1999. RNA-binding proteins TIA-1 and TIAR link the phosphorylation of eIF-2 alpha to the assembly of mammalian stress granules. *J Cell Biol*. 147:1431-42.

Kelley, R.L., J. Wang, L. Bell, and M.I. Kuroda. 1997. Sex lethal controls dosage compensation in Drosophila by a non-splicing mechanism. *Nature*. 387:195-9.

Kerekatte, V., B.D. Keiper, C. Badorff, A. Cai, K.U. Knowlton, and R.E. Rhoads. 1999. Cleavage of Poly(A)-binding protein by coxsackievirus 2A protease in vitro and in vivo: another mechanism for host protein synthesis shutoff? *J Virol*. 73:709-17.

Kessler, S.H., and A.B. Sachs. 1998. RNA recognition motif 2 of yeast Pab1p is required for its functional interaction with eukaryotic translation initiation factor 4G. *Mol Cell Biol*. 18:51-7.

Khacho, M., K. Mekhail, K. Pilon-Larose, J. Payette, and S. Lee. 2008. Cancer-causing mutations in a novel transcription-dependent nuclear export motif of VHL abrogate oxygen-dependent degradation of hypoxia-inducible factor. *Mol Cell Biol*. 28:302-14.

Khaleghpour, K., A. Kahvejian, G. De Crescenzo, G. Roy, Y.V. Svitkin, H. Imataka, M. O'Connor-McCourt, and N. Sonenberg. 2001a. Dual interactions of the translational repressor Paip2 with poly(A) binding protein. *Mol Cell Biol*. 21:5200-13.

Khaleghpour, K., Y.V. Svitkin, A.W. Craig, C.T. DeMaria, R.C. Deo, S.K. Burley, and N. Sonenberg. 2001b. Translational repression by a novel partner of human poly(A) binding protein, Paip2. *Mol Cell*. 7:205-16.

Kim-Ha, J., J.L. Smith, and P.M. Macdonald. 1991. oskar mRNA is localized to the posterior pole of the Drosophila oocyte. *Cell*. 66:23-35.

Kim, J.H., and J.D. Richter. 2006. Opposing polymerase-deadenylase activities regulate cytoplasmic polyadenylation. *Mol Cell*. 24:173-83.

Kim, J.H., and J.D. Richter. 2007. RINGO/cdk1 and CPEB mediate poly(A) tail stabilization and translational regulation by ePAB. *Genes Dev*. 21:2571-9.

Kimball, S.R., N.K. Heinzinger, R.L. Horetsky, and L.S. Jefferson. 1998. Identification of interprotein interactions between the subunits of eukaryotic initiation factors eIF2 and eIF2B. *J Biol Chem*. 273:3039-44.

Kimura, M., K. Ishida, S. Kashiwabara, and T. Baba. 2009. Characterization of two cytoplasmic poly(A)-binding proteins, PABPC1 and PABPC2, in mouse spermatogenic cells. *Biol Reprod*. 80:545-54.

Kleene, K.C. 1989. Poly(A) shortening accompanies the activation of translation of five mRNAs during spermiogenesis in the mouse. *Development*. 106:367-73.

Kleene, K.C. 1993. Multiple controls over the efficiency of translation of the mRNAs encoding transition proteins, protamines, and the mitochondrial capsule selenoprotein in late spermatids in mice. *Dev Biol*. 159:720-31.

Kleene, K.C., R.J. Distel, and N.B. Hecht. 1984. Translational regulation and deadenylation of a protamine mRNA during spermiogenesis in the mouse. *Dev Biol*. 105:71-9.

Kleene, K.C., E. Mulligan, D. Steiger, K. Donohue, and M.A. Mastrangelo. 1998. The mouse gene encoding the testis-specific isoform of Poly(A) binding protein (Pabp2) is an expressed retroposon: intimations that gene expression in spermatogenic cells facilitates the creation of new genes. *J Mol Evol*. 47:275-81.

Kleene, K.C., M.Y. Wang, M. Cutler, C. Hall, and D. Shih. 1994. Developmental expression of poly(A) binding protein mRNAs during spermatogenesis in the mouse. *Mol Reprod Dev*. 39:355-64.

Koloteva-Levine, N., D. Pinchasi, I. Pereman, A. Zur, M. Brandeis, and O. Elroy-Stein. 2004. The Apc5 subunit of the anaphase-promoting complex/cyclosome interacts with poly(A) binding protein and represses internal ribosome entry site-mediated translation. *Mol Cell Biol*. 24:3577-87.

Konecki, D.S., K.C. Aune, W. Tate, and C.T. Caskey. 1977. Characterization of reticulocyte release factor. *J Biol Chem*. 252:4514-20.

Koritzinsky, M., M.G. Magagnin, T. van den Beucken, R. Seigneuric, K. Savelkouls, J. Dostie, S. Pyronnet, R.J. Kaufman, S.A. Weppler, J.W. Voncken, P. Lambin, C. Koumenis, N. Sonenberg, and B.G. Wouters. 2006. Gene expression during acute and prolonged hypoxia is regulated by distinct mechanisms of translational control. *Embo J*. 25:1114-25.

Korner, C.G., and E. Wahle. 1997. Poly(A) tail shortening by a mammalian poly(A)-specific 3'-exoribonuclease. *J Biol Chem*. 272:10448-56.

Korner, C.G., M. Wormington, M. Muckenthaler, S. Schneider, E. Dehlin, and E. Wahle. 1998. The deadenylating nuclease (DAN) is involved in poly(A) tail removal during the meiotic maturation of Xenopus oocytes. *EMBO J*. 17:5427-37.

Koromilas, A.E., A. Lazaris-Karatzas, and N. Sonenberg. 1992. mRNAs containing extensive secondary structure in their 5' non-coding region translate efficiently in cells overexpressing initiation factor eIF-4E. *EMBO J*. 11:4153-8.

Kozak, M. 1987a. An analysis of 5'-noncoding sequences from 699 vertebrate messenger RNAs. *Nucleic Acids Res*. 15:8125-48.

Kozak, M. 1987b. Effects of intercistronic length on the efficiency of reinitiation by eucaryotic ribosomes. *Mol Cell Biol*. 7:3438-45.

Kozak, M. 1989. Circumstances and mechanisms of inhibition of translation by secondary structure in eucaryotic mRNAs. *Mol Cell Biol*. 9:5134-42.

Kozak, M. 1990. Downstream secondary structure facilitates recognition of initiator codons by eukaryotic ribosomes. *Proc Natl Acad Sci U S A*. 87:8301-5.

Kozak, M. 1991. An analysis of vertebrate mRNA sequences: intimations of translational control. *J Cell Biol*. 115:887-903.

Kozak, M. 1999. Initiation of translation in prokaryotes and eukaryotes. *Gene*. 234:187-208.

Kozak, S.L., M. Marin, K.M. Rose, C. Bystrom, and D. Kabat. 2006. The anti-HIV-1 editing enzyme APOBEC3G binds HIV-1 RNA and messenger RNAs that shuttle between polysomes and stress granules. *J Biol Chem*. 281:29105-19.

Kozlov, G., G. De Crescenzo, N.S. Lim, N. Siddiqui, D. Fantus, A. Kahvejian, J.F. Trempe, D. Elias, I. Ekiel, N. Sonenberg, M. O'Connor-McCourt, and K. Gehring. 2004. Structural basis of ligand recognition by PABC, a highly specific peptide-binding domain found in poly(A)-binding protein and a HECT ubiquitin ligase. *Embo J*. 23:272-81.

Kozlov, G., and K. Gehring. 2010. Molecular basis of eRF3 recognition by the MLLE domain of poly(A)-binding protein. *PLoS One*. 5:e10169.

Kozlov, G., J.F. Trempe, K. Khaleghpour, A. Kahvejian, I. Ekiel, and K. Gehring. 2001. Structure and function of the C-terminal PABC domain of human poly(A)-binding protein. *Proc Natl Acad Sci U S A*. 98:4409-13.

Kuhn, U., and T. Pieler. 1996. Xenopus poly(A) binding protein: functional domains in RNA binding and protein-protein interaction. *J Mol Biol*. 256:20-30.

Kuhn, U., and E. Wahle. 2004. Structure and function of poly(A) binding proteins. *Biochim Biophys Acta*. 1678:67-84.

Kuyumcu-Martinez, N.M., M. Joachims, and R.E. Lloyd. 2002. Efficient cleavage of ribosome-associated poly(A)-binding protein by enterovirus 3C protease. *J Virol*. 76:2062-74.

Kuyumcu-Martinez, N.M., M.E. Van Eden, P. Younan, and R.E. Lloyd. 2004. Cleavage of poly(A)-binding protein by poliovirus 3C protease inhibits host cell translation: a novel mechanism for host translation shutoff. *Mol Cell Biol*. 24:1779-90.

Kwon, S., E. Barbarese, and J.H. Carson. 1999. The cis-acting RNA trafficking signal from myelin basic protein mRNA and its cognate trans-acting ligand hnRNP A2 enhance cap-dependent translation. *J Cell Biol*. 147:247-56.

Lal, A., K. Mazan-Mamczarz, T. Kawai, X. Yang, J.L. Martindale, and M. Gorospe. 2004. Concurrent versus individual binding of HuR and AUF1 to common labile target mRNAs. *Embo J*. 23:3092-102.

Le, H., K.S. Browning, and D.R. Gallie. 2000. The phosphorylation state of poly(A)-binding protein specifies its binding to poly(A) RNA and its interaction with eukaryotic initiation factor (eIF) 4F, eIFiso4F, and eIF4B. *J Biol Chem*. 275:17452-62.

Le, H., R.L. Tanguay, M.L. Balasta, C.C. Wei, K.S. Browning, A.M. Metz, D.J. Goss, and D.R. Gallie. 1997. Translation initiation factors eIF-iso4G and eIF-

4B interact with the poly(A)-binding protein and increase its RNA binding activity. *J Biol Chem*. 272:16247-55.

Le Hir, H., E. Izaurralde, L.E. Maquat, and M.J. Moore. 2000. The spliceosome deposits multiple proteins 20-24 nucleotides upstream of mRNA exon-exon junctions. *EMBO J*. 19:6860-9.

Leegwater, P.A., G. Vermeulen, A.A. Konst, S. Naidu, J. Mulders, A. Visser, P. Kersbergen, D. Mobach, D. Fonds, C.G. van Berkel, R.J. Lemmers, R.R. Frants, C.B. Oudejans, R.B. Schutgens, J.C. Pronk, and M.S. van der Knaap. 2001. Subunits of the translation initiation factor eIF2B are mutant in leukoencephalopathy with vanishing white matter. *Nat Genet*. 29:383-8.

LeFebvre, A.K., N.L. Korneeva, M. Trutschl, U. Cvek, R.D. Duzan, C.A. Bradley, J.W. Hershey, and R.E. Rhoads. 2006. Translation initiation factor eIF4G-1 binds to eIF3 through the eIF3e subunit. *J Biol Chem*. 281:22917-32.

Levine, M., and R. Tjian. 2003. Transcription regulation and animal diversity. *Nature*. 424:147-51.

Lim, N.S., G. Kozlov, T.C. Chang, O. Groover, N. Siddiqui, L. Volpon, G. De Crescenzo, A.B. Shyu, and K. Gehring. 2006. Comparative peptide binding studies of the PABC domains from the ubiquitin-protein isopeptide ligase HYD and poly(A)-binding protein. Implications for HYD function. *J Biol Chem*. 281:14376-82.

Lin, A.C., and C.E. Holt. 2007. Local translation and directional steering in axons. *Embo J*.

Ling, J., S.J. Morley, and J.A. Traugh. 2005. Inhibition of cap-dependent translation via phosphorylation of eIF4G by protein kinase Pak2. *Embo J*. 24:4094-105.

Liu, H., N.D. Rodgers, X. Jiao, and M. Kiledjian. 2002. The scavenger mRNA decapping enzyme DcpS is a member of the HIT family of pyrophosphatases. *EMBO J*. 21:4699-708.

Lu, L., A.P. Han, and J.J. Chen. 2001. Translation initiation control by heme-regulated eukaryotic initiation factor 2alpha kinase in erythroid cells under cytoplasmic stresses. *Mol Cell Biol*. 21:7971-80.

Maag, D., M.A. Algire, and J.R. Lorsch. 2006. Communication between eukaryotic translation initiation factors 5 and 1A within the ribosomal pre-initiation complex plays a role in start site selection. *J Mol Biol*. 356:724-37.

Maag, D., C.A. Fekete, Z. Gryczynski, and J.R. Lorsch. 2005. A conformational change in the eukaryotic translation preinitiation complex and release of eIF1 signal recognition of the start codon. *Mol Cell*. 17:265-75.

Macejak, D.G., and P. Sarnow. 1991. Internal initiation of translation mediated by the 5' leader of a cellular mRNA. *Nature*. 353:90-4.

Maciejowski, J., J.H. Ahn, P.G. Cipriani, D.J. Killian, A.L. Chaudhary, J.I. Lee, R. Voutev, R.C. Johnsen, D.L. Baillie, K.C. Gunsalus, D.H. Fitch, and E.J. Hubbard. 2005. Autosomal genes of autosomal/X-linked duplicated gene pairs and germ-line proliferation in Caenorhabditis elegans. *Genetics*. 169:1997-2011.

Majumdar, R., A. Bandyopadhyay, and U. Maitra. 2003. Mammalian translation initiation factor eIF1 functions with eIF1A and eIF3 in the formation of a stable 40 S preinitiation complex. *J Biol Chem*. 278:6580-7.

Mangus, D.A., M.C. Evans, and A. Jacobson. 2003. Poly(A)-binding proteins: multifunctional scaffolds for the post-transcriptional control of gene expression. *Genome Biol*. 4:223.

Manzella, J.M., and P.J. Blackshear. 1990. Regulation of rat ornithine decarboxylase mRNA translation by its 5'-untranslated region. *J Biol Chem*. 265:11817-22.

Marash, L., and A. Kimchi. 2005. DAP5 and IRES-mediated translation during programmed cell death. *Cell Death Differ*. 12:554-62.

Marash, L., N. Liberman, S. Henis-Korenblit, G. Sivan, E. Reem, O. Elroy-Stein, and A. Kimchi. 2008. DAP5 promotes cap-independent translation of Bcl-2 and CDK1 to facilitate cell survival during mitosis. *Mol Cell*. 30:447-59.

Marcotrigiano, J., A.C. Gingras, N. Sonenberg, and S.K. Burley. 1999. Cap-dependent translation initiation in eukaryotes is regulated by a molecular mimic of eIF4G. *Mol Cell*. 3:707-16.

Marintchev, A., K.A. Edmonds, B. Marintcheva, E. Hendrickson, M. Oberer, C. Suzuki, B. Herdy, N. Sonenberg, and G. Wagner. 2009. Topology and regulation of the human eIF4A/4G/4H helicase complex in translation initiation. *Cell*. 136:447-60.

Martineau, Y., M.C. Derry, X. Wang, A. Yanagiya, J.J. Berlanga, A.B. Shyu, H. Imataka, K. Gehring, and N. Sonenberg. 2008. Poly(A)-binding protein-interacting protein 1 binds to eukaryotic translation initiation factor 3 to stimulate translation. *Mol Cell Biol*. 28:6658-67.

Melo, E.O., R. Dhalia, C. Martins de Sa, N. Standart, and O.P. de Melo Neto. 2003. Identification of a C-terminal poly(A)-binding protein (PABP)-PABP interaction domain: role in cooperative binding to poly (A) and efficient cap distal translational repression. *J Biol Chem*. 278:46357-68.

Mendell, J.T., N.A. Sharifi, J.L. Meyers, F. Martinez-Murillo, and H.C. Dietz. 2004. Nonsense surveillance regulates expression of diverse classes of mammalian transcripts and mutes genomic noise. *Nat Genet*. 36:1073-8.

Mendez, R., and J.D. Richter. 2001. Translational control by CPEB: a means to the end. *Nat Rev Mol Cell Biol*. 2:521-9.

Messias, A.C., C. Harnisch, A. Ostareck-Lederer, M. Sattler, and D.H. Ostareck. 2006. The DICE-binding activity of KH domain 3 of hnRNP K is affected by c-Src-mediated tyrosine phosphorylation. *J Mol Biol*. 361:470-81.

Methot, N., M.S. Song, and N. Sonenberg. 1996. A region rich in aspartic acid, arginine, tyrosine, and glycine (DRYG) mediates eukaryotic initiation factor 4B (eIF4B) self-association and interaction with eIF3. *Mol Cell Biol*. 16:5328-34.

Meyuhas, O. 2000. Synthesis of the translational apparatus is regulated at the translational level. *Eur J Biochem*. 267:6321-30.

Michel, Y.M., D. Poncet, M. Piron, K.M. Kean, and A.M. Borman. 2000. Cap-Poly(A) synergy in mammalian cell-free extracts. Investigation of the requirements for poly(A)-mediated stimulation of translation initiation. *J Biol Chem*. 275:32268-76.

Micklem, D.R., J. Adams, S. Grunert, and D. St Johnston. 2000. Distinct roles of two conserved Staufen domains in oskar mRNA localization and translation. *EMBO J*. 19:1366-77.

Millevoi, S., and S. Vagner. 2010. Molecular mechanisms of eukaryotic pre-mRNA 3' end processing regulation. *Nucleic Acids Res*. 38:2757-74.

Moraes, K.C., C.J. Wilusz, and J. Wilusz. 2006. CUG-BP binds to RNA substrates and recruits PARN deadenylase. *RNA*. 12:1084-91.

Morris, D.R., and A.P. Geballe. 2000. Upstream open reading frames as regulators of mRNA translation. *Mol Cell Biol*. 20:8635-42.

Munroe, D., and A. Jacobson. 1990. mRNA poly(A) tail, a 3' enhancer of translational initiation. *Mol Cell Biol*. 10:3441-55.

Muthukrishnan, S., G.W. Both, Y. Furuichi, and A.J. Shatkin. 1975. 5'-Terminal 7-methylguanosine in eukaryotic mRNA is required for translation. *Nature*. 255:33-7.

Nagy, E., and L.E. Maquat. 1998. A rule for termination-codon position within intron-containing genes: when nonsense affects RNA abundance. *Trends Biochem Sci*. 23:198-9.

Nakamura, A., K. Sato, and K. Hanyu-Nakamura. 2004. Drosophila cup is an eIF4E binding protein that associates with Bruno and regulates oskar mRNA translation in oogenesis. *Dev Cell*. 6:69-78.

Nanda, J.S., Y.N. Cheung, J.E. Takacs, P. Martin-Marcos, A.K. Saini, A.G. Hinnebusch, and J.R. Lorsch. 2009. eIF1 controls multiple steps in start codon recognition during eukaryotic translation initiation. *J Mol Biol*. 394:268-85.

Naranda, T., I. Sirangelo, B.J. Fabbri, and J.W. Hershey. 1995. Mutations in the NKXD consensus element indicate that GTP binds to the gamma-subunit of translation initiation factor eIF2. *FEBS Lett*. 372:249-52.

Nguyen Chi, M., F. Chalmel, E. Agius, N. Vanzo, K.S. Khabar, B. Jegou, and D. Morello. 2009. Temporally regulated traffic of HuR and its associated ARE-containing mRNAs from the chromatoid body to polysomes during mouse spermatogenesis. *PLoS One*. 4:e4900.

Nietfeld, W., H. Mentzel, and T. Pieler. 1990. The Xenopus laevis poly(A) binding protein is composed of multiple functionally independent RNA binding domains. *EMBO J*. 9:3699-705.

Noble, C.G., and H. Song. 2008. Structural studies of elongation and release factors. *Cell Mol Life Sci*. 65:1335-46.

Oberer, M., A. Marintchev, and G. Wagner. 2005. Structural basis for the enhancement of eIF4A helicase activity by eIF4G. *Genes Dev*. 19:2212-23.

Ogawa, H., S. Inouye, F.I. Tsuji, K. Yasuda, and K. Umesono. 1995. Localization, trafficking, and temperature-dependence of the Aequorea green fluorescent protein in cultured vertebrate cells. *Proc Natl Acad Sci U S A*. 92:11899-903.

Ogle, J.M., A.P. Carter, and V. Ramakrishnan. 2003. Insights into the decoding mechanism from recent ribosome structures. *Trends Biochem Sci*. 28:259-66.

Okochi, K., T. Suzuki, J. Inoue, S. Matsuda, and T. Yamamoto. 2005. Interaction of anti-proliferative protein Tob with poly(A)-binding protein and inducible poly(A)-binding protein: implication of Tob in translational control. *Genes Cells*. 10:151-63.

Ostareck-Lederer, A., D.H. Ostareck, N. Standart, and B.J. Thiele. 1994. Translation of 15-lipoxygenase mRNA is inhibited by a protein that binds to a repeated sequence in the 3' untranslated region. *Embo J*. 13:1476-81.

Ostareck, D.H., A. Ostareck-Lederer, I.N. Shatsky, and M.W. Hentze. 2001. Lipoxygenase mRNA silencing in erythroid differentiation: The 3'UTR regulatory complex controls 60S ribosomal subunit joining. *Cell*. 104:281-90.

Ostareck, D.H., A. Ostareck-Lederer, M. Wilm, B.J. Thiele, M. Mann, and M.W. Hentze. 1997. mRNA silencing in erythroid differentiation: hnRNP K and hnRNP E1 regulate 15-lipoxygenase translation from the 3' end. *Cell*. 89:597-606.

Otero, L.J., M.P. Ashe, and A.B. Sachs. 1999. The yeast poly(A)-binding protein Pab1p stimulates in vitro poly(A)-dependent and cap-dependent translation by distinct mechanisms. *EMBO J*. 18:3153-63.

Pacheco, A., S. Reigadas, and E. Martinez-Salas. 2008. Riboproteomic analysis of polypeptides interacting with the internal ribosome-entry site element of foot-and-mouth disease viral RNA. *Proteomics*. 8:4782-90.

Paraskeva, E., N.K. Gray, B. Schlager, K. Wehr, and M.W. Hentze. 1999. Ribosomal pausing and scanning arrest as mechanisms of translational regulation from cap-distal iron-responsive elements. *Mol Cell Biol*. 19:807-16.

Passmore, L.A., T.M. Schmeing, D. Maag, D.J. Applefield, M.G. Acker, M.A. Algire, J.R. Lorsch, and V. Ramakrishnan. 2007. The eukaryotic translation initiation factors eIF1 and eIF1A induce an open conformation of the 40S ribosome. *Mol Cell*. 26:41-50.

Patel, G.P., and J. Bag. 2006. IMP1 interacts with poly(A)-binding protein (PABP) and the autoregulatory translational control element of PABP-mRNA through the KH III-IV domain. *FEBS J*. 273:5678-90.

Patel, G.P., S. Ma, and J. Bag. 2005. The autoregulatory translational control element of poly(A)-binding protein mRNA forms a heteromeric ribonucleoprotein complex. *Nucleic Acids Res*. 33:7074-89.

Patel, J., L.E. McLeod, R.G. Vries, A. Flynn, X. Wang, and C.G. Proud. 2002. Cellular stresses profoundly inhibit protein synthesis and modulate the states of phosphorylation of multiple translation factors. *Eur J Biochem*. 269:3076-85.

Pause, A., G.J. Belsham, A.C. Gingras, O. Donze, T.A. Lin, J.C. Lawrence, Jr., and N. Sonenberg. 1994. Insulin-dependent stimulation of protein synthesis by phosphorylation of a regulator of 5'-cap function. *Nature*. 371:762-7.

Pelletier, J., G. Kaplan, V.R. Racaniello, and N. Sonenberg. 1988. Cap-independent translation of poliovirus mRNA is conferred by sequence elements within the 5' noncoding region. *Mol Cell Biol*. 8:1103-12.

Peng, S.S., C.Y. Chen, N. Xu, and A.B. Shyu. 1998. RNA stabilization by the AU-rich element binding protein, HuR, an ELAV protein. *EMBO J*. 17:3461-70.

Pestova, T.V., S.I. Borukhov, and C.U. Hellen. 1998a. Eukaryotic ribosomes require initiation factors 1 and 1A to locate initiation codons. *Nature*. 394:854-9.

Pestova, T.V., and C.U. Hellen. 2003. Translation elongation after assembly of ribosomes on the Cricket paralysis virus internal ribosomal entry site without initiation factors or initiator tRNA. *Genes Dev*. 17:181-6.

Pestova, T.V., and V.G. Kolupaeva. 2002. The roles of individual eukaryotic translation initiation factors in ribosomal scanning and initiation codon selection. *Genes Dev*. 16:2906-22.

Pestova, T.V., V.G. Kolupaeva, I.B. Lomakin, E.V. Pilipenko, I.N. Shatsky, V.I. Agol, and C.U. Hellen. 2001. Molecular mechanisms of translation initiation in eukaryotes. *Proc Natl Acad Sci U S A*. 98:7029-36.

Pestova, T.V., I.B. Lomakin, J.H. Lee, S.K. Choi, T.E. Dever, and C.U. Hellen. 2000. The joining of ribosomal subunits in eukaryotes requires eIF5B. *Nature*. 403:332-5.

Pestova, T.V., I.N. Shatsky, S.P. Fletcher, R.J. Jackson, and C.U. Hellen. 1998b. A prokaryotic-like mode of cytoplasmic eukaryotic ribosome binding to the initiation codon during internal translation initiation of hepatitis C and classical swine fever virus RNAs. *Genes Dev*. 12:67-83.

Petersen, C.P., M.E. Bordeleau, J. Pelletier, and P.A. Sharp. 2006. Short RNAs repress translation after initiation in mammalian cells. *Mol Cell*. 21:533-42.

Pillai, R.S., S.N. Bhattacharyya, C.G. Artus, T. Zoller, N. Cougot, E. Basyuk, E. Bertrand, and W. Filipowicz. 2005. Inhibition of translational initiation by Let-7 MicroRNA in human cells. *Science*. 309:1573-6.

Piron, M., P. Vende, J. Cohen, and D. Poncet. 1998. Rotavirus RNA-binding protein NSP3 interacts with eIF4GI and evicts the poly(A) binding protein from eIF4F. *Embo J*. 17:5811-21.

Pisarev, A.V., M.A. Skabkin, V.P. Pisareva, O.V. Skabkina, A.M. Rakotondrafara, M.W. Hentze, C.U. Hellen, and T.V. Pestova. 2010. The role of ABCE1 in eukaryotic posttermination ribosomal recycling. *Mol Cell*. 37:196-210.

Portela, V.M., G. Zamberlam, and C.A. Price. 2010. Cell plating density alters the ratio of estrogenic to progestagenic enzyme gene expression in cultured granulosa cells. *Fertil Steril*. 93:2050-5.

Poulin, F., A.C. Gingras, H. Olsen, S. Chevalier, and N. Sonenberg. 1998. 4E-BP3, a new member of the eukaryotic initiation factor 4E-binding protein family. *J Biol Chem*. 273:14002-7.

Proweller, A., and J.S. Butler. 1996. Ribosomal association of poly(A)-binding protein in poly(A)-deficient Saccharomyces cerevisiae. *J Biol Chem*. 271:10859-65.

Ptushkina, M., T. von der Haar, S. Vasilescu, R. Frank, R. Birkenhager, and J.E. McCarthy. 1998. Cooperative modulation by eIF4G of eIF4E-binding to the mRNA 5' cap in yeast involves a site partially shared by p20. *EMBO J*. 17:4798-808.

Pyronnet, S., H. Imataka, A.C. Gingras, R. Fukunaga, T. Hunter, and N. Sonenberg. 1999. Human eukaryotic translation initiation factor 4G (eIF4G) recruits mnk1 to phosphorylate eIF4E. *EMBO J*. 18:270-9.

Qin, X., and P. Sarnow. 2004. Preferential translation of internal ribosome entry site-containing mRNAs during the mitotic cycle in mammalian cells. *J Biol Chem*. 279:13721-8.

Qvist, R., L.F. Blackwell, H. Bourne, and J.B. Brown. 1990. Development of mouse ovarian follicles from primary to preovulatory stages in vitro. *J Reprod Fertil*. 89:169-80.

Racki, W.J., and J.D. Richter. 2006. CPEB controls oocyte growth and follicle development in the mouse. *Development*. 133:4527-37.

Reynolds, P.R. 2002. In sickness and in health: the importance of translational regulation. *Arch Dis Child*. 86:322-4.

Richter, J.D. 1999. Cytoplasmic polyadenylation in development and beyond. *Microbiol Mol Biol Rev*. 63:446-56.

Richter, J.D. 2007. CPEB: a life in translation. *Trends Biochem Sci*. 32:279-85.

Richter, N.J., G.W. Rogers, Jr., J.O. Hensold, and W.C. Merrick. 1999. Further biochemical and kinetic characterization of human eukaryotic initiation factor 4H. *J Biol Chem*. 274:35415-24.

Roll-Mecak, A., P. Alone, C. Cao, T.E. Dever, and S.K. Burley. 2004. X-ray structure of translation initiation factor eIF2gamma: implications for tRNA and eIF2alpha binding. *J Biol Chem*. 279:10634-42.

Ross, A.F., Y. Oleynikov, E.H. Kislauskis, K.L. Taneja, and R.H. Singer. 1997. Characterization of a beta-actin mRNA zipcode-binding protein. *Mol Cell Biol*. 17:2158-65.

Roy, G., G. De Crescenzo, K. Khaleghpour, A. Kahvejian, M. O'Connor-McCourt, and N. Sonenberg. 2002. Paip1 interacts with poly(A) binding protein through two independent binding motifs. *Mol Cell Biol*. 22:3769-82.

Ruggiu, M., R. Speed, M. Taggart, S.J. McKay, F. Kilanowski, P. Saunders, J. Dorin, and H.J. Cooke. 1997. The mouse Dazla gene encodes a cytoplasmic protein essential for gametogenesis. *Nature*. 389:73-7.

Sachs, A.B., M.W. Bond, and R.D. Kornberg. 1986. A single gene from yeast for both nuclear and cytoplasmic polyadenylate-binding proteins: domain structure and expression. *Cell*. 45:827-35.

Sachs, A.B., and R.W. Davis. 1989. The poly(A) binding protein is required for poly(A) shortening and 60S ribosomal subunit-dependent translation initiation. *Cell*. 58:857-67.

Sachs, A.B., R.W. Davis, and R.D. Kornberg. 1987. A single domain of yeast poly(A)-binding protein is necessary and sufficient for RNA binding and cell viability. *Mol Cell Biol*. 7:3268-76.

Saini, A.K., J.S. Nanda, J.R. Lorsch, and A.G. Hinnebusch. 2010. Regulatory elements in eIF1A control the fidelity of start codon selection by modulating tRNA(i)(Met) binding to the ribosome. *Genes Dev*. 24:97-110.

Sakugawa, N., T. Miyamoto, H. Sato, M. Ishikawa, M. Horikawa, H. Hayashi, and K. Sengoku. 2008. Isolation of the human ePAB and ePABP2 cDNAs and analysis of the expression patterns. *J Assist Reprod Genet*. 25:215-21.

Sala, C., G. Arrigo, G. Torri, F. Martinazzi, P. Riva, L. Larizza, C. Philippe, P. Jonveaux, F. Sloan, T. Labella, and D. Toniolo. 1997. Eleven X chromosome breakpoints associated with premature ovarian failure (POF) map to a 15-Mb YAC contig spanning Xq21. *Genomics*. 40:123-31.

Salaun, C., A.I. MacDonald, O. Larralde, L. Howard, K. Lochtie, H.M. Burgess, M. Brook, P. Malik, N.K. Gray, and S.V. Graham. 2010. Poly(A)-binding protein 1 partially relocalizes to the nucleus during herpes simplex virus type 1 infection in an ICP27-independent manner and does not inhibit virus replication. *J Virol*. 84:8539-48.

Sali, A., and T.L. Blundell. 1993. Comparative protein modelling by satisfaction of spatial restraints. *J Mol Biol*. 234:779-815.

Sanchez, R., and W.F. Marzluff. 2002. The stem-loop binding protein is required for efficient translation of histone mRNA in vivo and in vitro. *Mol Cell Biol*. 22:7093-104.

Sarkissian, M., R. Mendez, and J.D. Richter. 2004. Progesterone and insulin stimulation of CPEB-dependent polyadenylation is regulated by Aurora A and glycogen synthase kinase-3. *Genes Dev*. 18:48-61.

Scheper, G.C., N.A. Morrice, M. Kleijn, and C.G. Proud. 2001. The mitogen-activated protein kinase signal-integrating kinase Mnk2 is a eukaryotic initiation factor 4E kinase with high levels of basal activity in mammalian cells. *Mol Cell Biol*. 21:743-54.

Scheper, G.C., and C.G. Proud. 2002. Does phosphorylation of the cap-binding protein eIF4E play a role in translation initiation? *Eur J Biochem*. 269:5350-9.

Scheper, G.C., B. van Kollenburg, J. Hu, Y. Luo, D.J. Goss, and C.G. Proud. 2002. Phosphorylation of eukaryotic initiation factor 4E markedly reduces its affinity for capped mRNA. *J Biol Chem*. 277:3303-9.

Schuman, E.M., J.L. Dynes, and O. Steward. 2006. Synaptic regulation of translation of dendritic mRNAs. *J Neurosci*. 26:7143-6.

Schutz, P., M. Bumann, A.E. Oberholzer, C. Bieniossek, H. Trachsel, M. Altmann, and U. Baumann. 2008. Crystal structure of the yeast eIF4A-eIF4G complex: an RNA-helicase controlled by protein-protein interactions. *Proc Natl Acad Sci U S A*. 105:9564-9.

Schwartz, D.C., and R. Parker. 1999. Mutations in translation initiation factors lead to increased rates of deadenylation and decapping of mRNAs in Saccharomyces cerevisiae. *Mol Cell Biol*. 19:5247-56.

Schwartz, E.I., R.V. Intine, and R.J. Maraia. 2004. CK2 is responsible for phosphorylation of human La protein serine-366 and can modulate rpL37 5'-terminal oligopyrimidine mRNA metabolism. *Mol Cell Biol*. 24:9580-91.

Searfoss, A., T.E. Dever, and R. Wickner. 2001. Linking the 3' poly(A) tail to the subunit joining step of translation initiation: relations of Pab1p, eukaryotic translation initiation factor 5b (Fun12p), and Ski2p-Slh1p. *Mol Cell Biol*. 21:4900-8.

Seli, E., M.D. Lalioti, S.M. Flaherty, D. Sakkas, N. Terzi, and J.A. Steitz. 2005. An embryonic poly(A)-binding protein (ePAB) is expressed in mouse oocytes and early preimplantation embryos. *Proc Natl Acad Sci U S A*. 102:367-72.

SenGupta, D.J., B. Zhang, B. Kraemer, P. Pochart, S. Fields, and M. Wickens. 1996. A three-hybrid system to detect RNA-protein interactions in vivo. *Proc Natl Acad Sci U S A*. 93:8496-501.

Shantz, L.M., R.H. Hu, and A.E. Pegg. 1996. Regulation of ornithine decarboxylase in a transformed cell line that overexpresses translation initiation factor eIF-4E. *Cancer Res*. 56:3265-9.

Shapiro, A.L., E. Vinuela, and J.V. Maizel, Jr. 1967. Molecular weight estimation of polypeptide chains by electrophoresis in SDS-polyacrylamide gels. *Biochem Biophys Res Commun*. 28:815-20.

Shatkin, A.J. 1985. mRNA cap binding proteins: essential factors for initiating translation. *Cell*. 40:223-4.

Sheiness, D., L. Puckett, and J.E. Darnell. 1975. Possible relationship of poly(A) shortening to mRNA turnover. *Proc Natl Acad Sci U S A*. 72:1077-81.

Shelling, A.N. 2010. Premature Ovarian Failure. *Reproduction*.

Shen-Orr, S.S., Y. Pilpel, and C.P. Hunter. 2010. Composition and regulation of maternal and zygotic transcriptomes reflects species-specific reproductive mode. *Genome Biol*. 11:R58.

Siddiqui, N., D.A. Mangus, T.C. Chang, J.M. Palermino, A.B. Shyu, and K. Gehring. 2007. Poly(A)-nuclease interacts with the PABC domain from poly(A)-binding protein. *J Biol Chem*.

Sigrist, S.J., P.R. Thiel, D.F. Reiff, P.E. Lachance, P. Lasko, and C.M. Schuster. 2000. Postsynaptic translation affects the efficacy and morphology of neuromuscular junctions. *Nature*. 405:1062-5.

Silva, A.L., P. Ribeiro, A. Inacio, S.A. Liebhaber, and L. Romao. 2008. Proximity of the poly(A)-binding protein to a premature termination codon inhibits mammalian nonsense-mediated mRNA decay. *RNA*. 14:563-76.

Silva, A.L., and L. Romao. 2009. The mammalian nonsense-mediated mRNA decay pathway: to decay or not to decay! Which players make the decision? *FEBS Lett*. 583:499-505.

Simmer, F., C. Moorman, A.M. van der Linden, E. Kuijk, P.V. van den Berghe, R.S. Kamath, A.G. Fraser, J. Ahringer, and R.H. Plasterk. 2003. Genome-wide RNAi of C. elegans using the hypersensitive rrf-3 strain reveals novel gene functions. *PLoS Biol*. 1:E12.

Singh, G., S. Jakob, M.G. Kleedehn, and J. Lykke-Andersen. 2007. Communication with the exon-junction complex and activation of nonsense-mediated decay by human Upf proteins occur in the cytoplasm. *Mol Cell*. 27:780-92.

Singh, G., I. Rebbapragada, and J. Lykke-Andersen. 2008. A competition between stimulators and antagonists of Upf complex recruitment governs human nonsense-mediated mRNA decay. *PLoS Biol*. 6:e111.

Skabkina, O.V., D.N. Lyabin, M.A. Skabkin, and L.P. Ovchinnikov. 2005. YB-1 autoregulates translation of its own mRNA at or prior to the step of 40S ribosomal subunit joining. *Mol Cell Biol*. 25:3317-23.

Skabkina, O.V., M.A. Skabkin, N.V. Popova, D.N. Lyabin, L.O. Penalva, and L.P. Ovchinnikov. 2003. Poly(A)-binding protein positively affects YB-1 mRNA translation through specific interaction with YB-1 mRNA. *J Biol Chem*. 278:18191-8.

Sladic, R.T., C.A. Lagnado, C.J. Bagley, and G.J. Goodall. 2004. Human PABP binds AU-rich RNA via RNA-binding domains 3 and 4. *Eur J Biochem*. 271:450-7.

Smith, R.W., and N.K. Gray. 2010. Poly(A)-binding protein (PABP): a common viral target. *Biochem J*. 426:1-12.

Sneddon, S.F., N. Walther, and P.T. Saunders. 2005. Expression of androgen and estrogen receptors in sertoli cells: studies using the mouse SK11 cell line. *Endocrinology*. 146:5304-12.

Sonenberg, N., D. Guertin, and K.A. Lee. 1982. Capped mRNAs with reduced secondary structure can function in extracts from poliovirus-infected cells. *Mol Cell Biol*. 2:1633-8.

Sonenberg, N., M.A. Morgan, W.C. Merrick, and A.J. Shatkin. 1978. A polypeptide in eukaryotic initiation factors that crosslinks specifically to the 5'-terminal cap in mRNA. *Proc Natl Acad Sci U S A*. 75:4843-7.

Sonenberg, N., H. Trachsel, S. Hecht, and A.J. Shatkin. 1980. Differential stimulation of capped mRNA translation in vitro by cap binding protein. *Nature*. 285:331-3.

Spirin, A.S. 2009. How does a scanning ribosomal particle move along the 5'-untranslated region of eukaryotic mRNA? Brownian Ratchet model. *Biochemistry*. 48:10688-92.

Spriggs, K.A., M. Bushell, S.A. Mitchell, and A.E. Willis. 2005. Internal ribosome entry segment-mediated translation during apoptosis: the role of IRES-trans-acting factors. *Cell Death Differ*. 12:585-91.

Spriggs, K.A., M. Stoneley, M. Bushell, and A.E. Willis. 2008. Re-programming of translation following cell stress allows IRES-mediated translation to predominate. *Biol Cell*. 100:27-38.

Stebbins-Boaz, B., Q. Cao, C.H. de Moor, R. Mendez, and J.D. Richter. 1999. Maskin is a CPEB-associated factor that transiently interacts with elF-4E. *Mol Cell*. 4:1017-27.

Stebbins-Boaz, B., L.E. Hake, and J.D. Richter. 1996. CPEB controls the cytoplasmic polyadenylation of cyclin, Cdk2 and c-mos mRNAs and is necessary for oocyte maturation in Xenopus. *EMBO J*. 15:2582-92.

Stolovich, M., H. Tang, E. Hornstein, G. Levy, R. Cohen, S.S. Bae, M.J. Birnbaum, and O. Meyuhas. 2002. Transduction of growth or mitogenic signals into translational activation of TOP mRNAs is fully reliant on the phosphatidylinositol 3-kinase-mediated pathway but requires neither S6K1 nor rpS6 phosphorylation. *Mol Cell Biol*. 22:8101-13.

Stripecke, R., C.C. Oliveira, J.E. McCarthy, and M.W. Hentze. 1994. Proteins binding to 5' untranslated region sites: a general mechanism for translational regulation of mRNAs in human and yeast cells. *Mol Cell Biol*. 14:5898-909.

Svitkin, Y.V., H. Imataka, K. Khaleghpour, A. Kahvejian, H.D. Liebig, and N. Sonenberg. 2001a. Poly(A)-binding protein interaction with elF4G stimulates picornavirus IRES-dependent translation. *RNA*. 7:1743-52.

Svitkin, Y.V., A. Pause, A. Haghighat, S. Pyronnet, G. Witherell, G.J. Belsham, and N. Sonenberg. 2001b. The requirement for eukaryotic initiation factor 4A (elF4A) in translation is in direct proportion to the degree of mRNA 5' secondary structure. *RNA*. 7:382-94.

Tanaka, M., and W. Herr. 1990. Differential transcriptional activation by Oct-1 and Oct-2: interdependent activation domains induce Oct-2 phosphorylation. *Cell*. 60:375-86.

Tang, H., E. Hornstein, M. Stolovich, G. Levy, M. Livingstone, D. Templeton, J. Avruch, and O. Meyuhas. 2001. Amino acid-induced translation of TOP mRNAs is fully dependent on phosphatidylinositol 3-kinase-mediated signaling, is partially inhibited by rapamycin, and is independent of S6K1 and rpS6 phosphorylation. *Mol Cell Biol*. 21:8671-83.

Tarun, S.Z., Jr., and A.B. Sachs. 1995. A common function for mRNA 5' and 3' ends in translation initiation in yeast. *Genes Dev*. 9:2997-3007.

Tarun, S.Z., Jr., and A.B. Sachs. 1996. Association of the yeast poly(A) tail binding protein with translation initiation factor eIF-4G. *Embo J*. 15:7168-77.

Tarun, S.Z., Jr., S.E. Wells, J.A. Deardorff, and A.B. Sachs. 1997. Translation initiation factor eIF4G mediates in vitro poly(A) tail-dependent translation. *Proc Natl Acad Sci U S A*. 94:9046-51.

Tay, J., and J.D. Richter. 2001. Germ cell differentiation and synaptonemal complex formation are disrupted in CPEB knockout mice. *Dev Cell*. 1:201-13.

Taylor, D.J., J. Frank, and T.G. Kinzy. 2007a. Structure and Function of the Eukaryotic Ribosome and Elongation Factors. *Cold Spring Harb Laboratory Press*. 48:59-85.

Taylor, D.J., J. Nilsson, A.R. Merrill, G.R. Andersen, P. Nissen, and J. Frank. 2007b. Structures of modified eEF2 80S ribosome complexes reveal the role of GTP hydrolysis in translocation. *Embo J*. 26:2421-31.

Teleman, A.A., Y.W. Chen, and S.M. Cohen. 2005. 4E-BP functions as a metabolic brake used under stress conditions but not during normal growth. *Genes Dev*. 19:1844-8.

Tharun, S., and R. Parker. 2001. Targeting an mRNA for decapping: displacement of translation factors and association of the Lsm1p-7p complex on deadenylated yeast mRNAs. *Mol Cell*. 8:1075-83.

Thoma, C., A. Ostareck-Lederer, and M.W. Hentze. 2004. A poly(A) tail-responsive in vitro system for cap- or IRES-driven translation from HeLa cells. *Methods Mol Biol*. 257:171-80.

Tran, H., M. Schilling, C. Wirbelauer, D. Hess, and Y. Nagamine. 2004. Facilitation of mRNA deadenylation and decay by the exosome-bound, DExH protein RHAU. *Mol Cell*. 13:101-11.

Uchida, N., S. Hoshino, H. Imataka, N. Sonenberg, and T. Katada. 2002. A novel role of the mammalian GSPT/eRF3 associating with poly(A)-binding protein in Cap/Poly(A)-dependent translation. *J Biol Chem*. 277:50286-92.

Uchida, N., S. Hoshino, and T. Katada. 2004. Identification of a human cytoplasmic poly(A) nuclease complex stimulated by poly(A)-binding protein. *J Biol Chem*. 279:1383-91.

Ueda, T., R. Watanabe-Fukunaga, H. Fukuyama, S. Nagata, and R. Fukunaga. 2004. Mnk2 and Mnk1 are essential for constitutive and inducible phosphorylation of eukaryotic initiation factor 4E but not for cell growth or development. *Mol Cell Biol*. 24:6539-49.

Unbehaun, A., S.I. Borukhov, C.U. Hellen, and T.V. Pestova. 2004. Release of initiation factors from 48S complexes during ribosomal subunit joining and the link between establishment of codon-anticodon base-pairing and hydrolysis of eIF2-bound GTP. *Genes Dev*. 18:3078-93.

Valasek, L., K.H. Nielsen, F. Zhang, C.A. Fekete, and A.G. Hinnebusch. 2004. Interactions of eukaryotic translation initiation factor 3 (eIF3) subunit NIP1/c with eIF1 and eIF5 promote preinitiation complex assembly and regulate start codon selection. *Mol Cell Biol*. 24:9437-55.

Van Eden, M.E., M.P. Byrd, K.W. Sherrill, and R.E. Lloyd. 2004. Translation of cellular inhibitor of apoptosis protein 1 (c-IAP1) mRNA is IRES mediated and regulated during cell stress. *RNA*. 10:469-81.

Vasudevan, S., Y. Tong, and J.A. Steitz. 2007. Switching from repression to activation: microRNAs can up-regulate translation. *Science*. 318:1931-4.

Vattem, K.M., K.A. Staschke, and R.C. Wek. 2001. Mechanism of activation of the double-stranded-RNA-dependent protein kinase, PKR: role of dimerization and cellular localization in the stimulation of PKR phosphorylation of eukaryotic initiation factor-2 (eIF2). *Eur J Biochem*. 268:3674-84.

Ventoso, I., R. Blanco, C. Perales, and L. Carrasco. 2001. HIV-1 protease cleaves eukaryotic initiation factor 4G and inhibits cap-dependent translation. *Proc Natl Acad Sci U S A*. 98:12966-71.

Voeltz, G.K., J. Ongkasuwan, N. Standart, and J.A. Steitz. 2001. A novel embryonic poly(A) binding protein, ePAB, regulates mRNA deadenylation in Xenopus egg extracts. *Genes Dev*. 15:774-88.

Volpon, L., M.J. Osborne, I. Topisirovic, N. Siddiqui, and K.L. Borden. 2006. Cap-free structure of eIF4E suggests a basis for conformational regulation by its ligands. *EMBO J*. 25:5138-49.

von Der Haar, T., P.D. Ball, and J.E. McCarthy. 2000. Stabilization of eukaryotic initiation factor 4E binding to the mRNA 5'-Cap by domains of eIF4G. *J Biol Chem*. 275:30551-5.

Wahle, E. 1991. A novel poly(A)-binding protein acts as a specificity factor in the second phase of messenger RNA polyadenylation. *Cell*. 66:759-68.

Wang, Z., X. Jiao, A. Carr-Schmid, and M. Kiledjian. 2002. The hDcp2 protein is a mammalian mRNA decapping enzyme. *Proc Natl Acad Sci U S A*. 99:12663-8.

Wang, Z., and M.S. Sachs. 1997. Ribosome stalling is responsible for arginine-specific translational attenuation in Neurospora crassa. *Mol Cell Biol*. 17:4904-13.

Wei, C.C., M.L. Balasta, J. Ren, and D.J. Goss. 1998. Wheat germ poly(A) binding protein enhances the binding affinity of eukaryotic initiation factor 4F and (iso)4F for cap analogues. *Biochemistry*. 37:1910-6.

Wells, S.E., P.E. Hillner, R.D. Vale, and A.B. Sachs. 1998. Circularization of mRNA by eukaryotic translation initiation factors. *Mol Cell*. 2:135-40.

Wendel, H.G., R.L. Silva, A. Malina, J.R. Mills, H. Zhu, T. Ueda, R. Watanabe-Fukunaga, R. Fukunaga, J. Teruya-Feldstein, J. Pelletier, and S.W. Lowe. 2007. Dissecting eIF4E action in tumorigenesis. *Genes Dev*. 21:3232-7.

Wilkie, G.S., K.S. Dickson, and N.K. Gray. 2003. Regulation of mRNA translation by 5'- and 3'-UTR-binding factors. *Trends Biochem Sci*. 28:182-8.

Wilkie, G.S., P. Gautier, D. Lawson, and N.K. Gray. 2005. Embryonic poly(A)-binding protein stimulates translation in germ cells. *Mol Cell Biol*. 25:2060-71.

Willett, M., S.A. Flint, S.J. Morley, and V.M. Pain. 2006. Compartmentalisation and localisation of the translation initiation factor (eIF) 4F complex in normally growing fibroblasts. *Exp Cell Res*. 312:2942-53.

Woods, A.J., T. Kantidakis, H. Sabe, D.R. Critchley, and J.C. Norman. 2005. Interaction of paxillin with poly(A)-binding protein 1 and its role in focal adhesion turnover and cell migration. *Mol Cell Biol*. 25:3763-73.

Woods, A.J., M.S. Roberts, J. Choudhary, S.T. Barry, Y. Mazaki, H. Sabe, S.J. Morley, D.R. Critchley, and J.C. Norman. 2002. Paxillin associates with poly(A)-binding protein 1 at the dense endoplasmic reticulum and the leading edge of migrating cells. *J Biol Chem*. 277:6428-37.

Yamashita, A., T.C. Chang, Y. Yamashita, W. Zhu, Z. Zhong, C.Y. Chen, and A.B. Shyu. 2005. Concerted action of poly(A) nucleases and decapping enzyme in mammalian mRNA turnover. *Nat Struct Mol Biol*. 12:1054-63.

Yan, R., W. Rychlik, D. Etchison, and R.E. Rhoads. 1992. Amino acid sequence of the human protein synthesis initiation factor eIF-4 gamma. *J Biol Chem*. 267:23226-31.

Yanagiya, A., G. Delbes, Y.V. Svitkin, B. Robaire, and N. Sonenberg. In press. The poly(A)-binding protein partner Paip2a controls translation during late spermiogenesis in mice. *J Clin Invest*.

Yanagiya, A., Y.V. Svitkin, S. Shibata, S. Mikami, H. Imataka, and N. Sonenberg. 2009. Requirement of RNA binding of mammalian eukaryotic translation initiation factor 4GI (eIF4GI) for efficient interaction of eIF4E with the mRNA cap. *Mol Cell Biol*. 29:1661-9.

Yang, H., C.S. Duckett, and T. Lindsten. 1995. iPABP, an inducible poly(A)-binding protein detected in activated human T cells. *Mol Cell Biol*. 15:6770-6.

Yoshida, M., K. Yoshida, G. Kozlov, N.S. Lim, G. De Crescenzo, Z. Pang, J.J. Berlanga, A. Kahvejian, K. Gehring, S.S. Wing, and N. Sonenberg. 2006. Poly(A) binding protein (PABP) homeostasis is mediated by the stability of its inhibitor, Paip2. *Embo J*. 25:1934-44.

Zekri, L., E. Huntzinger, S. Heimstadt, and E. Izaurralde. 2009. The silencing domain of GW182 interacts with PABPC1 to promote translational repression and degradation of microRNA targets and is required for target release. *Mol Cell Biol*. 29:6220-31.

Zhang, B., B. Kraemer, D. SenGupta, S. Fields, and M. Wickens. 1999. Yeast three-hybrid system to detect and analyze interactions between RNA and protein. *Methods Enzymol*. 306:93-113.

Zhang, J., X. Sun, Y. Qian, J.P. LaDuca, and L.E. Maquat. 1998. At least one intron is required for the nonsense-mediated decay of triosephosphate isomerase mRNA: a possible link between nuclear splicing and cytoplasmic translation. *Mol Cell Biol*. 18:5272-83.

Zhu, J., A. Hayakawa, T. Kakegawa, and R.L. Kaspar. 2001. Binding of the La autoantigen to the 5' untranslated region of a chimeric human translation elongation factor 1A reporter mRNA inhibits translation in vitro. *Biochim Biophys Acta*. 1521:19-29.

Zimmer, S.G., A. DeBenedetti, and J.R. Graff. 2000. Translational control of malignancy: the mRNA cap-binding protein, eIF-4E, as a central regulator of tumor formation, growth, invasion and metastasis. *Anticancer Res*. 20:1343-51.